THE MODIFICATION AND USE OF SUPPORTED PLATINUM CATALYSTS FOR ASYMMETRIC HYDROGENATION REACTIONS

A Thesis Presented to
the University of Glasgow
for the Degree of
Doctor of Philosophy
by

Elaine Allan

October 1995

ProQuest LLC.
789 East Eisenhower Parkway
P.O. Box 1346
Ann Arbor, MI 48106 – 1346

SUMMARY

This thesis describes a study of the adsorption of chiral substituted binaphthalene molecules (2,2'-dihydroxy-1,1'-binaphthalene, 2,2'-diamino-1,1'-binaphthalene, 2,2-dimethoxy-1,1'-binaphthalene and 2,2',7,7'-tetrahydroxy-1,1'-binaphthalene) on to supported Pt catalysts (1% w/w Pt/γ-alumina, 1% w/w Pt/Grace silica C10 and 1% w/w Pt/Cab-O-Sil) with a view to establishing a system which could be capable of inducing asymmetric hydrogenation of prochiral starting materials.

The 2,2'-dihydroxy-1,1'-binaphthalene modifier was found to adsorb irreversibly on to the 1% w/w Pt/γ-alumina and 1% w/w Pt/Grace silica C10 catalysts, prior to the ageing of the 1% w/w Pt/Grace silica C10 catalyst. The 2,2'-dihydroxy-1,1'-binaphthalene modifier was also found to irreversibly adsorb on to the γ-alumina support, to a similar extent as that on to the 1% w/w Pt/γ-alumina catalyst. The 2,2'-diamino-1,1'-binaphthalene modifier was adsorbed irreversibly on to the 1% w/w Pt/γ-alumina, 1% w/w Pt/Grace silica C10 and 1% w/w Pt/Cab-O-Sil catalysts. In the case of the 1% w/w Pt/Cab-O-Sil catalyst, the 2,2'-diamino-1,1'-binaphthalene was found to undergo a chemical reaction which resulted in the formation of 2-hydroxy-2'-amino-1,1'-binaphthalene and 2,2'-dihydroxy-1,1'-binaphthalene. 2,2-Dimethoxy-1,1'-binaphthalene modifier was found not to adsorb on to the (1% w/w Pt/γ-alumina, 1% w/w Pt/Grace silica C10 and 1% w/w Pt/Cab-O-Sil catalysts. The 2,2',7,7'-tetrahydroxy-1,1'-binaphthalene modifier was found to be adsorbed on to the 1% w/w Pt/γ-alumina and 1% w/w Pt/Cab-O-Sil catalysts, with the γ-alumina support adsorbing the 2,2',7,7'-tetrahydroxy-1,1'-binaphthalene to a similar extent as that on to the 1% w/w Pt/γ-alumina catalyst. Evidence is presented for the adsorption of 2,2'-dihydroxy-1,1'-binaphthalene, 2,2'-diamino-1,1'-binaphthalene and 2,2',7,7'-tetrahydroxy-1,1'-binaphthalene modifiers are in a near vertical mode via their substituent groups, via the dissociation of a hydrogen atom.

The adsorption of R-(-)-1-(9-anthryl)-2,2,2-trifluoroethanol was studied with respect to the 1% w/w Pt/γ-alumina and 1% w/w Pt/Cab-O-Sil catalysts as well as the respective supports. It was found that only the 1% w/w Pt/γ-alumina catalyst adsorbed this modifier.

The adsorption of (S,S)-di-(2-propyl)-6,12-dioxa-2,5,13,16-tetraoxo-3,15,19-triazabicyclo [15.3.1] heneicosa-1 (21),17,19-triene and (S,S)-di-(2-propyl)-6,13-dioxa-2,5,14,17-tetraoxo-3,16,20-triazabicyclo [16.3.1] docosa-1 (22),18,20-triene macrocycles were also studied, with the result that both the macrocycles were adsorbed on to both the 1% w/w Pt/γ-alumina and 1% w/w Pt/Cab-O-Sil catalysts as well as the γ-alumina support.

The 1% w/w Pt/γ-alumina and 1% w/w Pt/Cab-O-Sil catalysts were studied for their co-adsorption properties with respect to the 2,2'-dihydroxy-1,1'-binaphthalene and 2,2'-

diamino-1,1'-binaphthalene modifiers. In the case of the 1% w/w Pt/Cab-O-Sil catalyst, 2,2'-dihydroxy-1,1'-binaphthalene and 2-hydroxy-2'-amino-1,1'-binaphthalene were formed as well as 2,2'-diamino-1,1'-binaphthalene being adsorbed.

The hydrogenation of methyl tiglate and tiglic acid over the various modified supported Pt catalysts resulted in the formation of the racemate (methyl-2-methyl butyrate and 2-methyl butyric acid, respectively). However, the hydrogenation of 3-coumaranone over diamine modified supported Pt catalysts resulted in the inducement of enantioselectivity, that is, R-(+)-2,2'-diamino-1,1'-binaphthalene modified supported Pt catalysts induced S-3-benzofuranol and S-(-)-2,2'-diamino-1,1'-binaphthalene modified supported Pt catalysts induced R-3-benzofuranol. While the hydrogenation of 3-coumaranone over 2,2'-dihydroxy-1,1'-binaphthalene modified supported Pt catalysts resulted in the racemate. Modification of the supported Pt catalysts with either (S,S)-di-(2-propyl)-6,12-dioxa-2,5,13,16-tetraoxo-3,15,19-triazabicyclo[15.3.1]heneicosa-1(21),17,19-triene or (S,S)-di-(2-propyl)-6,13-dioxa-2,5,14,17-tetraoxo-3,16,20-triazabicyclo [16.3.1] docosa-1 (22),18,20-triene macrocycles led to the formation of the racemate with respect to the hydrogenation of 3-coumaranone.

The hydrogenation of methyl tiglate and 3-coumaranone were studied over the supported Pt catalysts modified with L-histidine, R-(+)-N,N-dimethyl-1-phenylethylamine, L-tryptophan, R-(+)-α-methoxy-α-trifluoromethylphenylacetic acid, L-phenylalaninol, L-(+)-α-phenylglycinol and (+)-pseudoephedrine. The racemate was obtained from the hydrogenation of methyl tiglate over supported Pt catalysts modified with these modifiers, and the formation of methyl angelate was observed when the 1% w/w Pt/γ-alumina catalyst was modified with L-histidine, R-(+)-N,N-dimethyl-1-phenylethylamine, (+)-pseudoephedrine and R-(+)-α-methoxy-α-trifluoromethylphenylacetic acid. An unidentified additional product was observed in the hydrogenation of 3-coumaranone over either the unmodified supported Pt catalysts or the modified supported Pt catalysts.

ACKNOWLEDGEMENTS

I would like to thank my academic supervisor Prof. Geoff Webb and industrial supervisor Dr. David Jackson for their help and the other members of research group:-

Dr. E. Colvin, Miss N. Young and Mr. D. Hunter (University of Glasgow),
Dr. W. Moss and Dr. G. Robinson (Zeneca Pharmaceuticals, Macclesfield),
Dr. S. Korn (Zeneca Fine Chemicals Manufacturing Organisation, Huddersfield),
Prof. Peter B. Wells, Dr. P. Johnston and Mr. S. R. Watson (University of Hull),
Dr. A. Ibbotson and
Dr. R. Sampson.

I would also like to thank the Technical Staff in the Chemistry Department for all their help, especially Jim McIver, Rose Millar and Victoria Yates. Thanks to the other members of the Inorganic Research Office. Thanks to Ian Dalgleish, Principle Teacher of Chemistry, Ardrossan Academy for scanning of some of the diagrams in the thesis.

Thanks to EPSRC for funding and I.C.I. Katalco for providing me with sponsorship.

Finally, I would like to thank my parents because without their support, encouragement and belief in my abilities, I could never have got this far.

TABLE OF CONTENTS

CHAPTER 1
INTRODUCTION

1.1 INTRODUCTION

1.1.1 Chirality

Stereochemistry, from the Greek word, stereos = solid, is the study in three dimensions of the relationship between molecular structure and properties of organic molecules. Compounds that share the same molecular formula but have different molecular structures are known as isomers (Greek: isos, equal; meros, part), that is, they contain the same numbers of the same kinds of atoms, but the atoms are attached to one another in different ways. A less extreme form of isomers exists where instead of the difference in the way the atoms are bound together, the difference is the way in which the atoms are orientated in space. These particular type of isomers are known as stereoisomers, that is, the orientation of an atom of two separate molecules in space. This type of isomerism is not reflected by the condensed structural formula. Unlike true isomers, stereoisomers have identical properties, for example boiling point, except for the effect they have on plane polarised light. Stereoisomers may be classed as either conformational or configurational isomers. Conformational isomers at room temperature permit the rotation around a C-C single bond. On the other hand configurational isomers do not permit inter-conversion by rotation around the bonds in the molecules.

Enantiomers are configurational stereoisomers that are mirror images of each other (Greek; enantio-, opposite). Enantiomers have identical physical properties, except for the direction of rotation of the plane polarised light (discussed in section 3.4.3.6) and they also have identical chemical properties except towards optically active reagents. An example of enantiomers are shown in Figure 1.1.

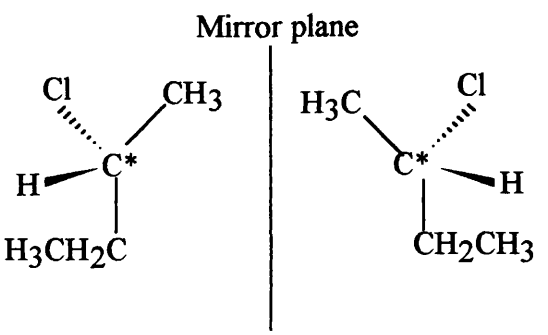

(a) (-)-2-chlorobutane (b) (+)-2-chlorobutane
(a) is non-superimposable on (b)

Figure 1.1:-Enantiomers of 2-chlorobutane

Configurational stereoisomers which are not enantiomers are diastereoisomers.

The carbon atom in Figure 1.1 marked with the asterisk; that is, C*, is described as the chiral centre of the molecules because it is attached to four different groups. An alternative name for the chiral centre is asymmetric or stereogenic centre. Enantiomeric molecules that contain a chiral centre and whose mirror images are not superimposable are chiral. The resulting molecules are superimposable if by any manipulation except bending or breaking bonds, the molecules coincide in all their parts. Structure (a) and (b) in Figure 1.1 are mirror images and non-superimposable and so therefore 2-chlorobutane is chiral.

The ability of a molecule to rotate plane polarised light in nearly all cases is due to a tiny amount of interaction with the charged particles of the molecules; the direction and the extent of rotation varies with the orientation of the particular molecule in the beam. For most compounds, because of the random distribution of a large number of molecules that make up even the smallest sample of a single pure compound, for every molecule that the light encounters, there is another (identical) molecule (mirror image) which cancels its effect. The net result is no rotation, that is no optical activity. Optical inactivity is a property of the random distribution of molecules that exist as mirror images of each other rather than the property of individual molecules. In the case of chiral molecules whose mirror images are not identical but in fact different, isomeric compounds; optical activity is observed when a pure sample of a single enantiomer is studied, that is, no molecule has its mirror image present to cancel out the rotation of the pure enantiomer. The pure sample of a single enantiomer is described as optically pure. While a sample which contains an equal amount of the two enantiomers is known as a racemate and is optically inactive as the rotation of one enantiomer is cancelled by the rotation of the second enantiomer. Enantiomers rotate plane polarised light to the same extent except in opposite directions.

The exact origin of the studies of chirality in nature remains something of a mystery. The founder of stereochemistry has been regarded as van't Hoff following the publication of his famous paper in 1874.[1] It was the existence of enantiomers that convinced van't Hoff that the carbon atom is tetrahedral.

Louis Pasteur is believed to be one of the first that had thoughts on stereochemistry (molecular asymmetry). Pasteur's idea involved relating the asymmetric structure of the crystals to the molecules themselves. Pasteur[2] observed that crystals of racemic sodium ammonium tartrate could be divided into two types due to the presence of small hemihedral facets on the crystals. The experiment in 1848 by Pasteur[3] in which he divides the crystals into the two groups was done by hand using a pair of tweezers and a hand lens. The crystals together were optically inactive in solution, but once separated they were

seen to be mirror images of each other. The separated crystals were either right- or left-handed and each set of dissolved crystals were optically active. Furthermore, the extent (specific) rotations of the two solutions were exactly equal, but of opposite sign, that is the right-handed crystals rotated to the right and the left-handed to the left but by the same extent. Since the difference in optical rotation in solution, Pasteur concluded that it was characteristic, not of the crystals, but of the molecules. He proposed that the molecules making up the two sets of crystals were mirror images of each other and so the existence of isomers whose structures differ only in being mirror images of each other was demonstrated.

Historically racemic sodium ammonium tartrate was referred to as sodium ammonium "racemate" because "racemic acid" was the name for racemic tartaric acid, while the right-handed enantiomer, was called "tartaric acid" which was obtained during the manufacture of wine.

Pasteur found that not all compounds could be resolved by hand at room temperature because of their inability to form crystals at this temperature. So by 1852, Pasteur had discovered a new method to resolve "racemic acid" and other compounds. This new method involved the use of optically active reagents, for example, the use of naturally occurring bases such as (-)-quinine. The process of using optically active reagents can be summarised in terms of modern theory as shown in Figure 1.2. The separation of the diastereoisomeric salts could be performed using the differences in their solubilities. The acid enantiomers are also recovered from the salts without much difficulty.

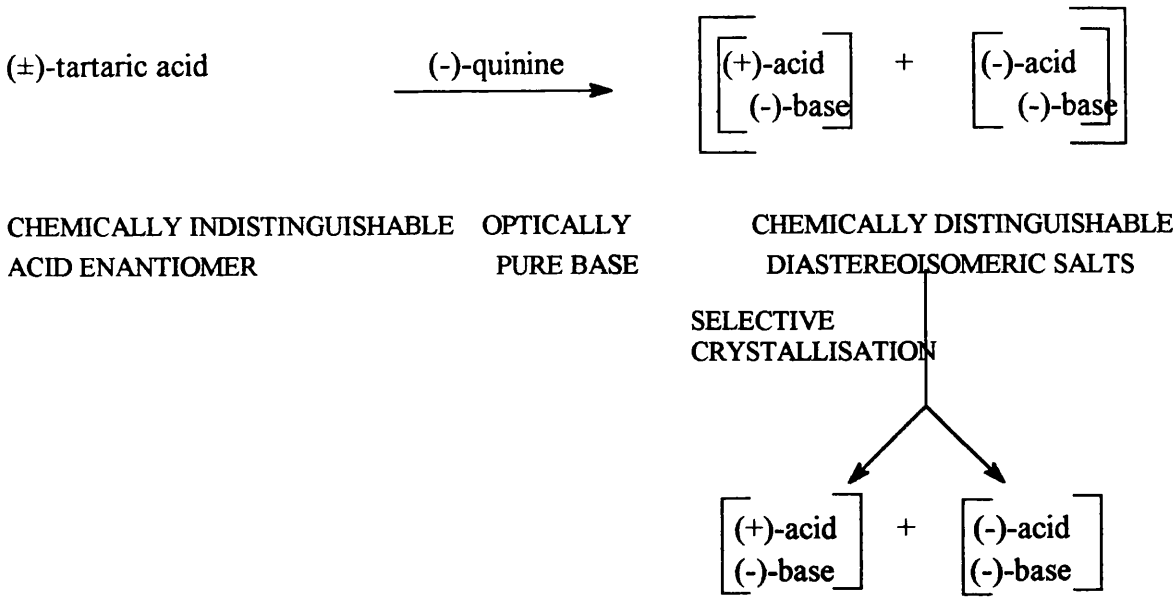

Figure 1.2:- Modern theory of diastereomeric separation

Configuration is the arrangement of atoms that characterises a particular stereoisomer. A stereoisomer that rotates the plane of polarised light to the right is labelled by the symbol (+) and to the left by (-) as shown by Figure 1.1. The (+) and (-) preceding an enantiomeric name indicates the direction of optical activity, they give no indication as to the actual configuration of each enantiomer. The system used to distinguish one enantiomer from the other, by using a naming system which gives the configuration of each enantiomer is known as the Cahn-Ingold-Prelog rules.

The Cahn-Ingold-Prelog rules can be split into two of steps as follows:

STEP 1: Following the sequence rules (see later), the sequence of priority of the four groups (that is, four ligands) attached to the chiral centre is assigned. For example in CHClBrI, the four atoms attached to the chiral centre are all different and priority depends simply on atomic number, the atom of higher number having higher priority. Thus I > Br > Cl > H.

STEP 2: The molecule is orientated so that the ligand of lowest priority, in the case of CHClBrI, the H atom, is directed away. If, in preceding from the ligand of highest priority (I) to the ligand of second priority (Br) and then to the third (Cl), the direction of travel is in a clockwise direction, the configuration is specified R (Latin: rectus, right); if counterclockwise, the configuration is specified S (Latin: sinister, left).

The sequence rules mentioned previously are as follows:

SEQUENCE RULE 1: If the four atoms attached to the stereogenic centre are all different, priority depends of atomic number, with the atom of higher atomic number getting higher priority. If two atoms are isotopes of the same element, the atom of higher mass number has the higher priority e.g. D > H.

SEQUENCE RULE 2: If the relative priority of two groups cannot be decided by Rule 1, it is determined by comparing of the next atoms in the group. That is, if two atoms attached to the chiral centre are the same, the atoms attached to each of the first atoms are compared. For example, in 2-chlorobutane (Figure 1.1), there are two carbon atoms attached to the chiral centre. In the CH_3 the second atoms are H, H, H; and in C_2H_5 they are C, H, H. Since carbon has a higher atomic number than hydrogen, C_2H_5 has the higher priority. The complete sequence for 2-chlorobutane is therefore Cl > C_2H_5 > CH_3 > H.

SEQUENCE RULE 3: This rule takes into account how to give priority to ligands which contain double and triple bonds. Where there is a double or triple bond, both atoms are considered to be duplicated or triplicated. For example (Figures 1.3 and 1.4),

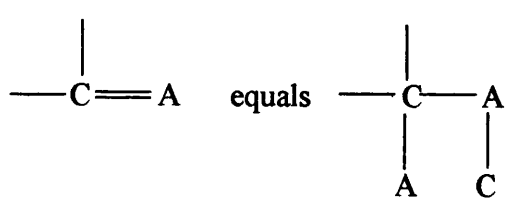

Figure 1.3:- Priority of double bonds

and

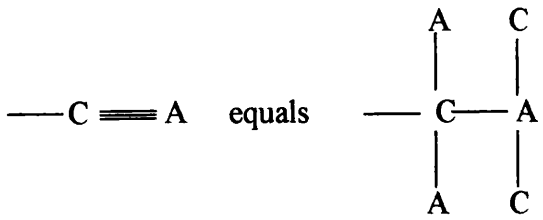

Figure 1.4:- Priority of treble bonds

The phenyl group, C_6H_5-, is handled as though it had one of the Kekulé structures as shown by Figure 1.5,

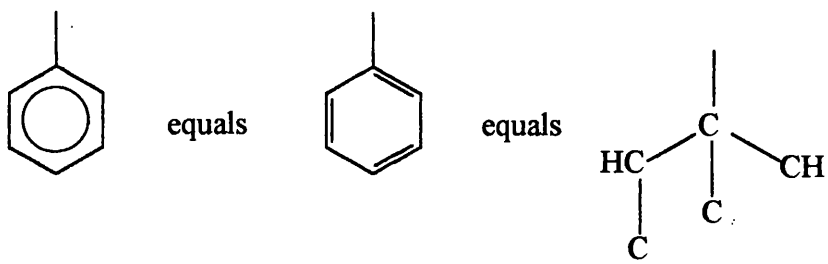

Figure 1.5:- Priority of phenyl group

It is matter of convention that when naming enantiomers using the Cahn-Ingold-Prelog rules to include the sign (+ or -) relating to the direction of rotation of plane polarised light.

1.2 CATALYSIS

In the early 19th century there had been discoveries that the presence of trace amounts of substances although not consumed, affected a chemical reaction.[4] An example of such observation was the decomposition of hydrogen peroxide in the presence of metal ions even at low concentrations. While Michael Faraday[5] demonstrated the oxidation of ethanol vapour with platinum; J.W. Döbereiner showed the oxidation of hydrogen with platinum[6] and in 1831 Peregrine Philips[7] patented the oxidation of SO_2 with platinum.

The first rationalisation of catalysis took place in 1836 by J.J. Berzelius.[8] Berzelius' definition of catalysis was

"I shall ... call it the catalytic power of substances, and the decomposition by means of the power catalysis"

although over the years the definition has changed slightly and the most acceptable

definition is that of a substance that increases the rate of reaction towards equilibrium without being consumed in the reaction. The word catalysis arrives from the two Greek words, the prefix cata meaning down, and the verb lysein meaning to split or break.

The definition of a catalyst assumes that the equilibrium position attained in the presence of a catalyst is the same as that obtained when no catalyst is employed, as required by the laws of thermodynamics.

Catalysis can be divide into three main categories, that is, heterogeneous, homogeneous and enzymatic. A heterogeneous catalyst, is a catalyst which is in a different phase from the reactants and so a phase boundary exists; a homogeneous catalyst, is a catalyst which is in the same phase as the reactants and no phase boundary exists; and an enzymatic catalyst, this is a catalyst that is a large complex molecule which is neither a heterogeneous nor a homogeneous catalyst but usually a protein which forms lyophilic colloid.

Catalysts these days are important in the pharmaceutical, agrochemicals and fine chemical industries.

Hydrogenation reactions involve the addition of molecular hydrogen, H_2 (dihydrogen), to a multiple bond. The addition of hydrogen can take place across carbon-carbon double bonds (C=C), carbon-carbon treble bonds (C≡C) or carbon-oxygen double bonds (C=O). Catalytic addition of hydrogen is one of the most studied catalytic reactions. Metals are good catalysts for the hydrogenation; for example, platinum, palladium or nickel are employed to hydrogenate alkenes to alkanes; and are used in a variety of physical forms, wires, finely divided metal powders or most commonly when supported on a carrier.

A catalyst that has been shown to hydrogenate alkenes to alkanes can also hydrogenate unsaturated alcohols to saturated alcohols and unsaturated esters to saturated esters under similar conditions. However, by varying the catalyst and the conditions it is possible to selectively hydrogenate one multiple bond, but not the other, in the same molecule, for example, a C=C double bond but not a C=O double bond; a C≡C triple bond but not a C=C double bond; even one C=C double bond over another C=C double bond. Also hydrogenation of an optically inactive unsaturated compound into an optically active saturated product can occur.

Hydrogenation is of two general kinds: (a) heterogeneous and (b) homogeneous. The support is the vehicle for the active phase and its function can maximise the surface area of the active phase. The support constitutes 80 to 99.9% of total weight of the catalyst.

One of many uses for supported metal catalysts is for hydrogenation reactions. The

main use of hydrogenation reactions is in the pharmaceutical, agrochemicals and food industries. The food industry employs hydrogenation catalysts to harden animal and vegetable oils to edible fats in the preparation of margarine.[7] Food flavouring and fragrances are prepared from the hydrogenation of precursors by catalyst.[9]

The need for the production of one enantiomer over the other, especially where biological activity is concerned, is of great importance to the pharmaceutical, agrochemical and fine chemical industries. Biological systems (enzymes[10]) can distinguish one enantiomer and its mirror images as a result of the natural occurrence in nature of only one enantiomer of carbohydrates and proteins. Enzymes, therefore, can distinguish one enantiomer of a compound to be a hormone or active as medication, while the other enantiomer is biologically inactive. Alternatively, one enantiomer may be active and have an undesired effect as shown by the well documented case of thalidomide (Figure 1.6), where both enantiomers showed sedative effects, but the S-(-)-enantiomer had teratogenic properties.[11]

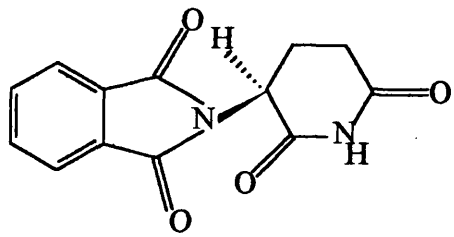

Figure 1.6:- S-(-)-thalidomide

The method in which one enantiomer is selectively produced is known as stereoselective or more specifically enantioselective reaction. The preferential formation of one enantiomer over the other involves selective addition of the reagent, for example, dihydrogen, to one side of the plane of symmetry that contains the prochiral group and so such processes are termed asymmetric.

Asymmetric synthesis, in general, can be termed either first, second, third or fourth generation.[12] The first, second and third generation asymmetric synthesis is an organic synthetic approach involving chiral reagents or substrates, while the fourth generation uses catalysts which control the asymmetry, that is, the substrates and reagents are achiral and the catalysts are chiral.

The fourth generation catalysts include heterogeneous, homogeneous and enzymatic catalysts. Asymmetric syntheses require enantiomerically pure compounds to influence the

stereochemical outcome of an asymmetric reaction. The naturally occurring enantiomerically pure compounds used have been classified as follows:

(1) Amino acids and amino alcohols

(2) Amines and alkaloids

(3) Hydroxy acids (for example, tartaric acid[13])

(4) Terpenes (for example, pinene, camphor)

(5) Carbohydrates

(6) Enzymes and other proteins

Compounds (1) and (3) have been used with heterogeneous nickel catalysts in the formation of asymmetric products. Compounds (2), for example, cinchonidine has been used with heterogeneous platinum catalysts in the asymmetric hydrogenation of ethyl pyruvate[14] and methyl pyruvate.[15] The formation of one alcohol[16] enantiomer as a result of the hydrolysis of an intermediate formed from the reaction of diisopincampheyl (4) with an alkene.

1.2.1 Asymmetric hydrogenation reactions

A number of asymmetric hydrogenation reactions have been studied for both homogeneous and heterogeneous asymmetric catalysts. Wilkinson's catalyst $RhCl(PPh_3)_3$,[17] is one of the best known homogeneous hydrogenation catalysts, although previous to the discovery of Wilkinson's catalyst, homogeneous solution[18] of Ag^+ and MnO_4^- ions had been shown to be able to activate molecular hydrogen and add the hydrogen to unsaturated compounds. The introduction of chirality into the tertiary phosphines of the Wilkinson's catalyst led to the possibility for asymmetric homogeneous catalytic hydrogenation of prochiral unsaturated substances. An example of a chiral phosphine ligand used is (- or +)-2,3-O-isopropylidene-2,3-dihydroxy-1,4-bis(diphenylphosphino)-butane (Figure 1.7) which is usually known as (- or +)-DIOP. An

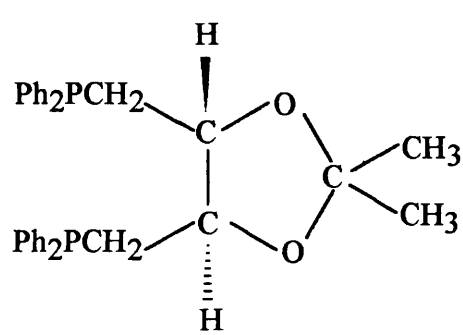

Figure 1.7:- DIOP

example of a chiral compound obtained from asymmetric homogeneous hydrogenation catalyst is L-DOPA (Figure 1.8) used in the treatment of Parkinson's disease. From a

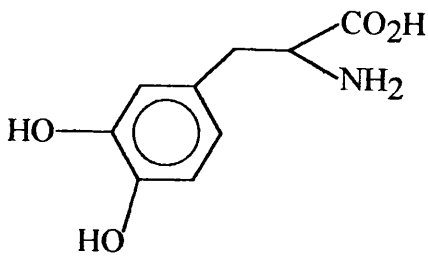

Figure 1.8:- L-DOPA

technical point of view, homogeneous asymmetric catalysts are more difficult to separate from the products and since heterogeneous catalyst are in a different phase from the reactants/products, separation is easier.

The discovery by Wilkinson of that tris(triphenylphosphine)rhodium chloride (Wilkinson's catalyst) was a suitable catalyst for the asymmetric catalytic hydrogenation of prochiral unsaturated substances containing C=C, C=O and C=N bonds, led to a branch of homogeneous catalysis for asymmetric induction. Figure 1.9 shows some of the most successful ligands developed. Early attempts using simple resolved chiral phosphines were not very successful with enantiomeric excesses in the range 3 to 16%. However, the first major development in the use of resolved chiral phosphines was by Kagan and Dang.[19] They demonstrated that the use of a chiral chelating bisphosphine, (-) DIOP, gave good optical yields in the reduction of dehydroamino acid derivatives. A second major development of considerable significance was by Knowles and coworkers,[20] who developed DIPAMP, a chelating biphosphine ligand. The chelation of the Rh catalyst resulted in a 95% optical yield for the catalytic hydrogenation of sterically hindered and multifunction olefins. Such chemistry is now the basis of several large scale processes, the most famous being the Monsato process for the synthesis of L-DOPA. This was first commercialised in the mid 1970's and used a Rh-DIPAMP catalyst, which was highly enantioselective and active for the hydrogenation of the dehydroamino acid required.

In asymmetric hydrogenation using (-)-DIOP-Rh catalysts, the different optical yields obtained for *cis* and *trans* isomers of prochiral olefins, was interpreted to indicate that asymmetric induction takes place during or before the rhodium alkyl formation.[21] Almost all monophosphines were found without exception to be ineffective in asymmetric hydrogenation, and poor optical yields arose from the use of flexible chelate biphosphines.

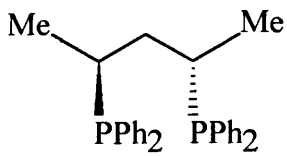

Bosnich 1978

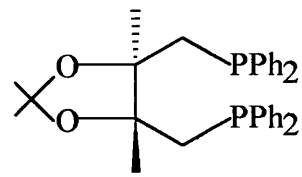

Kagan 1972
DIOP

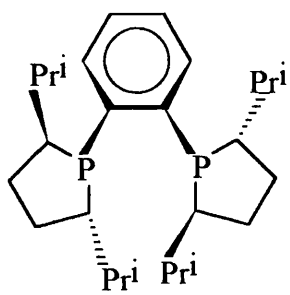

Burke 1990

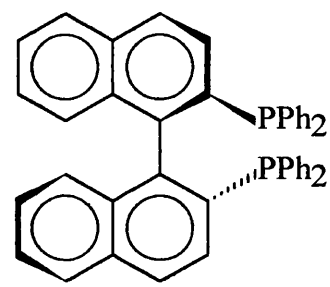

Noyori, Otsuka 1980
BINAP

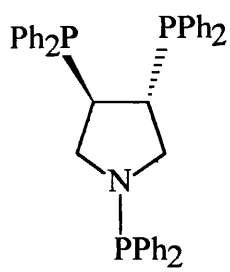

Nagel 1983

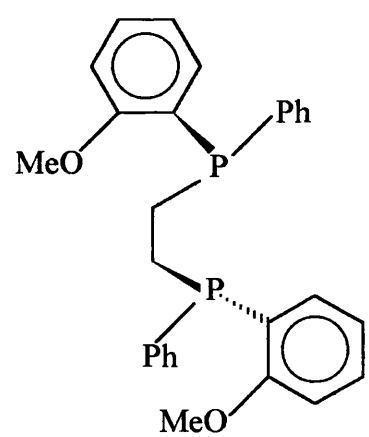

Knowles 1975
DIPAMP

Figure 1.9:- Homogeneous modifiers

X-ray studies were then used to show that the best chiral ligands were those that could maintain conformational rigidity and chirality upon chelation, to achieve a singular catalytic species.[22] It was thus proposed that the ligands of the metal must have been endowed with suitable functionality, configuration and conformational rigidity to achieve an enantioselective catalyst. This led the work to use of (R)-BINAP, a molecule which possessed only axial chirality. The BINAP ligand could accommodate a number of different transition metals, including Rh and Ru, by rotation about the binaphthyl C(1)-C(1') pivot and C(2 or 2')-P bonds without a serious increase in torsional strain.[23] A BINAP-Rh complex was able to enantioselectively hydrogenate prochiral olefins with up to 100% e.e.,[24] but the scope of this catalyst was not very wide. On the other hand, BINAP-Ru was a much more versatile catalyst and was extended to include the hydrogenation of a wide range of carboxylic acids[25] and allylic alcohols,[26] as well as ketonic substrates, such as β-keto-esters[27] with enantiomeric excesses of up to 100% in both cases.

All the reactions described have involved Rh or Ru catalysts. However, in synthetic organic chemistry, the reduction of carbonyl groups by borohydride or aluminohydride reagents is much more common. Chiral catalytic analogues of these species are now emerging and are already becoming very important, for example, trichloromethyl ketones can be hydrogenated with enantiomeric excesses of up to 98% using such catalysts.[27]

Within all these homogeneous catalysts the metal site is a single metal atom, with the ligands relatively strongly complexed around the metal core. The rigid nature of the best chiral ligands results in a steric cleft. The reactant is then attracted to the metal centre through an electrostatic attraction and the orientation of which is directed by the ligands. Chiral discrimination can then occur through steric effects.

The first heterogeneous enantiomeric catalysts used naturally occurring chiral materials as either an auxiliary or as a support. In 1956 Akabori[29] hydrogenated benzylidene oxazolinone with the use of a Pd/silk fibroin catalyst. Isoda[30] also used Pd/silk catalysts. Izumi[31,32,33] in 1959 repeated Akabori's work with different amounts of Pd on the silk and was unable to reproduce enantiomeric excesses up to 66%.[34] Other metals were studied using the silk fibroin as a support, namely, Pt[35,36] and Rh.[37] Platinum and nickel were first modified in 1940 with chiral acids by Nakamura[38] and, at a later date by Izumi.[34] The results of these studies led to the Ni/tartrate/NaBr catalyst which enantioselectively hydrogenates β-ketoesters with optical yields as high as 94%. Lipkin and Stewart[39] in the 1930's first described the other well known enantioselective catalyst, cinchona alkaloid modified Pt catalyst which asymmetrically hydrogenated α-ketoesters and Orito[40,41,42,43] then

examined in detail.

1.2.2 Platinum/cinchona alkaloid system

Since the initial report in 1978 by Orito[40,41,42,43] concerning the enantioselective hydrogenation of α-ketoesters by cinchona alkaloid modified platinum catalyst there has been considerable time and effort spent on this system. Palladium is now used as well as platinum and the range of prochiral starting materials extended from the α-ketoester ethyl pyruvate[44,45,46] to other derivatives. The highest optical yields have been obtained when platinum, not palladium, modified with the cinchona alkaloid, has been used for the hydrogenation of α-ketoesters and derivatives, in fact, the optimum enantiomeric excess was obtained from the hydrogenation of methyl pyruvate and ethyl pyruvate,[47] while lower optical yields were obtained from the derivatives.[48,49,50,51,52,53,54] The enantioselective hydrogenation of methyl- (Figure 1.10) or ethyl pyruvate (Figure 1.11) to methyl- or ethyl lactate has given the most information on the cinchona-modified platinum system and illustrates crucial factors determining the catalytic performance of the system.

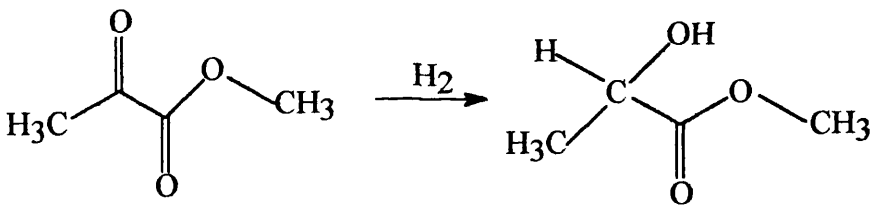

Methyl pyruvate Methyl lactate

Figure 1.10:- Hydrogenation of methyl pyruvate

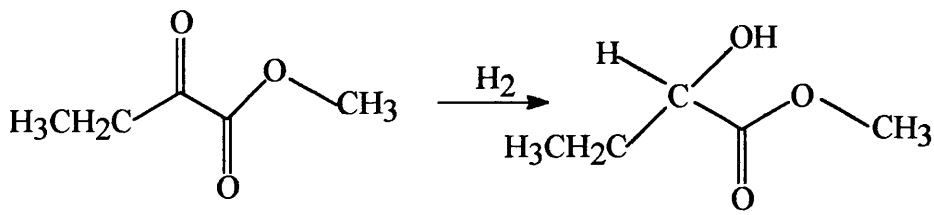

Ethyl pyruvate Ethyl lactate

Figure 1.11:- Hydrogenation of ethyl pyruvate

Figure 1.12 illustrates the main features of the cinchona alkaloid modified metal systems. A range of metals have been studied, platinum[15,40,41,42,43,48,55,56,57,8] was found to be suitable; while palladium,[48,53,54] rhodium[48] and iridium[59] were suitable but to a lesser extent; and Ru and Ni were not suitable.[48] The metals have been studied in supported form using, for example, alumina, silica and carbon supports.[40,41,42,43,48] The cinchona alkaloids which have been most successfully studied are cinchonidine and cinchonine, although derivatives

have also been studied, such as 10,11-dihydrocinchonidine[48] where similar or better enantio-differentiation was obtained.

STEREOCHEMICAL CONTROL

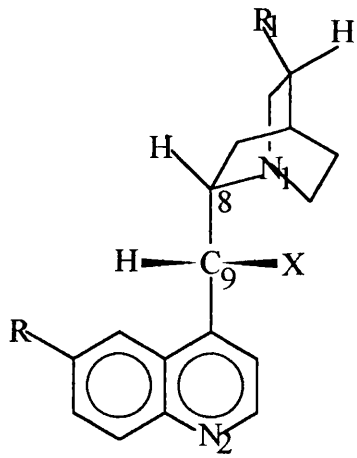

(a)

R = OMe,Quinine
R = H, Cinchonidine
$R_1 = C_2H_3$

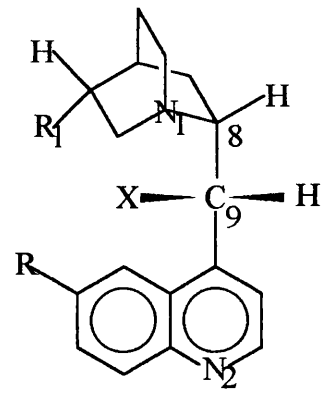

(b)

R = OMe, Quinidine
R = H, Cinchonine
$R_1 = C_2H_3$

ACTIVATING FUNCTION

Metals: Pt, Pd, Rh and Ir
Supports: Alumina, Carbon, Silica

Figure 1.12:- Schematic outline of the main features of the cinchona alkaloid system

Modification of the catalyst by the cinchona-alkaloid is achieved by stirring the metal catalyst in a solution of modifier in air, followed by decantation of the liquid, as described by Orito *et al*[40,41,42,43] or *in situ* addition of the modifier to the reactant mixture.[48,55,56,57] Reactions have been studied at ambient temperature at a range of hydrogen pressure (1-10MPa) where good optical yields are obtained irrespective of the modification procedure.

The enantioselectivity obtained from the hydrogenation of α-ketoesters by the Pt-cinchona alkaloid modified catalyst is dependent on a number of factors which include (a) the modifier, (b) the catalyst properties, (c) the solvents and additives, and (d) the temperature and pressure. The effect of these factors will be outlined below.

The cinchona-alkaloid modifier has the following functional groups: (a) the quinoline ring which has shown to be adsorbed on to the platinum surface via the π bond system,[56] (b) the asymmetric region of C-8, C-9 which determines the chirality of the product, (c) the nucleophilic quinuclidine N-1 which interacts with the reactants, and (d) the double R-1, which is relatively easily hydrogenated under reaction conditions and has no significant influence on the enantio-differentiation of the modifier.

The presence of a chiral modifier not only indices enantioselectivity but also increases the rate of reaction.[48,60,61] The presence of the modifier even in small quantities can show the effect of enantioselectivity and rate enhancement.[61,62,63] The optimal modifier concentration was shown to depend on the solvent, modifier and substrate type.

Blaser *et al*[64] have shown that the structure of the modifier influences the optical yields, for example; if the absolute configuration of C-8, C-9 of the modifier in Figure 1.12 is changed, the resultant chirality of the product changes. This phenomenon was also shown by Orito *et al*,[40,41,42,43] when they compared cinchonidine and cinchonine. Blaser *et al*[64] also showed the result of altering the cinchonidine and cinchonine at various positions and concluded that (1) the alkylation of N-1 led to optical induction being lost, while the protonation of N-1 enhanced the induction;[65] (2) altering X generally led to lower optical yields but the R enantiomer of ethyl lactate was still in excess and when X = OH or OCH_3 high enantioselectivity was observed; (3) lower enantioselectivity was observed with the hydrogenated quinoline nucleus; and (4) the nature of R-1 had little effect on the optical yield: that is the enantio-differentiation of cinchona-modified platinum catalysts are influenced with regard to the modifier structure.

The properties of the catalyst in an enantio-differentiation reaction was also dependent on the particle size of the dispersed metal; the morphology and contaminants stemming from the platinum precursor of reduction agent; size of pores and pretreatment of catalyst before use.

The optical yield increased with increased platinum particle size, that is optical yield is dependent on the dispersion of the metal on the support[55,57] and it was found that the platinum particle sizes had to be at least 3-4nm before good optical yields were obtained. Therefore the reactions are strong structure sensitive.[57] The platinum particles require to be large enough to allow the cinchona alkaloid to be adsorbed via the aromatic ring system, covering an L-shaped platinum surface area which contains 15 platinum atoms, according to Wells[46] but is now not accepted.[66]

Enantio-differentiation is also dependent[57] on the morphology of the platinum particles and contaminants on the support. The morphology and contaminants are

dependent on the platinum salt used to prepare the catalyst and reducing agent employed to obtain the platinum metal from the precursor. The support material can also influence the performance of the catalyst.[40,41,42,43,48]

The sizes of the pores also affects the activity, that is the catalyst with larger pores affords better optical yields.[64]

Orito *et al*[40,41,42,43] showed initially that pretreatment of the catalyst was important, that is, for example, the preheating of the catalyst in hydrogen at 573-673K, followed by soaking in modifier. The high temperature hydrogen pretreatment ensured complete reduction of platinum and removal of contaminants. For Pt/alumina catalyst, exposure to air during modification was shown to be crucial to high enantioselectivity and activity for ethyl pyruvate hydrogenation in ethanol.[58]

Although most of the studies have used ethanol and toluene, other solvents have been used. The polarity of the solvent has strong effects on the optical yields and the initial rates of ethyl pyruvate hydrogenation.[47,56,67] For example, (a) the rate and optical yield decreases with increasing polarity of the solvent; (b) good results are obtained with apolar solvents; (c) alcohols and acids allow high optical yields, but a solvent interaction is detected with the modifier or reactant;[66] and (d) although acidic solvents give high enantiomeric excesses, basic solvents give low optical activity. Acetic acid has been shown to give the highest optical yield, that is 95%. The presence of amines or weak acids as additives influence the enantioselectivity.[47,48]

A temperature range from ambient to 323K[48,58] has been shown to suitable and it has been reported that, as temperature increases, enantioselectivity drops. Hydrogenation pressure, at 1MPa, was found to be sufficient but beyond 7MPa the results of increased pressure showed an acceleration of the reaction rate and the enantioselectivity increased slightly.

A reaction pathway[62] has been proposed which can account for the enantiomeric hydrogenation of ethyl- and methyl pyruvate. Figure 1.13 outlines a two reaction cycle where the occurrence of an enantioselective reaction on the modified platinum surface with intrinsic selectivity, S, is observed and the racemic reaction on the unmodified platinum sites with the formation of racemic products. It has been proposed that the chiral active sites for the enantioselective hydrogenation are formed by the reversible adsorption of cinchona molecules on the platinum surface.

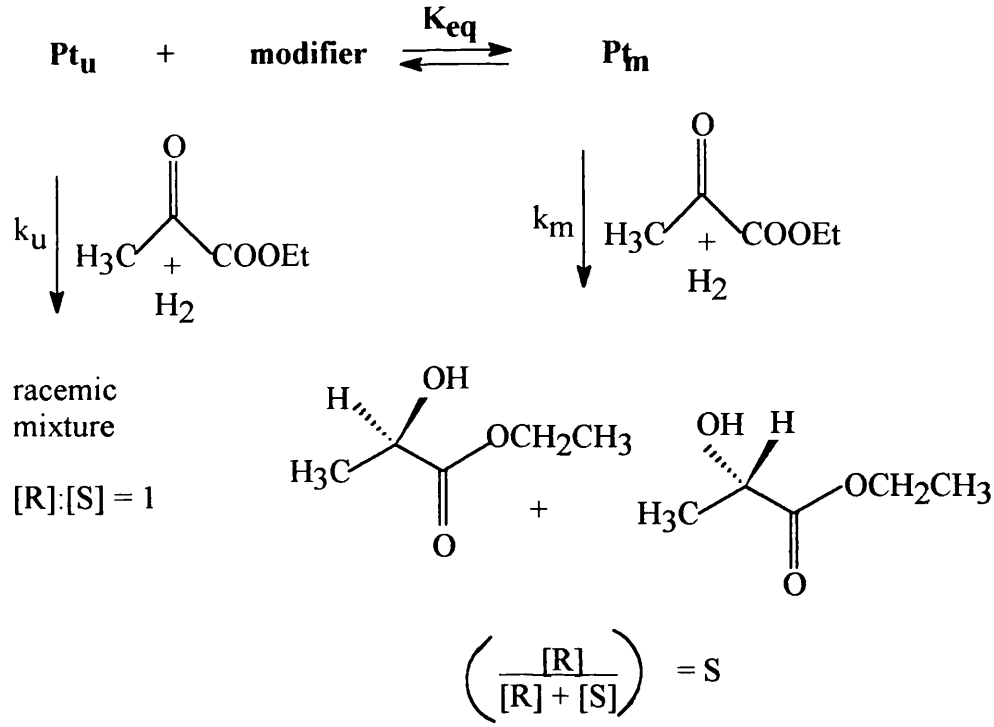

Figure 1.13:- Schematic outline of the two reaction pathway proposed for enantioselectivity

The pathways help to explain the enhanced rate as described by Blaser *et al.*[62,68] As shown by Figure 1.13, the model is based on a two-cycle mechanism, as predicted for ligand accelerated reaction,[69,70] where a slow unselective (unmodified catalyst) and a fast enantioselective reaction cycle are assumed to be in equilibrium. The modified platinum sites (Pt_m) are chirally active sites as a result of the reversible adsorption of the cinchona molecules. The enhanced rate of reaction is the combination of the chiral active sites and the hydrogen consumption rate; which is considered to be the sum of the enantioselective hydrogenation on Pt_m and racemic hydrogenation taking place on unmodified sites (Pt_u). For both the unselective and enantioselective hydrogenation of ethyl pyruvate (*ca* 3M) over Pt/alumina[56] and Pt/silica,[58] orders of approximately zero were observed with respect to ethyl pyruvate and first with respect to hydrogen.[15,56]

Two models have been proposed for the enantio-differentiation in the pyruvate hydrogenation over cinchona modified platinum catalyst, namely, the "template model" and the "1:1 interaction" between reactant and modifier.

The template model was proposed by Wells and coworkers[15,71] and depended upon the adsorption of the L-shaped cinchona alkaloid on to the metal surface of supported platinum. The supported platinum surface became chiral due to the formation of an ordered

non-closed packed array, leaving exposed ensembles of platinum atoms (the active sites) at which configurational selection occurred when the methyl pyruvate was adsorbed.

This model was shown not to be suitable to explain the enantio-differentiation, for example, because no evidence could be obtained for the ordered array of cinchona molecules on the platinum surface. A new model has now been proposed which can explain the induction of enantioselectivity and is explained by the presence of second type of sites at the edges of the platinum crystallites. These sites exhibit a 1:1 spatial relationship of the modifier and reactant.

Further studies[72,73] have shown that a 1:1 interaction of the modifier and reactant is crucial for enantio-differentiation. The '1:1 interaction' models differ from the template model in the way the modifier is adsorbed on to the platinum surface and the structure of the adduct formed upon interaction of the pyruvate with the modifier.

Augustine *et al*[72] proposed a model which relied upon the N-1 being adjacent to the hydroxyl group (in N_1-C_8-C_9-O position, Figure 1.12) to enable the formation of a "six-membered ring interaction" between the quinuclidine N-1 and the keto carbon as well as the C-9 oxygen and the ester carbon atoms. The assumption of the rigid six membered ring is not plausible because then the same importance would then have to be given to the N-1 and to the oxygen at C-9 during the interaction of pyruvate and cinchonidine. But experimental evidence has shown that the rigid six membered ring idea is not supported because the substitution of OH by OCH_3 has led to the best enantiomeric excess recorded.[64]

Theoretical studies using quantum chemistry techniques[73,74,75] have also been used to rationalise the 1:1 interaction. These studies were based on the experimental evidence that the quinuclidine nitrogen (N-1, Figure 1.12) plays an important role in the enantio-differentiation.[64] Calculations carried out in protic solvents (NH_3, NH_4^+, etc) showed that the cinchonidine could be protonated and that the protonated species will interact with the pyruvate. The cinchonidine favoured the formation of the R-lactate, while the cinchonine favoured the S-lactate.

Although the molecular modelling approach took into account the interaction of the pyruvate and the cinchona alkaloid and also the steric constraints imposed by the adsorption on to the platinum surface. In general, the 1:1 interaction does give a reasonable explanation for the enantio-differentiation of the system, it does not, however, take into account solvents of the system, mode of adsorption and conformation of adsorption of the modifier, interaction of modifier and substrate with the solvent and platinum surface or the mechanism of hydrogen transfer.

1.2.3 Nickel/tartaric acid system

The modification of nickel catalysts have developed over many years following the initial work by Nakamura[38] in the 1940's and later by Izumi.[34] Figure 1.14 shows the various substrates that have been successfully enantioselectively hydrogenated by the tartrate modified nickel catalysts. The highest optical yields having been obtained for β-ketoesters[76] and β-diketones.[76] Most investigations have been carried out with methyl acetoacetate (MAA) as the substrate. Due to substrate specificity of these catalysts, caution has to be taken when making generalisations.

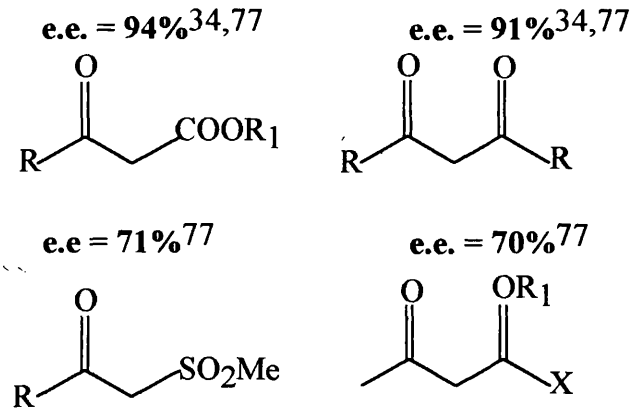

R, R_1 = alkyl
X = H, OMe

Figure 1.14:- Substrates successfully enantiomerically hydrogenated by nickel modified catalysts

Many factors influence the catalytic performance, each of which may be summarised as follows:

Tartaric acid is superior to α-amino acids and other α-hydroxy acids under optimum reaction conditions as a modifier for nickel catalysts.[34,77] Experimental observations have shown that the two carboxyl groups and at least one of the OH groups are necessary to create an effective modifier (Figure 1.15).[34,77,78] Keane and Webb[79] have shown, recently, that better enantioselectivities can be achieved for Ni/silica catalysts modified with L-alanine than tartaric acid for the hydrogenation of methyl acetoacetate.

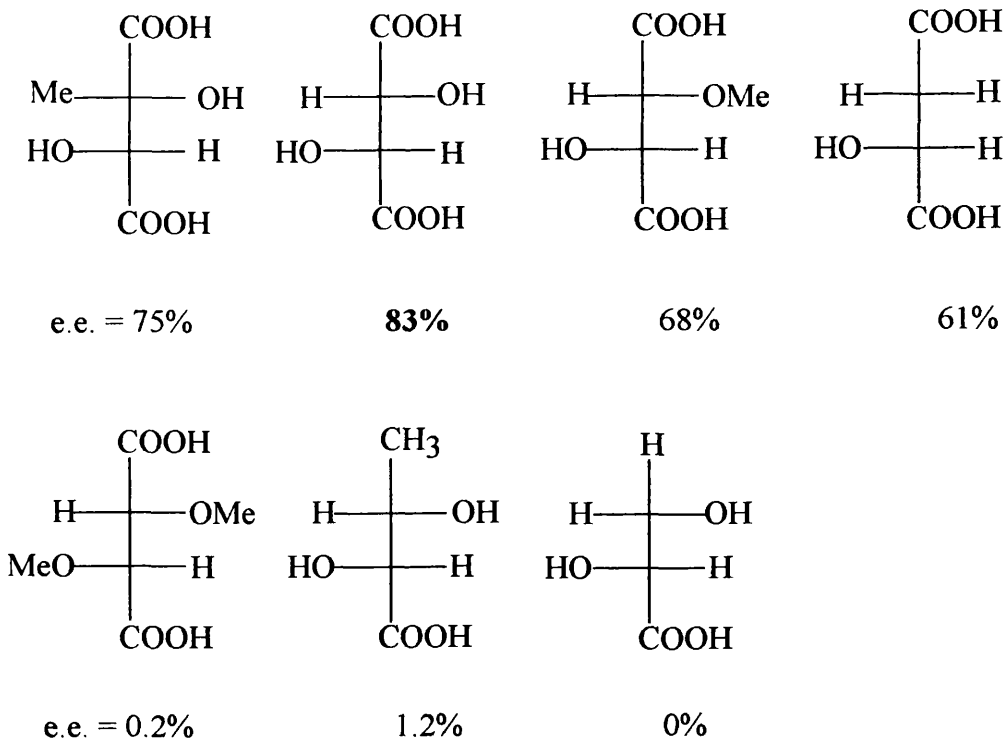

Figure 1.15:- Effective nickel catalyst modifiers

The preferred catalyst for these studies has been Raney nickel although other nickel catalysts have been used, such as Ni-powder[34,77,80] or supported nickel catalysts.[34,46,77] Bimetallic and noble metal catalysts have been studied but with the exception of NiPd/silica catalysts these give low enantiomeric excess.[81]

Best results have been obtained from freshly prepared Raney nickel, although nickel catalysts prepared from other methods (nickel-salt, impregnation, reduction procedure) has been shown to be important.[34,77,82] Tai and Harada[76] investigated ultrasonicated Raney nickel and found this to be the most selective (enantiomeric excesses up to 94%) and active catalyst for β-ketoesters and β-diketones hydrogenation.

Raney type catalysts are difficult to characterise and control structural features. Since the modification step is corrosive the nature of the nickel surface is strongly changed. Nitta *et al*[83,84,85,86] have shown for supported nickel catalysts, the dispersion of the metal influences the enantioselectivity. Sachtler *et al*[87] showed that the enantiomeric excesses are not affected by the crystallite size, if the nickel dispersion was changed by Ostwald ripening. The optimal nickel particle size was estimated to be 10-20nm. Although there has been no general valid correlation between enantioselectivity and any catalyst parameter.[34,77]

During the modification procedure of a nickel catalyst, which involves a separate step of placing the catalyst into an aqueous medium, nickel is leached into solution.[79,82,88,89,90] Catalyst performance of a good catalyst is crucial upon modifier concentration, pH, temperature, time and procedure.[34,77] Conditions must be optimized for each type of catalyst. Co-modifiers can enhance the optical yield, for example, NaBr can enhance optical yield by 10-30% and others have been studied.[34,77] Keane and Webb[79,82,88,9,90] have described in detail the affect of the modification procedure on the catalytic properties of nickel/silica catalysts modified with tartaric acid and amino acids.

A serious problem encountered is the corrosion of the catalyst by the acid modifiers. Embedding of the modified catalyst in a silicone polymer or treatment with an amine enhances the catalyst stability and allows re-use.[34,91,92]

Aprotic semipolar solvents give the highest enantiomeric excesses,[34] especially methyl propionate, but other trends have been reported.[93] The sequence: n-alcohols > methyl propionate ~ ethyl acetate >> THF >> toluene ~ acetonitrile is given by Webb.[94] The addition of weak acids have shown to increase the enantiomeric excess.[93] Addition of water is detrimental.[34,77]

Good results have been obtained for studies at temperatures between 333-373K and the dihydrogen pressures between 80-120 bar. No simple correlation between enantiomeric excess and pressure or temperature can be made.[34,77] Webb reported that pressures in excess of 90 bar gave optical yields in excess of 80%.[94] The reaction can also be carried out in the gas phase but optical yields are found to be lower.[95]

A range of techniques, namely, IR, UV, XPS, EM, electron diffraction and electrochemical studies have been used to study the adsorption of both the modifier and substrate on the nickel catalyst.[34,77] Other investigations have shown the effect of pH on the amount of adsorbed tartrate and methyl acetoacetate[88,89,94] that there is a corrosive effect on the nickel surface under optimum modification conditions. It is generally accepted that the tartaric acid molecule is chemically bonded to the nickel via the two carbonyl groups. During the hydrogenation (which is carried out in an organic solvent), all groups agreed that the adsorbed tartrate does not leave the surface. Two thoughts have been proposed as to the exact nature of the modified catalyst: Sachtler[95] suggests that the adsorbed nickel tartrate is the chiral active site; and the Japanese[34,77] suggested direct adsorption of the tartrate on modified sites on the nickel surface. Gas phase hydrogenation of methyl acetoacetate has shown the methyl acetoacetate to be adsorbed on to the catalyst as the enolate and there are indications that the adsorption of the substrate is stronger if the catalyst is modified.[95]

Kinetic studies have been undertaken in the liquid[34,77] and the gas phase.[95] The reaction was observed to be first order with respect to the catalyst, whilst the order in dihydrogen ranged from 0 to 0.2 in the gas phase and from 0 to 1 in the liquid phase, and that for methyl acetoacetate in the gas phase was 0.4 to 1 and 0.2 to 0.8 in the liquid phase.

Izumi's group[34,77] proposed a mechanism for the enantioselective hydrogenation based on a classical Langmuir-Hinshelwood approach. That is the adsorbed substrates reacts with activated hydrogen on the nickel surface in a stepwise fashion. The orientation of the adsorbed β-ketoester was controlled by the tartrate via hydrogen bonding. Experimental results suggest that the enantio-differentiation is determined in the adsorption step of the ketoester, not the addition of the hydrogen, although there is no structural evidence. The NaBr co-modifier blocks out unmodified sites and, since the ratio of unmodified to modified sites determines the optical yield, the optical yield increases.[34,77] The ultra-sound treatment is also claimed to block unmodified sites.

Sachtler[95] proposed a mechanism where hydrogen dissociation occurs on the nickel surface and migrates to the substrate which is coordinated to the adsorbed dimeric nickel-tartrate species.

1.3 THE CATALYSTS

1.3.1 Support materials

For a long time it has been recognised that the best heterogeneous catalysts for hydrogenation reactions are those of Group VIII metals.[7] These metals are very expensive and, as catalysts, are used mostly on support materials. A support can hopefully optimise the activity of the catalyst by dispersing the metal, such as platinum, to ensure its most effective use and improving the mechanical strength of an inherently weak catalyst. The activity of a metal depends on factors such as surface area, porosity, geometry of the surface, and resistance to sintering of small metal particles. The support, however, can sometimes contribute towards the catalytic activity. For example, it is generally accepted that, as shown by Weisz[96,97] among others in catalytic reforming the catalysts act through a bifunctional mechanism, that is the dehydrogenation of saturated hydrocarbons takes place on the metallic function (usually platinum) while isomerisation takes place on the acidic support (usually alumina).

Among of the main reasons a support is employed in catalysts are the following:

1. Economic
   (a) the cost of an expensive catalyst (for example platinum) is reduced by increasing its lifetime

2. Mechanical
   (a) mechanical strength introduced
   (b) bulk density optimised
   (c) provides a heat sink or source
   (d) overactive phases diluted
3. Geometric
   (a) surface area of catalysts increased
   (b) porosity of catalysts optimised
   (c) crystal and particle sizes optimised
   (d) particles allowed to adopt the most favourable configurations
4. Chemical
   (a) specific activity improved and the sintering of the catalyst minimized
   (b) accept or donate chemical entities
5. Deactivation
   (a) catalyst is stabilised against sintering
   (b) minimises poisoning

Obviously no support can exhibit all these properties. Typical supports include silica-alumina, carbon black, titania, zinc oxide, natural clays, alumina, magnesia, activated carbon, silica, and asbestos. In this study the supports used are γ-alumina and silica (Cab-O-Sil and Grace Cariact 10 (C10)).

1.3.2 Silica

Pure silica occurs in two forms, quartz and cristobalite. The silicon is always tetrahedrally bound to four oxygen atoms but the bonds have considerable ionic character. In cristobalite the silicon atoms are placed as are the carbon atoms in diamond,with the oxygen atoms midway between each pair. In quartz, there are helices so that enantiomorphic crystals[98] are possible.

The other three silica are of commercial interest in catalyst preparation. The preparation of the commercial silica are dependent on temperature, pressure, pH, manufacturing process, ageing process, etc.

Colloidal silica — Colloidal silica available to industry can contain up to 40 wt % of spherical, non-porous particles of SiO_2. The colloid is stabilized by ammonium or sodium ions.

Flamed silica — A finely divided non-porous and highly pure silica powder (Cab-O-Sil, Aerosil) is manufactured by flame hydrolysis of $SiCl_4$. Particle size are about 40-50nm.

Silica gels

These consist of three dimensional networks of contiguous particles of colloidal silica. Silica gels usually have a high surface area, as high as about $700m^2g^{-1}$. The average pore diameter is, correspondingly, very low, typically in the range of 2.5-4nm. Although silica gel supports have been created where the pore diameter is approximately 10nm (Grace Cariact 10 (C10)) and are of bead type and contain 99.8%+ silica, and are chemically very stable.[99]

Silica is relatively unreactive towards Cl_2, H_2, acids and most metals at 298K and even at slightly elevated temperatures, but is attacked by F_2, aqueous HF, alkali hydroxides and fused carbonates.[100]

Flamed silica has been shown by Parry,[101] in the case of the Cab-O-Sil, to contain no Brønsted acid or Lewis acid sites on the surface and Vortz *et al*[102] have shown that no proton acidity occurs. On the other hand silica gels have been shown to have a weakly acidic surface due to the surface silanol groups. The silanol groups present are those shown by (a), (b) and (c) in Figure 1.16. The surface of the silica gel consists of physically adsorbed water as well as the silanol groups. Heating of the silica in air at 400-500K removes the physically adsorbed water and causes two of the isolated hydroxyl silanol groups (Figure 1.16a) to condense together to form siloxane bridges (Figure 1.16d).

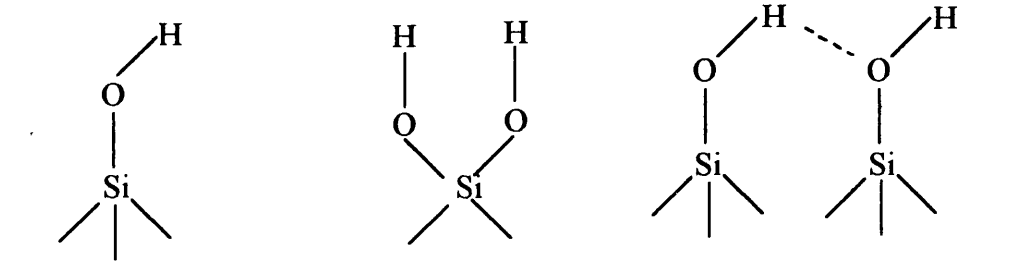

(a) isolated hydroxyl (b) vicinal hydroxyl (c) hydroxylated surface

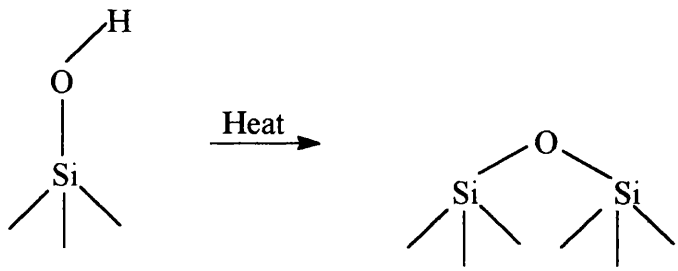

(d) siloxane formation

Figure 1.16:- Surface silanol groups of silica gel

1.3.3 γ-Alumina

A large variety of alumina exist and are generally prepared by the dehydration of various aluminum hydroxides. Figure 1.17 outlines the formation of the different alumina.[103,104]

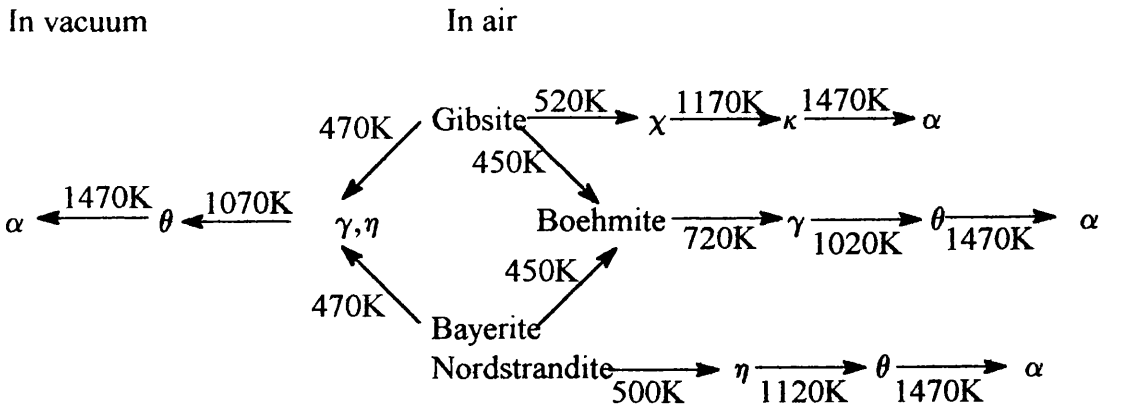

Figure 1.17:- Schematic outline for alumina formation from aluminum hydroxides

The most important alumina used as carriers or supports in catalysis are α-alumina, γ-alumina and η-alumina. Both γ- and η-alumina are important because of their high areas and stability over the range of temperatures at which catalytic reactions are carried out. Although both the γ- and η-alumina forms have defect spinel structures,[103,104,105] the η-form is more distorted than the γ-form and the η-form is more acidic than the γ-form.

The acidic sites found in γ-alumina are composed of both Brønsted acid and Lewis acid sites. The Lewis acid sites are stronger than the Brønsted acid sites.[106] A Lewis acid is defined as an acid which is an electron pair acceptor, that is the site has a vacant coordination site to form a new bond with a Lewis base (an electron pair). A Brønsted acid is an acid which is a proton donor. In general the surface area of γ-alumina is 150 - 250m^2g^{-1}, with pores with diameters 1-10nm.

1.3.4 Catalyst sintering

Sintering is a well known phenomenon in metallurgy and ceramic science, although the sintering of supported metal crystallites (catalysts) is complicated and in most cases results in catalyst deactivation. The sintering of supported catalyst is more complicated than that for pure metals because supported catalysts have extremely small crystallites, porous supports, and are used in systems which have reactive atmospheres and use relatively low temperatures.[107] Sintering is primarily a thermal process of pore collapse and crystallite growth. However, the process of interest is crystal growth. The main result of

sintering is the loss of activity as the surface area and, therefore, the number of active sites is reduced.[108] There are at least two accepted mechanisms of crystallite growth.

The first is known as crystallite migration as shown in Figure 1.18. Crystallite migration involves the movement of small crystallites which have a large fraction of the surface, at low temperature, than the bulk. Shape displacement then results which leads to a statistical number of movements. The migration depends upon the following parameters; temperature, crystallite size, surface wetting and support substrate interaction.

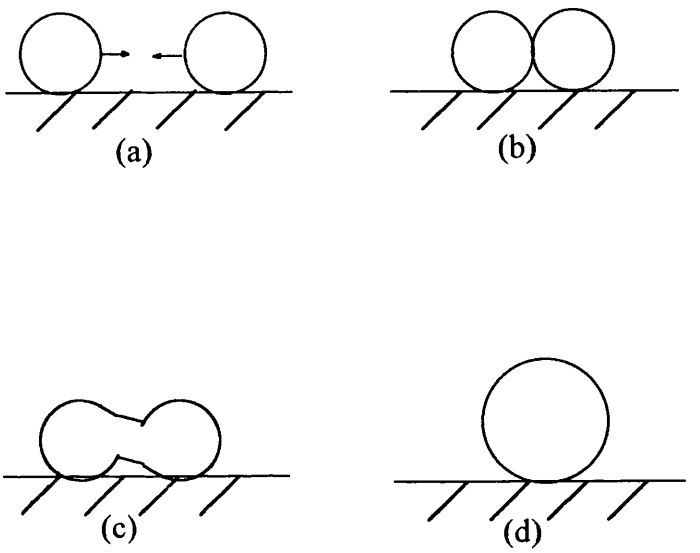

Figure 1.18:- Crystallite migration

The second mechanism, shown by Figure 1.19, involves inter-particle transfer of atoms from small to large crystallites. The driving force being the larger free energy of the small crystallites, which increase vapour pressure and evaporation, with condensation occurring on larger crystallites.

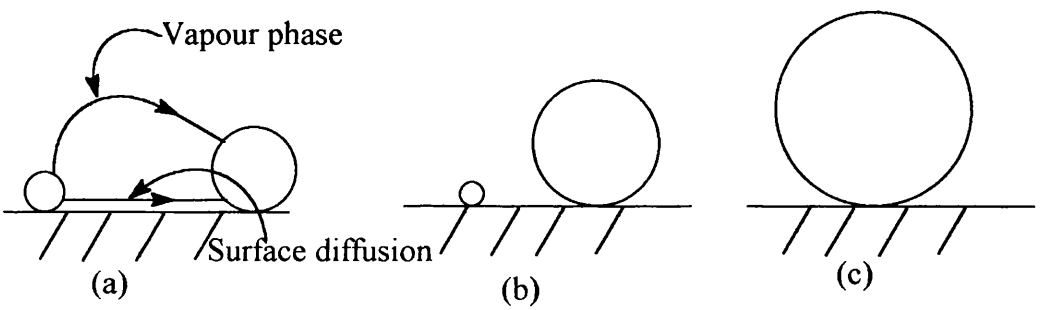

Figure 1.19:- Inter particle transfer

The migration and collision of crystallites give rise to particles which become substantially immobile and the size of these particles is limited, as in the case of Pt/alumina, the limiting crystallite diameter appears to be about 5nm.[109]

Sintering of the platinum group metals has been shown to occur in an oxidising, reducing or inert atmosphere. Although the mechanism in the oxidising atmosphere is much different to that in a reducing or inert atmosphere, due to the formation of slightly volatile oxides which may diffuse along the surface of the support or through the vapour from higher-energy sites to lower-energy sites. Sintering of platinum group metals in oxygen is markedly different from that in hydrogen due to the higher temperatures required to vapourise the metal atoms in the reducing atmosphere compared to the lower temperatures required to vapourise the oxides.

1.4 CATALYST CHARACTERISATION

Among the techniques available, the following are used to characterise the catalysts.

1.4.1 Ultra violet-visible spectroscopy

Chemical spectroscopy can be defined as the study of the interaction of electromagnetic radiation with chemical species, particularly the variation of absorption or emission with wavelength or frequency, and the deduction of chemical information about the species being emitted.

The characterisation of an absorption or emission spectrum includes a specification of some or all of the following:

1. the region of the electromagnetic spectrum involved and hence the type of energy changes occurring (for example; Ultra-violet absorption (electronic energy), infra-red absorption (vibrational energy)).
2. the number and position of the major lines or bands.
3. the absolute or relative intensity of each line or band.
4. the nature and character of any fine structure.

Ultra-violet and visible (UV-VIS) spectroscopy ranges from wavelength 100nm to 800nm where the visible ranges, sensitive to the human eye, corresponds to the wavelengths 400 to 800nm and the ultra-violet range corresponds to the wavelengths 100 to 400nm.[110]

As well as giving details of the electronic structure of supported catalyst precursors, UV-VIS gives information on the elemental analysis, crystal defects and local structure.

In solid state chemistry UV-VIS, photons of visible and ultra-violet light are directed to the sample and when they strike the electrons in the atoms in the platinum precursors cause shifts of electrons from one region to another. In the process some

photons are absorbed.

Various types of electronic transitions occur and may be detected[111] as shown in Figure 1.20. The two atoms A and B are neighbouring atoms in some kind of solid structure; they may be, for instance, an anion and a cation in an ionic crystal. The inner electron shells are localised on the individual atoms. The outermost shells may overlap to form delocalised bands of energy levels. Four basic types of transitions are indicated by Figure 1.20.:

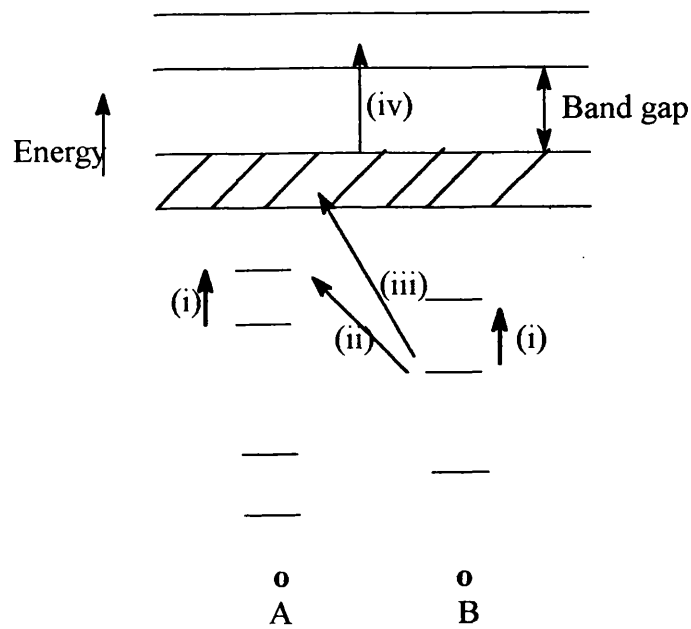

Figure 1.20:- Possible electronic transitions in a solid. These involve electrons in localised and delocalised bands

(i) Promotion of an electron from a localised orbital on one atom to a higher energy level but still localised orbital on the same atom. The spectroscopic absorption bands associated with this transition is sometimes known as an exciton band. Transitions in category (i) include (a) d-d and f-f transitions in transition metal compounds, (b) outer shell transitions in heavy metal compounds, (c) transitions associated with defects such as trapped electrons or holes, and (d) transitions involving, for example, silver atoms in photochromic glasses.

(ii) Promotion of an electron from a localised orbital on one atom to higher energy but still localised orbital on an adjacent atom. The associated absorption bands are known as charge transfer spectra. The transitions are usually "allowed transitions" according to the spectroscopic selection rules and hence the absorption bands are

intense. Charge transfer processes are, for example, responsible for the intense yellow colour of chromates; an electron is transferred from the oxygen atom in a $[CrO_4]^{2-}$ tetrahedral complex anion to the central chromium atom.

(iii) Promotion of an electron from a localised orbital on one atom to a delocalised energy band, the conduction band, which is characteristic of the entire solid.

(iv) promotion of an electron from one energy band (the valence band) to another band of higher energy (the conduction band).

The appearance of a typical UV-VIS absorption spectrum is shown schematically in Figure 1.21. It contains two principle features. Above a certain energy or frequency, intense absorption occurs - type (ii) and (iii). the second feature is the appearance of a broad absorption peaks or bands at frequencies below that of the absorption cut off - type (i).

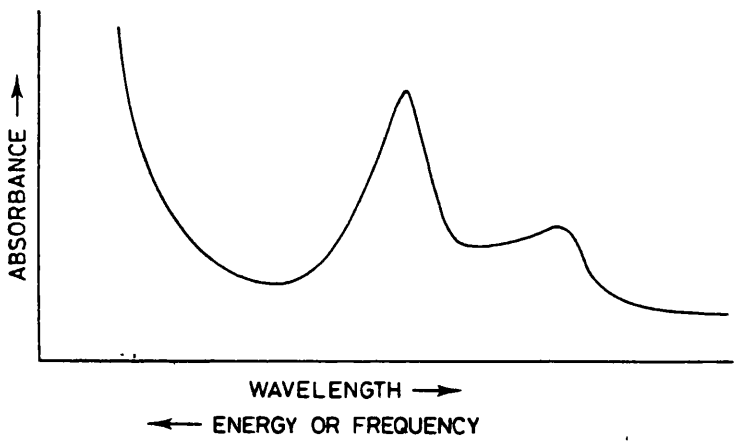

Figure 1.21:- Schematic outline of typical UV-VIS spectrum

The type of analyser required when solids are studied by UV-VIS spectrophotometers is a diffuse reflectance device. Diffuse reflectance is a particular type of reflectance from which the absorbance of a material can be determined. Reflectance, in general, can be represented by Figure 1.22.

Transmittance

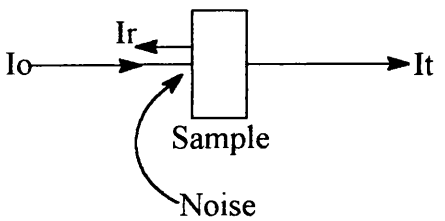

Surface reflectance accounts for approximately 4% and this is compensated for with the use of a blank

$$A = \log\left(\frac{Io}{It}\right) \quad \text{or} \quad A = \log\left(\frac{T1}{T2}\right) \begin{matrix}\text{Blank}\\ \text{Sample}\end{matrix}$$

Figure 1.22:-Schematic outline of reflectance, in general

1.4.2 Temperature Programmed Reduction

Temperature programmed reduction (TPR) is a technique used in the chemical characterisation of solids. The technique involves the reaction of a solid by a gas, as the temperature of the system is changed in a predetermined way. Analysis of the gaseous products provides chemical information about the solid.

In general, the solid is reduced by flowing dihydrogen, the concentration of which is monitored on existing the reactor. Assuming that the reduction has taken place over the temperature range of the reactor, the analysis record is simply the dihydrogen consumption and is displayed as a function of temperature of the reactor.

Figure 1.23 shows a typical reduction profile. Each peak represents a distinct reduction process of a particular component of the solid. The chemical nature and the environment of the chemical component can be determined from the position and size of the peak, the concentration of a component present in the solid being reflected by the peak area.

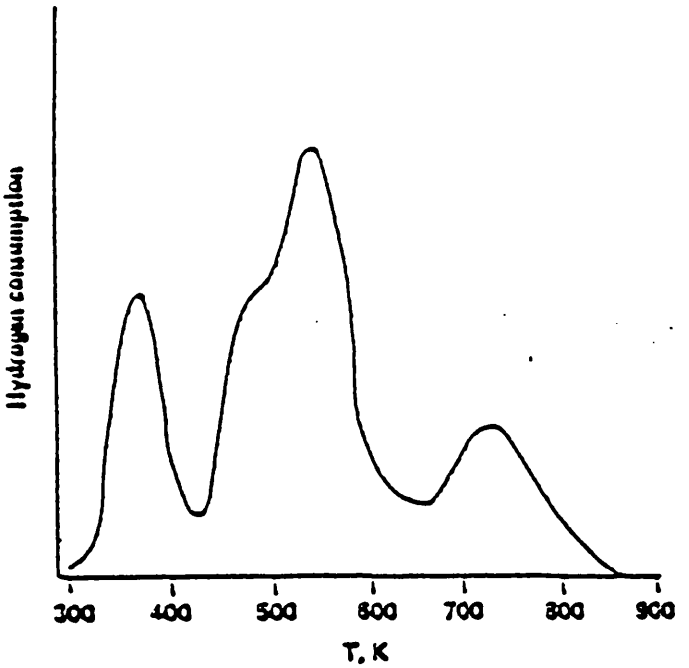

Figure 1.23:- Typical reduction profile

Although TPR is a relatively new technique for the characterisation of solids, it is highly sensitive and the only requirement of the technique is that the solid is reproducible. The technique was first investigated by Jenkins[112] and has been exploited till it was recognised as a characterisation technique for solids.[113,114]

On the basis of the type of information TPR can provide, the technique can be classified with spectroscopic techniques that have been traditionally and currently used to characterise solids. TPR does not impose such severe requirements on the solid or on the investigation conditions as other characterisation techniques tend to do, therefore the information obtained from TPR is not limited.

The profiles, "fingerprints", obtained from TPR of a complex solid shows in great detail the reduction processes of the complex, providing rapid assessment of the correctness of the composition of the solid.

As a result of the sensitivity of TPR and the fact that it does not impose constraints, except reducibility, this technique is a very suitable method to characterise supported metal catalysts. Difficulty usually arises from the other characterisation techniques because of the very high metal dispersions and low concentration of active component in the heterogeneous catalyst.

For the Pt/silica catalyst system, Jenkins *et al*[115] have shown that the preparation of a supported metal catalyst affects the TPR profile. Usually, Pt/silica catalysts prepared by an ion exchange method led to better dispersions of the platinum upon reduction,

because the hydroxyl groups of silica are exchanged during the catalyst preparation and so a true chemical interaction exists between the platinum species and the support. Jenkins *et al*[115] prepared their ion-exchange catalyst using $[Pt(NH_3)_4](OH)_2$ and an impregnated catalyst using H_2PtCl_6.

The TPR profiles obtained for the ion-exchange catalyst and the impregnated catalyst were quite different. The reduction to the platinum metal for the ion-exchanged catalyst occurred at a higher temperature than for the unsupported $[Pt(NH_3)_4](OH)_2$ as a result of the interaction with the silica support. The dihydrogen consumption corresponded to a two-electron reduction. The impregnated catalyst, however, showed a different temperature maxima and had a dihydrogen consumption which corresponded to a four-electron reduction. Jenkins *et al*[115] showed three peaks; the low temperature peak (~350K) corresponding to unsupported bulk $PtCl_4$ and H_2PtCl_6 still present after the drying step.

1.4.3 Chemisorption

Chemisorption is another physical characterisation technique which can be applied to heterogeneous catalysts. This technique enables the surface area of the metallic phase of a supported catalyst to be determined, since the surface area determines the effectiveness of the catalyst. Chemisorption is a simple and cheap method which relies upon the selective adsorption of gases. Molecules such as dihydrogen, dioxygen and carbon monoxide chemisorb selectively on the metal at room temperature, allowing a volumetric measurement of the monolayer to be determined and so count the number of adsorption sites. The ratio of the adsorbed molecules to surface atoms has to be determined, in the case of dioxygen, the ratio is usually taken to be one O atom per metal surface atom. The gases can be adsorbed either dissociatively or associatively, for example hydrogen atoms adsorb on to surface nickel atoms dissociatively[7] from dihydrogen, while carbon monoxide adsorbs associatively as the CO molecule.

The dispersion of metal on the surface can be calculated from the total metal content. Dispersion, D, can be defined as the active fraction of the catalyst, by Equation 1.1.

$$D = \frac{N_S}{N_{tot}} \qquad \text{Eqn 1.1}$$

Where N_s is the number of the active atoms exposed at the surface as calculated from chemisorption experiments and N_{tot} is the total number of potentially active atoms present in the catalyst as is determined by bulk chemical analysis.[116]

From the dispersion figures of a catalyst, assuming the shape of the metal particle,

the size of the particles can be determined and the surface area of the catalyst calculated. However, before any of these calculations can be made, it is necessary to produce a clean surface for the chemisorption of the gas.

1.4.4 Transmission electron microscopy

Examination of solids is usually done under magnification and this requires a polarising or electron microscope depending on the particle sizes being studied. Particle sizes of submicrometre require electron microscopy which can measure diameters as small as nanometres. Electron microscopy use two types of instrument in that the sample can viewed in transmission (that is, a beam of light or electrons passes through the sample) or in reflection (that is, a beam of light or electrons is reflected off the sample).[110]

Electron microscopy is an extremely versatile technique capable of providing structural information over a wide range of magnifications.

The particle sizes obtained from transmission electron microscopy (TEM) are a true reflection of the range of particle sizes. The particle size can be related to the dispersion value of the metal as obtained from chemisorption, although dispersion figures are based on an average size of metal particles.

CHAPTER 2

OBJECTIVES

2 OBJECTIVES

The importance in the pharmaceutical and fine chemical industries in the manufacture of optically pure chemicals using cleaner technology has increased over the past decade. Heterogeneous catalysis has the advantage over homogeneous and enzymatic catalysis, in that the catalysts are more robust and separation of the product from the catalyst is straight forward. Since the surfaces of heterogeneous catalysts possess no inherent chiral quality, hydrogenation of a prochiral material results in the formation of a racemic mixture. Modification of heterogeneous catalyst by the adsorption of a chiral substance on to the active catalyst surface has been shown to induce enantioselectivity.

The main objective of the work described in this thesis was to attempt to establish a general framework for the generation of chiral centres on heterogeneous catalytic surfaces and, using the principles, thus established, to develop new chirally modified catalyst systems and new heterogeneously catalysed chiral hydrogenation reactions. This work forms part of a large project embracing alumina-, silica- and carbon-supported nickel, palladium and platinum catalysts, specially involving the modification , by irreversible adsorption of chiral modifier molecules, and use of alumina- and silica-supported platinum catalysts.

The adsorption studies are based mainly upon the substituted binaphthalenes: (±), R and S 2,2'-dihydroxy-1,1'-binaphthalene; (±), R and S 2,2'-diamino-1,1'-binaphthalene; (±) 2,2'-dimethoxy-1,1'-binaphthalene, and (-) 2,2',7,7'-tetrahydroxy-1,1'-binaphthalene (Appendix 1). The adsorption studies were undertaken to:

(1) examine the extent of adsorption of the modifier.

(2) determine the type of adsorption.

(3) determine the mode of adsorption.

(4) study the potential of the modified catalysts for asymmetric hydrogenation reactions with respect to the R and S enantiomers.

These modifiers were chosen to extend the asymmetric work being carried out with homogeneous catalysts where binaphthalene substituted molecules are used as ligands to create chiral Rh complexes. Another modifier which had increased aromaticity was also examined, R-(-)-1-(9-anthryl)-2,2,2-trifluoroethanol (Appendix 1).

The use of macrocyclic ligands in homogeneous catalysis systems was extended to the heterogeneous catalyst system where it was hoped that chiral centres would be generated using macrocyclic ligands. The macrocyclic ligands were to be used as modifiers in the generation of chiral surfaces by the irreversible adsorption of chiral substances. The studies of the (S,S)-di-(2-propyl)-6,12-dioxa-2,5,13,16-tetraoxo-3,15,19-triazabicyclo

[15.3.1]heneicosa-1(21),17,19-trieneand(S,S)-di-(2-propyl)-6,13-dioxa-2,5,14,17-tetraoxo-3,16,20-triazabicyclo [16.3.1] docosa-1(22),18,20-triene macrocyles (Appendix 2) were undertaken to:

(1) examine the extent of adsorption of the macrocycle.

(2) determine the type of adsorption.

(3) to determine the mode of adsorption.

(4) to study the potential of the modified catalysts for asymmetric hydrogenation reactions.

The potential of the binaphthalene based and macrocyclic modified supported Pt catalysts as well as the modification of the catalysts with modified with PhGly, PhAla, Pseudo, Trp, His, DMPEA and MTFMPAA (Appendix 3) which were chosen for their aromaticity and the presence of the chiral centre, for asymmetric hydrogenation studies in order to determine the different spatial and chemical requirements, in terms of their site specificity of the chiral centres. The hydrogenation of the following prochiral reactants was examined:

(1) methyl tiglate

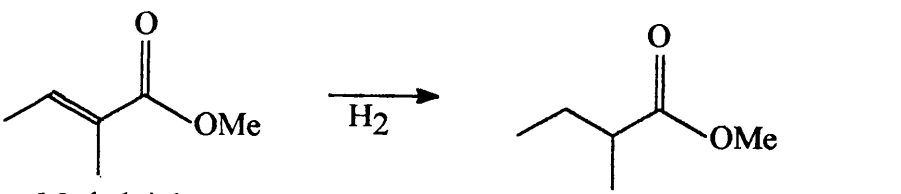

Methyl tiglate

2-Methyl butyric acid methyl ester
Methyl-2-methyl butyrate

(2) tiglic acid

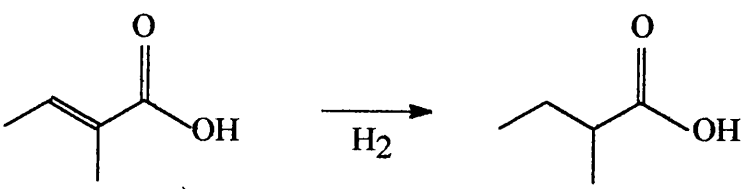

Tiglic acid

2-Methyl butyric acid

(3) 3-coumaranone

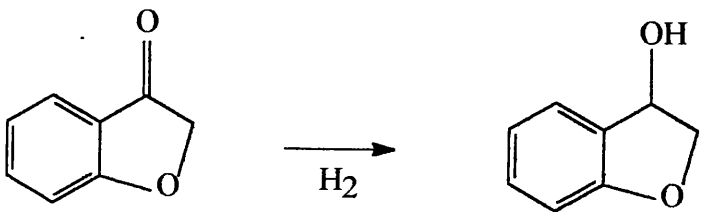

3-Coumaranone

3-Benzofuranol

The former two representing the hydrogenation of substituted alkenes, the latter an isolated C=O group.

CHAPTER 3

EXPERIMENTAL

3.1 INTRODUCTION

Three supported Pt catalysts were prepared, characterised, modified and tested for enantioselectivity in the hydrogenation of methyl tiglate, tiglic acid and 3-coumaranone. The catalysts were prepared using a wet impregnation method, the platinum precursors being impregnated on to the γ-alumina support and two different silica supports.

Several methods were used to characterise the catalysts. Ultra-violet and visible spectroscopy (UV-VIS), temperature-programmed reduction (TPR), O_2 and CO chemisorption and transmission electron microscopy (TEM).

The catalysts were then tested for enantiohydrogenation using a specially designed liquid phase reactor and the results were analysed by chiral gas chromatography (GC).

3.2 CATALYST PREPARATION

The catalysts were prepared in the ICI Katalco laboratories in Billingham.

The precursor used in the preparation of the three catalysts used in this study was $H_2PtCl_6.xH_2O$. The supports used were γ-alumina from Degussa, Grace silica C10 from Fuji-Davidson Chemical Ltd and Cab-O-Sil from M5 Cab-O-Sil. Each of the catalyst precursors were prepared using a wet impregnation method.

3.2.1 Pt/γ-alumina (P5211)

A known weight (1000g) of γ-alumina was placed in a Pascall rotatory tumbler and H_2PtCl_6 (21g), dissolved in de-ionised water (1000ml), was added. The container was purged with nitrogen and a water vacuum pump connected. The $[PtCl_6]^{2-}$/γ-alumina was dried in a rotatory vacuum at room temperature for 2 days and in an oven at 313K for 16 hours and calcined at 823K for 3 hours.

3.2.2 Pt/Grace silica C10 (P5450)

A known weight (250g) of Grace silica C10 was placed in a round bottomed flask and H_2PtCl_6 (5.253g, Aldrich Chemicals, assay 47.6% w/w Pt), dissolved in de-ionised water (425ml), was added. The flask was rotated in a Buchi Rotavap for 5 hours at 333K under a purge of nitrogen. The $[PtCl_6]^{2-}$/Grace silica C10 was dried in an oven at 333K for 16 hours and then at 393K for a further 2 hours.

3.2.3 Pt/Cab-O-Sil (P5578)

A known weight (250g) Cab-O-Sil was prepared as a slurry, using a minimum volume of deionised water in a round bottomed flask (3000ml). H_2PtCl_6 (6.35g, Aldrich Chemicals, assay 39.400% w/w Pt) dissolved in de-ionised water (50g) was added. The flask was connected to a Buchi Rotavap with a rotary pump for 1 hour and heated to 335K. The Buchi Rotavap was then connected to a water pump and heated to 354K until the catalyst was dried.

A full list of catalysts used in this study and their metal loadings is given in Table 3.1.

Table 3.1:- Summary of catalysts	
Catalyst	Nominal % w/w Pt metal loadings
Pt/γ-alumina	1
Pt/Grace silica C10	1
Pt/Cab-O-Sil	1

3.3 CATALYST CHARACTERIZATION

3.3.1 Ultra-violet-Visible spectroscopy

Ultra-violet-Visible spectroscopy (UV-VIS) was undertaken of the solid catalyst precursors over the range of 190 to 900nm using a Philips 8800 uv-visible spectrometer with a diffuse reflectance attachment to determine the electronic spectra.

Solid state UV-VIS absorption spectra were obtained by grinding a sample of catalyst precursor into a very fine powder and mounting the sample into an $1cm^3$ cell. The cell was then placed in the cell compartment and the spectra run.

3.3.2 Temperature programmed reduction

Temperature programmed reduction (TPR) experiments were carried out using the apparatus shown in Figure 3.1. A known weight (*ca.* 0.2g) of catalyst sample was placed on the sinter of the reactor vessel. Initially the catalyst was flushed with helium gas in order to detect any leaks in the system and until a steady baseline was obtained on the integrator. The helium was switched over in favour of the reducing gas 6% dihydrogen in dinitrogen, at ambient temperature and the baseline as indicated by the integrator was then allowed to settle once again, with the reducing gas flowing over the catalyst at a rate of 30ml min^{-1}. The temperature was then ramped steadily at a linear rate of 5K min^{-1}. As the reduction temperature of a specific species was reached, dihydrogen was consumed and the corresponding change in the composition of the effluent gas was detected by the TCD, resulting in a peak on the integrator. The temperature at the peak maximum was noted.

A deoxygenating catalyst followed by molecular sieves are placed in line to purify the gases before use. The deoxygenated catalyst had been previously prepared as follows: a known weight of palladium chloride (0.34g) had been dissolved in water (100ml) and impregnated on to WO_3 (20g), with the rotary evaporator used to remove the water. The catalyst was activated in a small glass vessel by the passage of dihydrogen gas over it for

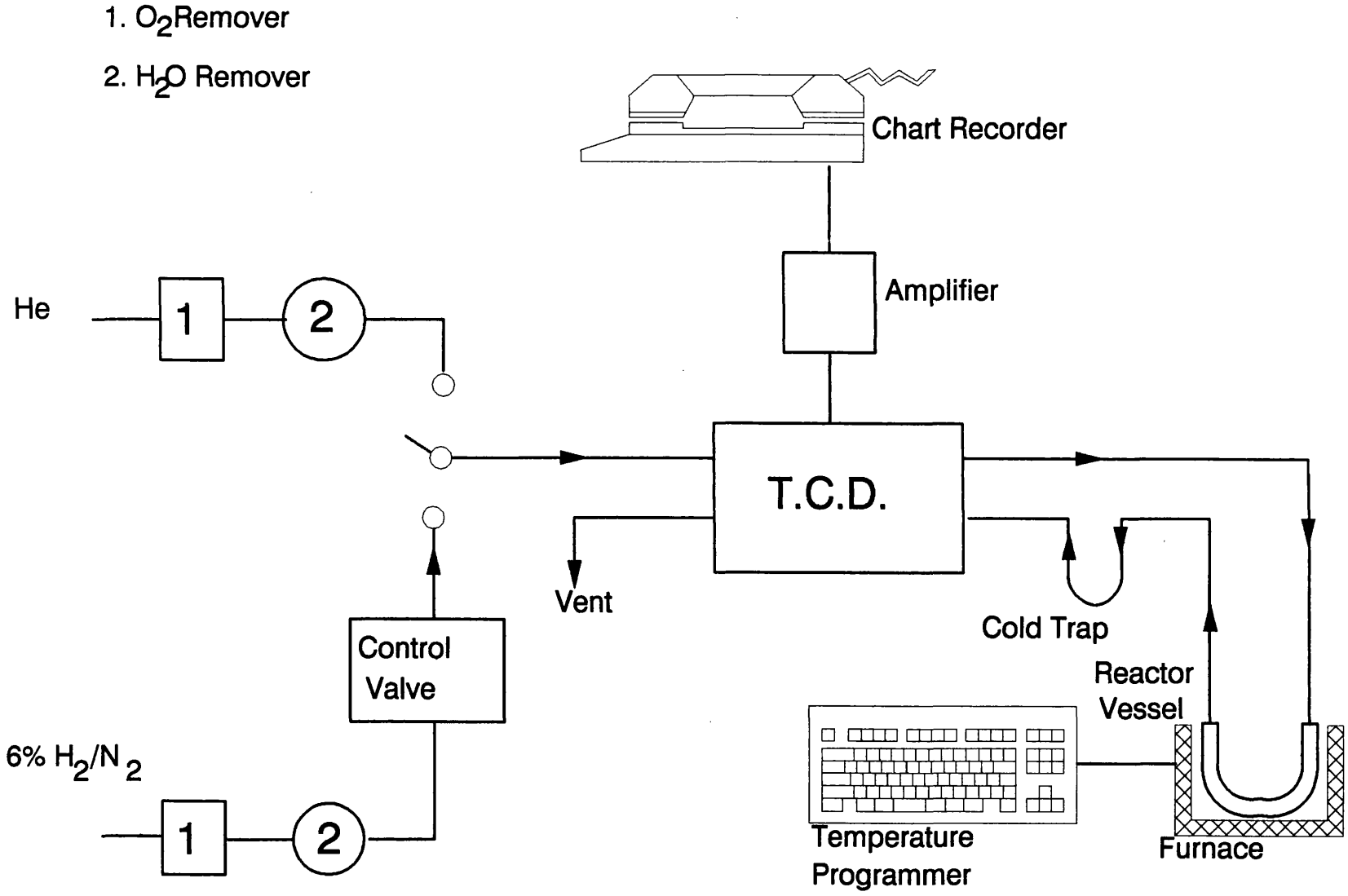

Figure 3.1:- Temperature-Programmed Reduction

60 minutes. Once the gases are deoxygenated, the gases are dried by passage over an activated Linde 5a molecular sieves in a brass vessel. The sieves were activated by heating to 423K.

The desired flow of the dihydrogen/dinitrogen gases is achieved by the use of mass flow controllers, which unlike volumetric flow controllers, are not affected by environmental factors such as temperature and pressure and so the flow of gas is consistent. Mass flow controllers consist of three basic units; a flow sensor, a control valve and an electronic control system. The flow through the sensor is measured thermodynamically. The heat is directed to the midpoint of a flow carrying sensor tube. At equidistant points up- and downstream of the heat input, are placed resistance temperature elements (T1 and T2) (Figure 3.2). During carrier gas flow, the gas stream carries an increasing amount of heat towards the downstream element, T2, from the upstream element, T1. The temperature difference is proportional to the amount of gas flow which is interpreted by a bridge circuit and an amplifier provides the output to the control readout. The power supply to the controllers can be adjusted to between 0% and 100% to produce a range of flows. The dihydrogen and dinitrogen gas flows are calibrated from a bubble meter attached to the reactor effluent stream. A reducing gas of 94% dinitrogen and 6% dihydrogen can be obtained this way.

The thermal conductivity detector (TCD) consists of a set of twin filaments. One set of the filaments was in contact with a stream of reference gas (unreacted gas) while the second was in contact with the gas to be analysed. Heat transferred from these hot wires, situated in the gases, at a rate proportional to the thermal conductivity of the gas which was in turn related to its composition. The filaments were connected to a Wheatstone bridge circuit with a sample and reference arm. The reducing gas was directed through the reactor reference side, then through the reactor vessel containing the catalyst sample and finally, via a cold trap, through the other arm of the TCD. Any differentiation in the gas composition between arms of the detector resulted in an imbalance in the Wheatstone which was measured and, after amplification plotted as a peak on the integrator. A TCD was therefore used to detect dihydrogen uptake by the catalyst. The cold trap consisted of a dewar flask containing dry ice and acetone and was incorporated to remove any reduction products from the gas stream which may have been harmful to the tungsten filaments of the TCD.

Reactor vessel is shown by Figure 3.3. The reactor was surrounded by a furnace which was connected to a temperature programmer. The temperature in the reactor was measured by a thermocouple. The Furnace and the temperature programmer were supplied

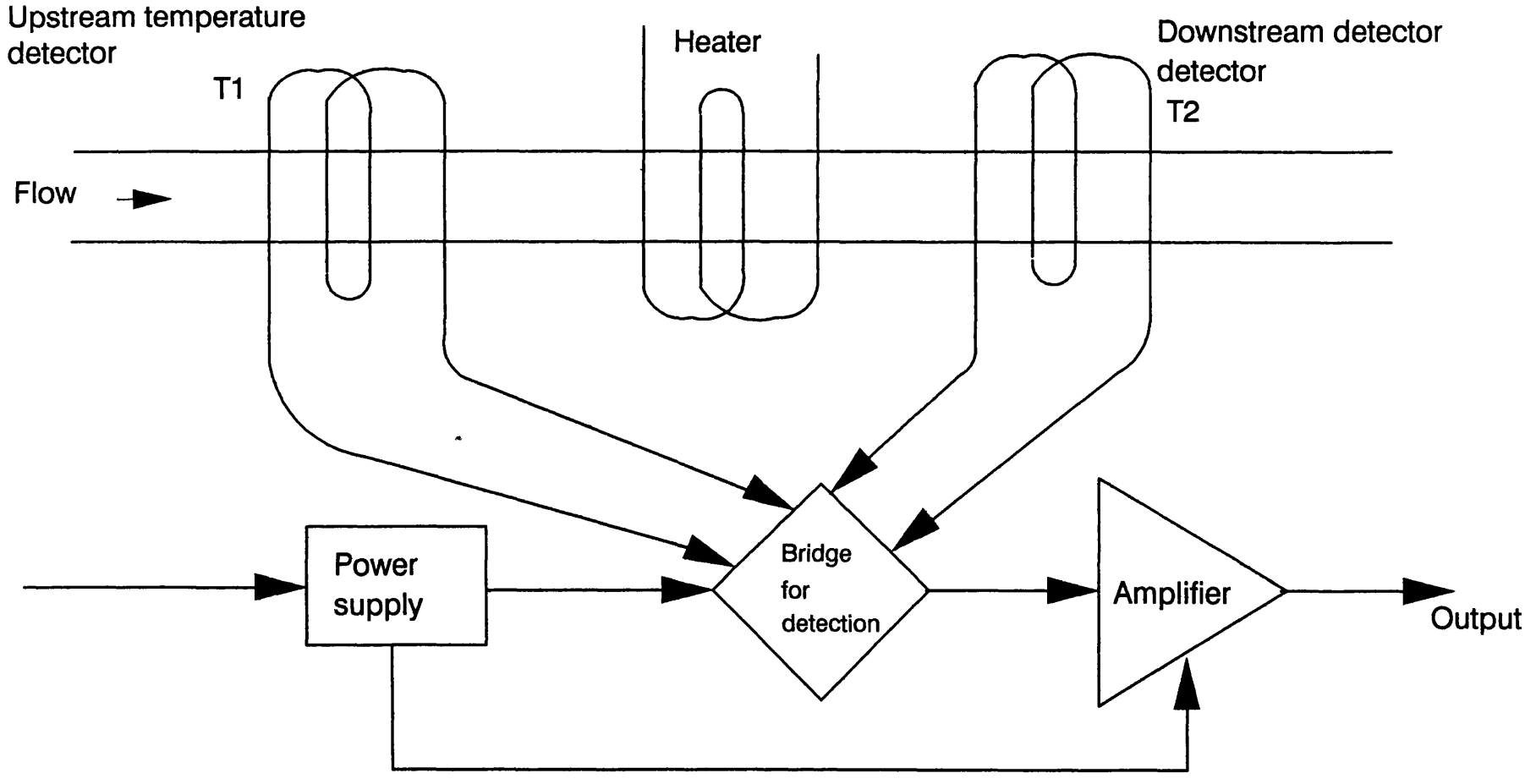

Figure 3.2:- Schematic diagram of a mass flow controller

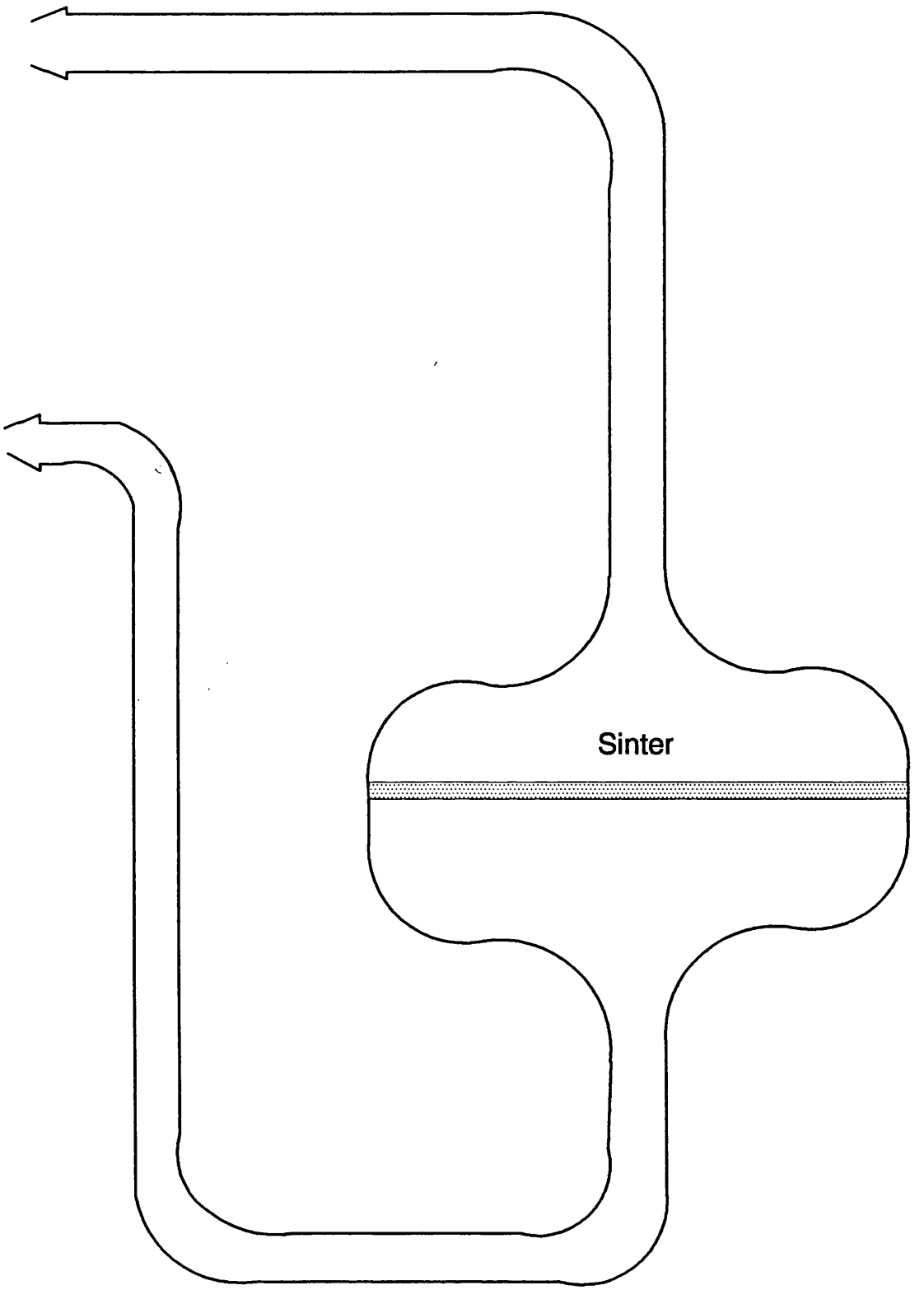

Figure 3.3:- Schematic diagram of TPR vessel

by Cambridge Process Controls, the amplifier was supplied by Gow-Mac Ltd, the integrator was supplied by Hewlett Packard and the mass flow controllers were supplied by Brooks Control Ltd.

3.3.3 Chemisorption of O_2(g) and CO(g)

Dioxygen and carbon monoxide chemisorption experiments were performed using the glass vacuum line shown schematically in Figure 3.4. A known weight (*ca.* 0.15g) of a catalyst precursor was placed in the reaction vessel. The catalyst precursor was flushed initially with helium (30ml min^{-1}), followed by dihydrogen gas. The catalyst precursor was then heated to the required temperature at which complete reduction of the precursor was attained, for approximately two hours in flowing dihydrogen (30ml min^{-1}). The active catalyst was cooled in flowing helium.

With the aid of a vacuum line, known volumes of dioxygen or carbon monoxide were pulsed from a sample loop in flowing helium; initially on by-pass and finally over the catalyst bed, *in situ*, at ambient temperature until saturation of the metal surface was reached.

The pulse volume is so chosen that a few pulses will be completely consumed by the catalyst. Knowing the pulse volume and the number of pulses consumed, that is gas reacted plus newly adsorbed on the metal (see Figure 3.5), including the fraction of pulses, the amount of gas chemisorbed by the catalyst to obtain a monolayer coverage on the exposed metal surface can be calculated.

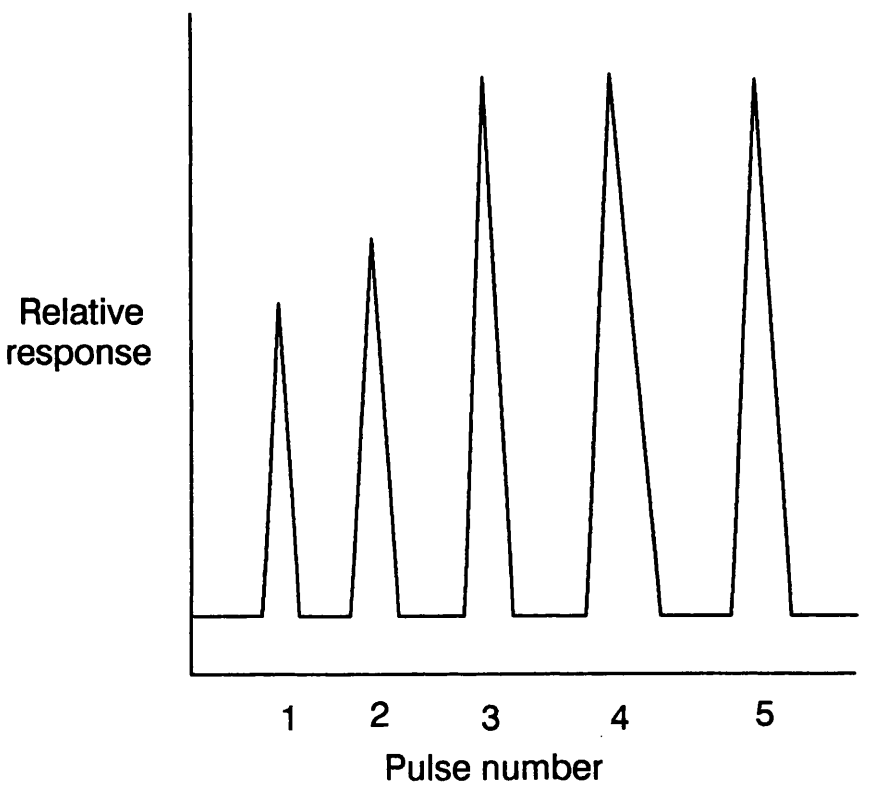

Figure 3.5:- Typical response obtained from chemisorption

Figure 3.4:- Schematic outline of Chemisorption system

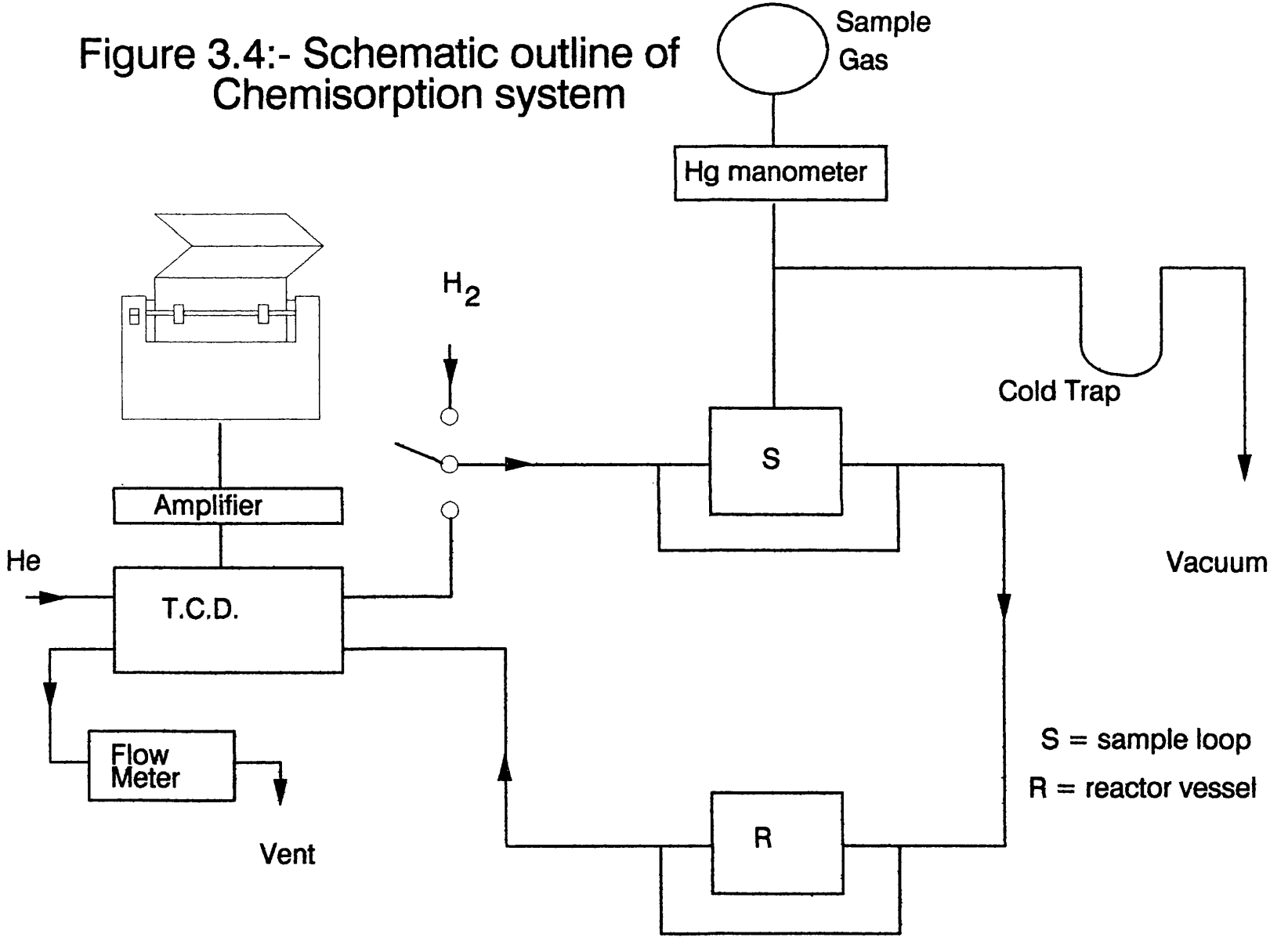

As with TPR, the detection of the changes in the helium flow contaminated with either dioxygen or carbon monoxide was effected using a TCD.

3.3.4 Transmission electron microscopy

A sample of catalyst which was to be examined in the Philips 1200 microscope was prepared using the following method.

A weight (approx. 0.1g) of sample was ground into a fine powder, which was then suspended in distilled water and placed in an ultra-sonic water bath. The fine powder/water mixture was placed on to a 300 square mesh Cu 3.05mm carbon coated grid. The supported grid was then put in an oven overnight to dry at 308K.

3.4 ADSORPTION STUDIES

The adsorption of the chiral organic modifiers on to the active supported platinum catalysts which will be detailed in section 3.4.1 were carried out in the liquid phase in an inert atmosphere (dinitrogen) at both 293K and 273K. Tetrahydrofuran (THF) was used as the solvent for the catalyst modification.

3.4.1 Materials

THF (HPLC grade) was supplied by Rathburns and kept in a nitrogen atmosphere. The binaphthalene based modifiers were as shown by Table 3.2a and Appendix 1.

Table 3.2a:- Binaphthalene modifiers	
Modifier	Supplier
(±)-1,1'-bi-2-naphthol ((±)-2,2'-dihydroxy-1,1'-binaphthalene) (99%)	Aldrich Chemicals
R-(+)-1,1'-bi-2-naphthol (R-(+)-2,2'-dihydroxy-1,1'-binaphthalene) (99%)	Aldrich Chemicals/prepared as detailed in Appendix 4
S-(-)-1,1'-bi-2-naphthol (S-(-)-2,2'-dihydroxy-1,1'-binaphthalene) (99%)	Lancaster Chemicals
(±)-2,2'-diamino-1,1'-binaphthalene	prepared as detailed in Appendix 5
R-(+)-2,2'-diamino-1,1'-binaphthalene (99%)	Aldrich Chemicals
S-(-)-2,2'-diamino-1,1'-binaphthalene (> 99.5%)	Fluka Chemicals
(±)-2,2'-dimethoxy-1,1'-binaphthalene	prepared as detailed in Appendix 6
(-)-2,2',7,7'-tetrahydroxy-1,1'-binaphthalene	prepared as detailed in Appendix 7

Other modifiers studied are as follows as are shown by Table 3.2b and Appendices 1 and 3.

Table 3.2b:- Alternative modifiers	
Modifier	Supplier
R-(-)-1-(9-anthryl)-2,2,2-trifluoroethanol (>98%)	Fluka Chemicals
L-histidine (S-2-amino-3-(4-imidazoyl) propionic acid) (>99%)	Fluka Chemicals
L-tryptophan (>99%)	Fluka Chemicals
(+)-pseudoephedrine (~98%)	Fluka Chemicals
L-phenylalaninol (~99%)	Fluka Chemicals
L-(+)-α-phenylglycinol (purum)	Fluka Chemicals
R-(+)-α-methoxy-α-trifluoromethylacetic acid (>99%)	Fluka Chemicals
R-(+)-N,N-dimethyl-1-phenylethylamine (>97%)	Fluka Chemicals

A couple of pyridine based macrocycles (S,S)-di-(2-propyl)-6,12-dioxa-2,5,13,16-tetraoxo-3,15,19-triazabicyclo[15.3.1]heneicosa-1(21),17,19-trieneand(S,S)-di-(2-propyl)-6,13-dioxa-2,5,14,17-tetraoxo-3,16,20-triazabicyclo [16.3.1] docosa-1(22),18,20-triene

(Appendix 2) were prepared as detailed in Appendix 8 and 9 were studied as well.

Analysis of the binaphthalene derivatives, R-(-)-1-(9-anthryl)-2,2,2-trifluoroethanol and the macrocycles was carried out by High Performance Liquid Chromatography (HPLC) using a liquid phase prepared from HPLC grade acetonitrile and HPLC grade water (600ml:400ml) which were both supplied by Rathburns.

3.4.2 Reactor systems

The modification of the supported platinum catalysts was carried out, *in situ*, in one of two reaction vessels, reactor R1 or reactor R2 as shown in Figure 3.6 and Figure 3.7 respectively. Initial adsorption properties of the catalysts were studied using reactor R1 to activate the catalyst sample in static dihydrogen (Figure 3.8). Subsequently, the activation of the catalyst samples for adsorption studies took place in reactor R2 by static reduction (Figure 3.9); or by flowing dihydrogen over the catalyst sample (Figure 3.10). For the flow reduction method the flow rates were measured with a bubble flow meter attached to the exit from the reaction vessel. These are shown in Table 3.3. For the static reduction the amount of gas admitted to the reaction vessel was measured by a Hg manometer (1atm). The vacuum of the glass line used to evacuate either reactor R1 or R2 was measured by a Pirani gauge (10^{-2}atm).

Table 3.3:- Flow rates for gases used in flow reduction

Gas	Flow rate/mlmin^{-1}
Dihydrogen	30
Dinitrogen	30

The reactors R1 and R2 were surrounded by an electric furnace the current to which was controlled using of a Variac transformer. The temperature at the catalyst bed of reactor R1 was measured by thermocouple placed near the catalyst sample. For reactor R2, the temperature at the sinter was measured by placing the thermocouple into a well in the side of the reaction vessel.

3.4.3 Catalyst activation

3.4.3.1 Modification with one modifier

The standard procedure for modification with one modifier of a sample of activated catalyst (see sections 3.4.3.3, 3.4.3.4 and 3.4.3.5) was as follows. To a freshly prepared catalyst sample 10ml of a known concentration of modifier solution was injected into the reactor vessel via a septum. The modifier solution was then allowed to reach a point where

Figure 3.6:-
Schematic diagram of reactor R1

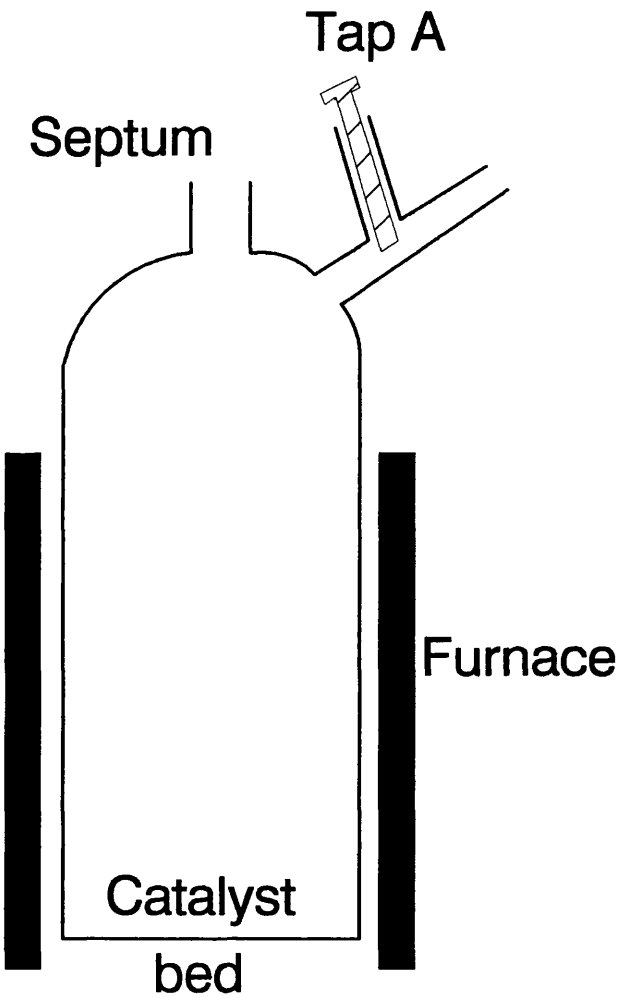

Figure 3.7:-
Schematic diagram of reactor R2

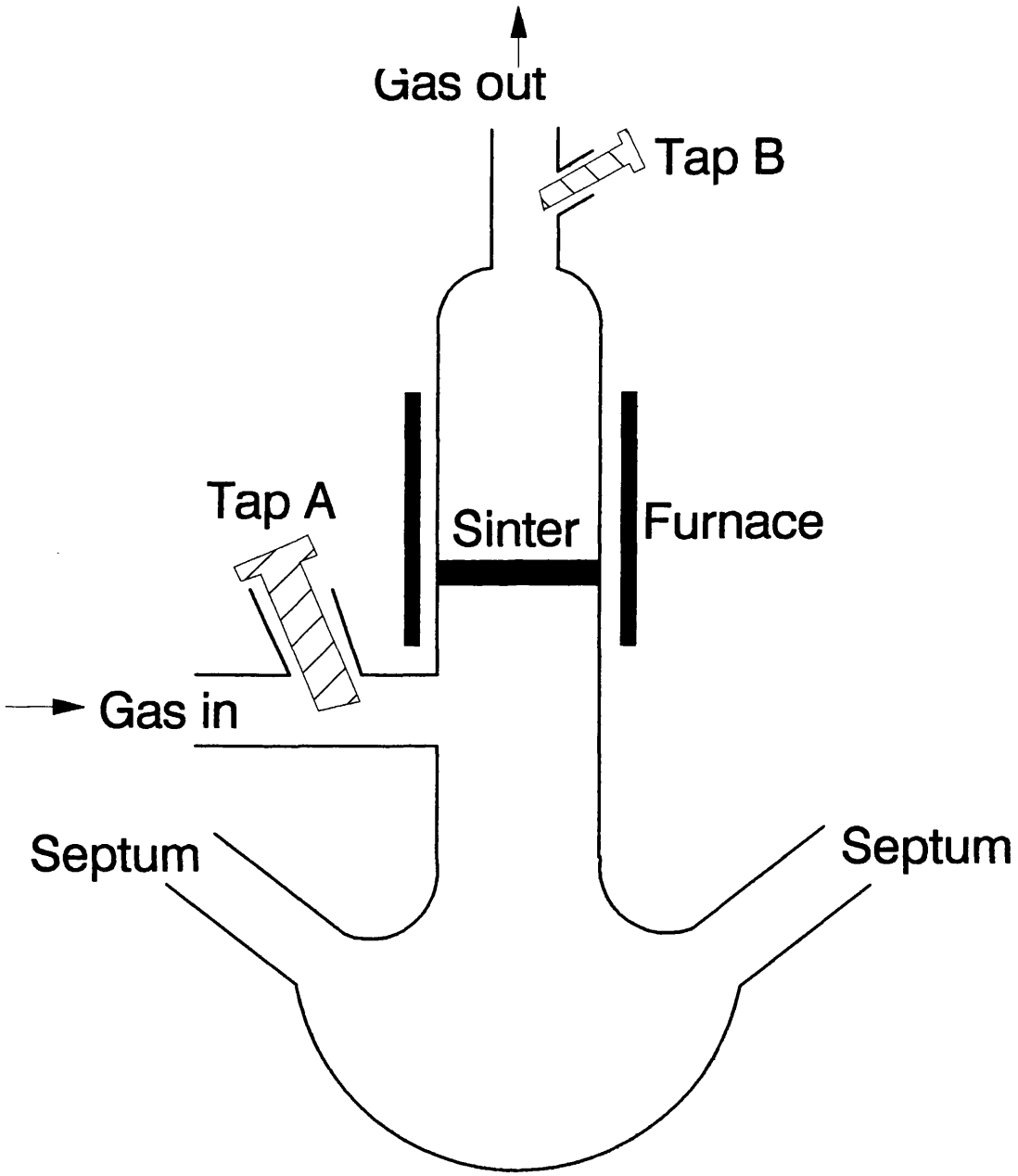

Figure 3.8:-
Schematic outline of reactor R1 and static reduction

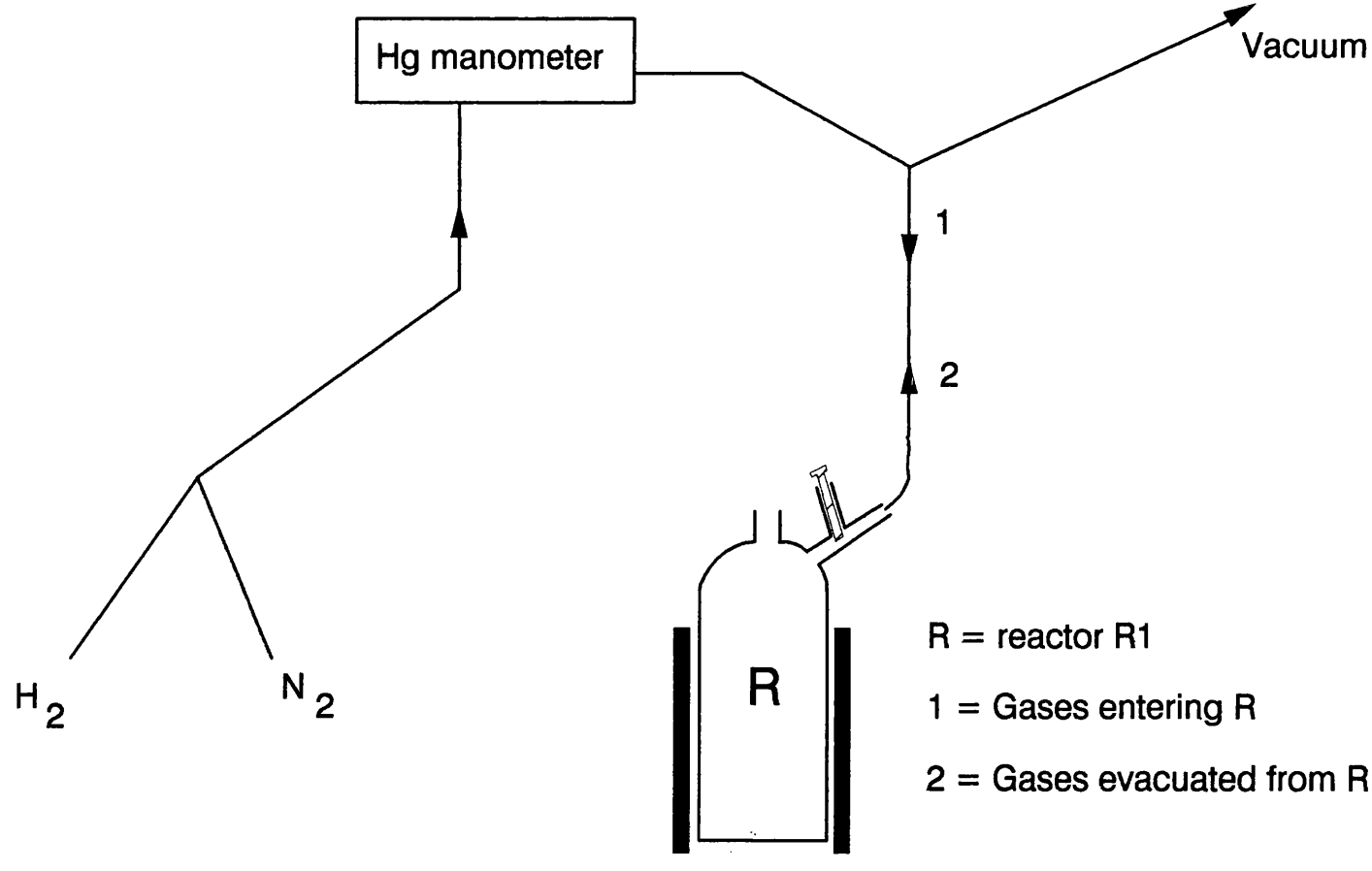

Figure 3.9:-
Schematic outline of static reduction and reactor R2

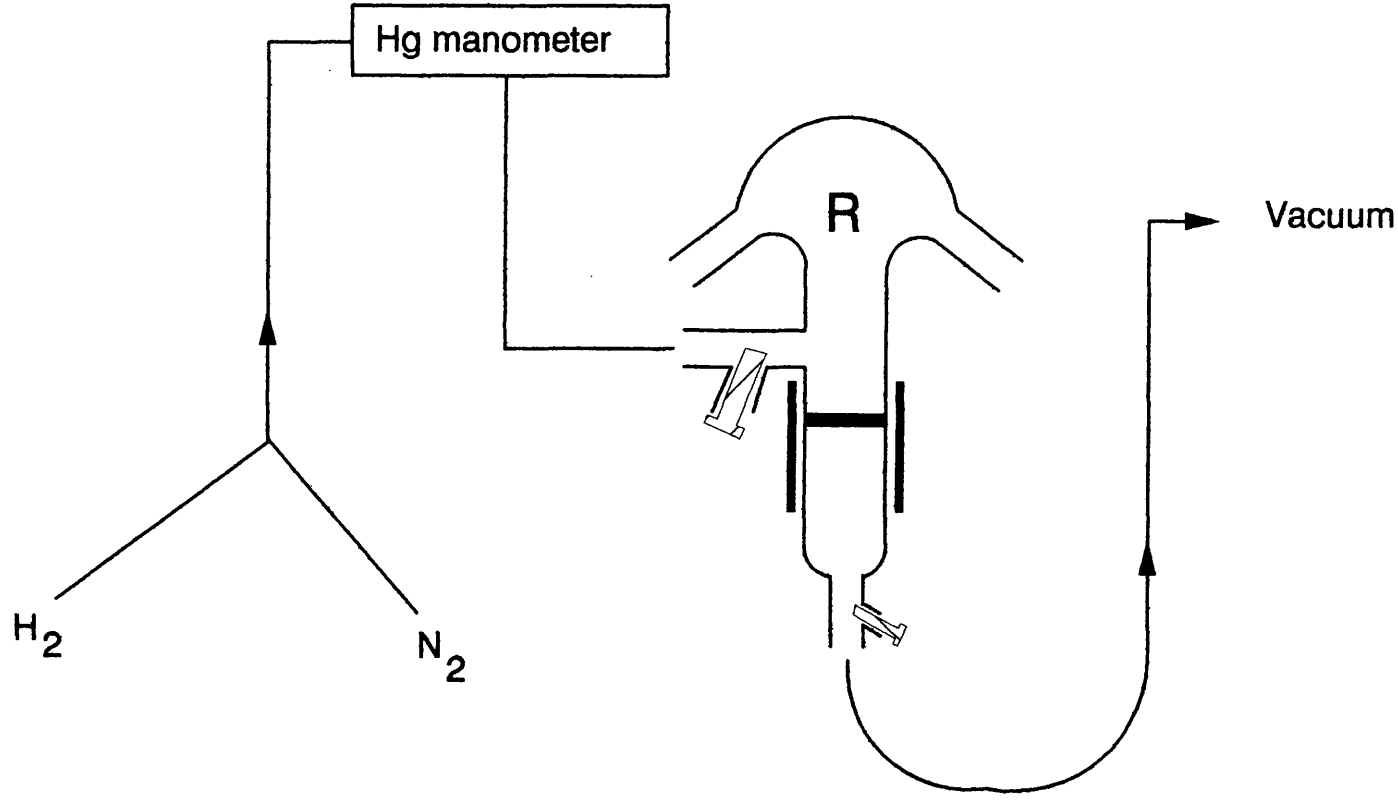

R = reactor R2

Figure 3.10:-
Schematic outline of flow reduction with reactor R2

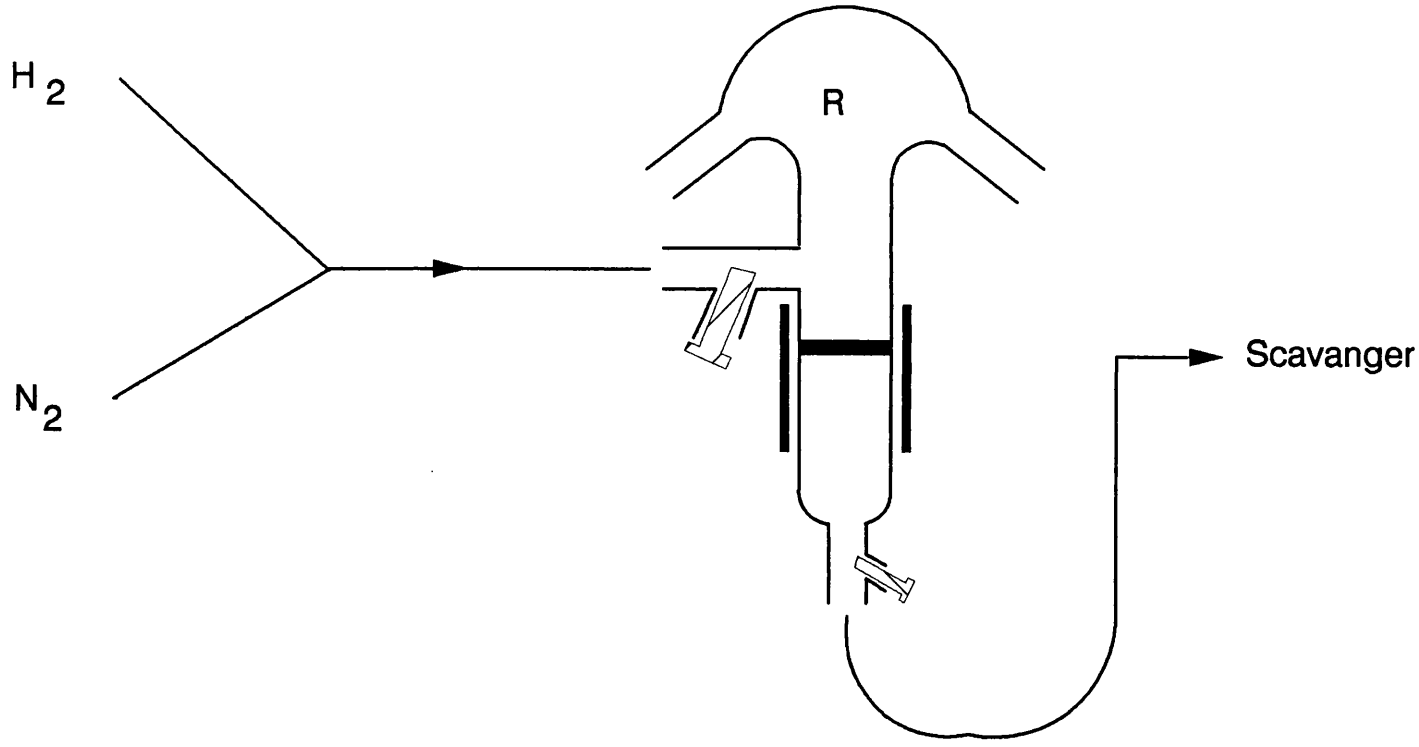

R = reactor R2

the modifier in solution was in equilibrium with the modifier adsorbed on to the catalyst.

3.4.3.2 Co-adsorption

The co-adsorption studies involved either the addition of a mixed modifier solution or the addition of a second modifier solution to a catalyst sample preconditioned with the first modifier. The preconditioning of the catalyst with the first modifier was carried out in one of two ways, that is, the first modifier was either removed from the reactor prior to the second one being added or the second modifier was mixed with the resultant solution of the first modifier.

3.4.3.3 Reactor R1 and static reduction

The precursors of the catalysts were reduced in the reactor before, *in situ*, modification. The reactor vessel was attached to a vacuum line as shown in Figure 3.8. A known weight of catalyst (*ca* 1.0g) was placed in the bottom of the reactor and the vessel then sealed with a septum cap (17mm diameter). The reactor was then evacuated with the aid of a Hg diffusion and rotary pump with tap A was in the open position. Following the evacuation of the reactor, the reactor was isolated from pumps, 1 atm of dihydrogen gas was admitted to the reactor and tap A closed. Excess hydrogen was evacuated from the manometer. After a period of time (*ca.* 10 minutes), the reactor again was evacuated and the procedure repeated for a period of 2 hours, at the appropriate reduction temperature, namely, Pt/γ-alumina at 573K and Pt/Grace silica C10 at 523K.

Following reduction the reactor was evacuated and dinitrogen gas admitted to the reactor at the reduction temperature and the catalyst allowed to cool to room temperature. The modifier solution (10ml) was introduced by injection through the septum cap and allowed to equilibrate. The modifier was allowed to adsorb on to the catalyst by being in contact with the catalyst without any agitation. The uptake of the modifier from solution was monitored by the removal of samples (0.2ml) of the modifier solution over a period of time and analysis using HPLC.

3.4.3.4 Reactor R2 and static reduction

As in section 3.4.3.3, the catalysts were activated before modification. The reactor vessel R2 was turned upside down as in Figure 3.9, clamped and connected to the vacuum line, at both taps A and B. A known weight of catalyst (*ca.* 1.0g) was placed on the sinter and the two arms of the reaction vessel were sealed with B14 (25mm diameter) septum caps. The reactor was evacuated via taps A and B. The Hg diffusion and rotary pump were isolated from the reactor as in section 3.4.3.3. Tap B was closed and 1 atm of dihydrogen was placed in the reactor after which tap A was then closed. The reduction procedure was similar to that for reactor R1 except that, after the activated catalyst was cooled in

dinitrogen, the reactor was re-inverted (Figure 3.11) and the modifier solution injected via one of the septa. As before, the modifier concentration in the solution was monitored by the removal of samples and HPLC analysis.

3.4.3.5 Reactor R2 and flow reduction

Reactor R2 was set up as described in section 3.4.3.4, that is, in the inverted position, catalyst sample on the sinter and clamped, except that tap A was connected to the gas supply and tap B to the gas scavenger system as shown in Figure 3.8. With taps A and B open dihydrogen gas was flowed (30ml min^{-1}) through the reactor for two hours at the appropriate reduction temperature for the catalyst, that is, Pt/γ-alumina, 573K and Pt/Grace silica C10 and Pt/Cab-O-Sil, 523K, unless otherwise stated (see section 3.4.3.7).

Following reduction the catalyst was purged with dinitrogen at the reduction temperature and then allowed to cool to room temperature in a steady flow of dinitrogen (30ml min^{-1}). The reactor vessel was then re-inverted and taps A and B closed. As in section 3.4.3.4, the modifier solution was injected into the reactor vessel and modifier concentration was monitored by HPLC analysis.

3.4.3.6 Polarimetry studies

Studies have shown that the physical properties such as melting points, boiling points, densities, indices of refraction, heats of formation and standard free energies for a pair of enantiomers are identical. However, a technique known as polarimetry can distinguish between a pair of enantiomers. The enantiomers are distinguished by their individual behaviour towards light and was measured by a polarimeter.

Plane polarised light consists of an electric field which oscillates in only one plane; while ordinary light contains oscillating electric and magnetic fields, of which the electric fields oscillate in all planes. Polarised light is obtained by passing ordinary light through a polariser. The orientation of the polariser's axis of polarisation determines the plane of the resulting polarised light.

Passing a plane of polarised light through an enantiomer of a chiral substance results on the re-emerged plane of polarised light being rotated. A substance which can rotate plane polarised light is optically active, that is, individual enantiomers of chiral substances are optically active.

Optically activity is measured by an instrument known as a polarimeter (Figure 3.12). This basically consists of two polarisers. The sample is placed in the light beam between the two polarisers. The light beam is monochromatic because optical activity changes with wavelength. The most common used light source is the yellow sodium arc, that is , the sodium D-line, λ = 5893Å.

Figure 3.11:-
Schematic outline of catalyst modification with reactor R2

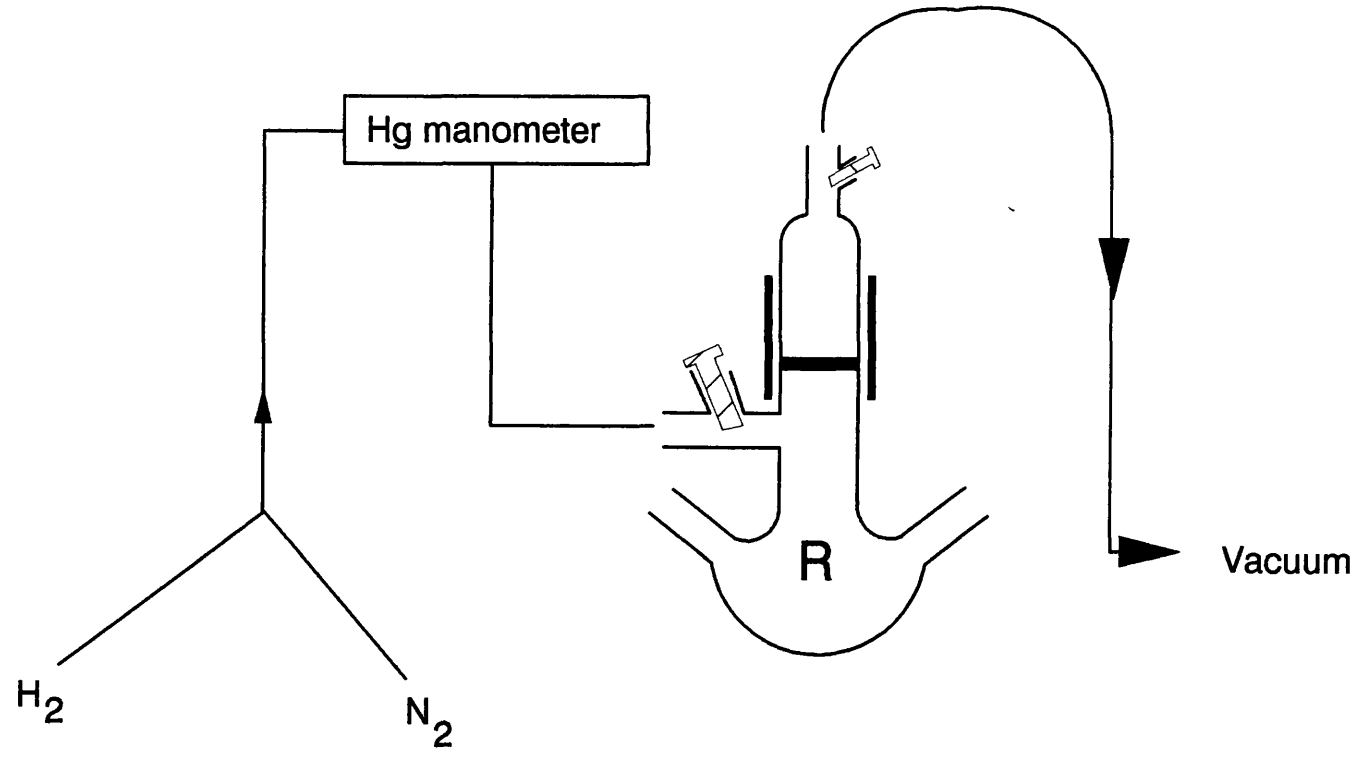

R = reactor R2

Figure 3.12:-
Schematic representation of a polarimeter

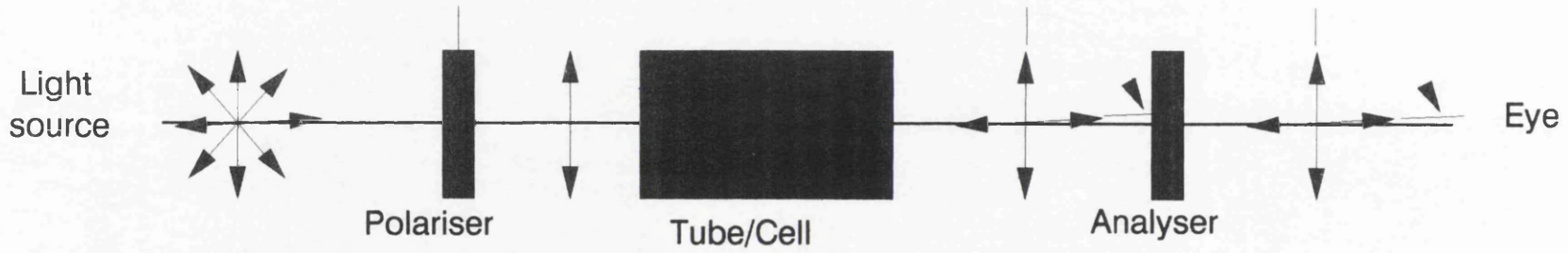

The first step in determining the optical rotation of a sample is to obtain a dark field in the analyser. A dark field is established by placing of an optically inactive sample, for example, solvent or air into the sample compartment and the polarised light passed through this inactive sample. The analyser is set at a zero optical rotation. The next step, is the replacing of the inactive sample by the sample whose optical activity is to be measured. The number of degrees, α, through which the analyser must be turned to re-establish the dark field corresponds to the optical activity or rotation of the sample. Plane polarised light rotated in a clockwise direction has a plus sign for the direction of optical rotation. Rotation of the plane polarised light in the counterclockwise direction, the optical rotation is given a minus sign.

The observed optical rotation, α, is proportional to the number of optically active molecules present in the light beam. Thus, α is proportional to both the concentration c of the optically active compound in the sample as well as the length l of the sample cell:

$$\alpha = [\alpha]cl \qquad \text{Eqn 3.1}$$

The constant of proportionality, $[\alpha]$, is called the specific rotation. The concentration of the sample is given in g ml^{-1}, and the path length in dm. Thus, the specific rotation is the observed rotation at a sample concentration of 1g ml^{-1} and a path length of 1dm. The specific rotation is conventionally reported as $[\alpha]^{20}_{D}$, where D indicates the wavelength of light used i.e. sodium D-line and 20 indicates an operating temperature of 20°C (293K). A acceptable concentration range over which optical rotation can be measured is c = 0.2 to 1g ml^{-1}.

The details of the polarimetry studies were as follows. Samples of catalyst precursors were activated and modified with either R-(+)-2,2'-dihydroxy-1,1'-binaphthalene or R-(+)-2,2'-diamino-1,1'-binaphthalene using the apparatus outlined in section 3.4.3.3. The concentration of these modifier solutions were prepared to approximately c = 1g ml^{-1} and the optical rotation measured. After allowing the modifier adsorption on to the catalyst to reach equilibrium, the modifier solution was then placed in a polarimeter and the optical rotation measured.

3.4.3.7 Sintering studies

Using the reactor vessel R2, samples of the Pt/Cab-O-Sil precursors subjected to a sintering process. This involved reducing the catalyst precursor as outlined in section 3.4.3.5 in flowing dihydrogen (30ml min^{-1}) at 723K for 2 hours. Instead of purging and cooling the activated sample in dinitrogen, air was used. The air was purged through the reactor at the reduction temperature and the catalyst was then cooled to room temperature in flowing air (30ml min^{-1}) for 30 minutes.

Adsorption studies of the sintered Pt/Cab-O-Sil catalyst involved the re-reduction of the new precursor at 723K in flowing dihydrogen (30ml min^{-1}) for a further 2 hours and cooled to room temperature in dinitrogen as previously described.

3.4.4 Analysis of modifier solution after equilibration

A Spectra Physics Isochrom LC pump High Performance Liquid Chromatograph fitted to a Spectra Physics Spectra 100 variable wavelength ultra-violet visible spectrophotometric (UV-VIS) detector was used to analyse the concentration of the modifier solution and, subsequently, the amount of modifier adsorbed by the catalyst. The UV-VIS was attached to a Philips Pye Unicam PU4810 computing integrator. Samples were injected on to a normal phase silica column, (length 25cm, internal diameter 4.6mm) modified by hydrocarbon chains consisting of 8 carbon atoms, using a 25µl syringe via a 10µl sample loop. The samples were injected and analysed at room temperature. Table 3.4 shows the wavelengths at which the modifiers were analysed and their approximate retention times. The column was a C8-SB5-19286, prepared for and supplied by Burke Analytical. The liquid mobile phase was a mixture of acetonitrile and water in the ratio 60 acetonitrile: 40 water. The mobile phase was degassed by bubbling helium through it for 5 minutes.

Table 3.4:- Summary of modifiers, wavelengths and retention times

Modifier	Retention time/Minutes
Wavelength = 340nm	
2,2'-Dihydroxy-1,1'-binaphthalene	6
2,2'-Diamino-1,1'-binaphthalene	8
2,2'-Dimethoxy-1,1'-binaphthalene	15
2,2'7,7'-Tetrahydroxy-1,1'-binaphthalene	3.5
(-)-1-(9-anthryl)-2,2,2-trifluoroethanol	9
Wavelength = 240nm	
(S,S)-di-(2-propyl)-6,12-dioxa-2,5,13,16-tetraoxo-3,15,19-triazabicyclo [15.3.1] heneicosa-1(21),17,19-triene	4
(S,S)-di-(2-propyl)-6,13-dioxa-2,5,14,17-tetraoxo-3,16,20-triazabicyclo [16.3.1] docosa-1(22),18,20-triene	4.5

The modifiers analysed with this technique were the

2,2'-dihydroxy-1,1'-binaphthalene,

2,2'-diamino-1,1'-binaphthalene,

2,2'-dimethoxy-1,1'-binaphthalene,

(-)-2,2',7,7'-tetrahydroxy-1,1'-binaphthalene,

R-(-)-1-(9-anthryl)-2,2,2-trifluoroethanol,

(S,S)-di-(2-propyl)-6,12-dioxa-2,5,13,16-tetraoxo-3,15,19-triazabicyclo [15.3.1] heneicosa-1(21),17,19-triene

and(S,S)-di-(2-propyl)-6,13-dioxa-2,5,14,17-tetraoxo-3,16,20-triazabicyclo[16.3.1] docosa-1(22),18,20-triene.

In the case of the dihydroxy-, diamino- and dimethoxy- binaphthalene derivatives the order of elution at 340nm was:

dihydroxy- < diamino- < dimethoxy-binaphthalene

During the analysis of a sample of modifier solution the liquid mobile phase flow rate was set at 1ml min^{-1}. The sample concentration was detected by the UV-VIS detector was attached to an integrator.

The sample was injected on to the HPLC column via a sample loop. Once on the column, the sample was moved along the column until it was eluted by the liquid mobile phase and passed through the UV-VIS detector. The change in liquid mobile phase composition of acetonitrile/water was detected by the UV-VIS and this appeared as a peak on the integrator. A typical plot from the integrator is shown in Figure 3.13.

Peak areas were calculated by the integrator. Amount of modifier adsorption was determined by the difference in the final modifier concentration with that of the initial concentration of the modifier solution added to the fresh catalyst sample, *in situ*.

The modification procedure was carried out as detailed earlier.

3.4.5 Desorption studies

Following the modification procedure, the modifier solution was removed from the reactor by a syringe. A sample of clean THF (10ml) was injected on to the modified catalyst and a magnetic stirrer was placed in the reactor after which an initial catalyst free liquid sample was taken. The reactor was placed on top of a magnetic stirrer hotplate (Figure 3.14). The modified catalyst/THF mixture was agitated for a standard time at room temperature of 1 hour unless stated otherwise. A sample of catalyst free liquid was removed and analysed. This procedure is referred to as the wash step.

3.4.5.1 Effect of temperature

The catalyst was washed at room temperature for 1 hour as before, then the temperature was increased and the catalyst washed for further hour. At each temperature, the temperature was noted and a sample of catalyst free liquid taken. This procedure was

Figure 3.13:-
A typical plot of a modifier from the integrator of the HPLC

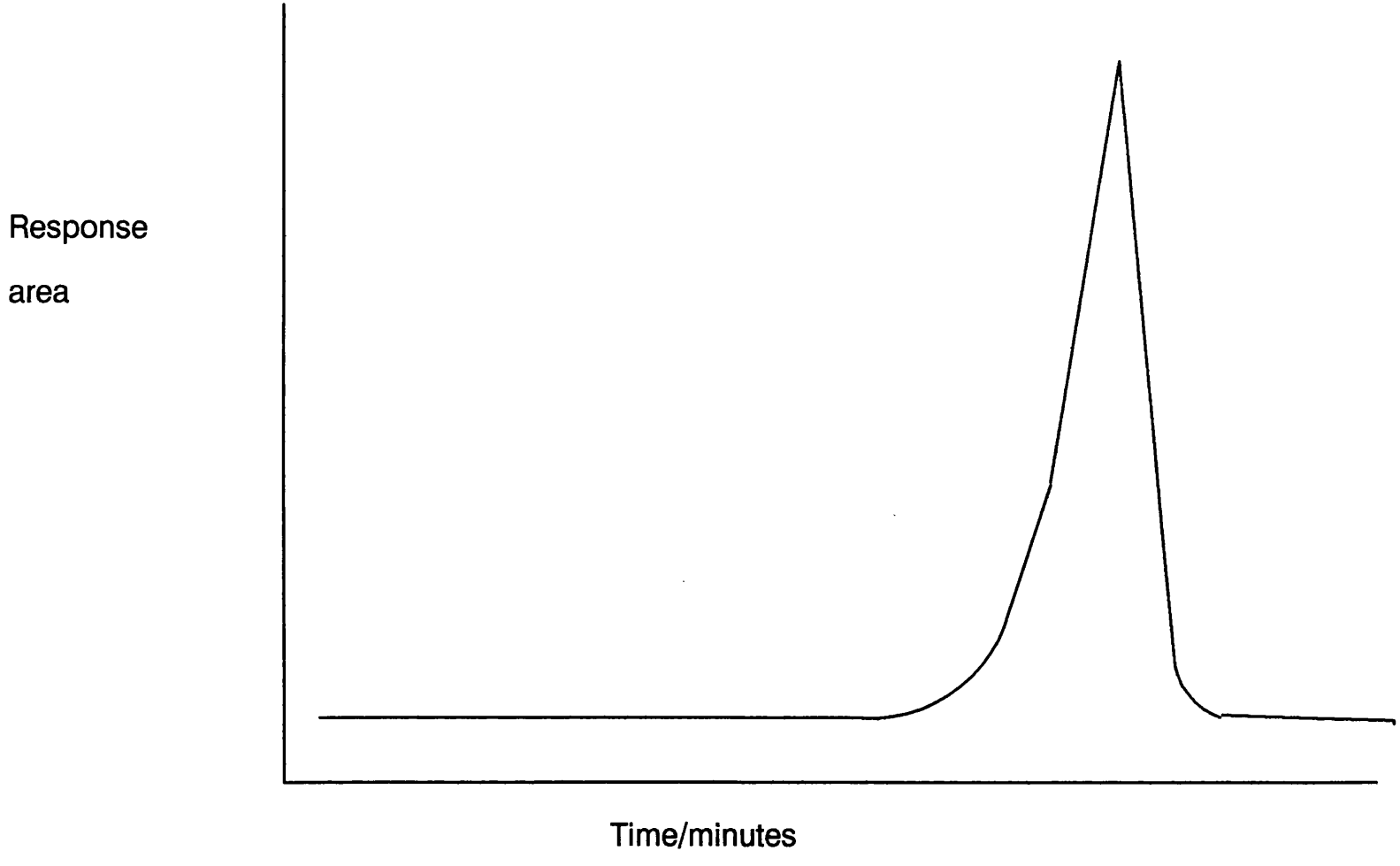

Figure 3.14:-
Schematic outline for wash procedure

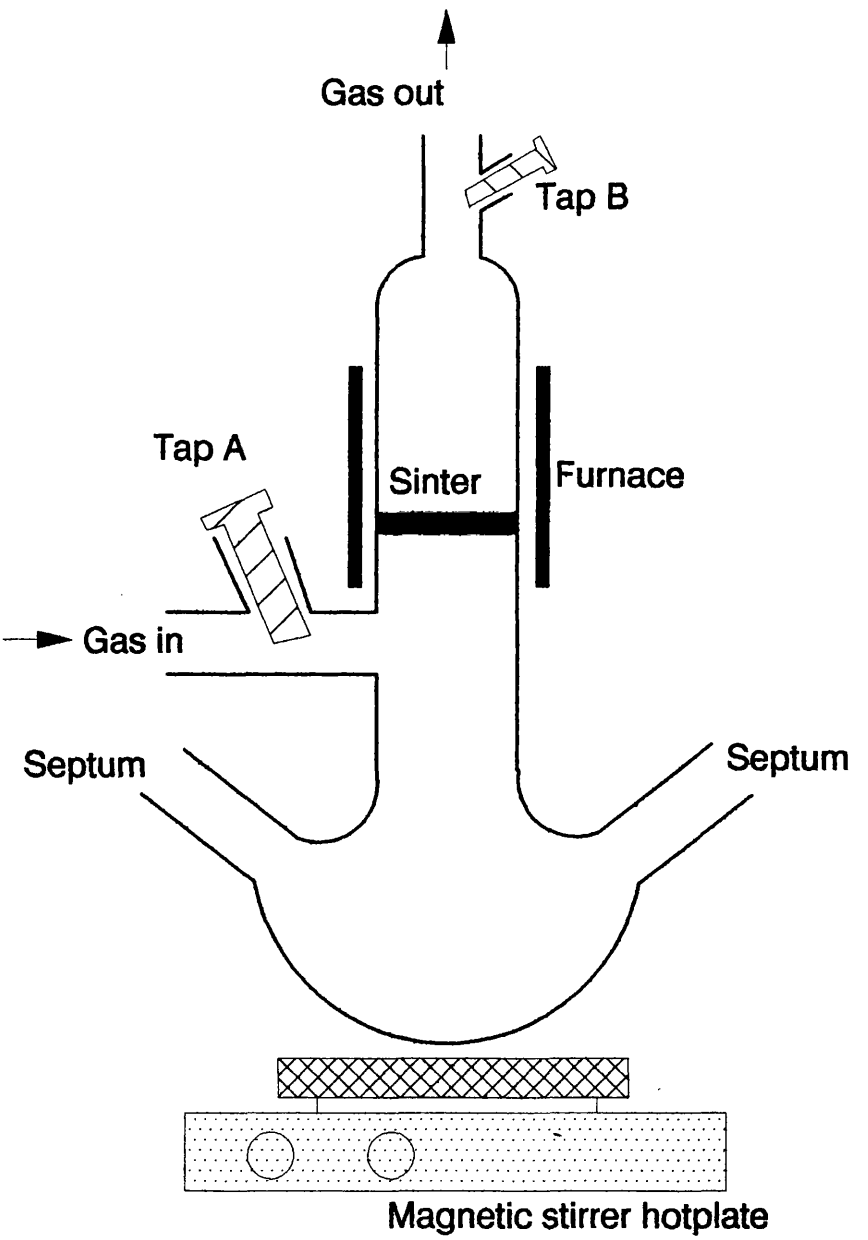

repeated at regular intervals until the boiling point of THF was reached.

3.4.5.2 Effect of time

The catalyst was washed at room temperature for an extended length of time. Samples of catalyst free liquid were removed every hour to monitor the extent of desorption of the modifier.

3.4.6 Calibration of polarimeter

Conversion of one pure enantiomer, R-(+)-2,2'-dihydroxy-1,1'-binaphthalene and R-(+)-2,2'-diamino-1,1'-binaphthalene to the other by Pt/silica Grace C10 and Pt/γ-alumina catalysts was determined as outlined in section 3.4.3.4.

A number of standard solutions of both modifiers were prepared and a calibration curve of concentration against α obtained for both the R-(+)-2,2'-dihydroxy-1,1'-binaphthalene, Figure 3.15 and R-(+)-2,2'-diamino-1,1'-binaphthalene, Figure 3.16.

3.4.7 Calibration of HPLC

The adsorption studies were carried out in either reactor R1 or R2 with the catalyst being activated for adsorption by either static or flow reduction as described in section 3.4.5. The HPLC was used to analyse the adsorption of the chiral modifiers. The adsorption of the modifier solution was monitored by the decrease in concentration of the modifier solution from the original solution injected on to the catalyst.

The origin of liquid chromatography was developed in 1903 by the Russian TSWETT and his studies on the separation of plant pigments using a glass column filled with chalk.

Chromatographic separation of a mixture of various compounds depends primarily on the fact that each of them is physiochemically different from the stationary or mobile phase. As a result of the physichemical differences, thermodynamic effects such as partition and adsorption are mostly involved. The physical state of the mobile phase determines whether the chromatography is gas (GC) of liquid (LC). The stationary phase creates a further distinction in gas chromatography, that is, gas solid (GSC) or gas liquid (GLC).

Gas chromatography although well established, before the introduction of high performance liquid chromatography, has limitations which include thermally unstable, easily oxidisable and non-volatile compounds. However, HPLC fills this gap left by GC.

In general two non-miscible phases take part in the chromatographic process, that is, the stationary and mobile phases. An equilibrium between the stationary and mobile phases is developed to create constant and reproducible conditions. The reproducible conditions are influenced by temperature, pressure and volume of the mobile phase (flow

Figure 3.15:-

Polarimetric calibration graph of

R-(+)-2,2'-dihydroxy-1,1'-binaphthalene

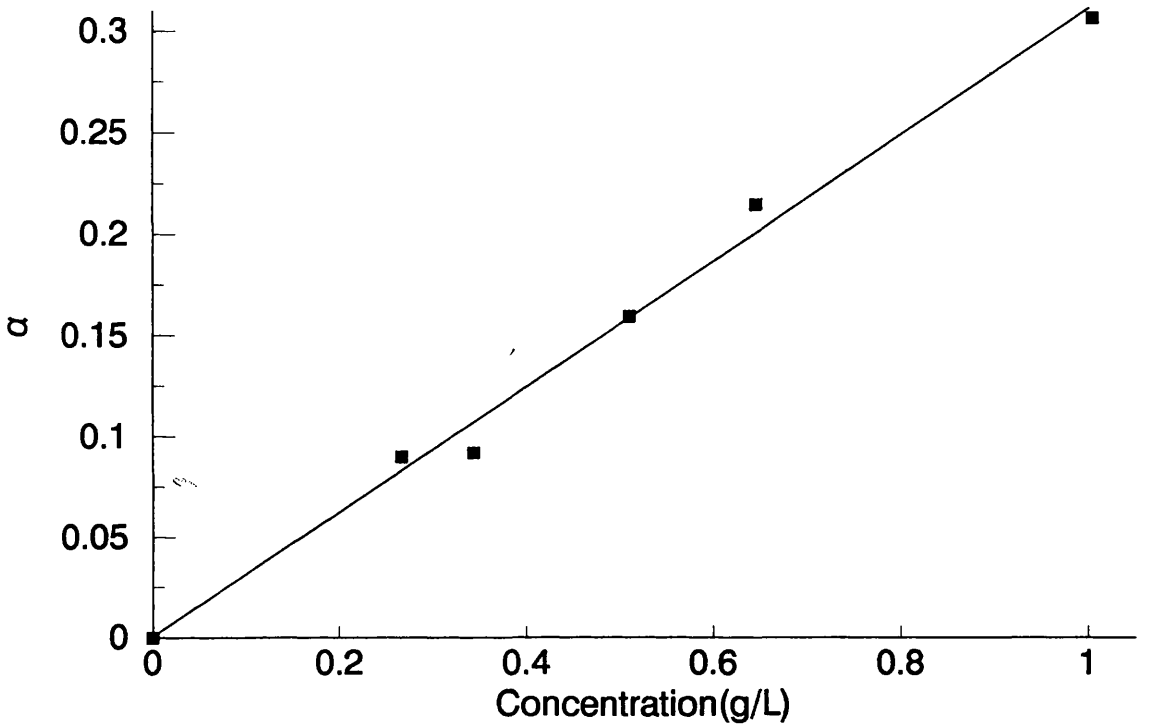

Figure 3.16:-

Polarimetric calibration graph of

R-(+)-2,2'-diamino-1,1'-binaphthalene

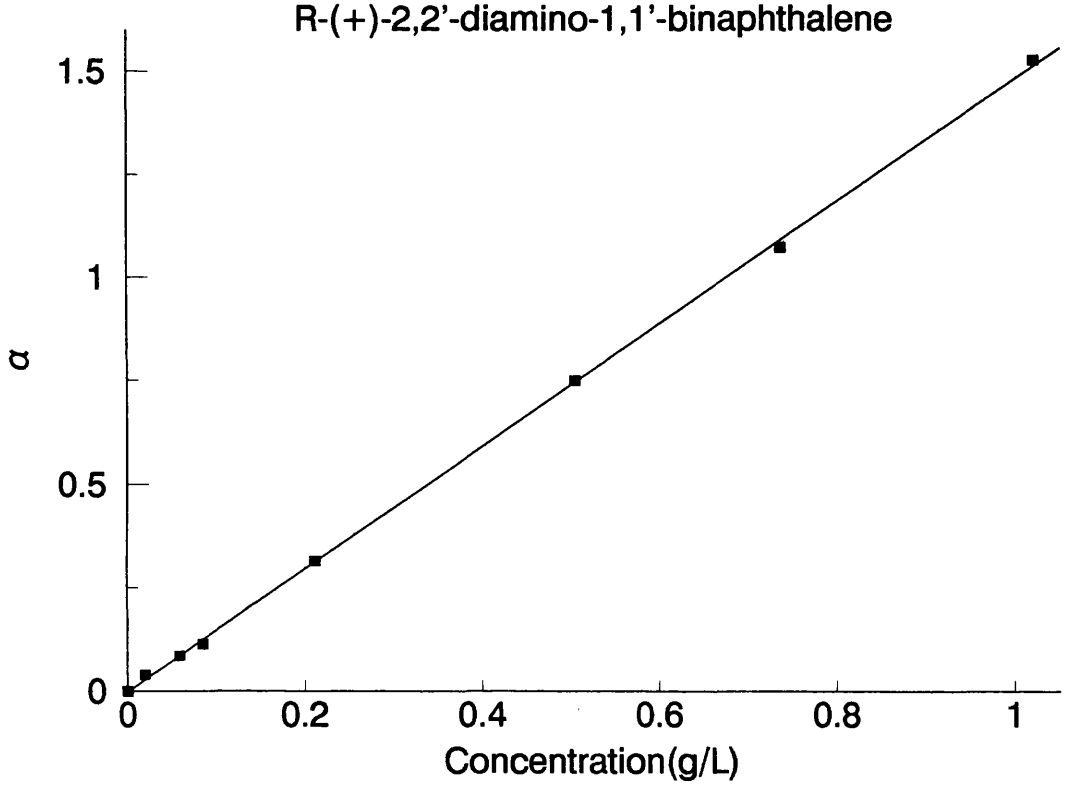

rate) and the nature of the stationary phase. The interaction of the solute components with the mobile and stationary phase results in a dynamic equilibrium.

The outline of the instrumentation is shown in Figure 3.17, that is, the following components are involved:

1. Solvent reservoir of mobile phase.
2. Mobile phase is delivered to the column by a pump system.
3. Sample loops is used to inject the sample into the flowing mobile phase just ahead of the separation column.
4. A pressure gauge is required at the front of the separation column to measure the column inlet pressure.
5. The separation column contains the packing needed to accomplish the desired HPLC separation.
6. A detector with some type of data handling device, that is, UV-VIS detector.

The concentration of a solution of modifier was determined from Beer's Law, which states

$$A = C\varepsilon l \qquad \text{Eqn 3.2}$$

that is

$$C = \frac{A}{\varepsilon l} \qquad \text{Eqn 3.3}$$

where A = absorbance of the solution

C = concentration of solution (mol l^{-1})

ε = molar absorptivity of the component (l mol^{-1} cm^{-1})

l = path length (cm)

In the case of a particular modifier both the path length and molar absorptivity remained constant. The HPLC was calibrated by the preparation of several standards of selected modifiers, that is, 2,2'-dihydroxy-1,1'-binaphthalene, 2,2'-diamino-1,1'-binaphthalene, and 2,2'-dimethoxy-1,1'-binaphthalene. Figures 3.18, 3.19, and 3.20 show the calibration curves for 2,2'-dihydroxy-1,1'-binaphthalene, 2,2'-diamino-1,1'-binaphthalene, and 2,2'-dimethoxy-1,1'-binaphthalene can be determined, respectively. From the appropriate calibration curve the concentration of the resultant modifier solution for 2,2'-dihydroxy-1,1'-binaphthalene, 2,2'-diamino-1,1'-binaphthalene, or 2,2'-dimethoxy-1,1'-binaphthalene was obtained.

For the remaining modifiers which were analysed by HPLC, the unknown concentration of the resultant solution was calculated by relating the area response of the resultant solution to the concentration and area response of the original solution by the

Figure 3.17:-
Schematic outline of HPLC

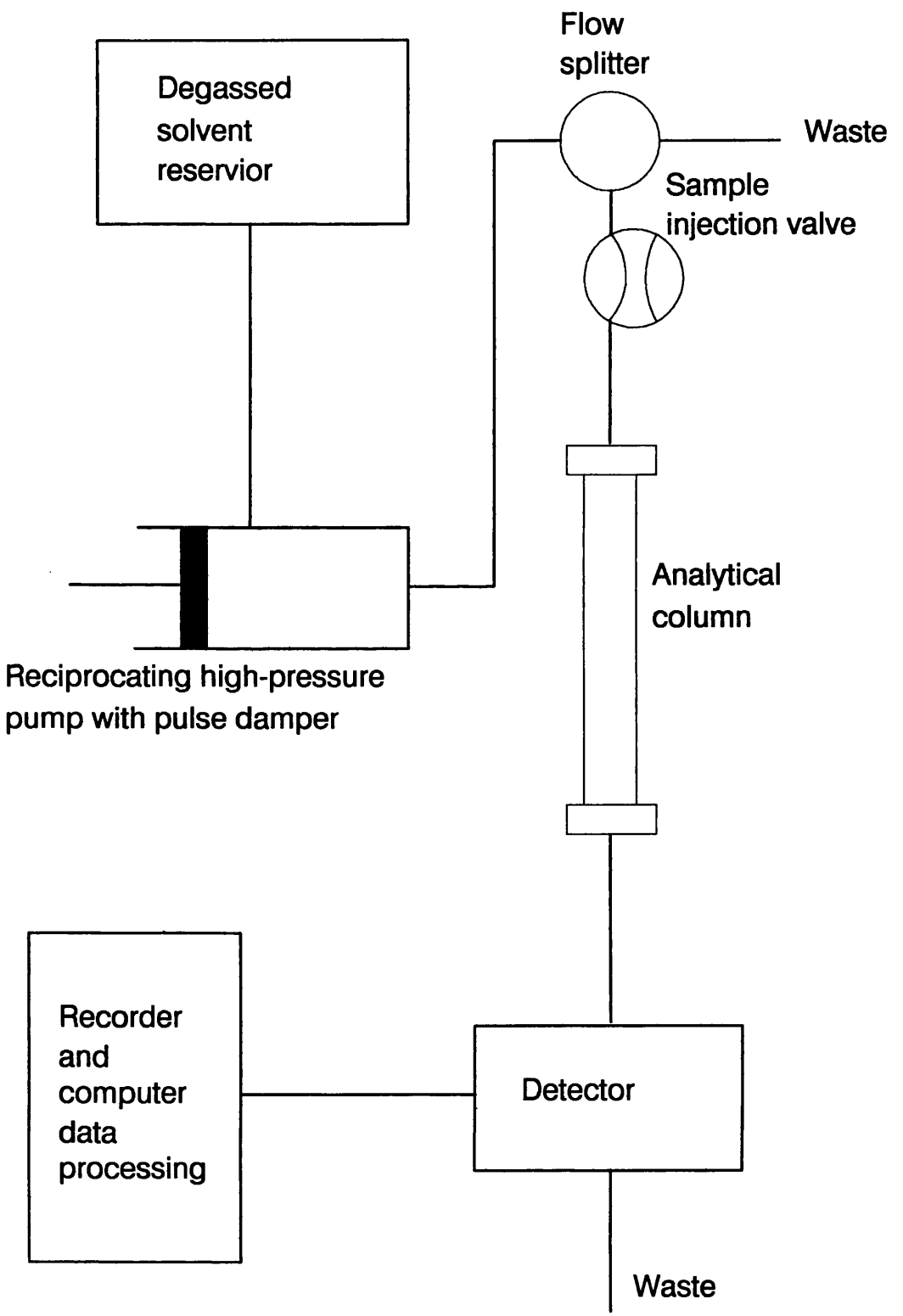

Figure 3.18:-

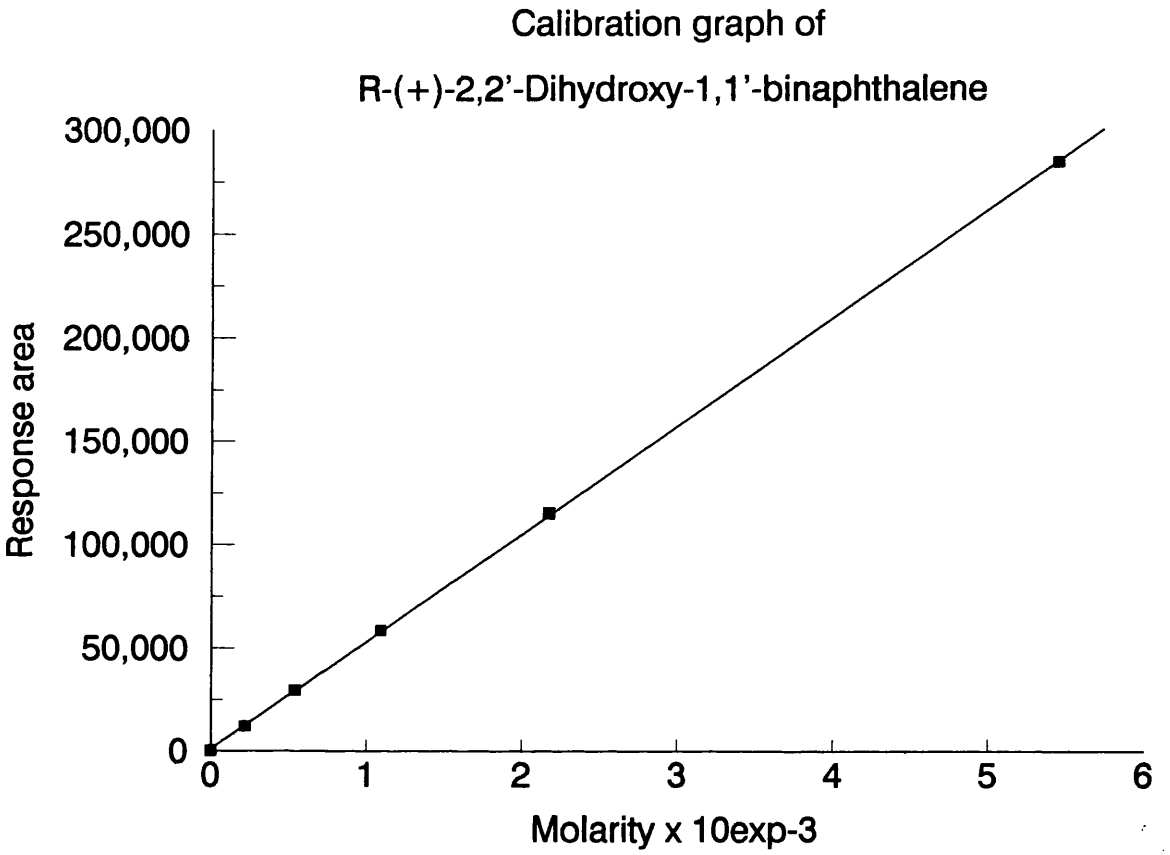

Figure 3.19:-

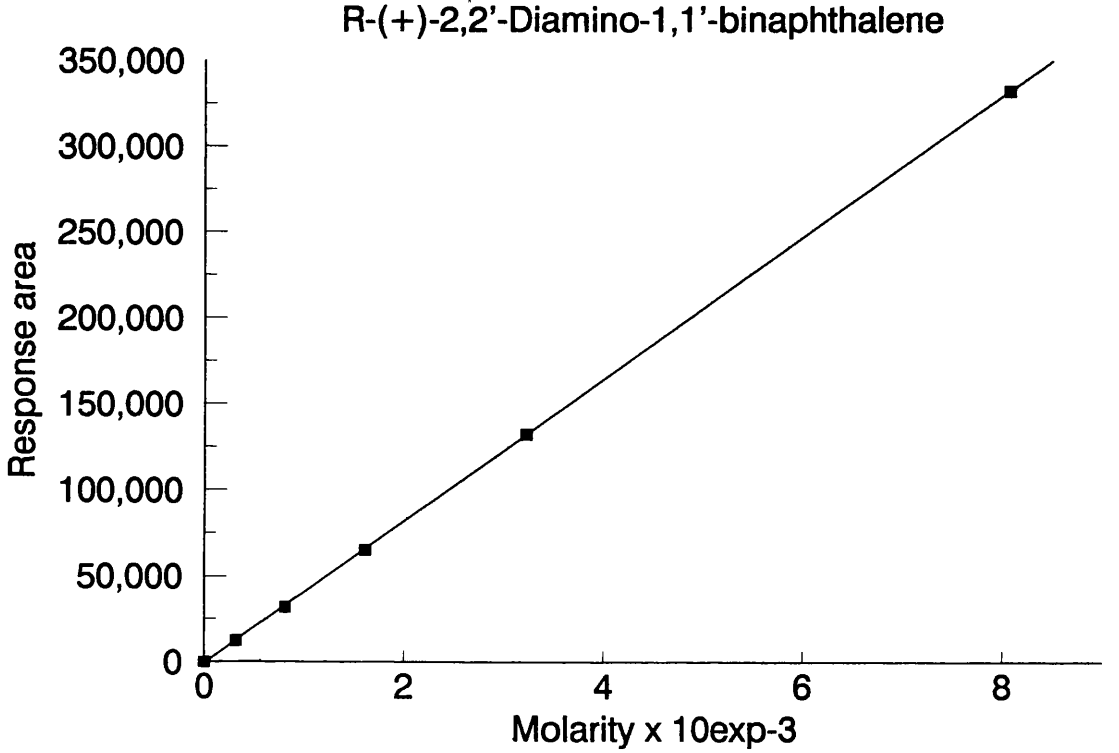

Figure 3.20:-

Calibration graph of

(±)-2,2'-Dimethoxy-1,1'-binaphthalene

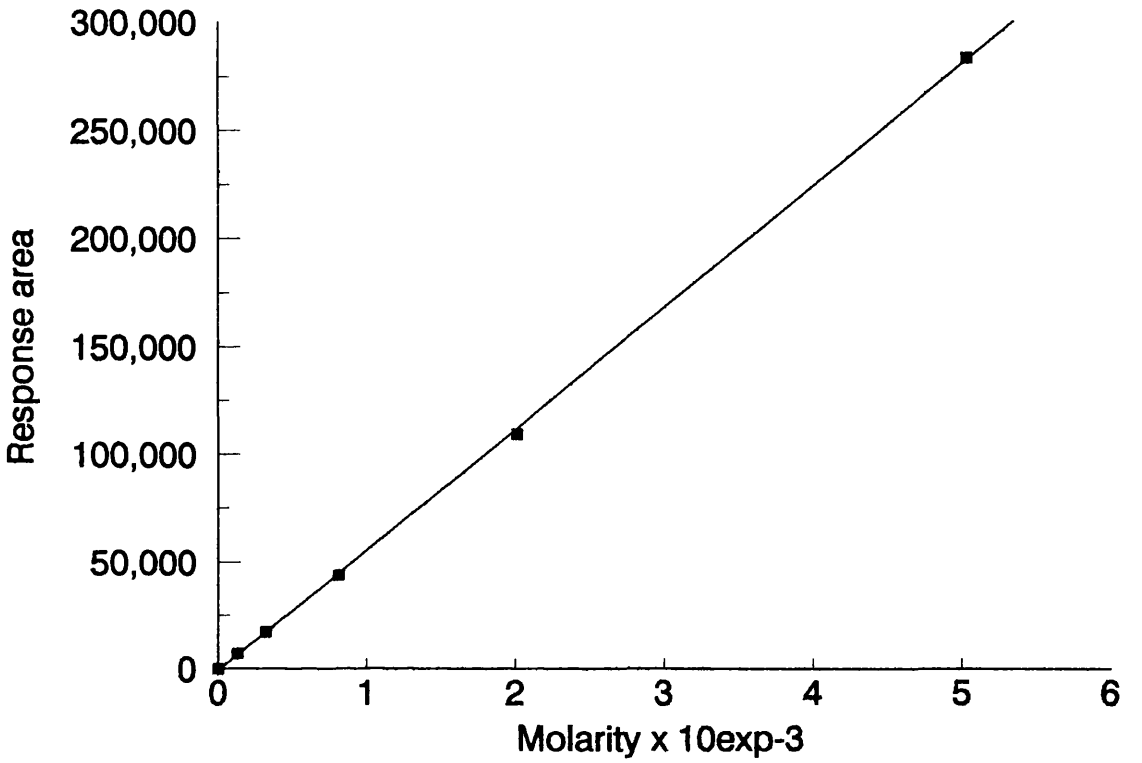

following equation:

$$C(u) = \frac{A(u) \times C(o)}{A(o)} \qquad \text{Eqn 3.4}$$

where C(u) = concentration of unknown solution.

C(o) = concentration of original solution.

A(u) = area response of resultant solution.

A(o) = area response of original solution.

The number of molecules of modifier adsorbed on to a catalyst surface was calculated by:

$$\text{Molecules}_{\text{adsorbed}} = \text{Molecules}_{\text{initially added}} - \text{Molecules}_{\text{in solution}} \qquad \text{Eqn 3.5}$$

where the molecules initially added was obtained from the concentration of the original solution added, that is,

$$\text{Moles}_{\text{added}} = \text{Molarity} \times \text{Volume}_{\text{solution added}} \qquad \text{Eqn 3.6}$$

$$\text{Molecules}_{\text{initially added}} = \text{Moles}_{\text{added}} \times 6.022 \times 10^{23} \qquad \text{Eqn 3.7}$$

The molecules remaining in solution following adsorption by the catalyst of the modifier was calculated as follows:

$$\text{Moles}_{\text{in solution}} = \text{Molarity} \times \text{Volume}_{\text{in solution}} \qquad \text{Eqn 3.8}$$

$$\text{Molecules}_{\text{in solution}} = \text{Moles}_{\text{in solution}} \times 6.022 \times 10^{23} \qquad \text{Eqn 3.9}$$

where the molarity in solution was determined either from the calibration curves in Figures 3.18, 3.19, and 3.20 or calculated from equation 3.4.

3.5 HYDROGENATION REACTIONS

The enantioselective hydrogenation of methyl tiglate, tiglic acid and 3-coumaranone (3-benzofuran) were carried out in the liquid phase at atmospheric pressure and at 293K. The 3-coumaranone hydrogenation was also examined at 273K. Tetrahydrofuran (THF) was used as the solvent for all reactions.

3.5.1 Materials

THF was supplied by Rathburns and kept under dinitrogen. Methyl tiglate (98%) was supplied by Avocado Research Chemicals and the product of the hydrogenation (±)-methyl-2-methyl butyrate (methyl butyric acid methyl ester) (99%) was supplied by Aldrich. Tiglic acid (98%) and the product of the hydrogenation 2-methyl butyric acid (98%) was supplied by Lancaster Chemicals. 3-Coumaranone (3-benzofuran) (97%) was supplied by Lancaster Chemicals and the hydrogenation product 3-benzofuranol, which was not available commercially was prepared by the reduction of C=O with sodium boronhydride and purified (see Appendix 10).

3.5.2 The reactor system

Liquid phase hydrogenations of methyl tiglate, tiglic acid and 3-coumaranone were carried out using the apparatus shown in Figure 3.10, that is, the reactor vessel R2 (see section 3.4.3.5) which had been previously used for catalyst activation and modification. The dihydrogen gas for the hydrogenations was supplied separately to the system using a bubbler inserted in one of the arms on the reactor vessel (Figure 3.21). The hydrogen gas flow rate was measured with a bubble flow meter attached to the exit from the reaction vessel and was adjusted to 1ml min^{-1}.

3.5.3 Experimental conditions

Each catalyst precursor was reduced, modified and washed in the reaction vessel, as described in sections 3.4.3.5 and 3.4.5, prior to a hydrogenation reaction, unless otherwise stated. THF was injected into the reactor vessel which was maintained under a positive pressure of dinitrogen through a septum. The volume of THF injected at this stage was dependent on the material being hydrogenated and the modification conditions of the catalyst. In all reactions the total volume of liquid was 22ml.

In the case of methyl tiglate, the total volume of THF was 20ml plus 2ml of methyl tiglate. For hydrogenation of both tiglic acid and 3-coumaranone, the total volume of THF added was 22ml. 7ml of the 22ml was used to dissolve 0.5g of either tiglic acid (5×10^{-3} moles) or 3-coumaranone (3.67×10^{-3} moles). When the modified catalyst was subjected to the wash step, the resultant solution was then removed and 15ml of clean THF added to the washed modified catalyst. In the case where the modified catalyst was not subjected to the wash step (that is, the resultant modifier solution was not removed after modification and the wash procedure outlined in section 3.4.5 omitted), 5ml of clean THF was added to the 10ml of the resultant modifier solution.

It was found that the catalyst was less susceptible to oxidation once immersed in the solvent and the two septa on the reaction vessel outlet could be removed at this stage to allow a condenser to be attached to one arm and a hydrogen bubbler to the other arm of the reaction vessel. Dihydrogen gas was bubbled through the solvent for 30 minutes. The dihydrogen bubbler contained a porous sinter to disperse the dihydrogen and enhance its solubility in the solvent, thus increasing the amount of dihydrogen available at the catalyst surface. The reactant was then added to the solvent using a syringe. The dinitrogen flow was then switched off and the reaction mixture was stirred using a magnetic stirrer. Dihydrogen gas was bubbled through the reaction mixture for a standard length of time (20 hours). Samples of the reaction mixture were withdrawn after 4 hours and at the end of the reaction time (20 hours).

Figure 3.21:-
Schematic diagram of hydrogenation system using reactor R2

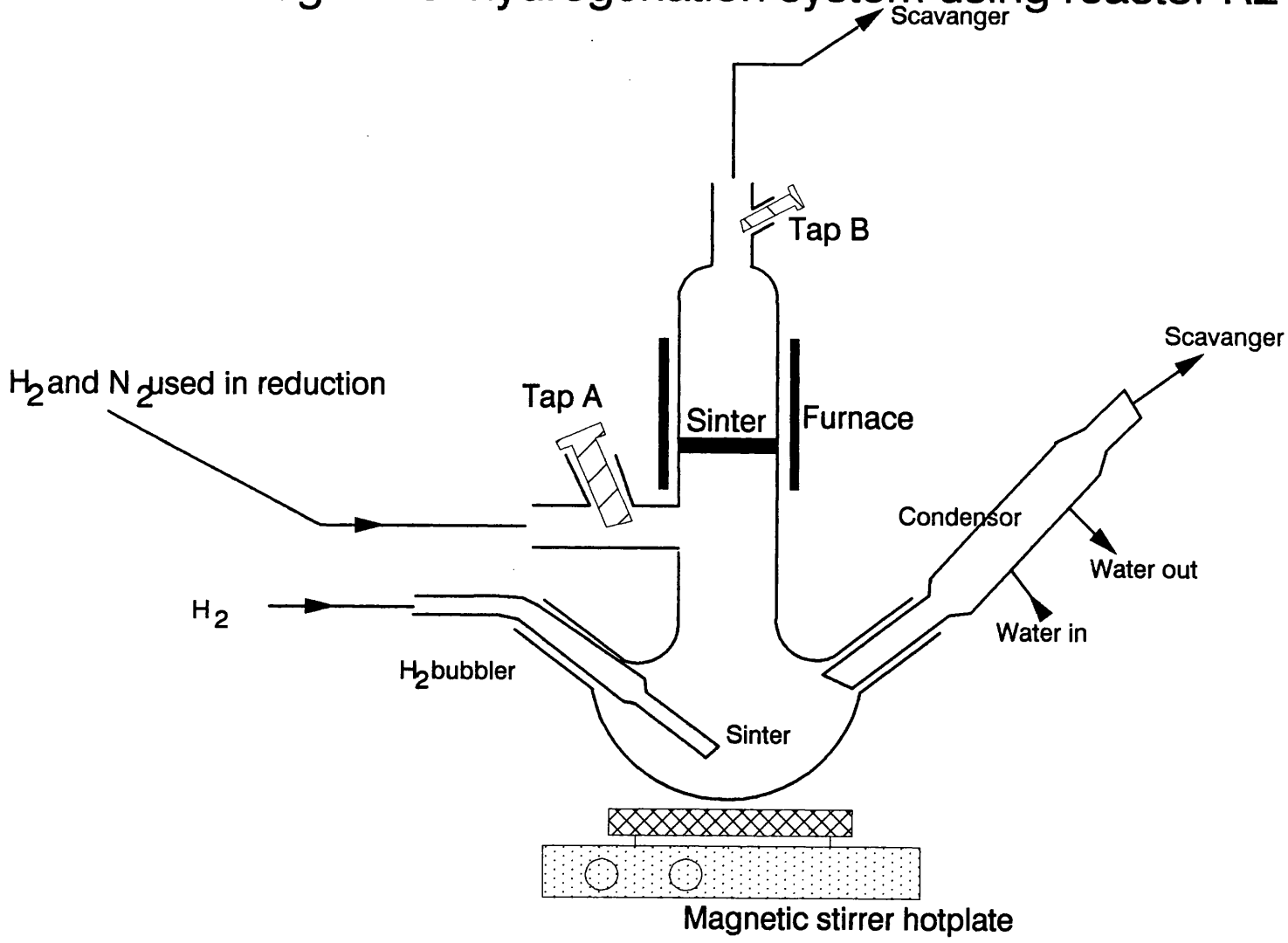

3.5.3.1 Hydrogenation of 3-coumaranone with a used R-(+)-2,2'-diamino-1,1'-binaphthalene modified Pt/γ-alumina catalyst

A sample of R-(+)-2,2'-diamino-1,1'-binaphthalene modified Pt/γ-alumina catalyst was prepared and washed as previously described (sections 3.4.3.3 and 3.4.5). This modified catalyst was used to hydrogenate one aliquot of 3-coumaranone as described in section 3.5.3. Following the 20 hours, the hydrogenation solution containing any unreacted starting material and product was removed under a positive pressure of dinitrogen, ensuring no dioxygen allowed in the system. A second aliquot of 3-coumaranone was then added and hydrogenated.

3.5.4 Analysis of the reaction mixture

A Chrompak CP 9000 Gas Chromatograph fitted with a flame ionisation detector (FID) was used to analyse both the reactants and hydrogenation products from the reaction of methyl tiglate, tiglic acid and 3-coumaranone. The FID was attached to a Hewlett Packard integrator. The column used was wall coated open tubular (WCOT) fused silica with a stationary phase (CP - Chirasil - DEX CB), prepared and supplied by Chrompak. Samples of 1μl were injected on to a chiral silica column (length 25m, outside diameter 0.39mm, internal diameter 0.25mm and film thickness 0.25mm) using a 5μl syringe.

For methyl tiglate the column was conditioned overnight at 20K above the working temperature, that is, 309K, in flowing helium (30ml min^{-1}). The column separated the solvent, reactants and the two enantiomers of the methyl-2-methyl butyrate. The order of elution was

THF < 2 enantiomers of methyl-2-methyl butyrate < methyl tiglate

For the analysis the helium carrier gas flow rate was set at 30ml min^{-1}, the air at 250ml min^{-1} and the dihydrogen at 30ml min^{-1}. A split flow ratio of 1:50 was used for the make-up gas. The column was held at 309K for the duration of the analysis. The sample constituents were vapourised at the injection port at 433K and detected using an FID at 433K. The FID was attached to an integrator.

A typical plot from the integrator is shown in Figure 3.22. Peak areas were calculated by the integrator.

In the case of tiglic acid hydrogenation, the column was conditioned overnight at 20K above the working temperature, that is 363K, in flowing helium (30ml min^{-1}). The column separated the solvent, reactant and the two enantiomers of methyl butyric acid. The order of elution was

THF < 2 enantiomers of methyl butyric acid < tiglic acid

The parameters used for separation were as follows; helium carrier gas flow rate

Figure 3.22:-

Typical GC plot for methyl tiglate hydrogenation

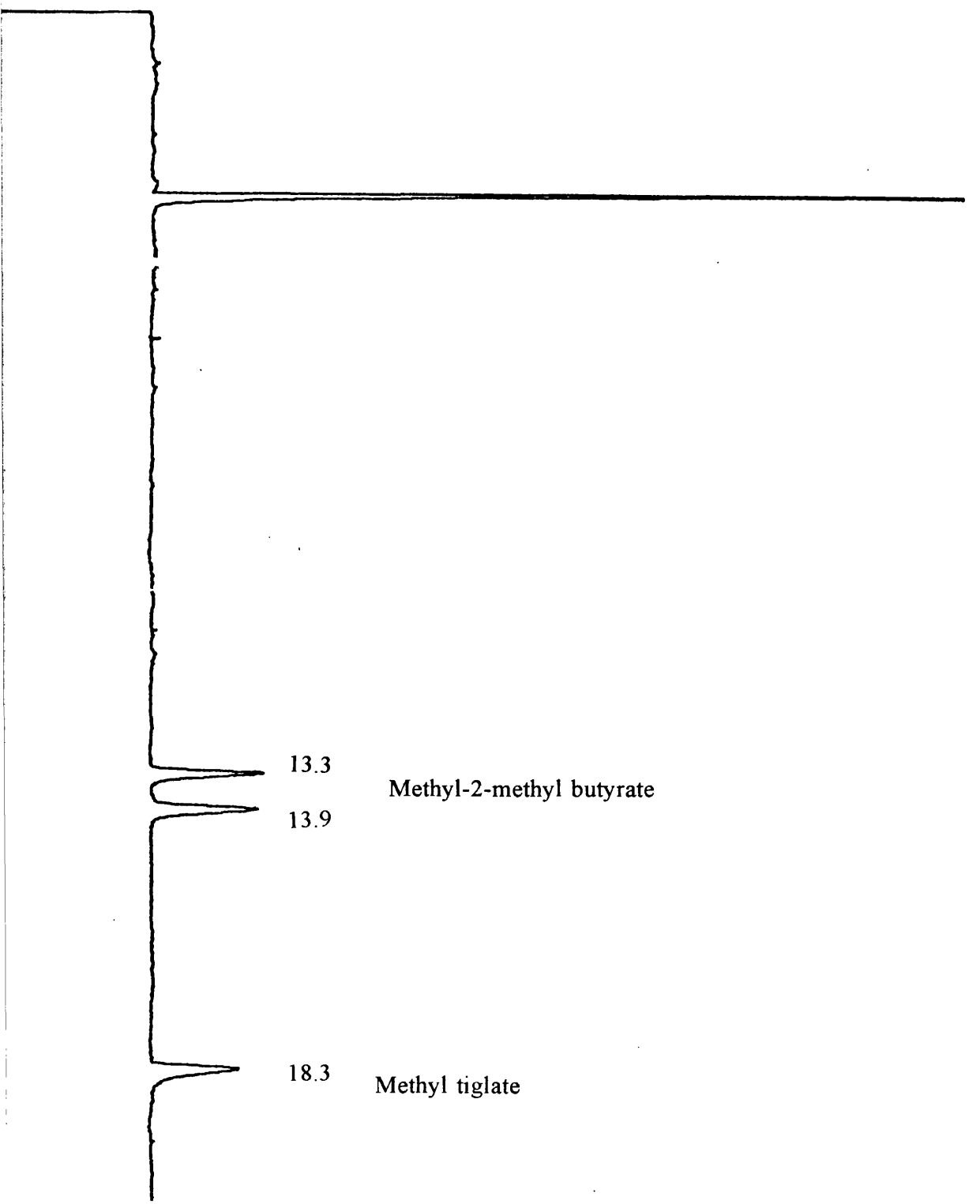

30ml min^{-1}, air 250ml min^{-1}, dihydrogen gas 30ml min^{-1}, split ratio of helium make-up gas was 1:50, isothermal separation at 363K, sample vapourisation at 453K and constituent detection by the FID at 453K. See Figure 3.23 for integrator plot.

While for 3-coumaranone, the column was conditioned overnight at 423K, in flowing helium (30ml min^{-1}). The column separated the solvent, reactant and 2 enantiomers of 3-benzofuranol. The order of elution was

THF < 3-coumaranone < S-3-benzofuranol < R-3-benzofuranol

The parameters used were; helium carrier gas flow rate 30ml min^{-1}, air 250ml min^{-1}, dihydrogen 30ml min^{-1} and split ratio of helium make-up gas 1:50. The column was held at 383K for ten minutes and then ramped to 413K at 1K min^{-1}. The integrator and detector were at 453K. Figure 3.24 shows a typical trace recorded by the integrator.

Table 3.5 shows an overall form for the approximate retention times for the three hydrogenation materials and their products.

Table 3.5:- Summary of retention times for methyl tiglate, tiglic acid and 3-coumaranone hydrogenation

Hydrogenation materials	Retention time/Minutes
Methyl tiglate hydrogenation	
2 Enantiomers of methyl-2-methyl butyrate	13.3
	13.9
Methyl tiglate	18.3
Tiglic acid hydrogenation	
2 Enantiomers of methyl butyric acid	13
	14
Tiglic acid	16
3-Coumaranone hydrogenation	
3-Coumaranone	17
Additional product	28
S-3-benzofuranol	31
R-3-benzofuranol	31.5

3.5.5 Calibration of GC

The hydrogenation reactions were carried out in a reactor system R2 as described in section 3.5.3. The GC was used to analyse the reactant products and the starting

Figure 3.23:-

Typical GC plot for tiglic acid hydrogenation

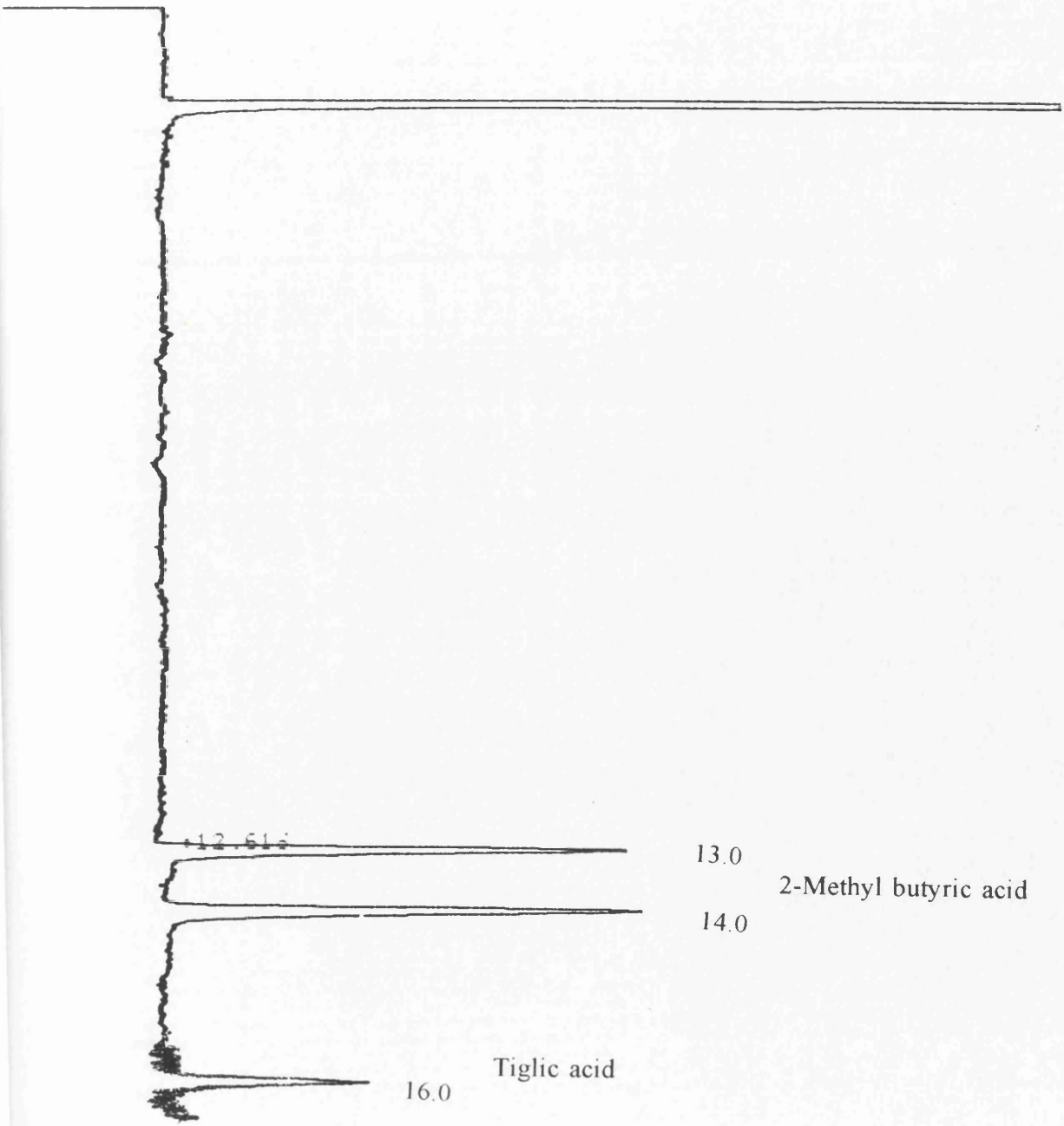

Figure 3.24:-

Typical GC plot for 3-coumaranone hydrogenation

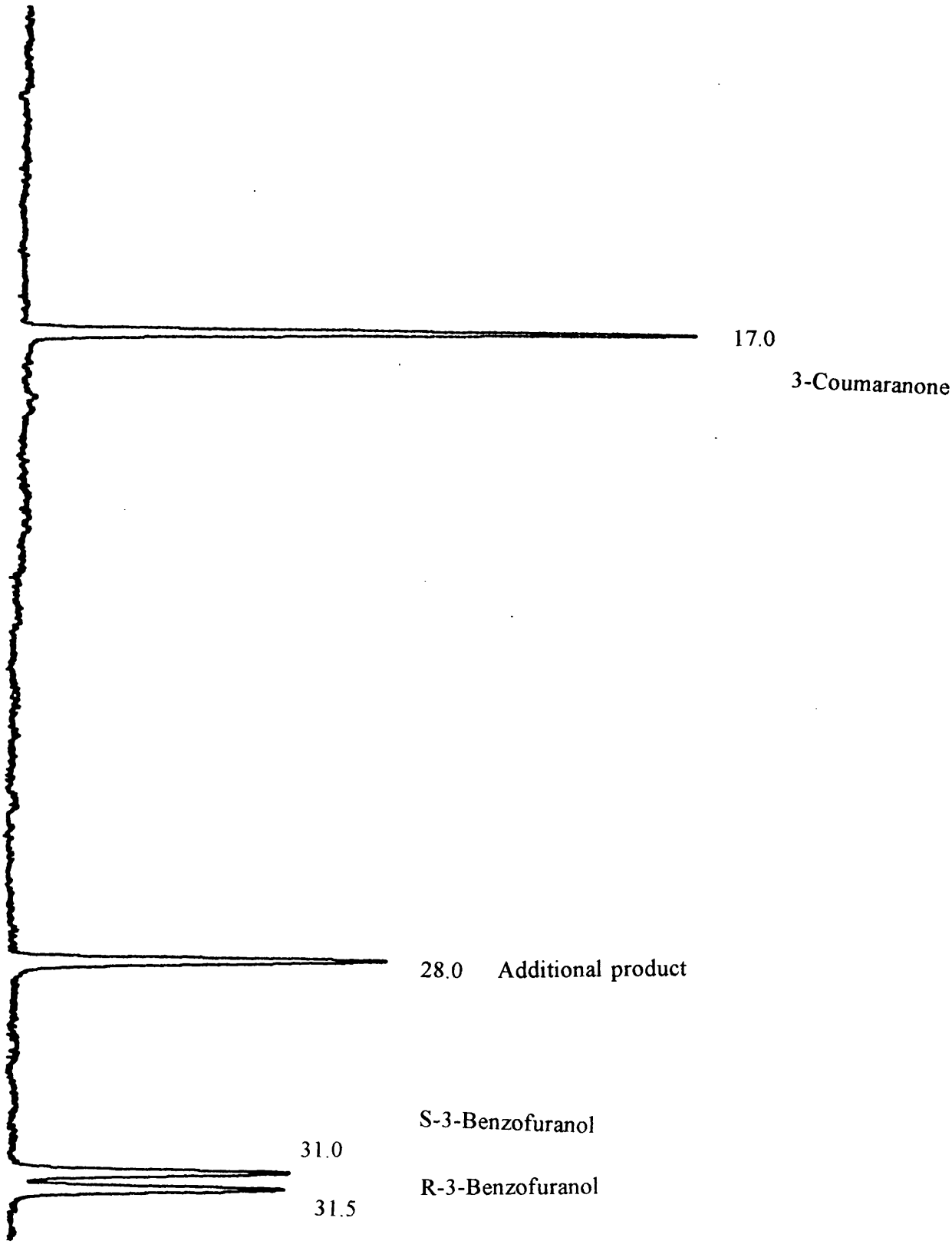

materials.

Gas chromatography is the technique of choice for the separation of thermally stable and volatile organic and inorganic compounds. GC is a remarkably sensitive and selective method for the qualitative and quantitative determination of substances. GC is based on the phenomenon that occurs when a mixture of volatile materials is transported by a carrier gas eluent through a column containing an adsorbing material coated on a solid material; each volatile component is partitioned between the stationary phase and carrier gas. The length of time required for a volatile analyte to traverse the column depends upon the degree to which it is retained by the stationary phase. A GC therefore consists of several basic modules joined together to (1) provide a constant flow of carrier gas (mobile phase), (2) permit the introduction of sample vapours into the flowing gas stream, (3) contain the appropriate length of stationary phase, (4) maintain the column at the appropriate temperature (or temperature-programme sequence), (5) detect the sample components as they elute from the column, and (6) provide a readable signal in magnitude to the amount of each component. The outline of the instrumentation is shown in Figure 3.25.

3.5.5.1 Chiral chromatographic separations

Chromatographic separation of a mixture of enantiomers can be done by one of two methods, that is, by either indirect or direct separation. Indirect separation which involves the formation of diastereomeric derivatives has a number of relatively unattractive disadvantages, for example, the derivatisation step can cause racemisation at the chiral centre to occur. The direct separation, namely, by the use of a chiral stationary phase is a more suitable mode for enantioselective separation.

As in all forms of chromatography, separation is based on differences in retention of some kind by the stationary phase. The introduction of immobilised coatings in fused silica capillary GC has led to the retention of the analyte being primarily of a molecular interaction with the stationary phase rather than a series of equilibria of the analyte with the stationary and mobile phases as seen for packed columns.

The theory of chiral chromatography, that is, the separation in which a chiral stationary phase selectively retains more of one enantiomer than the other is still rudimentary. A number of chiral recognition models have been proposed to account for optical resolution. The models are often based on the 'three-point interaction' theory put forward by Dalgleish in 1952.[117] According to this theory, three simultaneously operating interactions between an enantiomer and the stationary phase are needed for chiral discrimination. However, it has been shown that direct chromatographic optical resolution

Figure 3.25:-
Schematic outline of a gas chromatograph

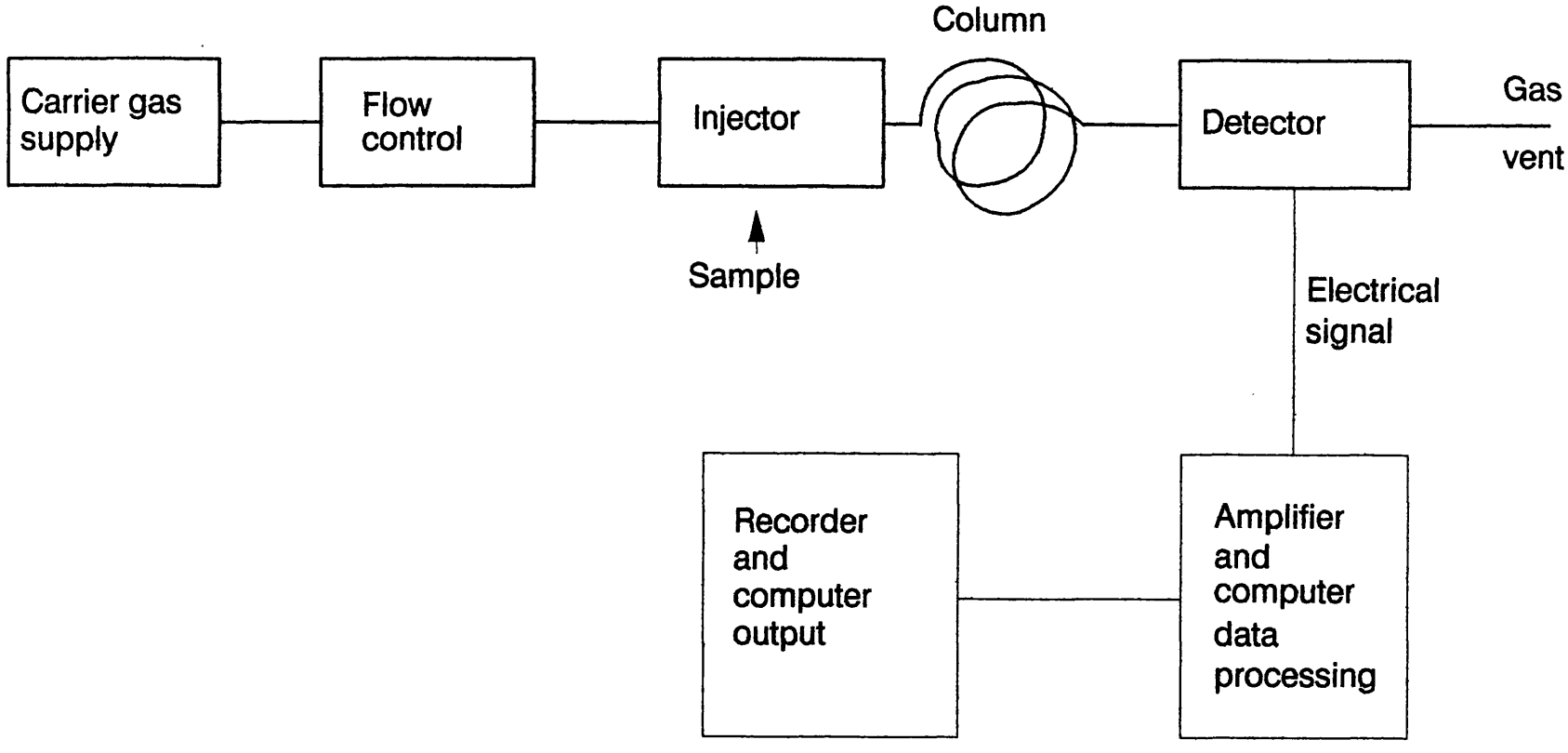

has been achieved from a range of many types of molecular interactions.

As a result of the molecular interaction of enantiomers with the stationary phase, the construction of chiral cavities has been attempted for the preferential inclusion of one enantiomer, that is, extend the idea that enantiomeric differentiation is based entirely on steric fit. Although no chiral stationary phase (CSP) has been prepared that is based entirely on steric exclusion from chiral cavities. However, CSPs exist where steric exclusion not is of primary importance. These CSPs include cyclodextrins and crown-ether phases which as based on the inclusion phenomena.

Chiral GC has evolved from CSPs based on (1) hydrogen bonding between amino acids and the analyte; and between diamides attached to a silicone polymer backbone by the amino function and the analyte; (2) chiral metal complexes and the analyte; and (3) on inclusion effects. All CSPs are limited, for example, the low temperatures at which the column can operate before column bleeding can occur, chiral discrimination and column efficiency. The inclusion effect is based on a cyclodextrin (CD) as a chiral selector. The β-CD has been shown to have a larger retention of compounds than α-CD, indicating β-CDs are more stable. However, the column must be used at very low temperatures, that is, at less than 343K. Although recent developments have led to the bonding of β-CD to the silica surface of a wall coated open tubular (WCOT) capillary GC column and allowed the temperature of operation to be successfully increased.

Though the concept of chiral GC is quite clear, that is, that enantiomers are separable with a chiral stationary phase, the situation is more complex for chiral liquid chromatography (LC). Separation by LC depends on whether enantiodifferentiation takes place through a chiral recognition effect by the stationary phase or by a constituent of the mobile phase forming a diastereomeric complex *in situ* during the chromatographic process.

The chiral GC used was calibrated by the preparation of several standards of mixtures of reactant products and starting materials with known mole fractions of each reactant and staring material in each mixture. For example, for the methyl tiglate hydrogenation, a mixture was prepared where 0.2ml of methyl tiglate and 0.2ml methyl-2-methyl butyrate were added to 2ml of THF. Table 3.6 shows the % Areas obtained for the appropriate mole fractions.

Table 3.6:- % Area of mole fraction of methyl tiglate hydrogenation		
Material	Mole fraction	% Area
Methyl-2-methyl butyrate[a]	0.25	22.1
Methyl-2-methyl butyrate[b]	0.25	22.0
Methyl tiglate	0.5	55.9

a 1st enantiomer eluted
b 2nd enantiomer eluted

The calibration curve in Figure 3.26 was obtained which shows a plot of mole fraction of methyl tiglate against % Area while Figure 3.27 shows a plot of mole fraction of methyl-2-methyl butyrate against % Area for the total of both enantiomers.

Similar standards were prepared for tiglic acid and 3-coumaranone hydrogenations and the results for one mixture for each of the starting materials and their reactant product are shown in Table 3.7 and Table 3.8, respectively.

Table 3.7:- % Area of mole fraction of tiglic acid hydrogenation		
Material	Mole fraction	% Area
Methyl butyric acid[a]	0.25	22.6
Methyl butyric acid[b]	0.25	22.4
Tiglic acid	0.50	55.0

a 1st enantiomer eluted
b 2nd enantiomer eluted

Table 3.8:- % Area of mole fraction of 3-coumaranone hydrogenation		
Material	Mole fraction	% Area
3-Coumaranone	0.50	53.0
3-Benzofuranol[a]	0.25	23.4
3-Benzofuranol[b]	0.25	23.6

a S enantiomer
b R enantiomer

As for methyl tiglate, calibration curves are obtained for mole fraction tiglic acid against % Area and mole fraction methyl butyric acid against % Area for both enantiomers and are shown by Figures 3.28 and 3.29, respectively. While Figure 3.30 and 3.31 show the calibration curves for mole fraction 3-coumaranone against % Area and mole fraction 3-

Figure 3.26:-

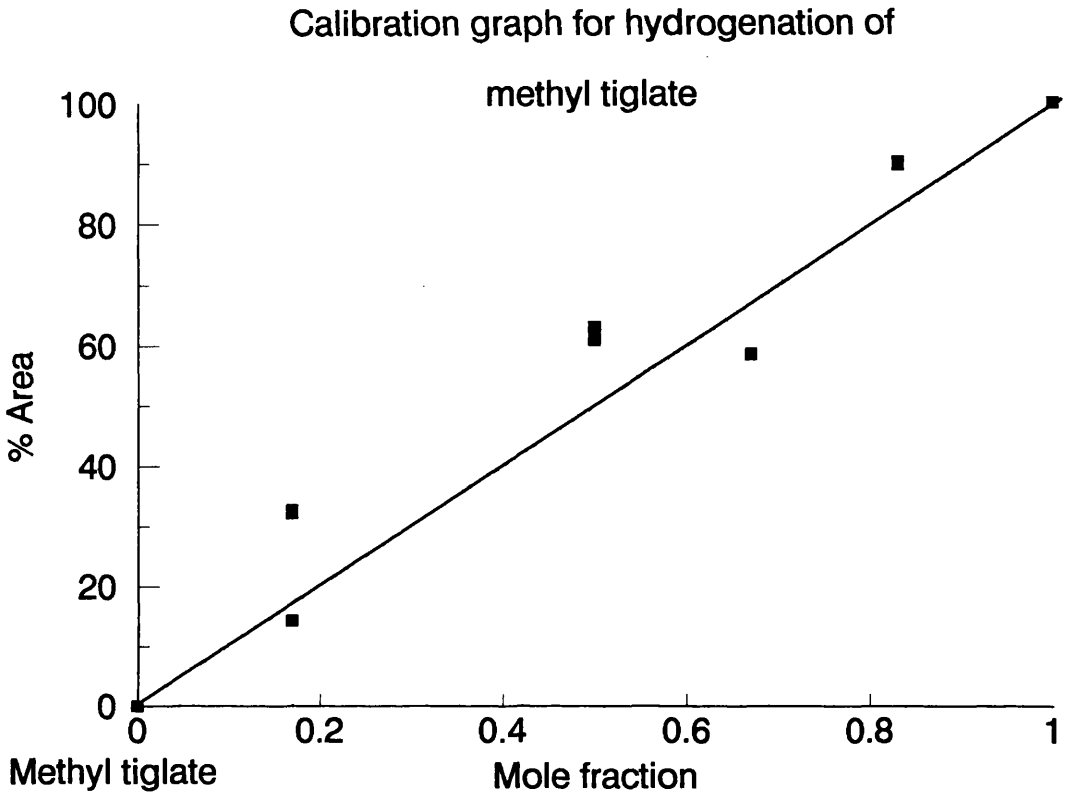

Figure 3.27:-

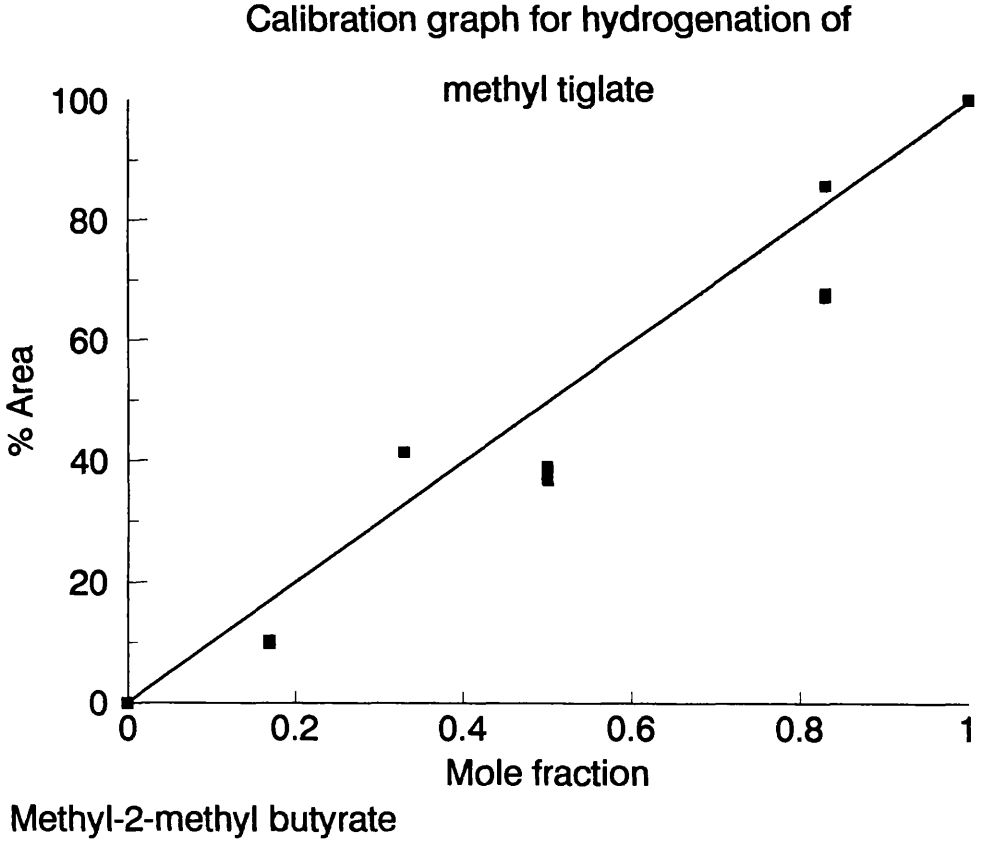

Figure 3.28:-

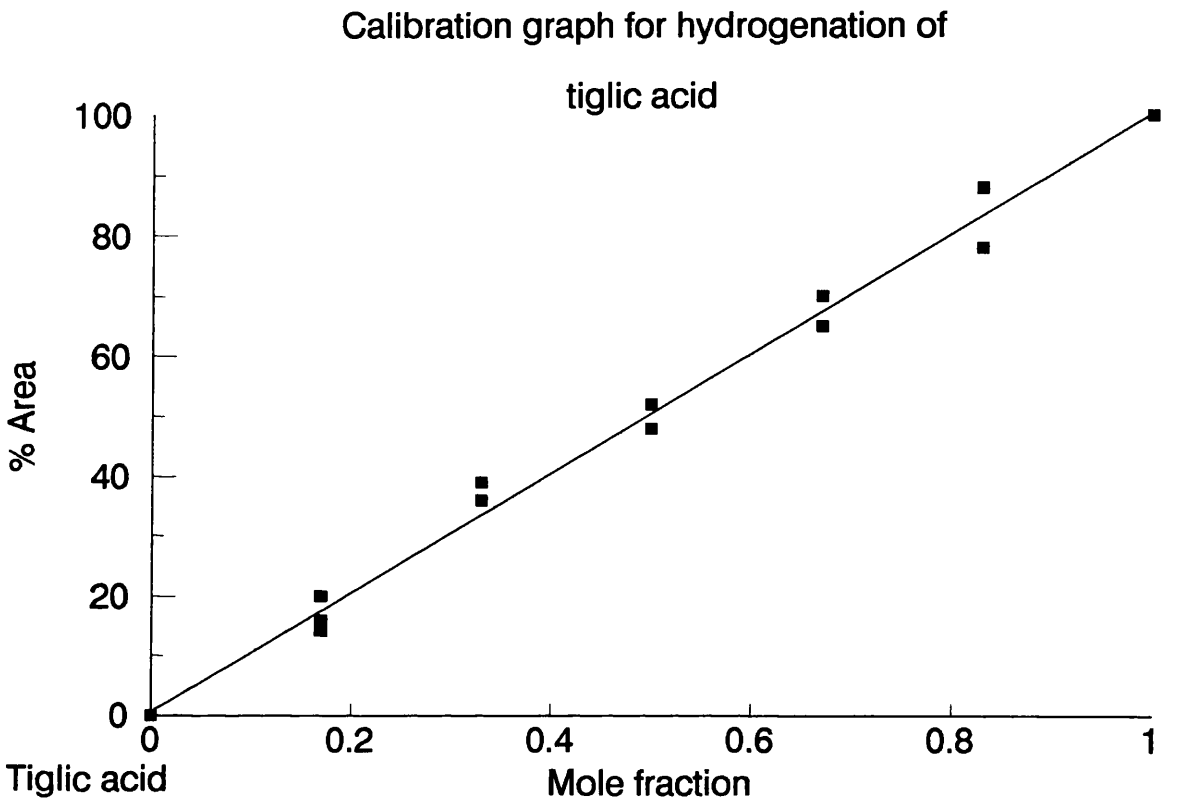

Figure 3.29:-

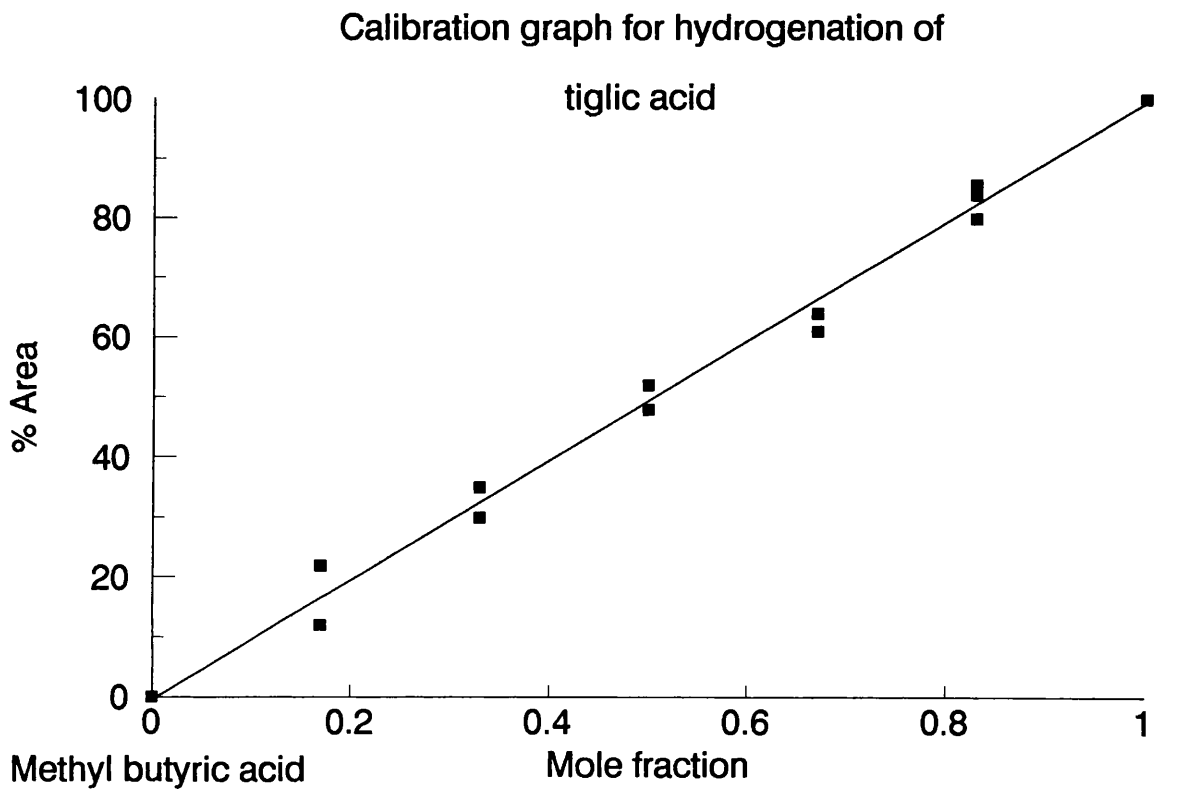

Figure 3.30:-

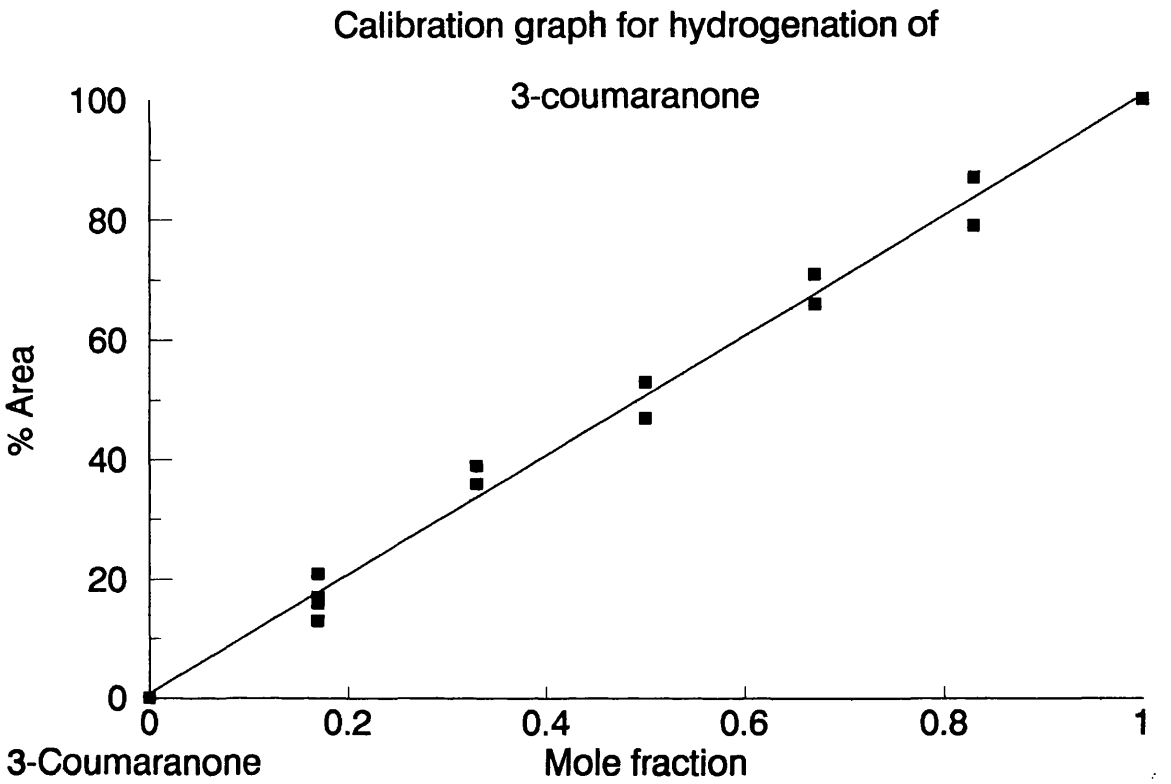

Figure 3.31:-

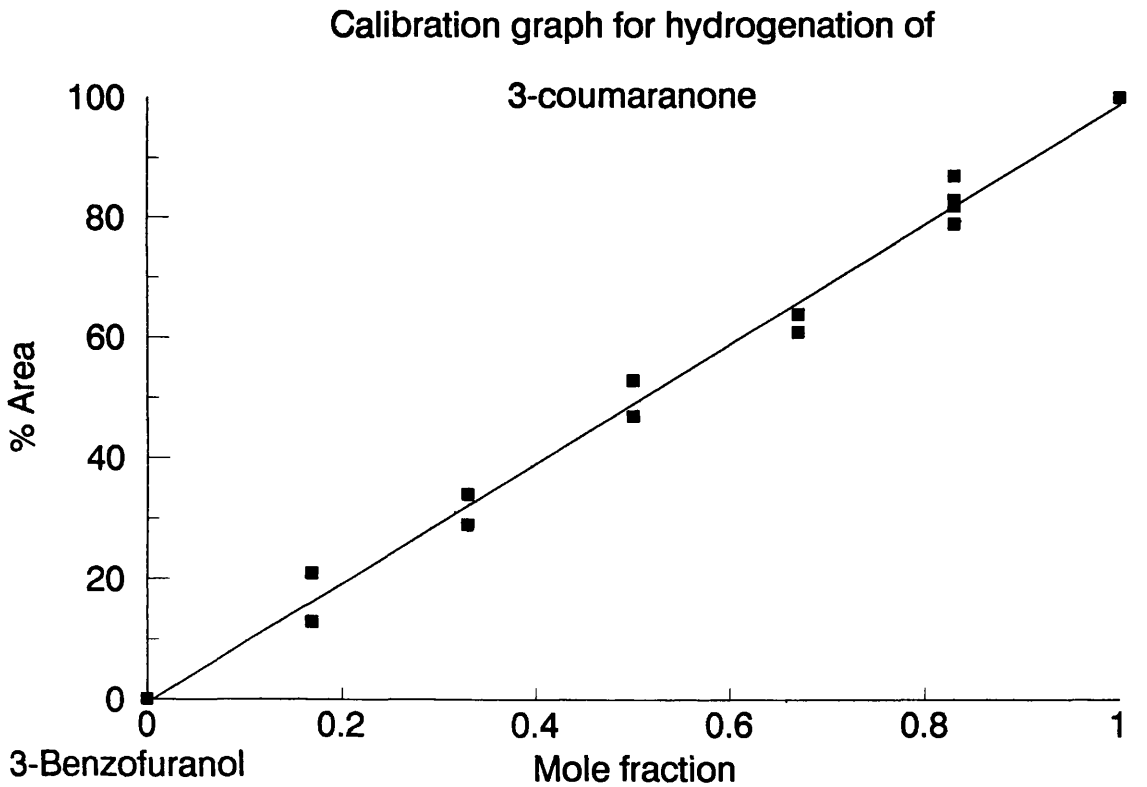

benzofuranol against % Area for both enantiomers.

3.5.5.2 Conversion levels

The mole fraction which has undergone hydrogenation is denoted as A. When either methyl tiglate, tiglic acid or 3-coumaranone are the reactant.

$$A = 1 - \text{mole fraction of reactant}$$

The % conversion is then given by

$$\% \text{ Conversion} = (A*100)\%$$

Hydrogenations in which the formation of an additional product is observed, the conversion of starting material is calculated as before ie.

$$A = 1 - \text{mole fraction of reactant}$$

However, the conversion of the additional product is determined by the use of the calibration plot of expected product against % Area of both enantiomers. The mole fraction which has been transformed to the expected and additional product is denoted by B. The mole fraction of additional product formed is denoted by C.

$$B = 1 - \text{mole fraction of expected product}$$

$$C = B - A$$

The % conversion is given as before, that is,

$$\% \text{ Conversion} = (B*100)\%$$

$$\% \text{ Conversion} = (C*100)\%$$

3.5.5.3 Enantiomeric excess

The enantiomeric excess (e.e.) of the chiral products can be described as the amount of excess of enantiomer over the other. The e.e. is defined as follows:

$$\text{Enantiomeric excess (e.e.)} = \frac{a - b}{a + b}$$

The % enantiomeric excess is given by

$$\% \text{ Enantiomeric excess (\% e.e.)} = [(e.e)*100\%]$$

where

a 1st enantiomer eluted

b 2nd enantiomer eluted

CHAPTER 4
RESULTS

4.1 CATALYST CHARACTERISATION

4.1.1 Ultra-violet-Visible spectroscopy

Solid state ultra-violet and visible (UV-VIS) spectroscopy was carried out in the instrument described in section 3.3.1. The absorption maxima and band assignments of the UV-VIS spectra of the dried, supported Pt salts are recorded in Table 4.1. The absorption maxima and band assignments for aqueous hexachloroplatinic acid and PtO_2/γ-alumina are also included in the table, as reported by Jackson *et al*[118] in a previous study of supported platinum catalysts.

Table 4.1:- Absorption maxima and band assignment of UV-VIS spectra of catalysts

Catalyst	Assignment of wavelength/nm ($^1A_{1g} \rightarrow$)					
	$^3T_{1g}$	$^3T_{2g}$	$^1T_{1g}$	$^1T_{2g}$	LMCT	
1% w/w Pt/γ-alumina		450	345			200
1% w/w Pt/Grace silica (OCTOBER 1992)		450	370		280	210
1% w/w Pt/Grace silica (APRIL 1994)		440	350		293	205
1% w/w Pt/Cab-O-Sil		450	360		275	210
$[PtCl_6]^{2-}$(aq)		452	362		263	205
PtO_2/γ-alumina		450	359			209

$^1A_{1g} \rightarrow {}^xT_{xg}$ = spin-allowed transitions of the d-electrons of Pt,
where x = 1 or 3 and xg = 1 or 2
$^xT_{xg}$ = d-d transitions
LMCT = Ligand-to-metal charge transfer

The UV-VIS spectroscopic data for the catalyst compares well with literature data available on octahedral Pt(VI) species.[119,120]

4.1.2 Temperature programmed reduction

Temperature-Programmed Reduction (TPR) experiments were carried out in the apparatus described in section 3.2.2. The TPR profiles reflect the reduction processes involved. The profile or 'fingerprint' reflects the correct composition of the catalyst. For the 1% w/w Pt/γ-alumina, 1% w/w Pt/Grace silica C10 and 1% Pt/Cab-O-Sil the reduction profile showed one peak. This peak was indicative of the species reduced to Pt metal. Table 4.2 summarises the maximum temperature of reduction, that is, the temperature at the maximum point of the reduction peak. The table also shows the temperature at which

complete reduction of the species is attained.

Table 4.2:- Temperature-programmed reduction results		
Catalyst	Optimum reduction temperature/K	Temperature for complete reduction/K
Pt/γ-alumina	491	573
Pt/Grace silica C10	409	483
Pt/Cab-O-Sil unsintered (JUNE 1994)	468	523
Pt/Cab-O-Sil unsintered (JUNE 1995)	613	673

The TPR profiles are shown by Figures 4.1 to 4.4.

4.1.3 Chemisorption

Chemisorption studies using O_2(g) and CO(g) as adsorbates were carried out in the apparatus described in section 3.3.3. The 1% w/w Pt/-alumina and 1% w/w Pt/Grace silica C10 were subjected to a reduction temperature at which, from TPR experiments, complete reduction of the platinum precursor was attained. The temperature used for 1% w/w Pt/-alumina was 573K and 1% w/w Pt/Grace silica C10 was 523K. Initial TPR results for 1% w/w Pt/Cab-O-Sil indicated complete reduction would be attained at 523K and so the chemisorption studies of O_2(g) and CO(g) on to Pt/Cab-O-Sil were undertaken following activation of the precursor at 523K. For the sintered 1% w/w Pt/Cab-O-Sil the chemisorptions were done after the activation of the precursor at 723K. The results are summarised in Table 4.3. The dispersion figures were calculated as follows: in the case of O_2(g), the molecule dissociates into two oxygen atoms and so two platinum atoms are required for the adsorption of one dioxygen molecule, that is $2M + O_2 \rightarrow 2M\text{-}O$; and the CO molecule is adsorbed via an associative mechanism in a linear mode and so for every CO molecule adsorbed one metal atom is required, that is $M + CO \rightarrow M\text{-}CO$.

Figure 4.1:-

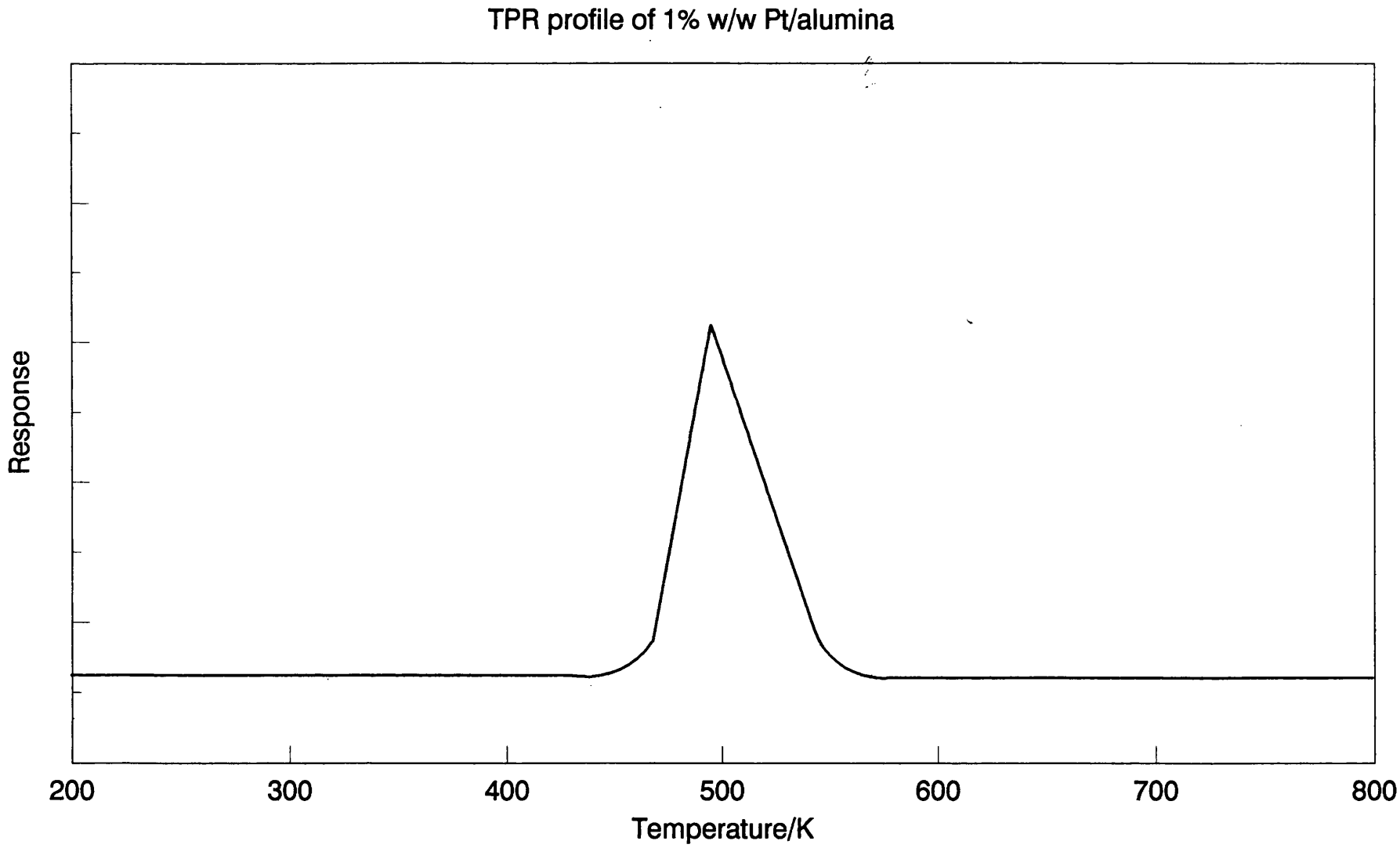
TPR profile of 1% w/w Pt/alumina
Response
200
300
400
500
600
700
800
Temperature/K

Figure 4.2:-

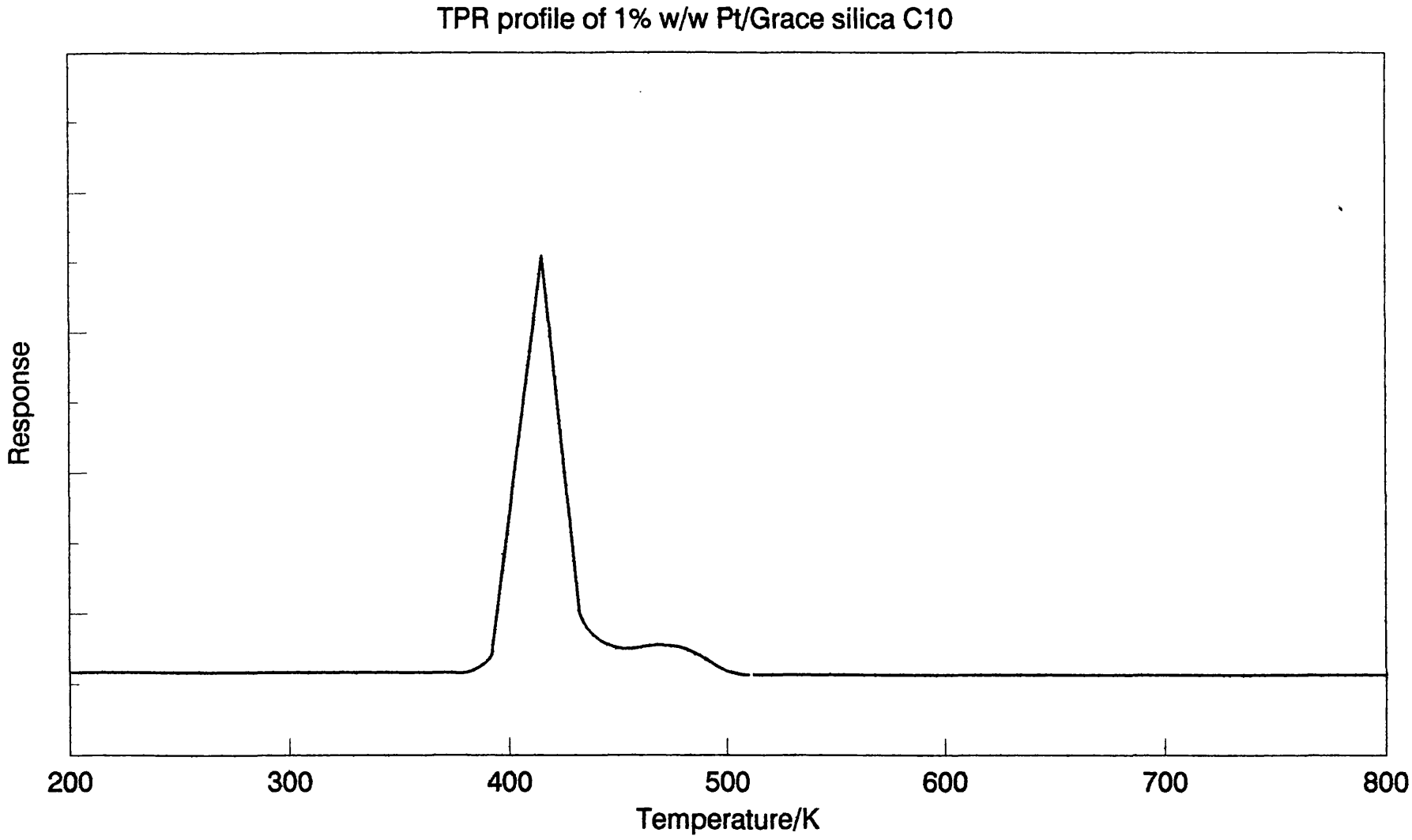
TPR profile of 1% w/w Pt/Grace silica C10
Response
200
300
400
500
600
700
800
Temperature/K

Figure 4.3:-

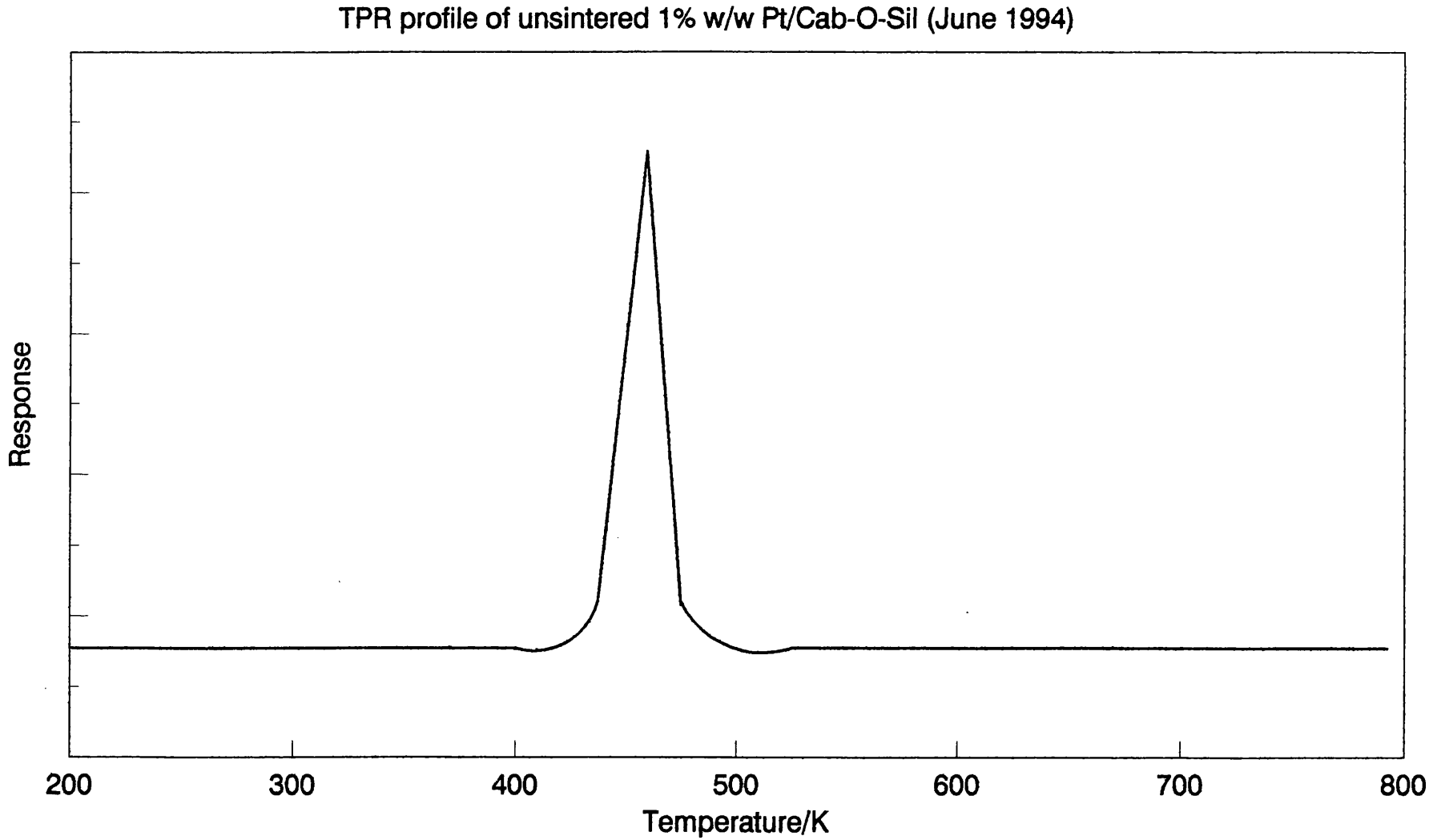
TPR profile of unsintered 1% w/w Pt/Cab-O-Sil (June 1994)
Response
200
300
400
500
600
700
800
Temperature/K

Figure 4.4:-

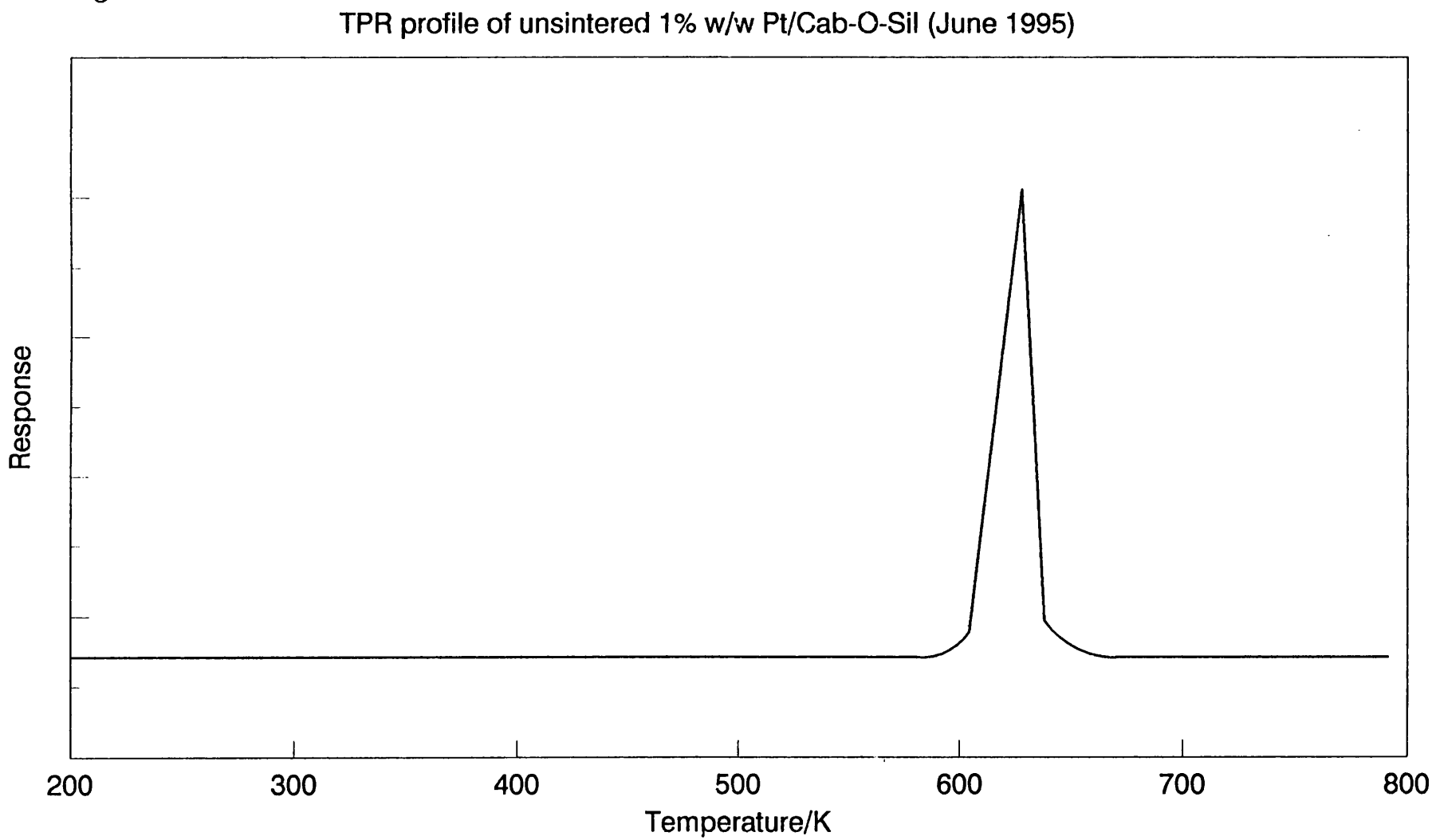
TPR profile of unsintered 1% w/w Pt/Cab-O-Sil (June 1995)
Response
200
300
400
500
600
700
800
Temperature/K

Table 4.3:- Chemisorption results		
Catalyst	% Dispersion of metal	
	O_2	CO
Pt/γ-alumina[1]	54.78	39.97
	46.75	
Pt/Grace silica C10[2]	19.20	15.11
	19.41	
Pt/Cab-O-Sil unsintered[3]	32.98	33.31
Pt/Cab-O-Sil sintered[4]	14.25	13.87

1 Reduced at 573 K
2 Reduced at 523 K
3 Reduced at 523 K
4 Reduced at 723 K

4.4 Transmission electron microscopy

Transmission electron microscopy experiments were carried out as described in section 3.3.4. The TEM of the catalysts in their post-reduction states are shown in Figures 4.5 to 4.8. The particle sizes for the 1% w/w Pt/-alumina, 1% w/w Pt/Grace silica C10, 1% w/w Pt/Cab-O-Sil and sintered 1% w/w Pt/Cab-O-Sil are summarised in Table 4.4.

Table 4.4:- TEM results	
Catalyst	Particle size/nm
1% w/w Pt/-alumina	1 - 2
1% w/w Pt/Grace silica C10	1 - 4
1% w/w Pt/Cab-O-Sil (unsintered)	2 - 6
Sintered 1% w/w Pt/Cab-O-Sil	15 - 22

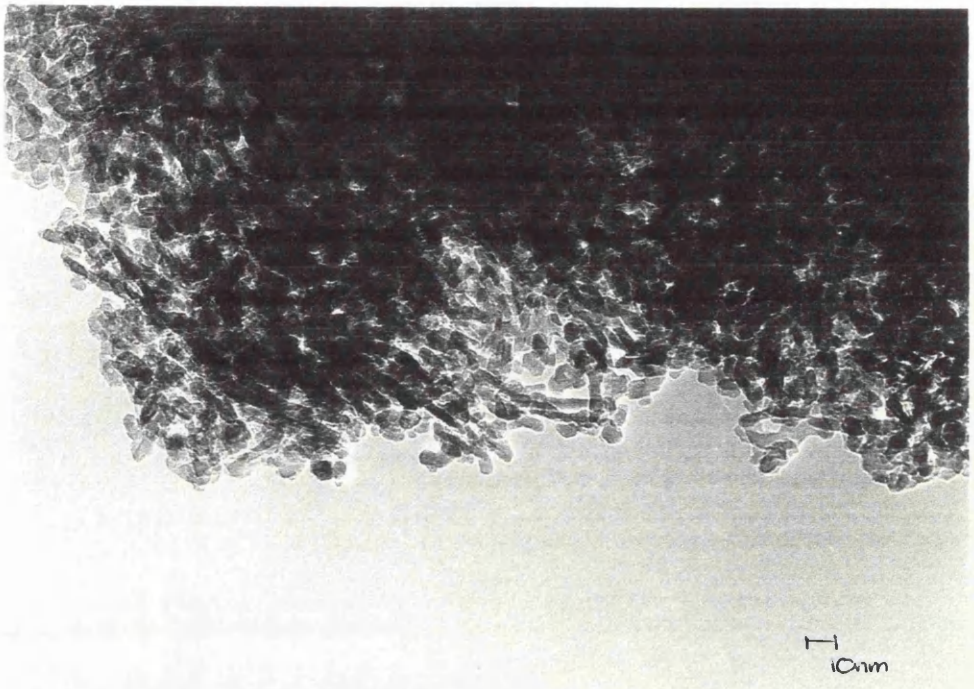

Figure 4.5: TEM of Pt/γ-alumina.
Magnification 392000 x (100nm = 3.92 cm)

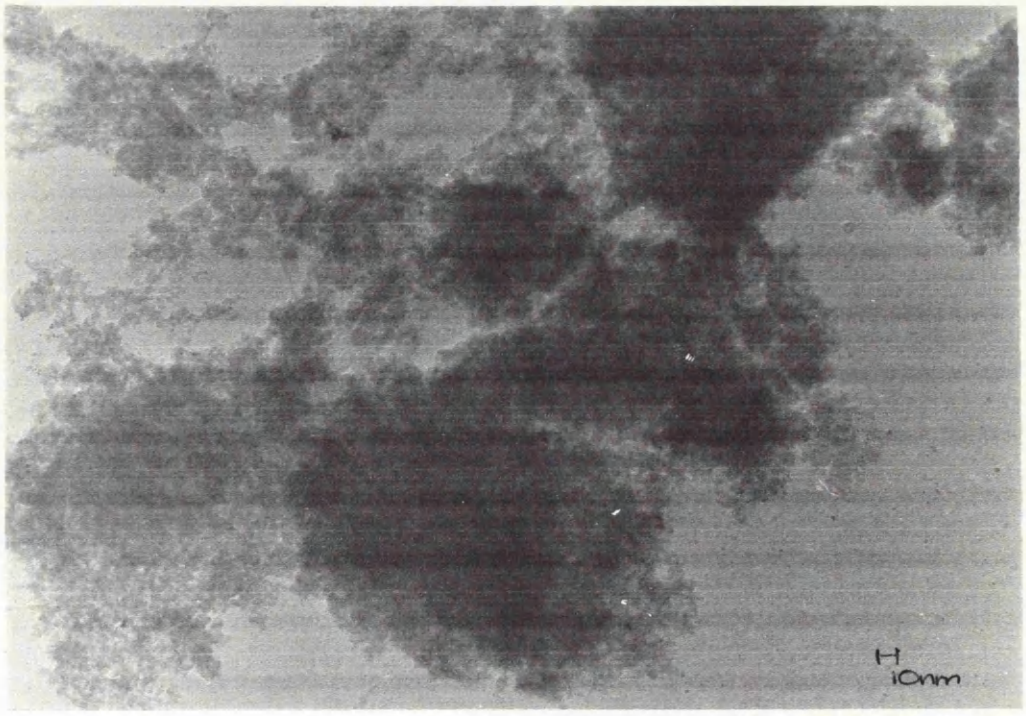

Figure 4.6: TEM of aged Pt/Grace silica C10.
Magnification 240000 x (100nm = 2.4 cm)

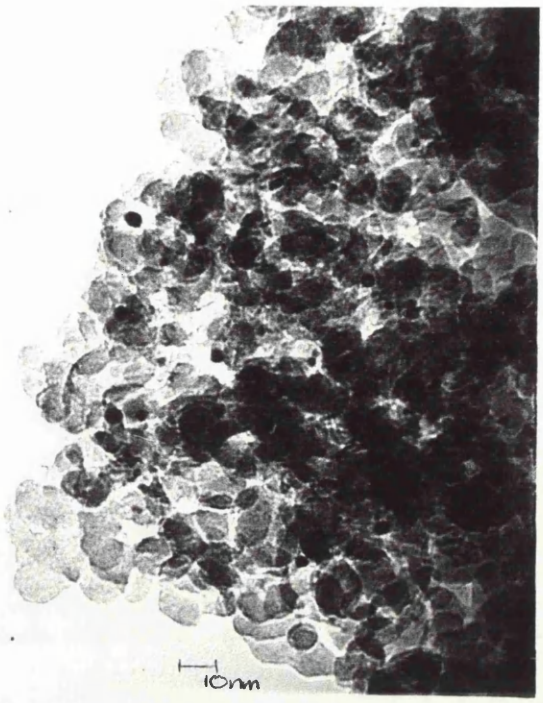

Figure 4.7: TEM of unsintered Pt/Cab-O-Sil.
Magnification 480000 x (100nm = 4.8 cm)

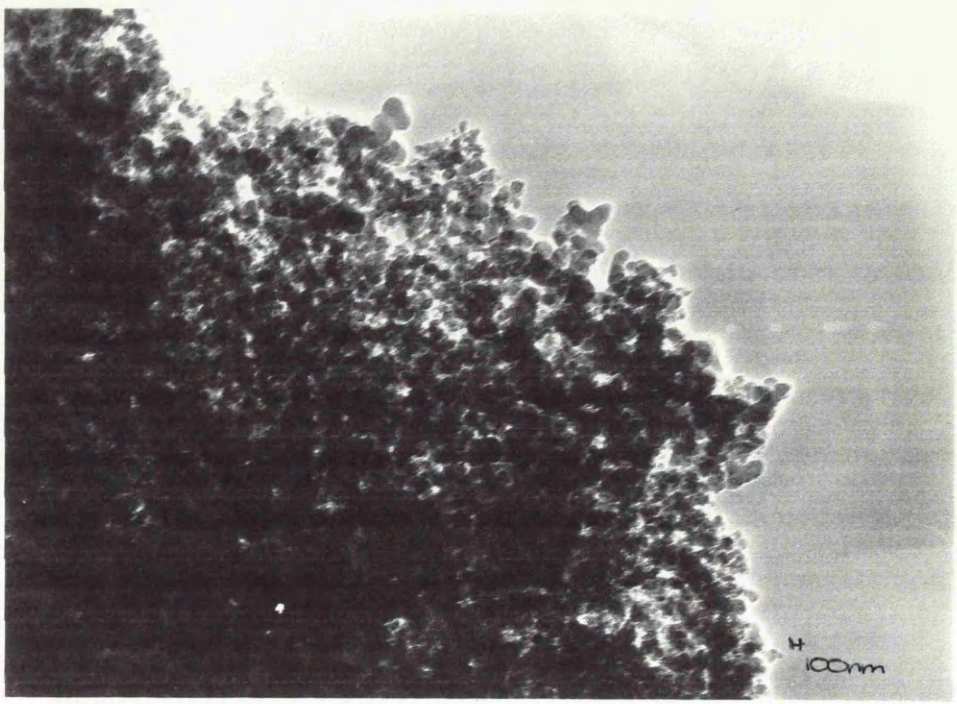

Figure 4.8: TEM of sintered Pt/Cab-O-Sil.
Magnification 91260 x (100nm = 0.91 cm)

4.2 ADSORPTION STUDIES OF CHIRAL MODIFIERS

4.2.1 Catalysts

Initial adsorption studies were carried out at ambient temperature using the apparatus described in section 3.4.1.3, that is, where the catalyst was activated in reactor R1 by static reduction as outlined in section 3.4.2.3. The initial adsorption studies involved the two original catalysts which had been prepared for this study. The catalysts were 1% w/w Pt/γ-alumina and 1% w/w Pt/Grace silica C10 and will be referred to as Pt/γ-alumina and Pt/silica C10, respectively.

4.2.1.1 Reactor R1 and static reduction

In the first instance the modification procedure as outlined in section 3.4.2.1 was carried out using 2,2'-dihydroxy-1,1'-binaphthalene, which will be referred to as 'diol'. The modifier solution was allowed to reach equilibrium with the catalyst. The racemic form of the diol was used initially in order to determine whether or not the molecule was adsorbed on to the catalyst surface, prior to the study of either pure enantiomer for the creation of a potential asymmetric catalyst. Adsorption of the modifier and the amount of adsorption was determined by HPLC as outlined in section 3.4.7. The initial number of molecules of modifier molecules added to a freshly prepared catalyst and the number of modifier molecules adsorbed are expressed per gram of catalyst and the nominal ratio is expressed per exposed surface metal atom. Table 4.5 shows the results of the adsorption of (±) diol on to supported Pt catalysts using reactor R1 and static reduction.

Table 4.5:- Adsorption of (±) diol on to supported Pt catalysts

Catalyst	Initial no. of molecules of modifier added x 10^{18}	No. of modifier molecules adsorbed x 10^{18}	Nominal ratio
Pt/silica C10	11.08	3.59	0.61
Pt/γ-alumina	10.61	11.22	0.77

Within Table 4.5, the first column shows the catalyst being studied; the second column refers to the initial number of molecules of modifier per gram of catalyst added in solution to the freshly prepared catalyst sample under a dinitrogen atmosphere; the third column shows the number of molecules modifier adsorbed per gram of catalyst at equilibrium; and the fourth column refers to the nominal ratio of modifier molecules adsorbed per gram of catalyst per exposed surface metal atom per gram of catalyst, since,

the exact amount of Pt in the catalysts is not known. The nominal ratio expresses the amount of modifier adsorbed per the number of exposed metal atoms on a catalyst surface, obtained from the CO(g) and O_2(g) chemisorption studies. In the case of the Pt/silica C10 the nominal ratio is calculated:

$$\frac{3.59 \times 10^{18}}{5.93 \times 10^{18}} = 0.61$$

where 3.59×10^{18} = the amount of modifier adsorbed and 5.93×10^{18} = the number of exposed Pt atoms (D = 19.41%, O_2(g)); and for Pt/γ-alumina the nominal ratio is:

$$\frac{11.22 \times 10^{18}}{14.43 \times 10^{18}} = 0.77$$

where 11.22×10^{18} = the amount of modifier adsorbed and 14.43×10^{18} = the number of exposed Pt atoms (D = 46.75%, O_2(g)).

The adsorption of R-(+)-2,2'-dihydroxy-1,1'-binaphthalene, referred to as R diol, on to the Pt/silica C10 catalyst gave the results presented in Tables 4.6 to 4.8. Table 4.6 shows the equilibrium adsorption results, while Tables 4.7 and 4.8 show the extent of adsorption as a function of time.

Table 4.6:- Adsorption of R diol on to Pt/silica C10

Initial no. of molecules of modifier added x 10^{18}	No. of modifier molecules adsorbed x 10^{18}	Nominal ratio
7.10	3.01	0.51
7.30	2.52	0.43
20.29	3.15	0.55
20.48	4.68	0.83

Table 4.7:- Adsorption of R diol on to Pt/silica C10		
5.84×10^{18} modifier molecules added initially		
Modification time/Minutes	No. of molecules modifier adsorbed x 10^{18}	Nominal ratio
0	0	0
30	0.26	0.04
60	0.73	0.12
90	1.45	0.24
150	1.15	0.19
180	1.41	0.24
240	1.45	0.24
270	1.54	0.26
300	1.65	0.28
1345	2.87	0.48
1375	3.01	0.51

Table 4.8:- Adsorption of R diol on Pt/silica C10		
7.30×10^{18} modifier molecules added initially		
Modification time/Minutes	No. of molecules modifier adsorbed x 10^{18}	Nominal ratio
0	0	0
30	0.09	0.02
60	0.19	0.03
90	0.46	0.08
120	0.52	0.09
180	0.99	0.17
210	1.08	0.18
240	1.05	0.18
270	1.22	0.21
300	1.45	0.25
1080	2.50	0.42
1140	2.52	0.43

Figures 4.9 and 4.10 show graphical representations of the adsorption of R diol on to

Figure 4.9:-

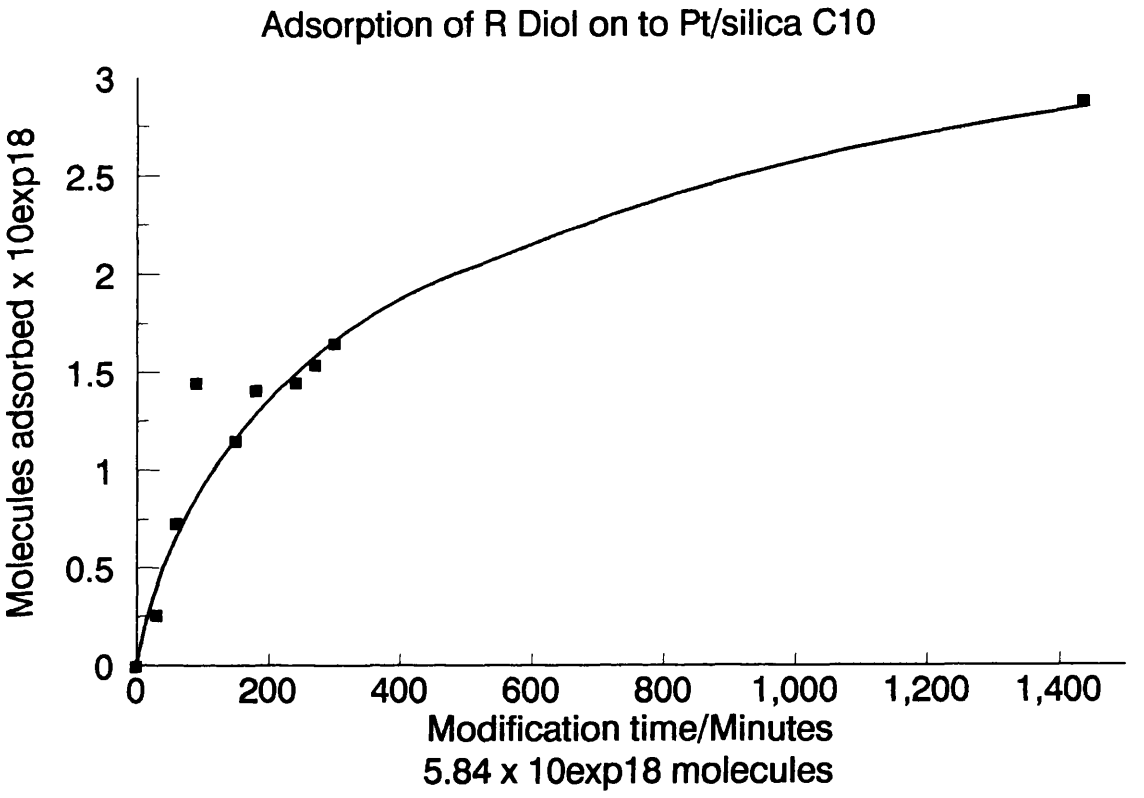

Figure 4.10:-

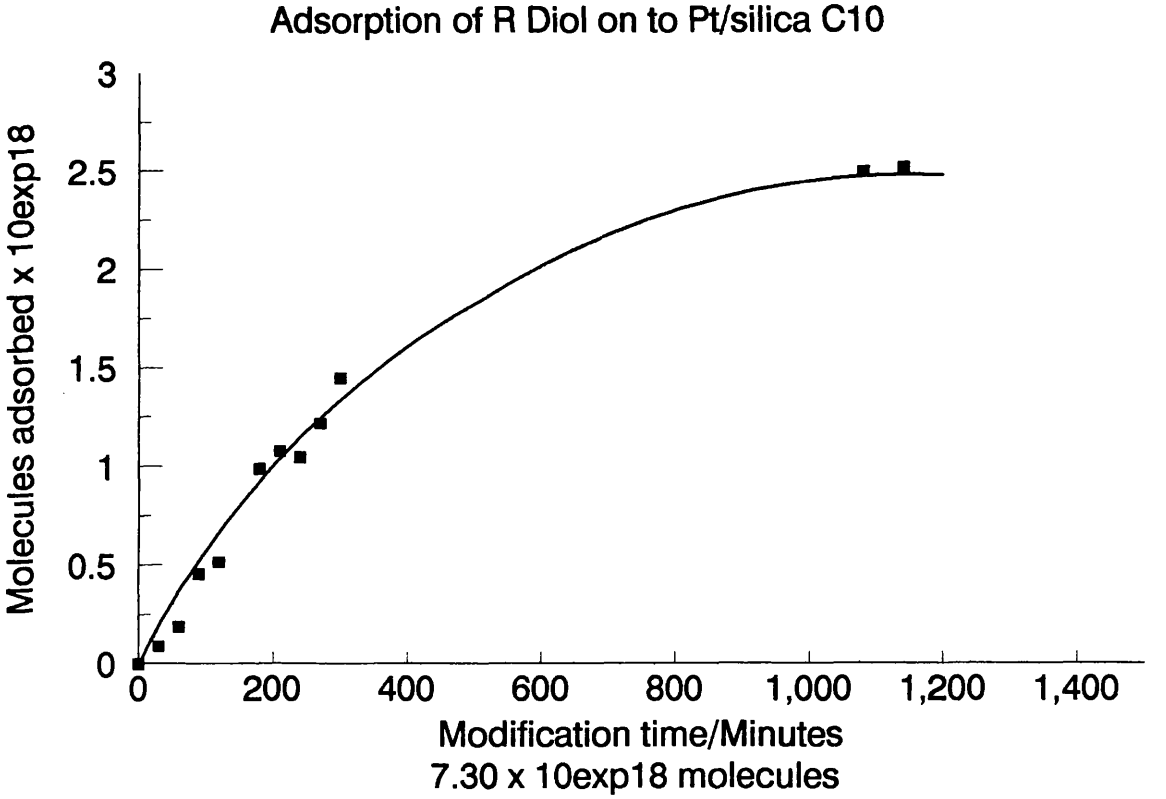

Pt/silica C10 catalyst.

4.2.1.2 Reactor R2 and static reduction

The reactor vessel design was changed from reactor R1 (Figure 3.1) to reactor R2 (Figure 3.2) in preparation for the hydrogenation reactions which were to be studied at a later stage in the programme. Also the change in reactor vessel enabled desorption studies to be undertaken with greater ease than would have been possible with the original reactor, R1.

Diol

The adsorption of R diol on to Pt/silica C10 catalyst was once again studied, see Tables 4.9, 4.11 and 4.13. The desorptions of R diol from diol modified Pt/silica C10 catalysts are shown in Tables 4.10, 4.12 and 4.14. Table 4.9 presents the adsorption results in an overall form, while Table 4.10 shows the desorption results. Tables 4.11 and 4.13 and Figures 4.11 and 4.13 show the variation in the extent of adsorption with time. Tables 4.12 and 4.14 and Figures 4.12 and 4.14 show the results of an in-depth study of the effect that temperature has on desorption.

Table 4.9:- Adsorption of R diol on to Pt/silica C10

Initial no. of molecules of modifier added x 10^{18}	No. of modifier molecules adsorbed x 10^{18}	Nominal ratio
5.35	1.95	0.33
6.10	4.10	069
6.79	2.09	0.35
9.08	1.91	0.32
13.63	2.57	0.43
23.90	6.39	1.08
24.88	9.28	1.56

Table 4.10:- Desorption of R diol from diol modified Pt/silica C10

Initial no. of modifier molecules added x 10^{18}	No. of molecules modifier remaining adsorbed after wash x 10^{18}	Nominal resultant ratio
5.35	1.85	0.31
6.79	2.05	0.35
13.63	2.10	0.35

Table 4.11:- Adsorption of R diol on to Pt/silica C10		
5.35×10^{18} modifier molecules added initially		
Modification time/Minutes	No. of molecules modifier adsorbed x 10^{18}	Nominal ratio
0	0	0
60	0.29	0.05
120	1.22	0.21
180	1.29	0.22
240	1.60	0.27
1290	1.90	0.32
1350	1.95	0.33

Table 4.12:- Desorption of R diol from diol modified Pt/silica C10		
5.35×10^{18} modifier molecules added initially		
Temperature of desorption/K	No. of molecules modifier remaining adsorbed after wash x 10^{18}	Nominal ratio
Before wash	1.95	0.33
298	1.85	0.31
304	1.78	0.30
323	1.84	0.31
340	1.86	0.31

Table 4.13:- Adsorption of R diol on to Pt/silica C10		
13.63×10^{18} modifier molecules added initially		
Modification time/Minutes	No. of molecules modifier adsorbed x 10^{18}	Nominal ratio
0	0	0
60	2.26	0.38
120	2.34	0.39
185	2.39	0.40
1275	2.56	0.43
1330	2.57	0.43

Figure 4.11:-

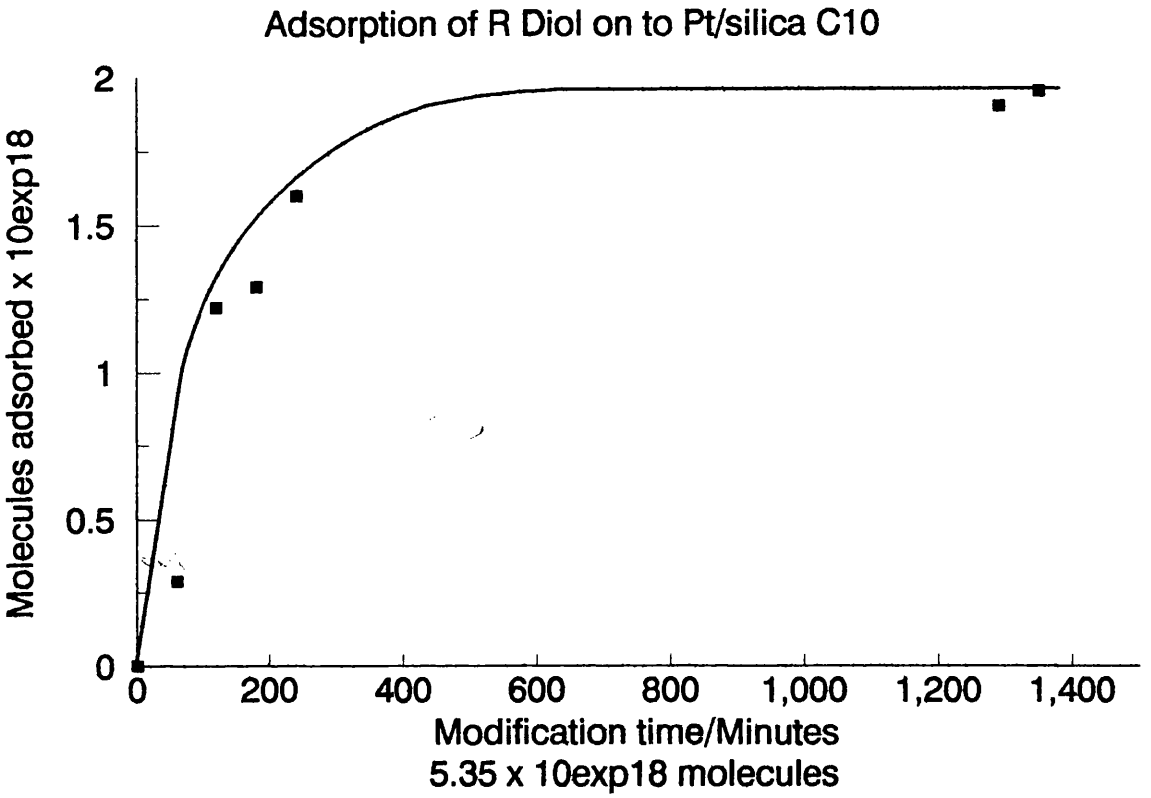

Figure 4.12:-

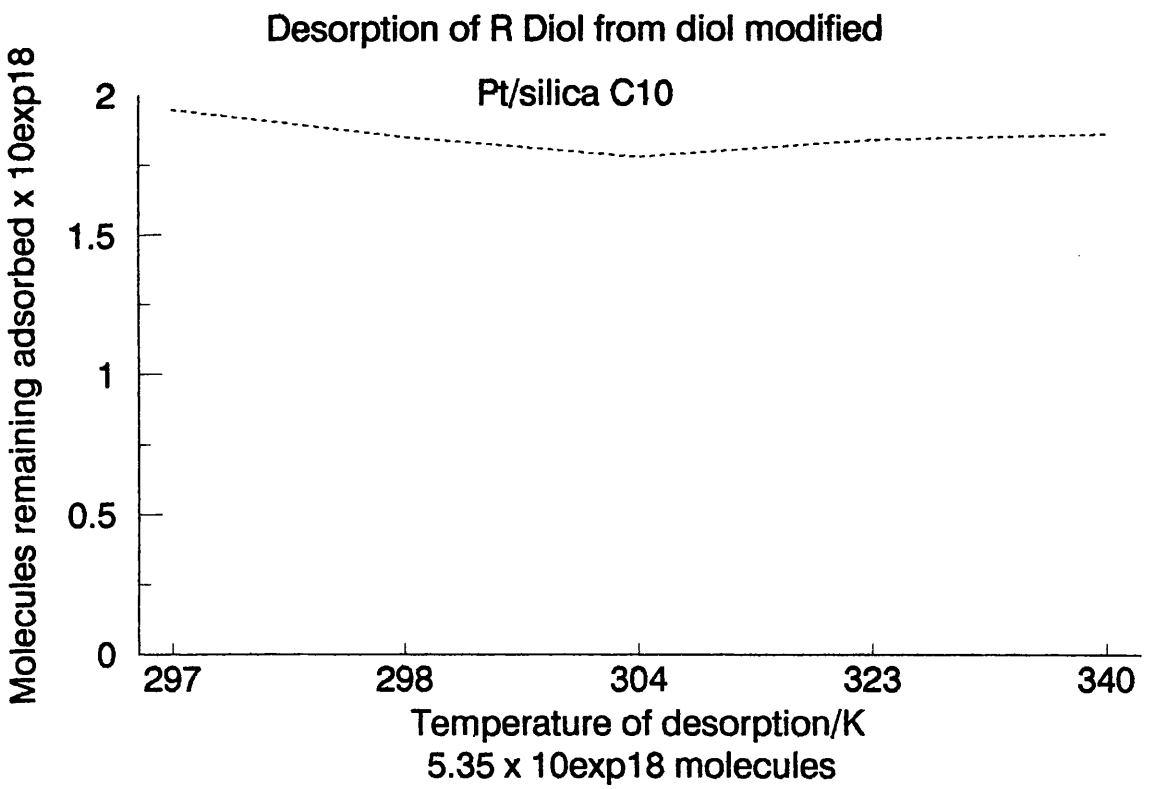

Table 4.14:- Desorption of R diol from diol modified Pt/silica C10		
13.63×10^{18} modifier molecules added initially		
Temperature of desorption/K	No. of molecules modifier remaining after wash x 10^{18}	Nominal ratio
Before wash	2.57	0.43
298	2.10	0.35
321	2.03	0.34
335	2.10	0.34
340	2.14	0.36

The adsorption and desorption of R diol was also examined on the Pt/γ-alumina catalyst. The results of the adsorption studies are presented in Table 4.15 and desorption studies in Table 4.16. Tables 4.17, 4.19, 4.21 and 4.23 and Figures 4.15, 4.17, 4.19 and 4.21 show the extent of adsorption as a function of time. Tables 4.16 and 4.24 and Figures 4.16 and 4.22 show the effect the length of washing time has on desorption at ambient temperature, while Tables 4.20 and 4.22 and Figures 4.18 and 4.20 show the effect that increasing the washing temperature has on modifier desorption.

Table 4.15:- Adsorption of R diol on to Pt/γ-alumina		
Initial no. of molecules of modifier added x 10^{18}	No. of modifier molecules adsorbed x 10^{18}	Nominal ratio
5.54	5.15	0.36
13.46	12.66	0.88
43.30	34.37	2.38
44.75	29.11	2.02

Table 4.16:- Desorption of R diol from diol modified Pt/γ-alumina		
Initial no. of modifier molecules added x 10^{18}	No. of molecules modifier remaining adsorbed after wash x 10^{18}	Nominal resultant ratio
5.54	4.90	0.34
13.46	12.15	0.84
43.30	30.47	2.12
44.75	28.20	1.95

Figure 4.13:-

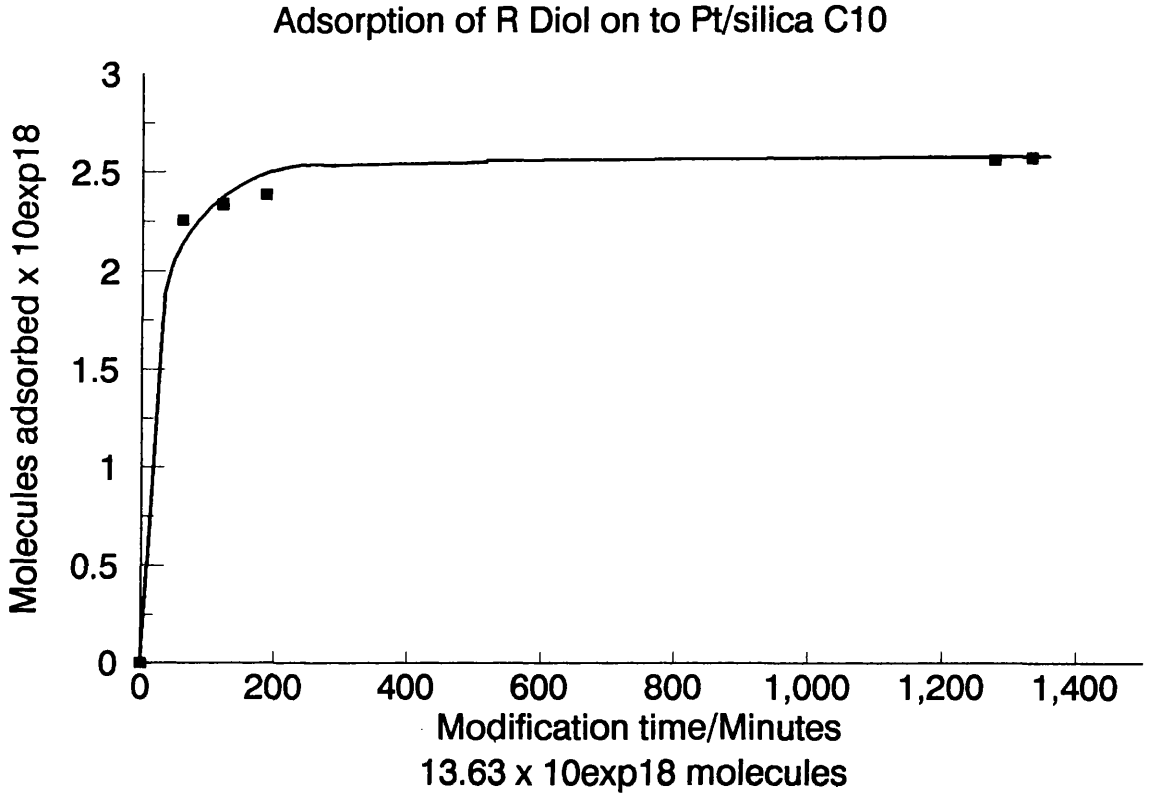

Figure 4.14:-

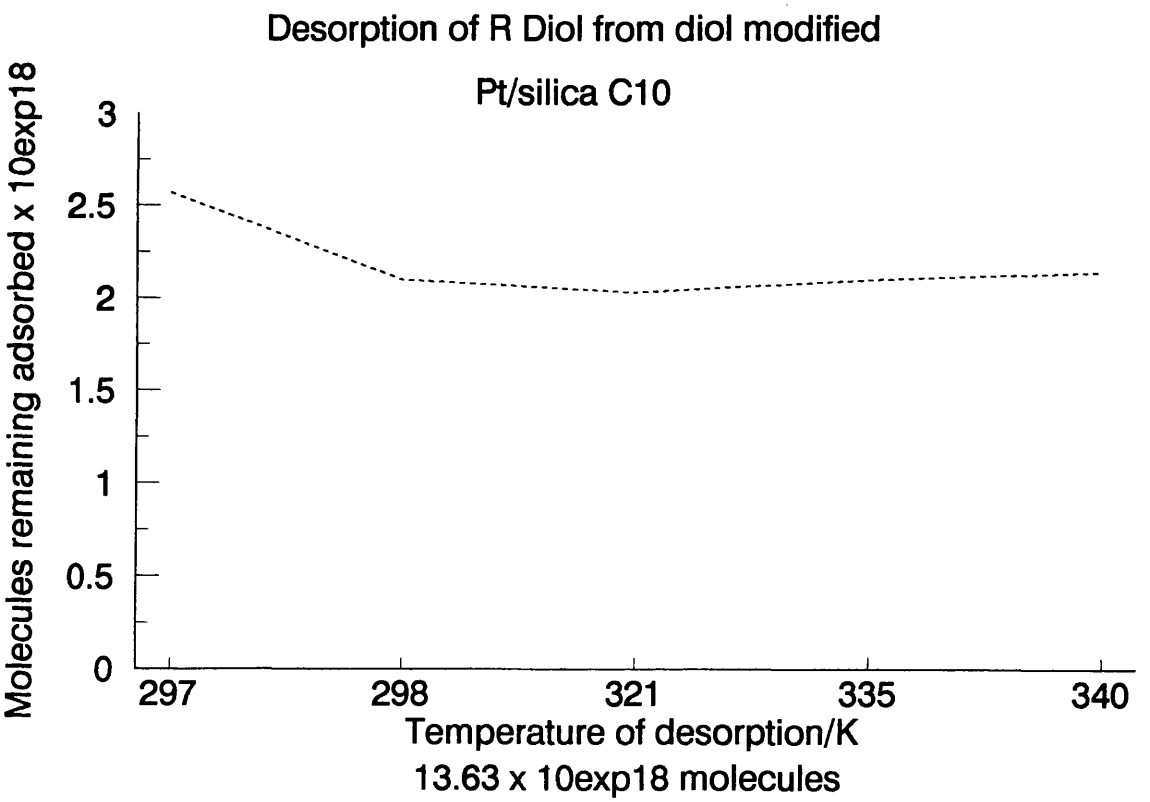

Table 4.17:- Adsorption of R diol on to Pt/γ-alumina		
5.54×10^{18} modifier molecules added initially		
Modification time/Minutes	No. of molecules modifier adsorbed x 10^{18}	Nominal ratio
0	0	0
60	3.09	0.21
120	4.10	0.28
180	4.73	0.33
240	4.86	0.34
1290	5.14	0.36
1350	5.14	0.36

Table 4.18:- Desorption of R diol from diol modified Pt/γ-alumina		
5.54×10^{18} modifier molecules added initially		
Desorption time at ambient temperature/Minutes	No. of molecules modifier remaining adsorbed after wash x 10^{18}	Nominal ratio
Before wash	5.14	0.36
60	4.90	0.34
120	4.90	0.34
180	4.90	0.34

Table 4.19:- Adsorption of R diol on to Pt/γ-alumina		
13.46×10^{18} molecules of modifier added initially		
Modification time/minutes	No. of molecules modifier adsorbed x 10^{18}	Nominal ratio
0	0	0
60	7.53	0.52
120	9.65	0.67
180	10.73	0.74
240	12.39	0.85
1290	12.66	0.88
1350	12.66	0.88

Figure 4.15:-

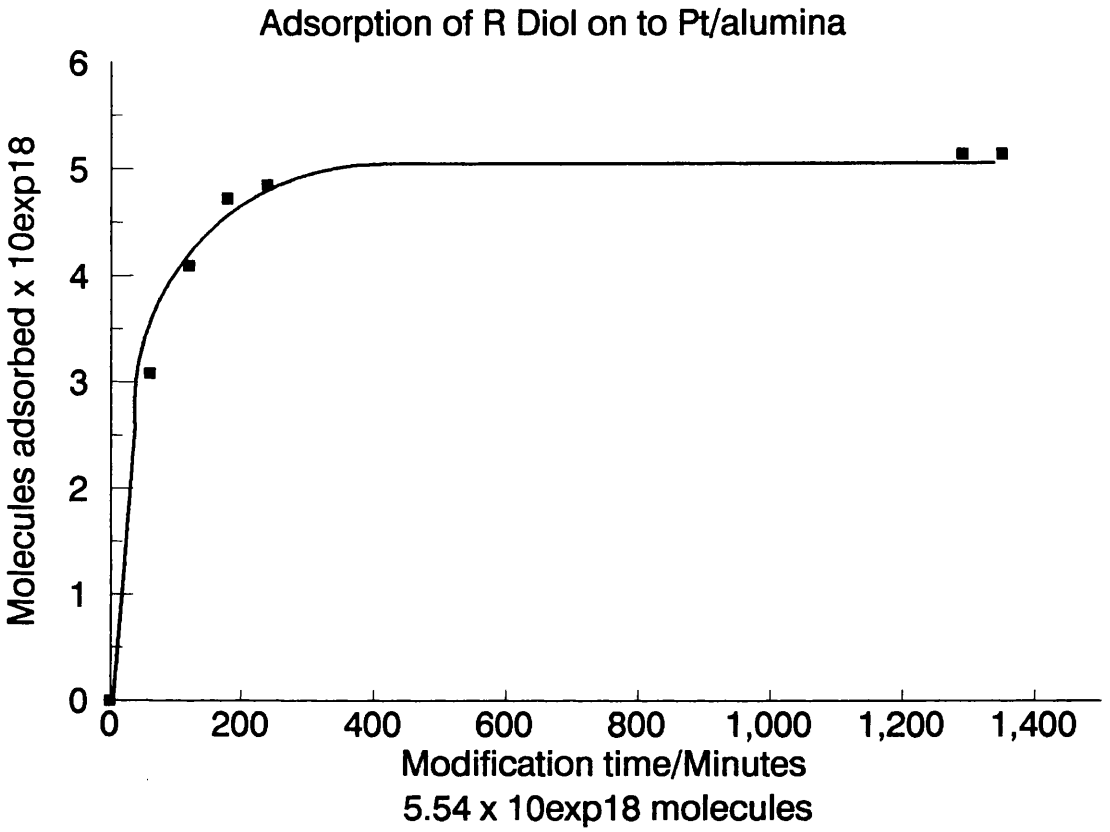

Figure 4.16:-

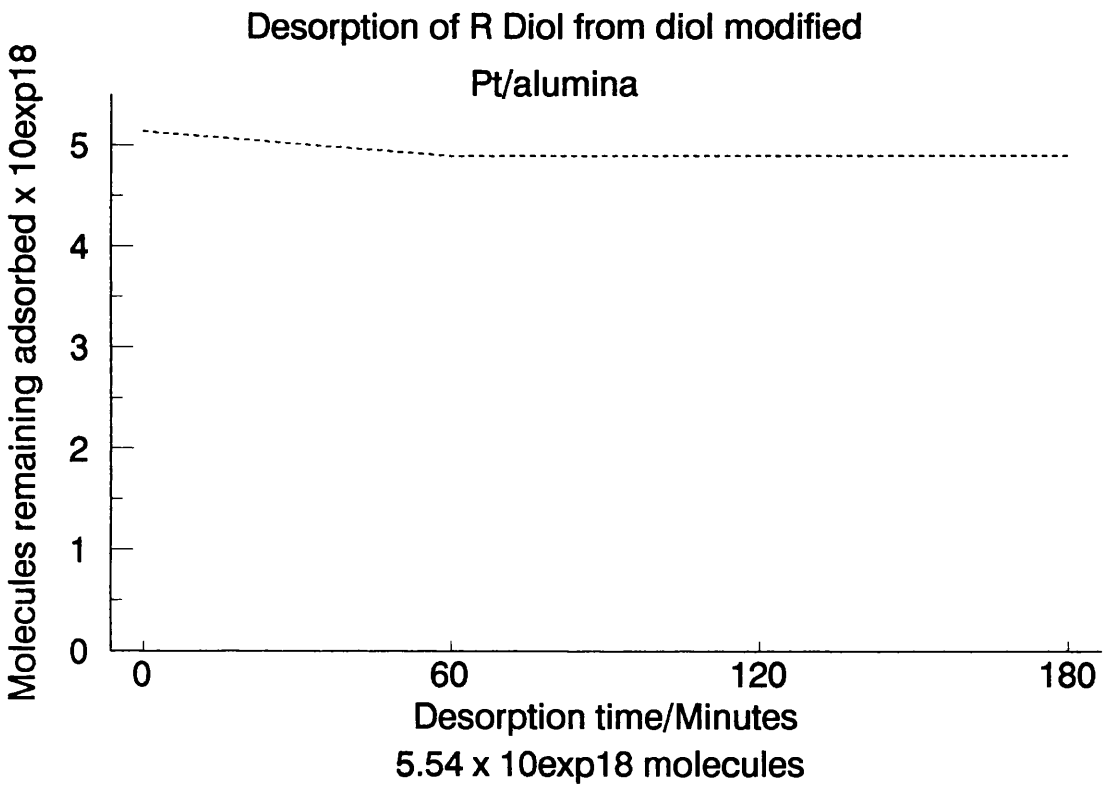

Table 4.20:- Desorption of R diol from diol modified Pt/γ-alumina		
13.46×10^{18} modifier molecules added initially		
Temperature of desorption/K	No. of molecules modifier remaining adsorbed after wash x 10^{18}	Nominal resultant ratio
Before wash	12.66	0.88
298	12.15	0.84
302	12.27	0.85
324	11.86	0.82
340	11.85	0.82

Table 4.21:- Adsorption of R diol on to Pt/γ-alumina		
43.30×10^{18} modifier molecules added initially		
Modification time/Minutes	No. of molecules modifier adsorbed x 10^{18}	Nominal ratio
0	0	0
60	16.31	1.13
120	23.02	1.60
180	26.89	1.86
240	28.68	1.99
1050	33.53	2.32
1110	34.14	2.37
1170	34.20	2.37
1195	34.37	2.38

Figure 4.17:-

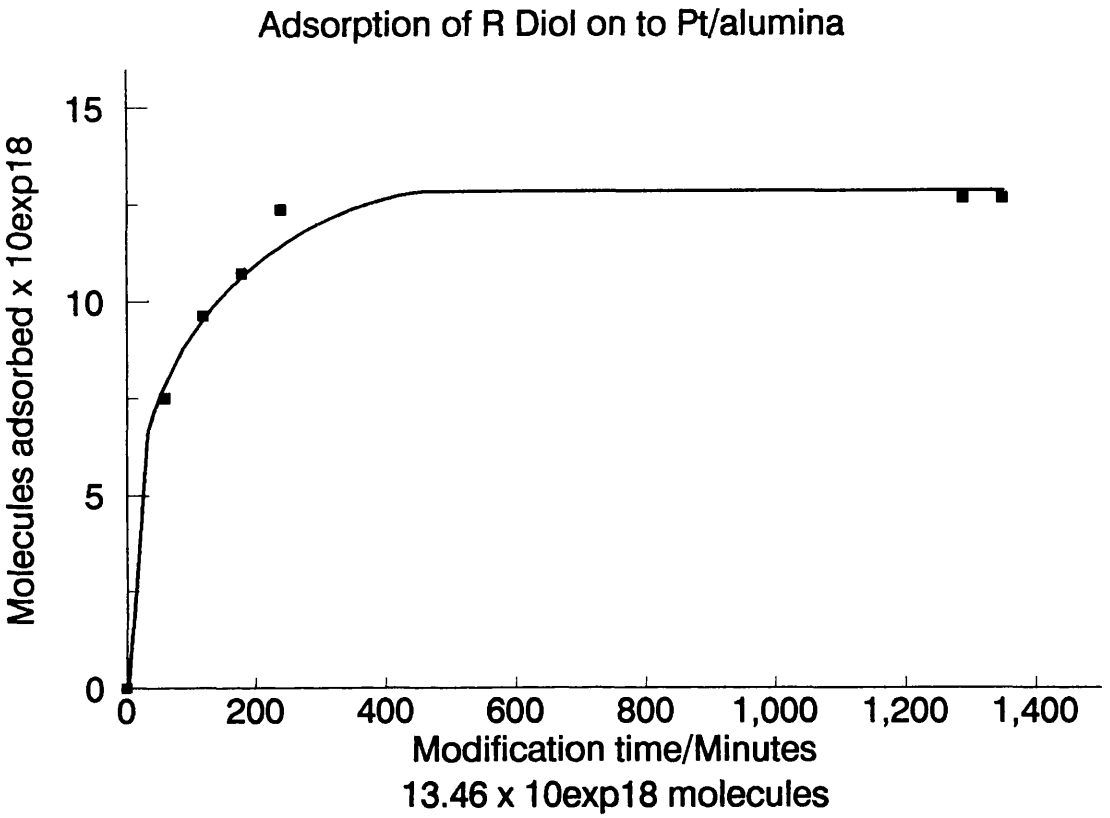

Figure 4.18:-

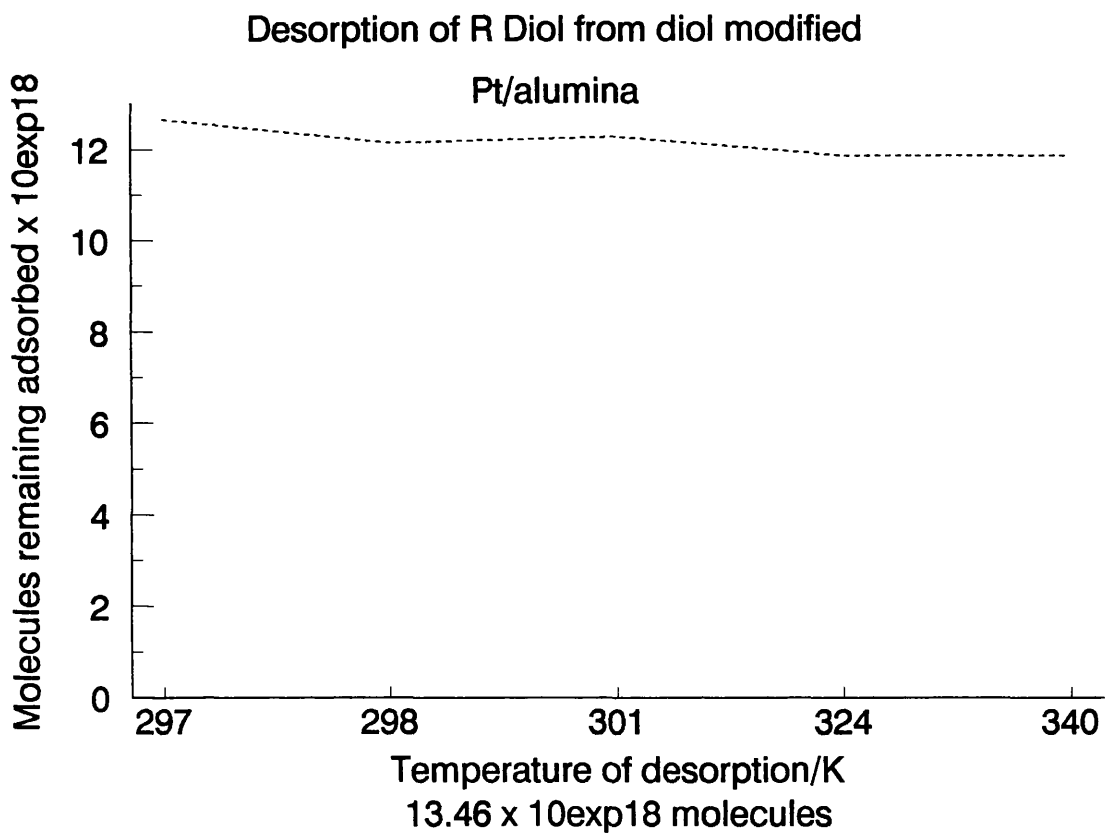

Table 4.22:- Desorption of R diol from diol modified Pt/γ-alumina		
43.30×10^{18} modifier molecules added initially		
Temperature of desorption/K	No. of molecules modifier remaining adsorbed after wash x 10^{18}	Nominal resultant ratio
Before wash	34.37	2.38
298	30.47	2.12
303	29.43	2.12
325	28.81	2.00
340	22.89	1.59

Table 4.23:- Adsorption of R diol on to Pt/γ-alumina		
44.75×10^{18} modifier molecules added initially		
Modification time/Minutes	No. of molecules modifier adsorbed x 10^{18}	Nominal ratio
0	0	0
60	17.15	1.19
120	21.76	1.51
180	24.56	1.70
240	28.84	2.00
1350	28.92	2.01
1410	29.11	2.02

Table 4.24:- Desorption of R diol from diol modified Pt/γ-alumina		
44.75×10^{18} modifier molecules added initially		
Desorption time at ambient temperature/Minutes	No. of molecules modifier remaining adsorbed after wash x 10^{18}	Nominal resultant ratio
Before wash	29.11	2.02
60	28.20	1.95
180	27.00	1.87

Diamine

A second binaphthalene derivative was introduced where the two hydroxyl groups

Figure 4.19:-

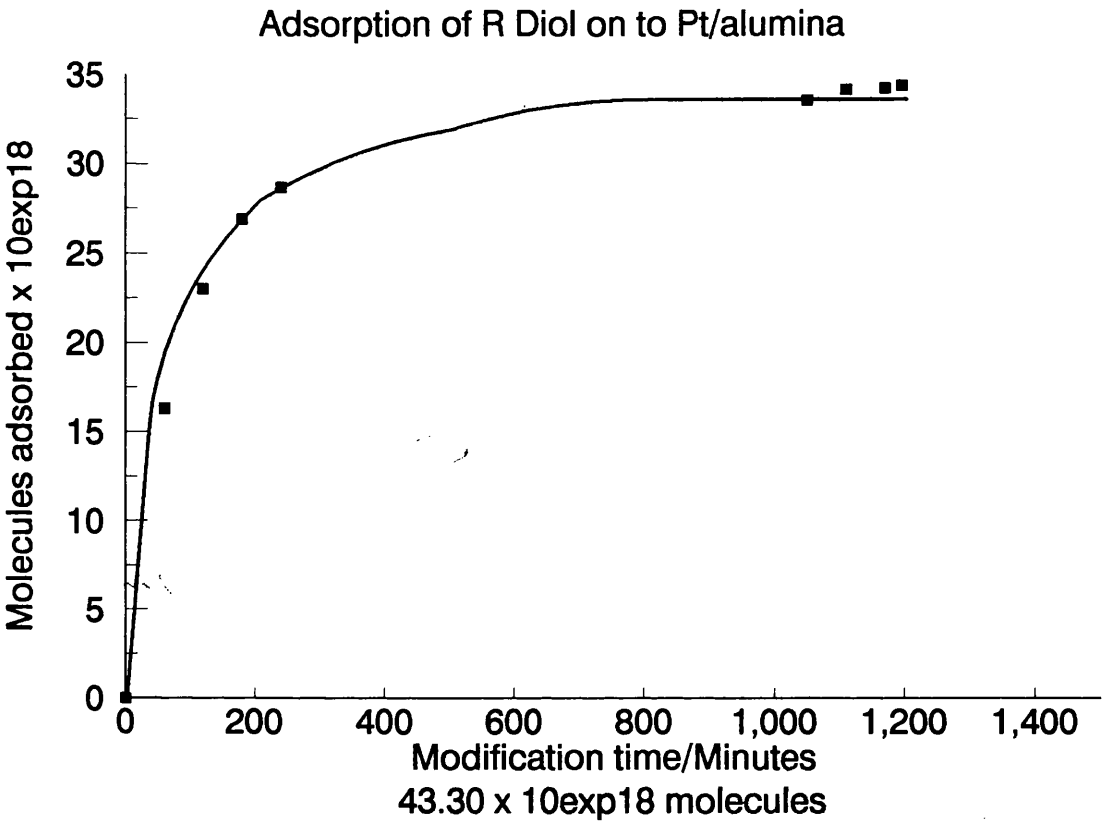

Figure 4.20:-

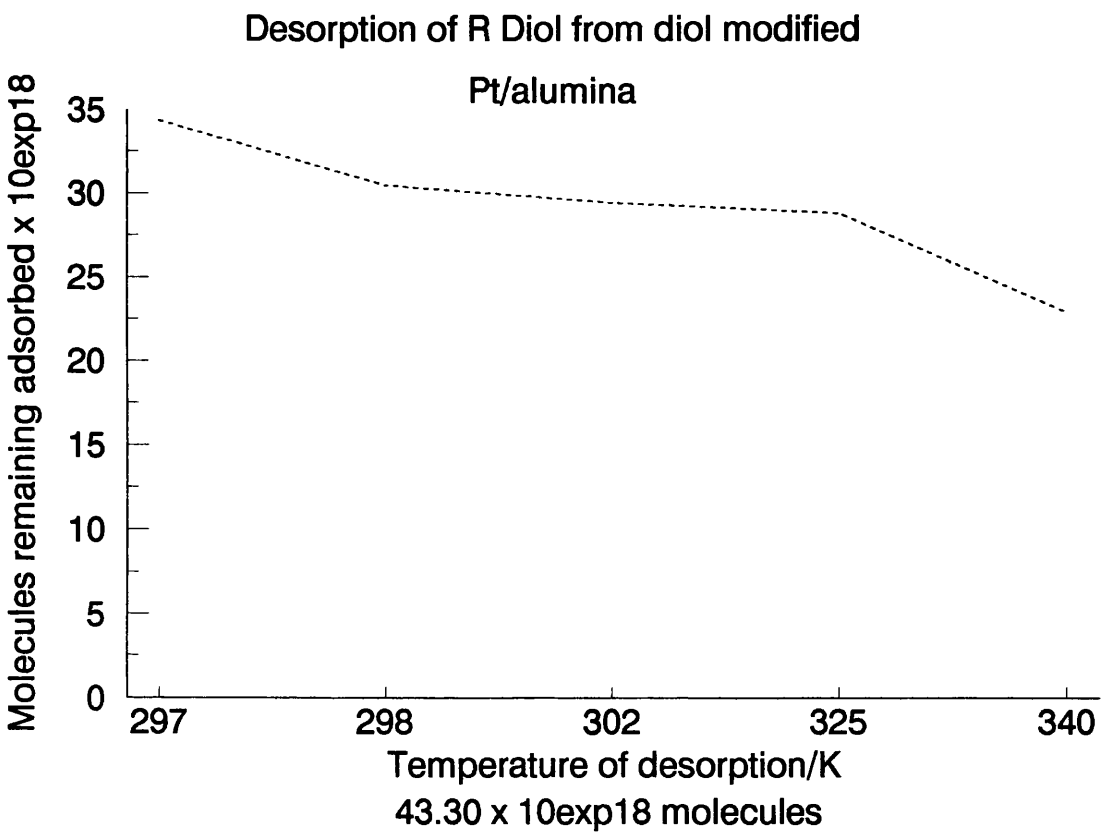

Figure 4.21:-

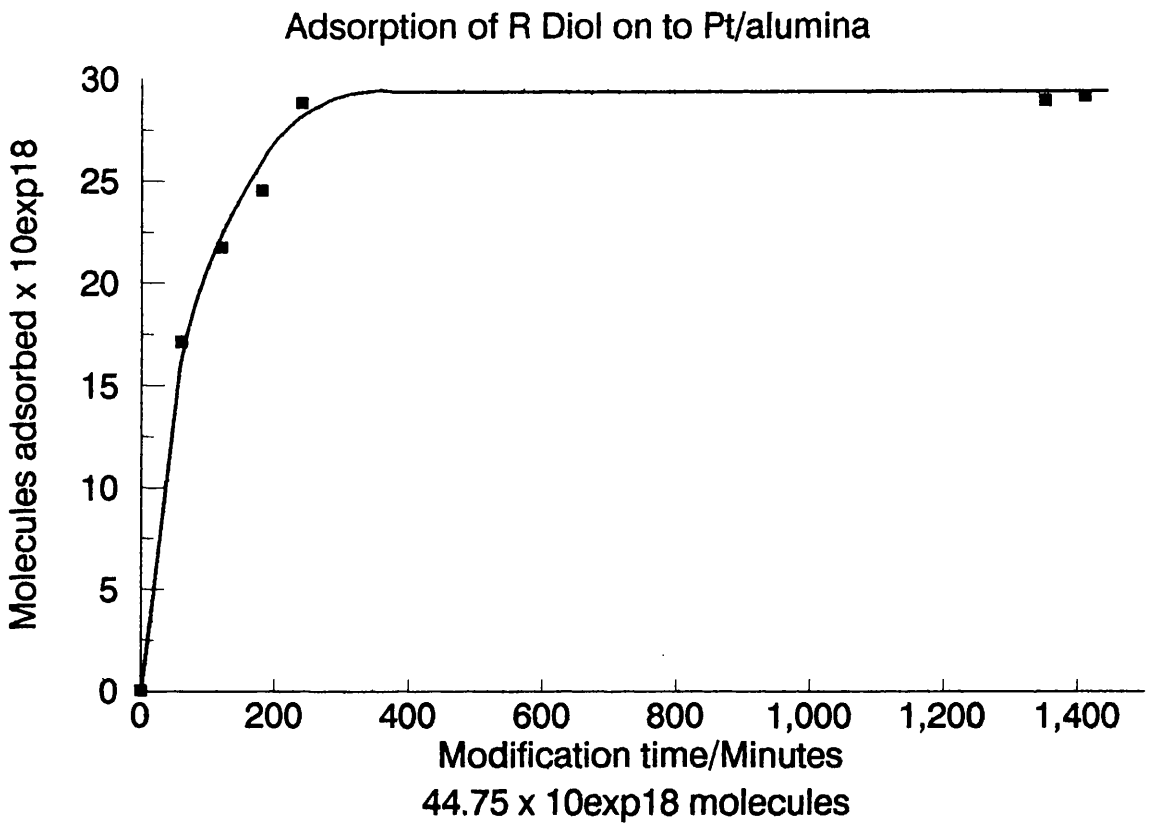

Figure 4.22:-

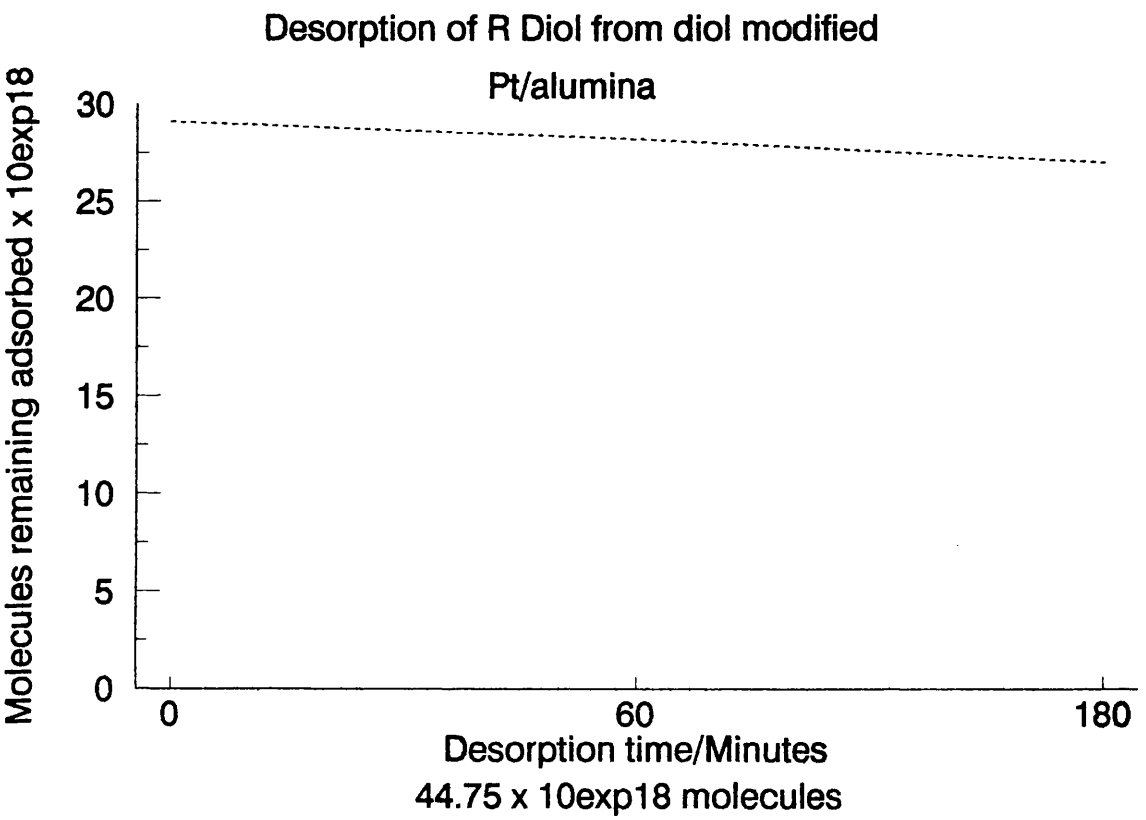

(-OH) were replaced by two amino groups (-NH_2). This new modifier, 2,2'-diamino-1,1'-binaphthalene which will from now on be referred to as the 'diamine' was initially studied in the racemic form. Although only one study with the (±) diamine was undertaken with the reactor vessel R2 and static reduction using the Pt/silica C10 catalyst. An adsorption as a function of time adsorption study was undertaken.The results are shown in Table 4.25 and Figure 4.23.

Table 4.25:- Adsorption of (±) diamine on to Pt/silica C10

8.73×10^{18} modifier molecules added initially

Modification time/Minutes	No. of molecules modifier adsorbed x 10^{18}	Nominal ratio
0	0	0
60	0.39	0.06
120	0.46	0.08
180	0.71	0.13
1290	3.76	0.63

Dimethoxy

Reactor R2 and static reduction system was used for a third binaphthalene derivative. This third binaphthalene derivative had the H atom of the hydroxyl groups replaced by a -CH_3 group. This modifier, 2,2'-dimethoxy-1,1'-binaphthalene, which will from now on be referred to as the 'dimethoxy' was studied initially in the racemic form as were the diol and the diamine. However, repeated studies of the dimethoxy with both the Pt/silica C10 and Pt/γ-alumina catalyst at various initial concentrations of the modifier led to no adsorption . Table 4.26 shows typical results from the dimethoxy adsorptions.

Table 4.26:- Adsorption of (±) dimethoxy			
Catalyst	Initial no. of molecules of modifier added x 10^{18}	No. of modifier molecules adsorbed x 10^{18}	Nominal ratio
Pt/silica C10	13.88	0.00	N/A
Pt/silica C10	24.25	0.00	N/A
Pt/silica C10	30.10	0.00	N/A
Pt/γ-alumina	14.58	0.00	N/A
Pt/γ-alumina	15.00	0.00	N/A

N/A Not applicable

4.2.1.3 Reactor R2 and flow reduction

To enable the number of studies to be undertaken to be increased the mode reduction was changed from static to flow reduction where the gas is flowed over the catalyst bed. Reactor vessel R2 was still used.

4.2.1.3.1 1% w/w Pt/γ-alumina catalyst

Adsorption studies using one modifier

Diol

Using 'flow' reduced catalysts, the adsorption of (±), R and S diol; and (±), R and S diamine, were studied in greater depth at ambient temperature, as well as a few studies at 273K, using the Pt/γ-alumina catalyst. The results for (±), R and S diol adsorption on to the Pt/γ-alumina catalyst are presented in Tables 4.27, 4.29 and 4.31, and the desorption of (±), R and S diol from the appropriate diol modified Pt/γ-alumina catalyst in Tables 4.28, 4.30 and 4.32, respectively. While Tables 4.33 and 4.34 and Figures 4.24 and 4.25 show typical results of the extent of adsorption as a function of time of the R and S diol, respectively. Figure 4.24 and 4.25 exhibit typical adsorption isotherms for R and S diol on to the Pt/γ-alumina catalyst.

Table 4.27:- Adsorption of (±) diol on to Pt/γ-alumina		
Initial no. of modifier molecules added x 10^{18}	No. of molecules modifier adsorbed x 10^{18}	Nominal ratio
10.27	10.14	0.70
10.29[1]	10.10	0.70

1 At 273K

Table 4.28:- Desorption of (±) diol from diol modified Pt/γ-alumina		
Initial no. of modifier molecules added x 10^{18}	No. of molecules modifier remaining adsorbed after wash x 10^{18}	Nominal resultant ratio
10.27	10.03	0.70
10.29[1]	9.85	0.68

1 At 273K

Table 4.29:- Adsorption of R diol on to Pt/γ-alumina		
Initial no. of modifier molecules added x 10^{18}	No. of molecules modifier adsorbed x 10^{18}	Nominal ratio
4.91	4.75	0.33
7.51	7.38	0.51
7.71	7.46	0.52
11.60	11.04	0.77
11.69	11.15	0.77
12.94	12.32	0.85
14.20	13.57	0.94
14.42	14.08	0.98
14.55	13.40	0.93
14.62	14.20	0.98
14.76	14.08	0.98
15.33	15.20	1.05
17.20	16.45	1.14
17.53	17.21	1.19
17.58	17.16	1.19
21.62	21.12	1.46
22.90	22.42	1.55
24.83	23.20	1.61
29.26	28.02	1.94
29.43	27.60	1.91
30.36	27.82	1.93
43.25	38.37	2.66
82.94	39.10	2.71
83.31	42.20	2.92

Table 4.30:- Desorption of R diol from diol modified Pt/γ-alumina		
Initial no. of modifier molecules added x 10^{18}	No. of molecules modifier remaining adsorbed after wash x 10^{18}	Nominal resultant ratio
4.91	4.70	0.33
7.51	7.29	0.51
7.71	7.40	0.51
11.60	10.81	0.75
11.69	10.95	0.76
12.94	12.17	0.84
14.42	13.90	0.96
15.33	14.48	1.00
17.20	15.50	1.07
17.53	16.94	1.17
17.58	16.69	1.16
21.62	20.52	1.42
22.90	22.11	1.53
24.83	15.01	1.04
29.26	27.13	1.88
29.43	26.85	1.86
30.36	25.98	1.80

Table 4.31:- Adsorption of S diol on to Pt/γ-alumina		
Initial no. of modifier molecules added x 10^{18}	No. of molecules modifier adsorbed x 10^{18}	Nominal ratio
14.11	13.04	0.90
14.22	13.32	0.92
14.31	14.07	0.98
15.72	15.52	1.08
27.59	26.04	1.80
27.79[1]	25.68	1.78
31.11	27.70	1.99
35.69[1]	28.72	1.99

1 At 273K

Table 4.32:- Desorption of S diol from diol modified Pt/γ-alumina		
Initial no. of modifier molecules added x 10^{18}	No. of molecules modifier remaining adsorbed after wash x 10^{18}	Nominal resultant ratio
14.31	13.95	0.96
15.72	15.05	1.04
27.59	24.82	1.72
27.79[1]	24.07	1.67
31.11	27.40	1.90
35.69[1]	27.35	1.90

1 At 273K

Table 4.33:- Adsorption of R diol on Pt/γ-alumina		
14.20×10^{18} modifier molecules added initially		
Modification time/Minutes	No. of molecules modifier adsorbed x 10^{18}	Nominal ratio
0	0	0
60	7.13	0.50
120	9.19	0.64
180	11.33	0.79
240	11.96	0.83
1380	13.49	0.93
1440	13.52	0.94

Table 4.34:- Adsorption of S diol on to Pt/γ-alumina		
14.11×10^{18} modifier molecules added initially		
Modification time/Minutes	No. of molecules modifier adsorbed x 10^{18}	Nominal ratio
0	0	0
60	7.12	0.49
120	8.96	0.62
180	10.43	0.72
240	10.79	0.75
1380	12.91	0.89
1440	13.04	0.90

Diamine

The adsorption of the (±), R and S diamine on to the Pt/γ-alumina catalyst are presented in Tables 4.35, 4.37 and 4.39, respectively. The subsequent (±), R and S diamine desorption from diamine modified Pt/γ-alumina is shown in Tables 4.36, 4.38 and 4.40, respectively. While Tables 4.41 to 4.44; 4.45 and 4.46; and 4.47 show typical results for the extent of adsorption as function of time of (±), R and S diamine, respectively. Figures 4.26 to 4.29; 4.30 and 4.31; and 4.32 show adsorption isotherms of the (±), R and S diamine on to Pt/γ-alumina catalyst, respectively.

Figure 4.23:-

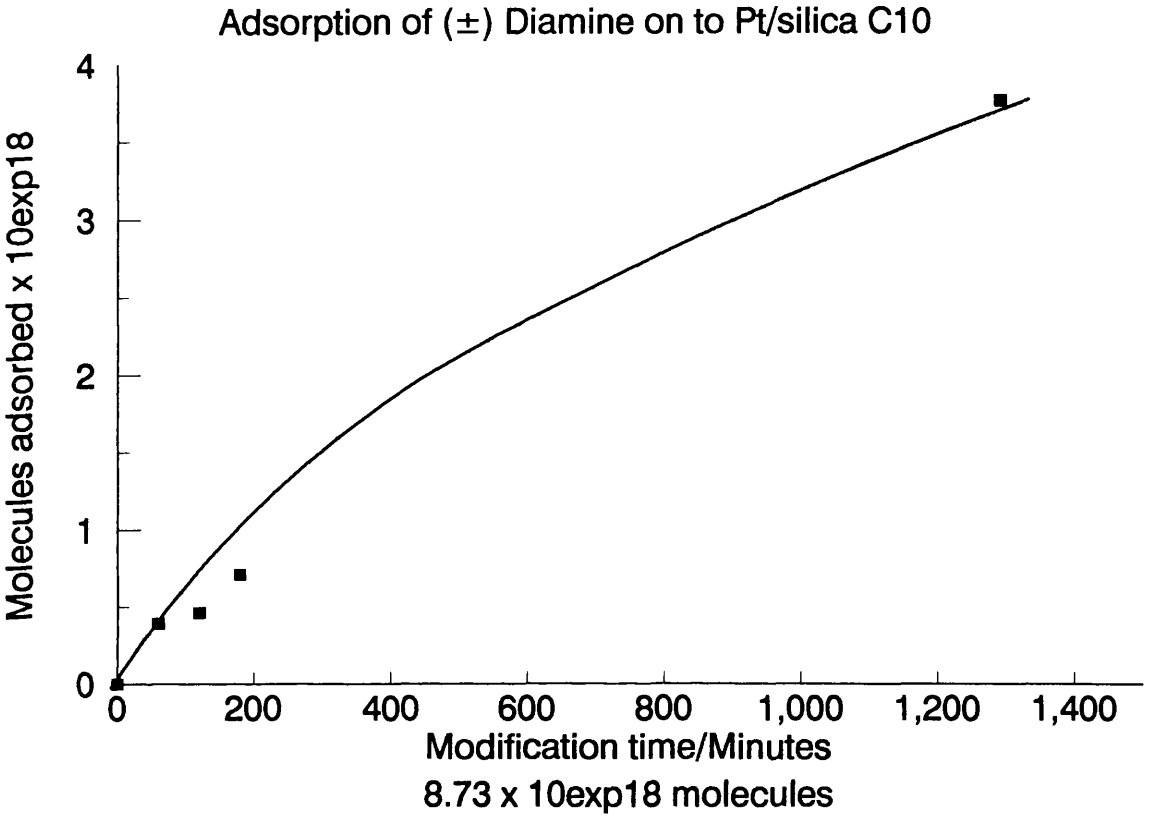

Figure 4.24:-

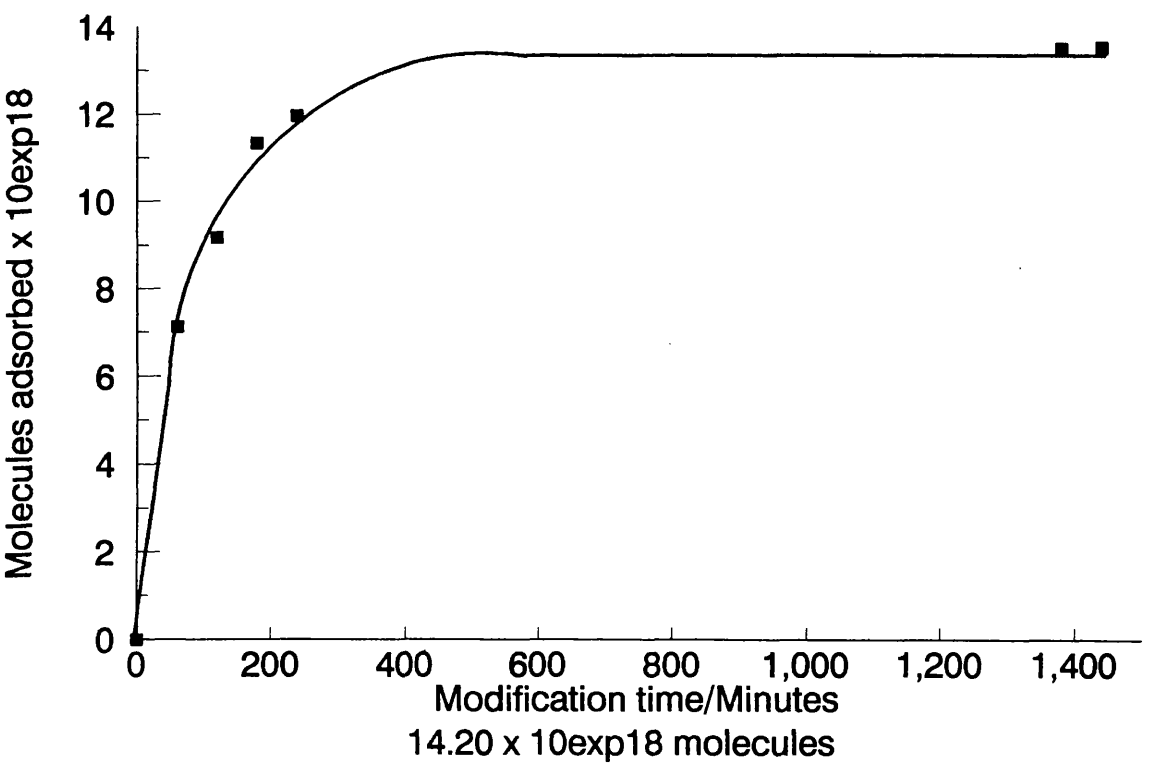

Table 4.35:- Adsorption of (±) diamine on to Pt/γ-alumina		
Initial no. of modifier molecules added x 10^{18}	No. of molecules modifier adsorbed x 10^{18}	Nominal ratio
10.42	6.90	0.48
10.33[1]	5.78	0.40
14.31	7.37	0.51
14.51	7.22	0.50
14.52	7.10	0.49
14.87	6.92	0.48
41.76	10.84	0.75
44.88	5.99	0.42

1 At 273K

Table 4.36:- Desorption of (±) diamine from diamine modified Pt/γ-alumina		
Initial no. of modifier molecules added x 10^{18}	No. of molecules modifier remaining adsorbed after wash x 10^{18}	Nominal resultant ratio
10.42	5.98	0.41
10.33[1]	5.02	0.35

1 At 273K

Table 4.37:- Adsorption of R diamine on to Pt/γ-alumina		
Initial no. of modifier molecules added x 10^{18}	No. of molecules modifier adsorbed x 10^{18}	Nominal ratio
9.18	5.77	0.40
10.04	5.49	0.38
13.08	3.95	0.27
13.22	5.28	0.36
13.98	7.15	0.50
14.03	5.45	0.38
14.08	6.42	0.44
14.11	4.74	0.33
14.22	8.64	0.60
14.28	9.01	0.62
14.33[1]	10.57	0.73
14.51	7.22	0.50
14.55	7.23	0.50
14.75	7.59	0.53
14.77	9.19	0.64
15.10	6.30	0.44
15.43[1]	6.40	0.44
15.82	10.20	0.71
17.97[1]	7.25	0.50
23.46	11.00	0.76
23.67[1]	9.75	0.68
31.93	14.00	0.97
47.03	14.41	1.00
47.44	9.21	0.64
48.15	10.35	0.72
60.22	5.04	0.35
60.89	4.05	0.28

1 At 273K

Table 4.38:- Desorption of R diamine from diamine modified Pt/γ-alumina		
Initial no. of modifier molecules added x 10^{18}	No. of molecules modifier remaining adsorbed after wash x 10^{18}	Nominal resultant ratio
7.50[1]	3.43	0.24
9.18	5.05	0.35
10.04	4.56	0.32
13.98	6.06	0.42
14.03	4.39	0.30
14.08	5.09	0.35
14.28	7.63	0.53
14.33[1]	9.63	0.67
14.55	6.00	0.42
14.77	8.13	0.56
15.10	4.92	0.34
15.43[1]	5.14	0.36
15.82	8.36	0.58
17.97[1]	5.83	0.40
23.46	8.64	0.59
23.67[1]	8.05	0.56
31.93	12.06	0.84
47.03	10.03	0.69
47.44	4.29	0.30
48.15	8.38	0.58
60.89	-9.86	N/A

1 At 273K
N/A Not available

Table 4.39:- Adsorption S diamine on to Pt/γ-alumina		
Initial no. of modifier molecules added x 10^{18}	No. of molecules modifier adsorbed x 10^{18}	Nominal ratio
11.95	5.60	0.39
11.98[1]	7.22	0.50
14.07	8.24	0.57
14.08	4.79	0.33
14.09	5.10	0.35
14.10	8.89	0.62
14.11	4.74	0.33
14.12[1]	6.86	0.48
14.16	7.68	0.53
14.23	10.18	0.71
14.24	2.63	0.18
14.26	10.18	0.71
14.30	6.22	0.43
15.82	7.44	0.52
19.93	8.65	0.60
24.88	8.48	0.59
42.53[1]	11.57	0.80
42.57	10.75	0.74

1 At 273K

Table 4.40:- Desorption of S diamine from diamine modified Pt/γ-alumina		
Initial no. of modifier molecules added x 10^{18}	No. of molecules modifier remaining adsorbed after wash x 10^{18}	Nominal resultant ratio
11.95	4.04	0.28
11.98[1]	6.44	0.45
14.07	6.62	0.46
14.10	8.44	0.59
14.12[1]	6.02	0.42
14.16	6.82	0.47
14.23	9.28	0.64
14.26	9.28	0.64
15.82	5.51	0.38
19.93	7.96	0.55
24.88	5.24	0.36
42.53[1]	8.05	0.56
42.57	6.41	0.44

1 At 273K

Table 4.41:- Adsorption of (±) diamine on Pt/γ-alumina		
14.31 x 10^{18} modifier molecules added initially		
Modification time/Minutes	No. of molecules modifier adsorbed x 10^{18}	Nominal ratio
0	0	0
60	3.98	0.28
120	4.19	0.29
180	5.33	0.37
240	5.97	0.41
1290	6.81	0.47
1350	7.37	0.51

Figure 4.25:-

Adsorption of S Diol on to Pt/alumina

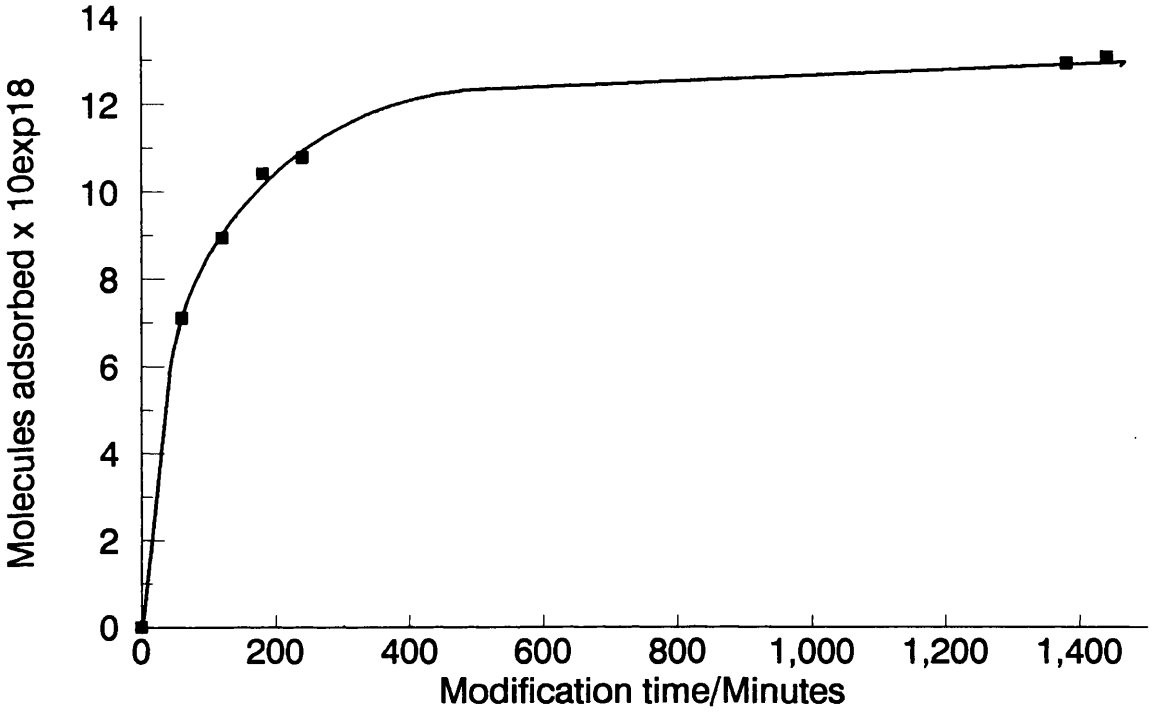

14.11 x 10exp18 molecules

Figure 4.26:-

Adsorption of (±) Diamine on to Pt/alumina

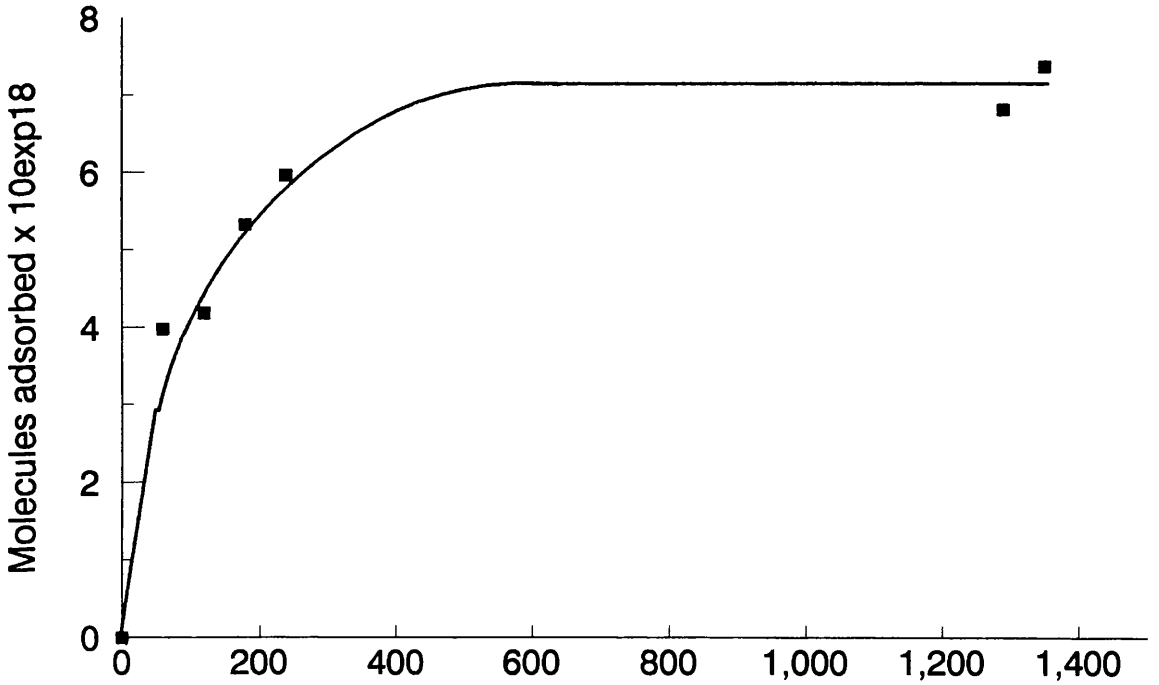

14.31 x 10exp18 molecules

Table 4.42:- Adsorption of (±) diamine on Pt/γ-alumina		
14.51×10^{18} modifier molecules added initially		
Modification time/Minutes	No. of molecules modifier adsorbed x 10^{18}	Nominal ratio
0	0	0
60	4.30	0.30
120	5.31	0.37
180	6.52	0.45
240	7.06	0.49
1380	7.36	0.51
1440	7.22	0.50

Table 4.43:- Adsorption of (±) diamine on Pt/γ-alumina		
14.87×10^{18} modifier molecules added initially		
Modification time/Minutes	No. of molecules modifier adsorbed x 10^{18}	Nominal ratio
0	0	0
60	3.38	0.23
120	4.29	0.30
180	4.98	0.35
240	5.77	0.40
1350	6.36	0.44
1410	6.92	0.48

Figure 4.27:-

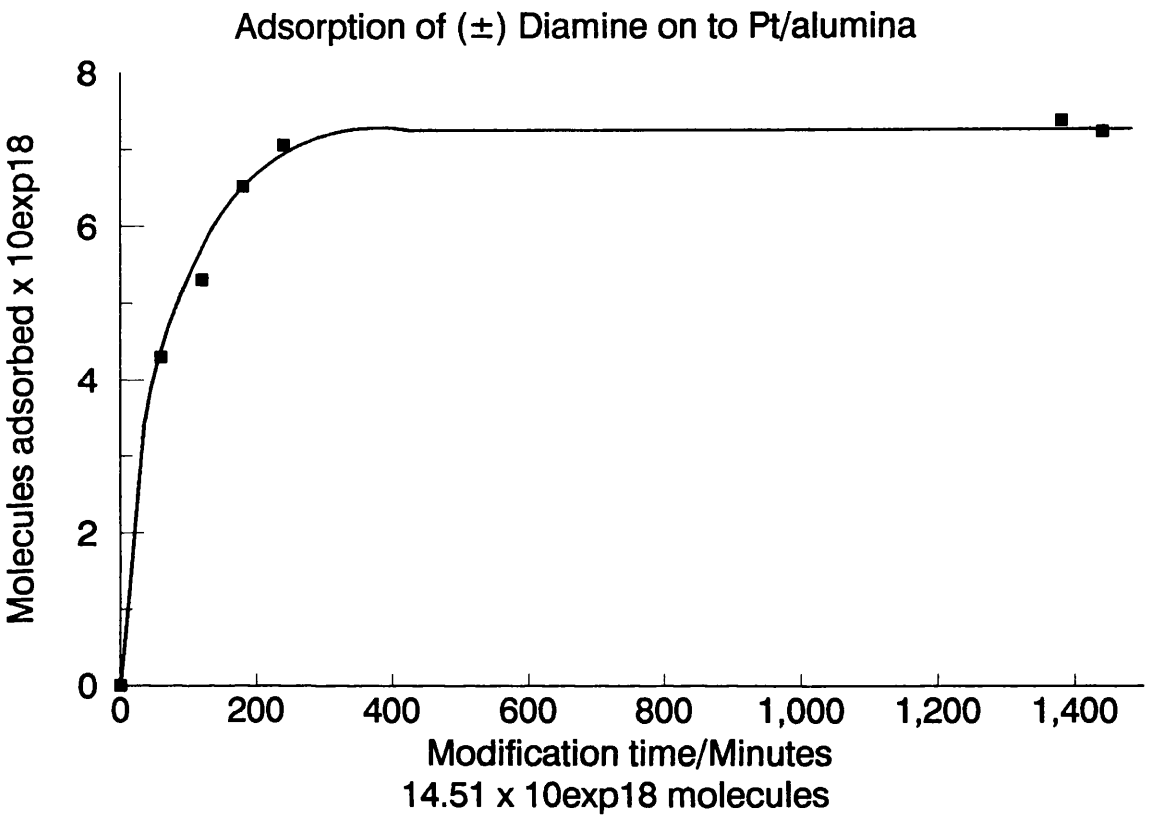

Figure 4.28:-

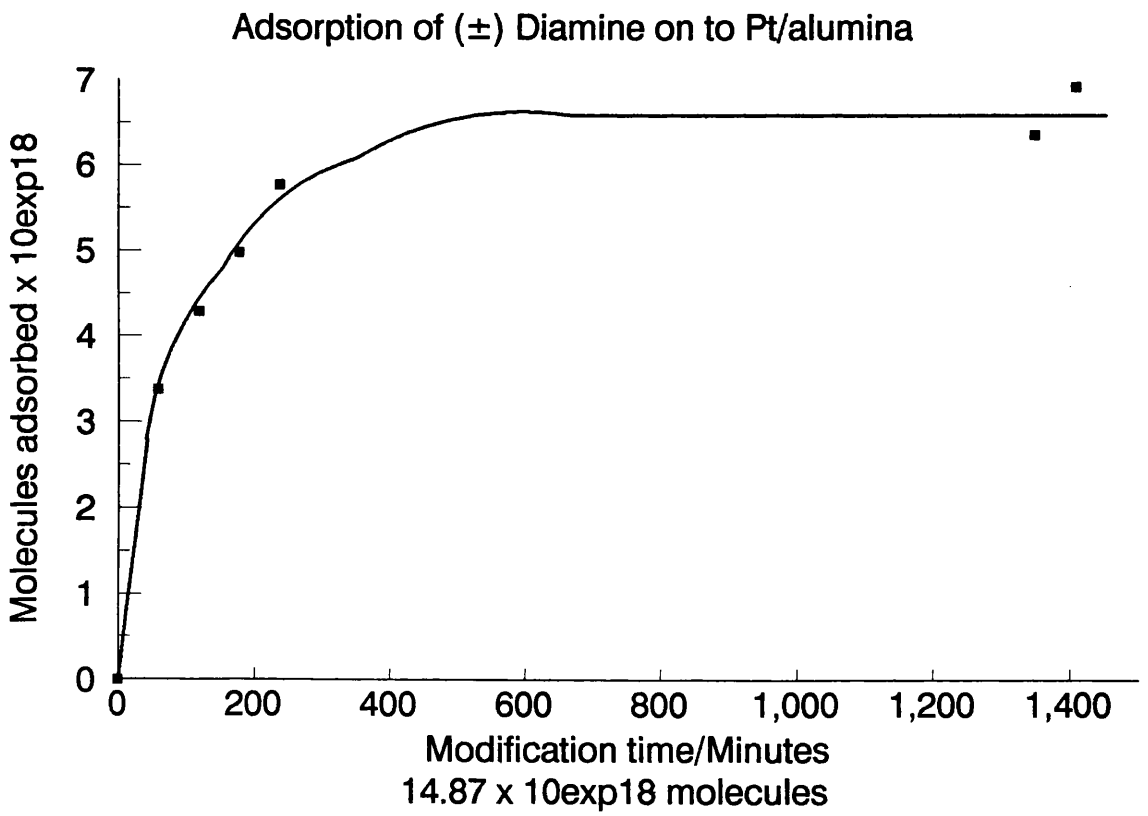

Table 4.44:- Adsorption of (±) diamine on Pt/γ-alumina		
41.76×10^{18} modifier molecules added initially		
Modification time/Minutes	No. of molecules modifier adsorbed x 10^{18}	Nominal ratio
0	0	0
60	7.77	0.54
120	8.29	0.57
180	8.36	0.58
240	9.20	0.64
1380	10.72	0.74
1440	10.84	0.75

Table 4.45:- Adsorption of R diamine on Pt/γ-alumina		
13.22×10^{18} modifier molecules added initially		
Modification time/Minutes	No. of molecules modifier adsorbed x 10^{18}	Nominal ratio
0	0	0
60	2.17	0.15
120	2.99	0.21
180	3.97	0.28
240	4.59	0.32
1380	4.90	0.34
1440	5.28	0.36

Figure 4.29:-

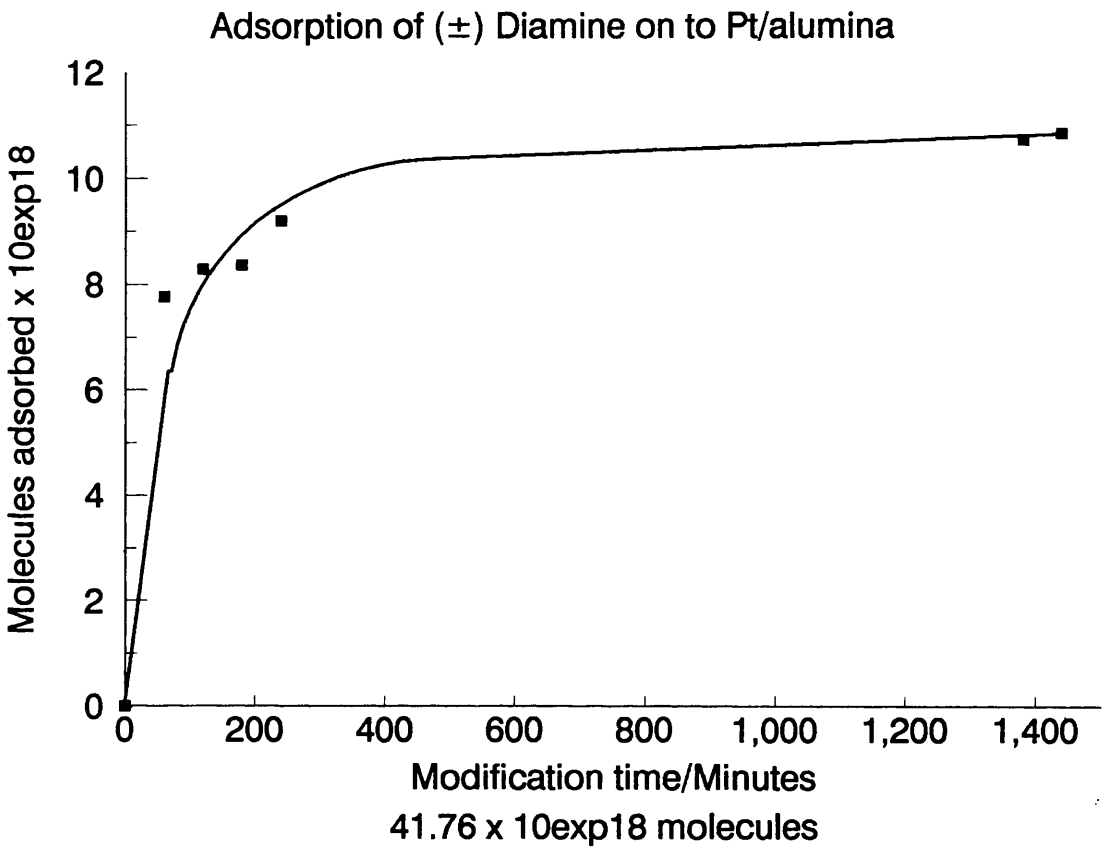

Figure 4.30:-

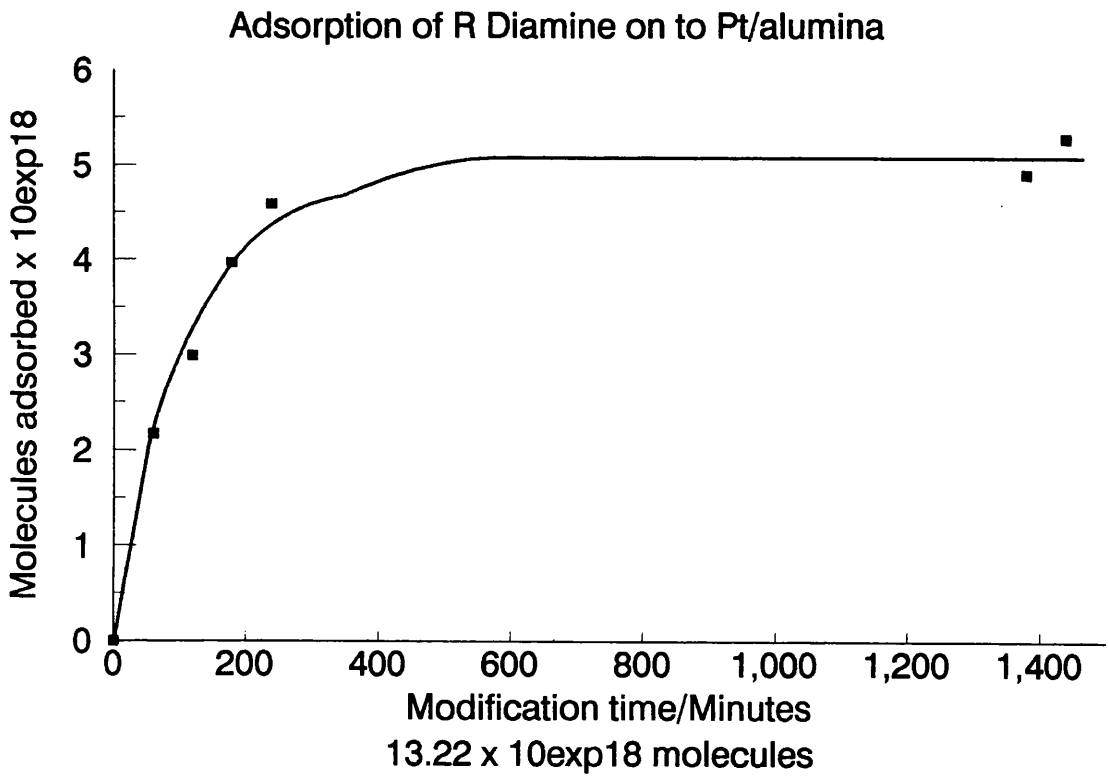

Table 4.46:- Adsorption of R diamine on to Pt/γ-alumina		
13.08×10^{18} modifier molecules added initially		
Modification time/Minutes	No. of molecules modifier adsorbed x 10^{18}	Nominal ratio
0	0	0
60	2.65	0.18
120	3.22	0.22
180	3.64	0.25
225	3.68	0.26
1380	3.92	0.27
1440	3.95	0.27

Table 4.47:- Adsorption S diamine on to Pt/γ-alumina		
14.30×10^{18} modifier molecules added initially		
Modification time/Minutes	No. of molecules modifier adsorbed x 10^{18}	Nominal ratio
0	0	0
60	2.94	0.20
120	3.93	0.27
180	3.95	0.27
240	4.46	0.31
1380	6.18	0.43
1440	6.22	0.43

Co-adsorption studies using two modifiers

The co-adsorption of diol and diamine on to the Pt/γ-alumina catalyst was examined in three different modes which are (i) addition of a mixture of diol and diamine, (ii) pre-conditioning of the freshly prepared catalyst sample prior to the addition of the second modifier, without the removal of the first modifier and (iii) pre-conditioning of the freshly prepared catalyst sample prior to the addition of the second modifier, with the removal of the first modifier before the addition of the second. Tables 4.48a and 4.48b show the overall results for the addition of a mixture of diol and diamine to a freshly prepared sample of catalyst following equilibration of the modifier with the catalyst.

Figure 4.31:-

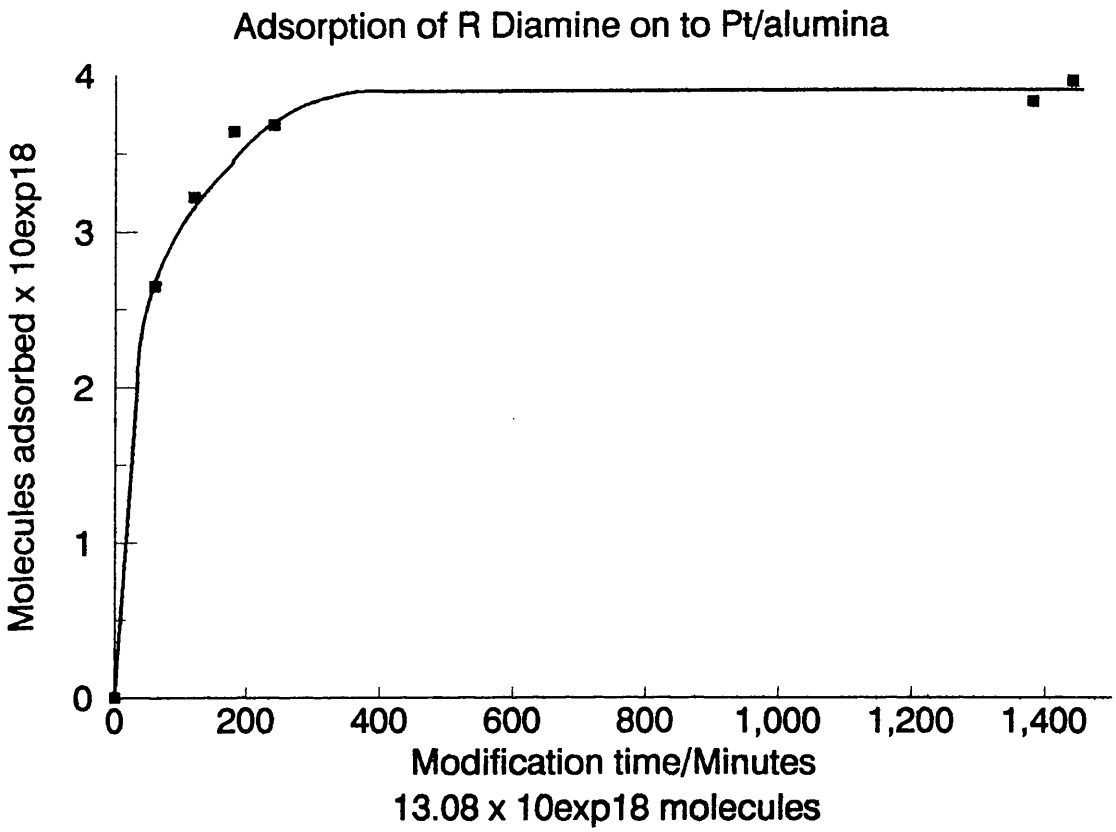

Figure 4.32:-

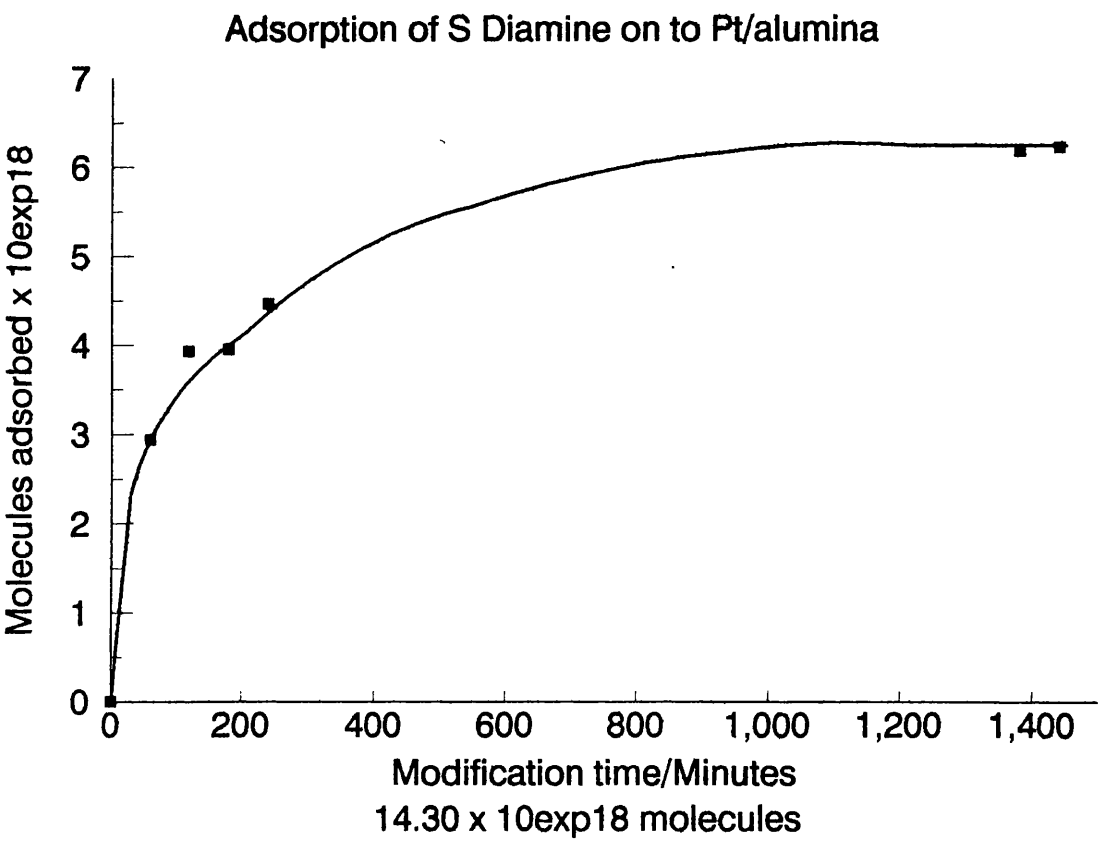

Table 4.48a:- Co-adsorption of diol and diamine on to Pt/γ-alumina			
Modifier	Initial no. of modifier molecules added x 10^{18}	No. of molecules modifier adsorbed x 10^{18}	Nominal ratio
R Diol	5.88	5.62	0.38
± Diamine	6.59	1.67	0.12
R Diol	16.56	16.01	1.11
± Diamine	23.31	7.73	0.54
R Diol	7.27	6.93	0.48
R Diamine	7.75	6.23	0.43
R Diol	7.35	6.53	0.45
S Diamine	7.48	4.68	0.32
R Diol	14.89	14.67	1.02
R Diamine	15.66	6.86	0.48
R Diol	7.71	7.61	0.53
R Diamine	7.93	4.91	0.34
R Diol	13.22	12.60	0.87
R Diamine	13.29	5.16	0.36
R Diol	7.77	7.68	0.53
R Diamine	7.99	4.67	0.32
R Diol	14.89	14.67	1.02
R Diamine	15.66	6.86	0.48
S Diol	7.87	7.67	0.53
S Diamine	7.25	5.46	0.38
R Diol	7.40	7.17	0.50
S Diamine	7.53	4.90	0.34
S Diol	7.38	7.05	0.49
S Diamine	12.90	6.20	0.43
S Diol	8.53	8.44	0.58
S Diamine	17.00	6.74	0.47
S Diol	7.90	7.63	0.53
S Diamine	7.28	5.48	0.40

1 At 273K

Table 4.48b:- Co-adsorption of diol and diamine on to Pt/γ-alumina			
Modifier	Initial no. of modifier molecules added x 10^{18}	No. of molecules modifier adsorbed x 10^{18}	Nominal ratio
S Diol[1]	13.21	12.83	0.89
S Diamine[1]	13.22	5.15	0.56
S Diol	13.41	13.14	0.91
S Diamine	13.33	6.76	0.47
S Diol	19.56	19.03	1.32
S Diamine	10.35	4.68	0.32
S Diol	19.63	19.46	1.35
S Diamine	10.39	1.46	0.10
S Diol	7.25	7.09	0.49
R Diamine	7.47	5.11	0.35
S Diol	7.30	7.08	0.49
R Diamine	7.52	4.57	0.32

1 At 273K

Table 4.49, on the other hand shows a summary of the adsorption data obtained when the catalyst was preconditioned with one enantiomer for the 20 hour equilibrium period, after which the second modifier was added. The superscript '2' indicates the modifier which was added after 20 hours into the original modifier solution and '2*' indicates the resultant adsorption of the original modifier following equilibrium of the second modifier.

Table 4.49:- Co-adsorption of diol and diamine on to Pt/γ-alumina			
Modifier	Initial no. of modifier molecules added x 10^{18}	No. of molecules modifier adsorbed x 10^{18}	Nominal ratio
R Diol	13..97	13.52 13.85^{2*}	0.94 0.96^{2*}
± Diamine[2]	14.06	7.96	0.55
R Diol	14.55	13.40 14.02^{2*}	0.93 0.97^{2*}
± Diamine[2]	14.65	3.60	0.25
R Diol	15.14	14.70 14.51^{2*}	1.02 1.01^{2*}
± Diamine[2]	14.38	1.42	0.10

Table 4.50 also shows the overall results of the adsorption of consecutive co-adsorption studies with the difference that the first modifier was removed prior to the addition of the second modifier to the preconditioned catalyst. The superscript '3' indicates the second modifier and the '3*' the adsorption of the first modifier following the adsorption and equilibration of the second modifier with the catalyst. Table 4.51 and Figure 4.33 show the adsorption of R diol on to the Pt/γ-alumina catalyst preconditioned with (±) diamine. A general overview of the desorption of modifier from the co-adsorbed modified Pt/γ-alumina catalyst is shown by Table 4.52.

Table 4.50:- Co-adsorption of diol and diamine on to Pt/γ-alumina			
Modifier	Initial no. of modifier molecules added x 10^{18}	No. of molecules modifier adsorbed x 10^{18}	Nominal ratio
R Diol	7.25	7.18	0.50
S Diamine[3]	7.30	7.19[3*]	0.50[3*]
		4.83	0.33
S Diol	7.27	7.16	0.50
S Diamine[3]	7.24	7.21[3*]	0.50[3*]
		4.37	0.30
± Diamine	14.87	6.92	0.48
R Diol[3]	14.76	11.82	0.82
S Diamine	7.25	5.46	0.38
S Diol[3]	7.28	7.10	0.49
		6.45[3*]	0.45[3*]
S Diamine	7.33	5.43	0.38
R Diol[3]	7.27	7.23[3*]	0.50[3*]
		6.70	0.46

Table 4.51:- Adsorption of R diol on (±) diamine modified Pt/γ-alumina		
14.87 x 10^{18} diamine molecules added initially		
No. of diamine molecules adsorbed = 6.92 x 10^{18} Nominal ratio 0.48		
14.76 x 10^{18} diol molecules added initially		
Modification time/Minutes	No. of molecules modifier adsorbed x 10^{18}	Nominal ratio
0	0	0
60	1.05	0.07
120	2.95	0.20
180	4.64	0.32
240	5.99	0.42
1290	11.69	0.81
1350	11.82	0.82

Table 4.52a:- Desorption of diol and diamine from diol/diamine modified Pt/γ-alumina			
Modifier	Initial no. of modifier molecules added x 10^{18}	No. of molecules modifier remaining adsorbed after wash x 10^{18}	Nominal resultant ratio
R Diol	7.27	6.64	0.46
R Diamine	7.75	N/A	N/A
R Diol	7.25	N/A	N/A
S Diamine[3]	7.30	7.09[3*]	0.49[3*]
		4.59	0.32
R Diol	7.35	6.34	0.44
S Diamine	7.48	N/A	N/A
R Diol	14.89	10.58	0.73
R Diamine	15.66	4.40	0.30
R Diol	7.71	7.55	0.52
R Diamine	7.93	4.46	0.31
R Diol	7.77	7.47	0.52
R Diamine	7.99	3.96	0.27
R Diol	14.89	10.58	0.73
R Diamine	15.66	4.40	0.30
S Diol	7.27	N/A	N/A
S Diamine[3]	7.24	7.11[3*]	0.49[3*]
		4.03	0.28
S Diol	7.87	7.42	0.51
S Diamine	7.25	N/A	N/A
S Diol	7.38	6.51	0.45
S Diamine	12.90	5.86	0.41
S Diol	7.90	7.06	0.49
S Diamine	7.28	N/A	N/A
S Diol	8.53	8.17	0.57
S Diamine	17.00	5.12	0.35

1 At 273K

Table 4.52b:- Desorption of diol and diamine from diol/diamine modified Pt/γ-alumina			
Modifier	Initial no. of modifier molecules added x 10^{18}	No. of molecules modifier remaining adsorbed after wash x 10^{18}	Nominal resultant ratio
S Diol[1]	13.21	12.68	0.88
S Diamine	13.22	6.89	0.48
S Diol	13.41	12.88	0.89
S Diamine	13.33	5.77	0.40
S Diol	19.56	18.50	1.28
S Diamine	10.35	4.21	0.29
S Diol	19.63	18.96	1.31
S Diamine	10.39	0.83	0.06
S Diol	7.25	6.74	0.47
R Diamine	7.47	4.81	0.33
S Diol	7.30	6.63	0.46
R Diamine	7.52	4.37	0.30
S Diamine	7.25	N/A	N/A
S Diol[3]	7.28	6.81	0.42
		6.20[3*]	0.43[3*]
S Diamine	7.33	N/A	N/A
R Diol[3]	7.27	N/A	N/A
		6.57	0.46

1 At 273K

Increased substitution of the binaphthalene derivatives was also examined by the introduction of hydroxyl groups at the 2 and 7 positions of both naphthalene rings. The adsorption of this (-)-2,2',7,7'-tetrahydroxy-1,1'-binaphthalene modifier, referred to as tetra-ol, was found to occur and Table 4.53 and Figure 4.34 show the extent of adsorption as a function of time.

Table 4.53:- Adsorption of tetra-ol on to Pt/γ-alumina		
5.71×10^{18} tetra-ol molecules added initially		
Modification time/Minutes	No. of molecules modifier adsorbed x 10^{18}	Nominal ratio
0	0	0
10	1.80	0.12
20	2.29	0.16
30	2.91	0.20
40	3.31	0.23
50	3.55	0.25
60	3.84	0.27
90	4.50	0.30
120	4.70	0.33
180	5.01	0.35
240	5.11	0.35
1380	5.26	0.36
1440	5.27	0.37

Adsorption studies of the alternative modifiers

As a result of initial hydrogenation reactions of methyl tiglate (see section 4.3), neither the R or S diol nor diamine were found to be capable of inducing enantioselectivity. This result suggested that the aromatic ring system, that is, naphthyl was not large enough, so to enable the introduction of the anthracene ring system R-(-)-1-(9-anthryl)-2,2,2-trifluoroethanol (TFAE) was studied. Initial studies showed that this molecule was adsorbed as shown by Table 4.54. However, as is be shown by Table 4.55, the case of desorption of TFAE from TFAE modified Pt/γ-alumina catalyst indicates that it is not a suitable modifier for asymmetric hydrogenation reactions.

Table 4.54:- Adsorption of TFAE on to Pt/γ-alumina		
Initial no. of modifier molecules added x 10^{18}	No. of molecules modifier adsorbed x 10^{18}	Nominal ratio
13.55	4.43	0.31

Figure 4.33:-

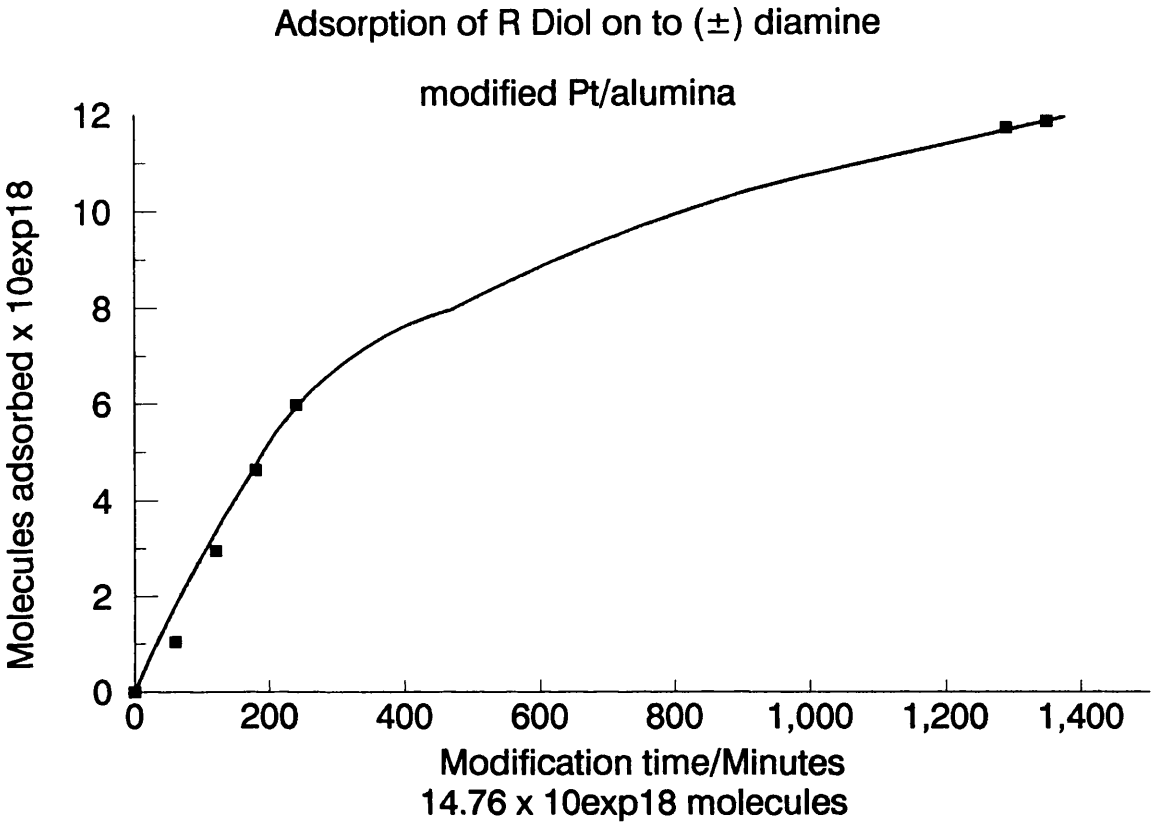

Figure 4.34:-

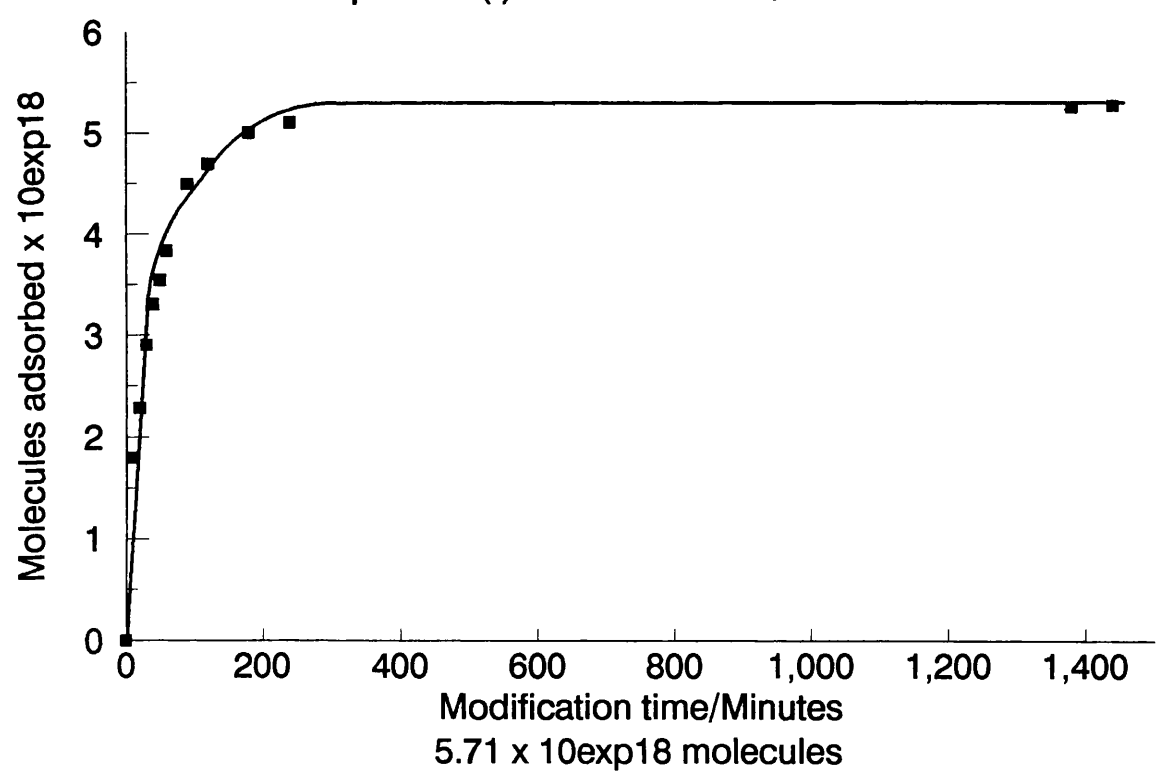

Table 4.55:- Desorption of R TFAE from TFAE modified Pt/γ-alumina		
Initial no. of modifier molecules added x 10^{18}	No. of molecules modifier remaining adsorbed after wash x 10^{18}	Nominal resultant ratio
13.55	0.83	0.06

In the case for support (Appendix 11), section 2.4, the theme of using macrocyclic ligands as modifiers to are used to extend the ideas from the homogeneous system where metal chelated macrocyclic compounds have been studied for their asymmetric hydrogenation properties. The (S,S)-di-(2-propyl)-6,12-dioxa-2,5,13,16-tetraoxo-3,15,19-triazabicyclo [15.3.1] heneicosa-1(21),17,19-triene and (S,S)-di-(2-propyl)-6,13-dioxa-2,5,14,17-tetraoxo-3,16,20-triazabicyclo [16.3.1] docosa-1(22),18,20-triene macrocycles used were those described by Kellogg[121] and will be referred to as $(CH_2)_5$- and $(CH_2)_6$-bridged, pyridine based macrocycles where the main section of the macrocycle was based on a pyridine ring with a bridging carbon chain. The two macrocycles studied had a 5 carbon and 6 carbon chain, respectively. The results for the adsorption of $(CH_2)_5$-bridged, pyridine based macrocycles are shown in Table 4.56 and desorption from the modified catalyst are shown in Table 4.57. The extent of adsorption as a function of time are shown in Tables 4.58 and 4.59 and Figures 4.35 and 4.36.

Table 4.56:- Adsorption of $(CH_2)_5$-bridged, pyridine-based macrocycle on to Pt/γ-alumina		
Initial no. of modifier molecules added x 10^{18}	No. of molecules modifier adsorbed x 10^{18}	Nominal ratio
2.67	2.04	0.14
2.69	2.12	0.15
25.33	5.22	0.36
27.93	2.23	0.15

Table 4.57:- Desorption of $(CH_2)_5$-bridged, pyridine-based macrocycle from $(CH_2)_5$-bridged, pyridine-based macrocycle modified Pt/γ-alumina		
Initial no. of modifier molecules added x 10^{18}	No. of molecules modifier remaining adsorbed after wash x 10^{18}	Nominal resultant ratio
2.69	1.93	0.13
25.33	4.86	0.34
27.93	1.98	0.14

Table 4.58:- Adsorption of $(CH_2)_5$-bridged, pyridine-based macrocycle on to Pt/γ-alumina		
2.67 x 10^{18} modifier molecules added initially		
Modification time/Minutes	No. of molecules modifier adsorbed x 10^{18}	Nominal ratio
0	0	0
60	0.88	0.06
120	1.24	0.09
180	1.26	0.09
240	1.55	0.11
1380	1.98	0.14
1440	2.04	0.14

Table 4.59:- Adsorption of $(CH_2)_5$-bridged, pyridine-based macrocycle on to Pt/γ-alumina		
25.33 x 10^{18} modifier molecules added initially		
Modification time/Minutes	No. of modifier molecules adsorbed x 10^{18}	Nominal ratio
0	0	0
60	6.00	0.42
120	6.04	0.42
180	6.14	0.43
240	5.95	0.41
1380	5.25	0.36
1440	5.22	0.36

Figure 4.35:-

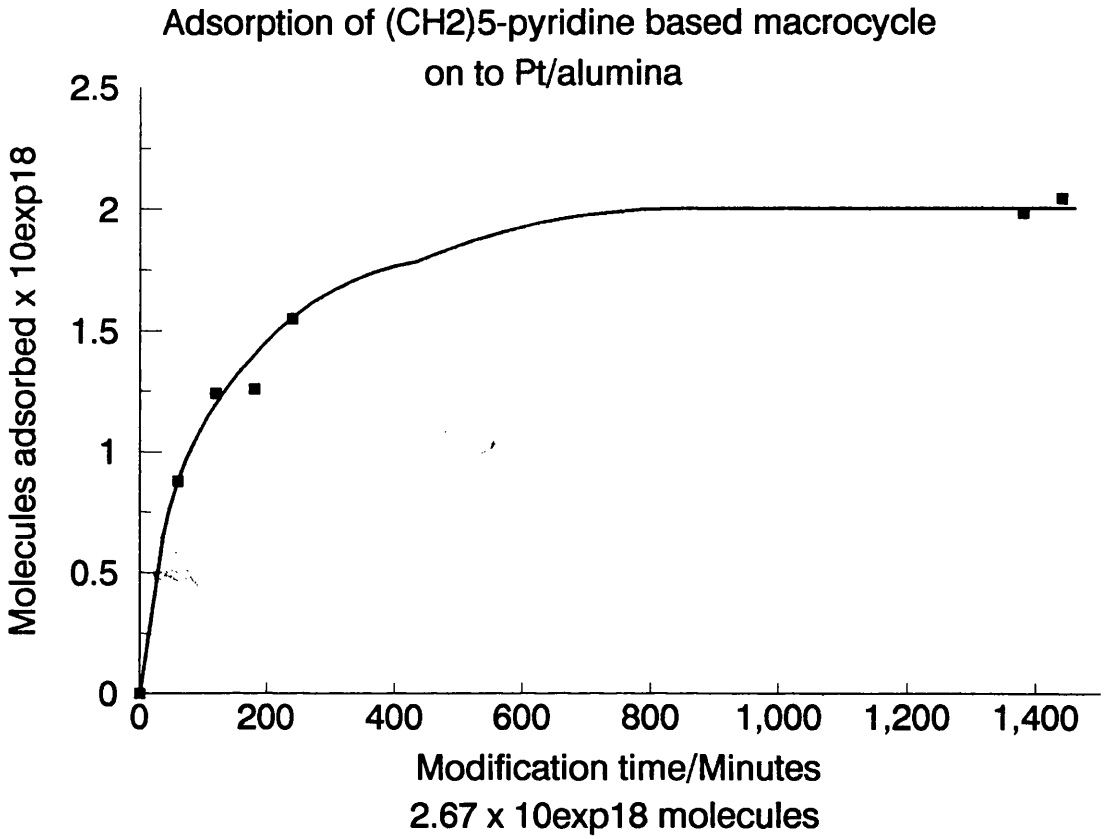

Figure 4.36:-

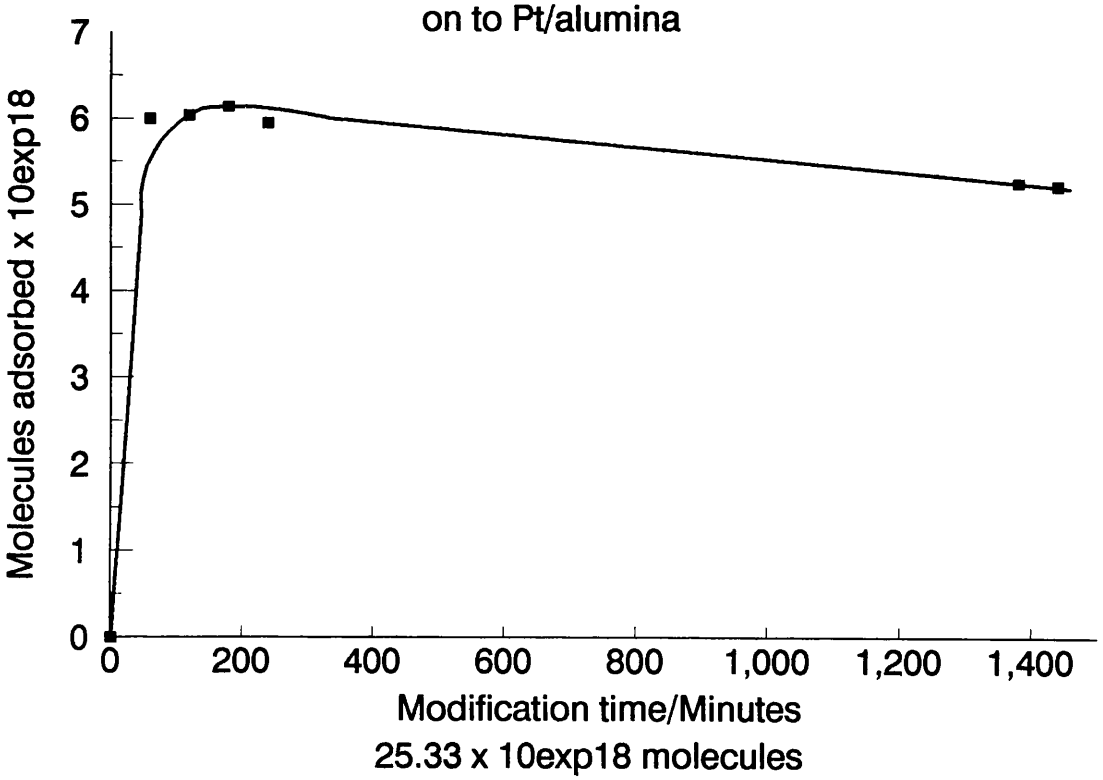

The results for the adsorption of $(CH_2)_6$-bridged, pyridine based macrocycle are shown in Table 4.60, whilst results for the desorption studies are shown in Table 4.61. The extent of adsorption as a function of time are shown in Table 4.62 and Figure 4.37.

Table 4.60:- Adsorption of $(CH_2)_6$-bridged, pyridine-based macrocycle on to Pt/γ-alumina		
Initial no. of modifier molecules added x 10^{18}	No. of molecules modifier adsorbed x 10^{18}	Nominal ratio
2.80	1.73	0.12
26.93	1.06	0.07

Table 4.61:- Desorption of $(CH_2)_6$-bridged, pyridine-based macrocycle from $(CH_2)_6$-bridged, pyridine-based macrocycle modified Pt/γ-alumina		
Initial no. of modifier molecules added x 10^{18}	No. of molecules modifier remaining adsorbed after wash x 10^{18}	Nominal resultant ratio
2.80	1.66	0.12
26.93	0.97	0.05

Table 4.62:- Adsorption of $(CH_2)_6$-bridged, pyridine-based macrocycle on to Pt/γ-alumina		
26.93 x 10^{18} modifier molecules added initially		
Modification time/Minutes	No. of modifier molecules adsorbed x 10^{18}	Nominal ratio
0	0	0
60	0.84	0.06
120	1.03	0.07
180	1.13	0.08
240	1.19	0.08
1380	1.10	0.08
1440	1.06	0.07

Figure 4.37:-

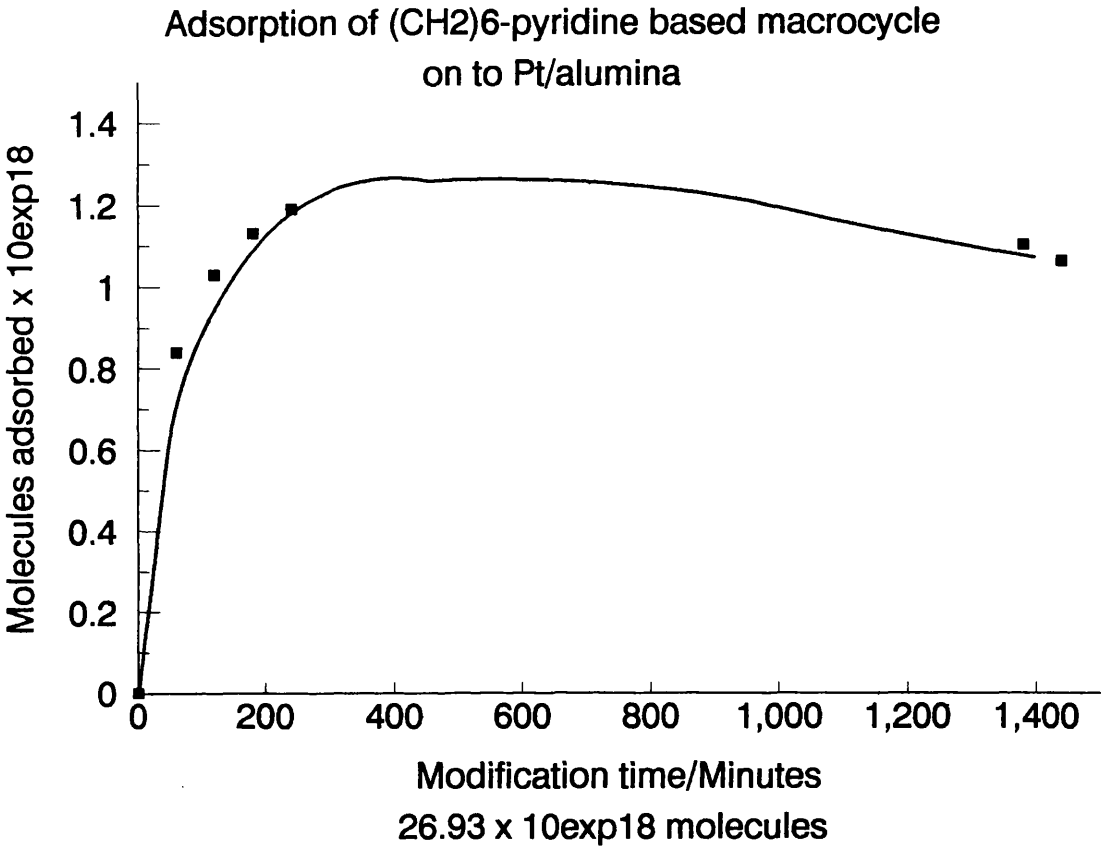
Adsorption of (CH2)6-pyridine based macrocycle
on to Pt/alumina
Molecules adsorbed x 10exp18
1.4
1.2
1
0.8
0.6
0.4
0.2
0
0
200
400
600
800
1,000
1,200
1,400
Modification time/Minutes
26.93 x 10exp18 molecules

4.2.1.3.2 1% w/w Pt/silica C10 catalyst

Diol

Pt/silica C10 was studied, using reactor vessel R2 and flow reduction, for the diol and diamine adsorption. Table 4.63 shows the results for the adsorption at equilibrium for R diol on to Pt/silica C10.

Table 4.63:- Adsorption of R diol on to Pt/silica C10		
Initial no. of modifier molecules added x 10^{18}	No. of molecules modifier adsorbed x 10^{18}	Nominal ratio
2.30	0.19	0.03
5.48	0.00	N/A
5.49	0.00	N/A
5.54	0.10	0.02
5.59[4]	0.00	N/A
5.71	0.00	N/A
5.77	0.11	0.02
5.79	0.21	0.04
5.85	0.61	0.10
6.02	0.64	0.11
6.24	0.21	0.04
6.70	0.14	0.02
15.39	2.83	0.48
21.64	0.00	N/A
23.16	0.00	N/A
23.57	0.00	N/A
24.04	0.00	N/A
44.46	0.00	N/A

4 Cooled in hydrogen

Diamine

While Table 4.64 shows a selection of results for the adsorption of (±) diamine on to Pt/silica C10 at equilibrium.

Table 4.64:- Adsorption of (±) diamine on to Pt/silica C10		
Initial no. of modifier molecules added x 10^{18}	No. of molecules modifier adsorbed x 10^{18}	Nominal ratio
5.35	0.83	0.14
5.46	2.60	0.43
14.46	3.70	0.62

4.2.1.3.3 1% w/w Pt/Cab-O-Sil catalyst

Adsorption studies using one modifier

Diol

As a result of ageing problems of the Pt/silica C10 catalyst, which will be discussed later, a third supported Pt catalyst was prepared. This third catalyst was a 1% w/w Pt/Cab-O-Sil and will be referred to as Pt/Cab-O-Sil. This catalyst was activated by (1) a straightforward reduction procedure and (2) a sintering process prior to the final reduction. Adsorption of both the R and S diol was attempted for the two catalyst activation modes. Tables 4.65 and 4.66 shows typical results of this study.

Table 4.65:- Adsorption of R diol on to Pt/Cab-O-Sil		
Initial no. of modifier molecules added x 10^{18}	No. of molecules modifier adsorbed x 10^{18}	Nominal ratio
2.17$^{\omega}$	0.00	N/A
3.37$^{\omega}$	0.00	N/A
6.61$^{\Phi}$	0.00	N/A
30.47$^{\Phi}$	0.00	N/A

ω Sintered
Φ Unsintered
N/A Not applicable

Table 4.66:- Adsorption of S diol on to Pt/Cab-O-Sil		
Initial no. of modifier molecules added x 10^{18}	No. of molecules modifier adsorbed x 10^{18}	Nominal ratio
4.95^{ω}	0.00	N/A
5.64^{Φ}	0.07	0.01
5.72^{ω}	0.00	N/A
$5.67^{\omega 5}$	0.14	0.03

ω Sintered
Φ Unsintered
N/A Not applicable
5 At 185K (Dry ice and acetone bath)

As noted earlier the nominal ratio is dependent on the number of exposed surface Pt atoms. For the unsintered catalyst the nominal ratio is

$$\frac{\text{No. of adsorbed molecules}}{10.08 \times 10^{18}} = \text{Nominal ratio} \quad (D = 32.98\%, O_2(g))$$

and for the sintered catalyst the nominal ratio is

$$\frac{\text{No. of adsorbed molecules}}{4.35 \times 10^{18}} = \text{Nominal ratio} \quad (D = 14.25\%, O_2(g)).$$

Diamine

The adsorption of the diamine modifier was also examined on this catalyst. As well as adsorption the diamine undergoes an inter-conversion to 2-hydroxy-2'-amino-1,1'-binaphthalene, which will be referred to as 'aminol' as shown by Figure 4.38, and the diol. The aminol was observed by the appearance by HPLC analysis as an extra peak which was eluted before the diamine as shown by Figure 4.39 and verified by injection of a sample of aminol through the HPLC. Tables 4.67 and 4.69 show results for the non-inter-converted adsorption of R and S diamine, respectively, on to both the sintered and unsintered catalyst. Tables 4.68 and 4.70 show the desorption of directly adsorbed R and S diamine from diamine modified Pt/γ-alumina catalyst, respectively. Table 4.71 and Figure 4.40 show the extent of adsorption as a function of time for the non-inter-converted R diamine on to sintered Pt/Cab-O-Sil, while Table 4.72 and Figure 4.41 show the extent of adsorption as a function of time for the non-inter-converted S diamine on to sintered Pt/Cab-O-Sil.

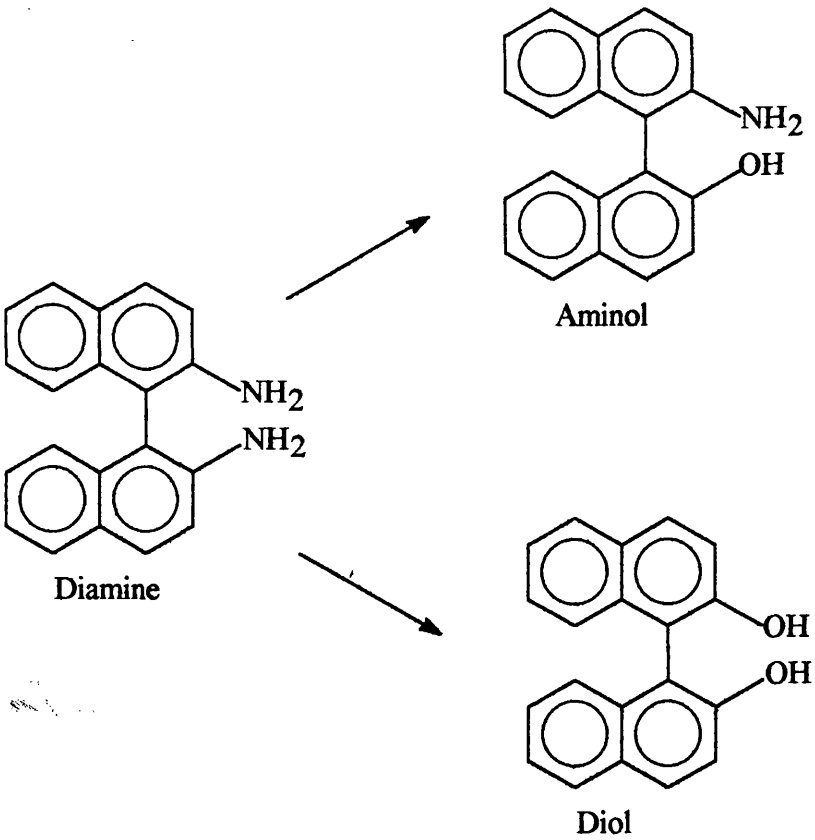

Figure 4.38:- Aminol formation

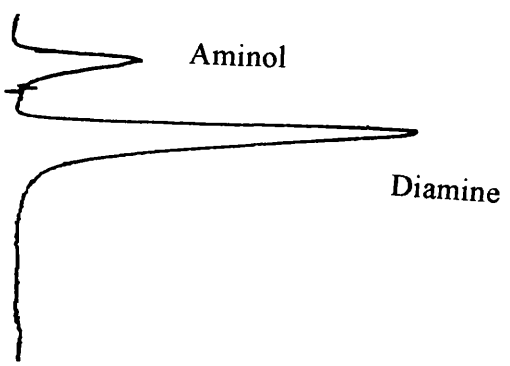

Figure 4.39:- HPLC plot of diamine and aminol

Table 4.67:- Adsorption of R diamine on to Pt/Cab-O-Sil		
Initial no. of modifier molecules added x 10^{18}	No. of molecules modifier adsorbed x 10^{18}	Nominal ratio
4.94$^{\omega}$	0.16	0.04
5.00$^{\Phi}$	0.16	0.02
5.34$^{\omega}$	0.48	0.11
5.76$^{\Phi}$	1.22	0.12
5.91$^{\Phi}$	1.28	0.13
5.93$^{\Phi}$	1.40	0.14
5.97$^{\Phi}$	1.10	0.11
6.71$^{\omega}$	0.93	0.21
7.90$^{\Phi}$	0.58	0.06
10.18$^{\Phi}$	0.53	0.05
10.65$^{\Phi}$	0.34	0.03
11.06$^{\Phi 1}$	5.71	0.56
18.93$^{\Phi}$	14.68	1.46

ω Sintered
Φ Unsintered
1 At 273K

Table 4.68:- Desorption of R diamine from diamine modified Pt/Cab-O-Sil		
Initial no. of modifier molecules added x 10^{18}	No. of molecules modifier remaining adsorbed after wash x 10^{18}	Nominal resultant ratio
5.00$^{\Phi}$	-0.31	N/A
5.34$^{\omega}$	0.19	0.04
5.93$^{\Phi}$	0.52	0.05
5.93$^{\Phi}$	1.20	0.12
7.90$^{\Phi}$	0.11	0.01
10.18$^{\Phi}$	-1.98(+ 0.05 Aminol)	N/A (+ < 0.01 Aminol)
18.93$^{\Phi}$	1.02	0.10

Φ Unsintered
ω Sintered
N/A Not applicable

Table 4.69:- Adsorption of S diamine on to Pt/Cab-O-Sil		
Initial no. of modifier molecules added x 10^{18}	No. of molecules modifier adsorbed x 10^{18}	Nominal ratio
4.97$^{\omega}$	0.89	0.20
4.99$^{\omega}$	1.37	0.31
5.36$^{\omega}$	0.69	0.16
5.88$^{\omega}$	0.96	0.22
6.03$^{\Phi}$	1.45	0.14
14.64$^{\Phi}$	2.03	0.20

ω Sintered
Φ Unsintered

Table 4.70:- Desorption of S diamine from diamine modified Pt/Cab-O-Sil		
Initial no. of modifier molecules added x 10^{18}	No. of molecules modifier remaining adsorbed after wash x 10^{18}	Nominal resultant ratio
4.97$^{\omega}$	0.55	0.13
5.36$^{\omega}$	0.27	0.06
6.03$^{\Phi}$	1.28	0.13

Φ Unsintered
ω Sintered

Table 4.71:- Adsorption of R Diamine on to Pt/Cab-O-Sil$^{\omega}$		
4.94 x 10^{18} modifier molecules added initially		
Modification time/Minutes	No. of molecules modifier adsorbed x 10^{18}	Nominal ratio
0	0	0
60	0.03	< 0.01
120	0.05	0.01
180	0.09	0.02
240	0.10	0.02
1380	0.13	0.03
1440	0.16	0.04

ω Sintered

Table 4.72:- Adsorption of S Diamine on to Pt/Cab-O-Sil$^{\omega}$		
4.98 x 10^{18} modifier molecules added initially		
Modification time/Minutes	No. of molecules modifier adsorbed x 10^{18}	Nominal ratio
0	0	0
60	0.17	0.04
120	0.21	0.05
180	0.24	0.06
240	0.22	0.05
1380	0.83	0.19
1440	0.89	0.20

ω Sintered

Adsorption of diamine where inter-conversion occurs is shown for R and S diamine for only the unsintered catalyst form in Tables 4.73 and 4.75. Desorptions from diamine modified Pt/γ-alumina catalyst where inter-conversion is observed are shown in Tables 4.74 and 4.76 for R and S diamine, respectively.

Table 4.73:- Adsorption of R Diamine on to Pt/Cab-O-Sil		
Initial no. of modifier molecules added x 10^{18}	No. of molecules modifier adsorbed x 10^{18}	Nominal ratio
7.97$^{\Phi}$	0.68 (+ 0.16 Aminol)	0.07 (+ 0.02 Aminol)
9.16$^{\Phi}$	1.76 (+ 3.19 Aminol + 0.30 Diol)	0.17 (+ 0.32 Aminol + 0.03 Diol)
9.21$^{\Phi 1}$	1.27 (+ 0.06 Aminol)	0.13 (+ < 0.01 Aminol)
10.65$^{\Phi 1}$	1.02 (+ 0.27 Aminol + 0.22 Diol)	0.10 (+ 0.03 Aminol + 0.02 Diol)
17.61$^{\Phi}$	0.86 (+ 0.15 Aminol + 0.06 Diol)	0.09(+ 0.0 Aminol + < 0.01 Diol)
19.12$^{\Phi 6}$	0.57 (+ 0.90 Aminol)	0.06 (+ 0.09 Aminol)
26.01$^{\Phi}$	7.87 (+ 0.45 Aminol)	0.78 (+ 0.04 Aminol)
26.17$^{\Phi}$	3.09 (+ 1.31 Aminol)	0.31 (+ 0.13 Aminol)

Φ Unsintered
1 At 273K
6 68 Hours

Figure 4.40:-

Adsorption of R Diamine on to Pt/Cab-O-Sil

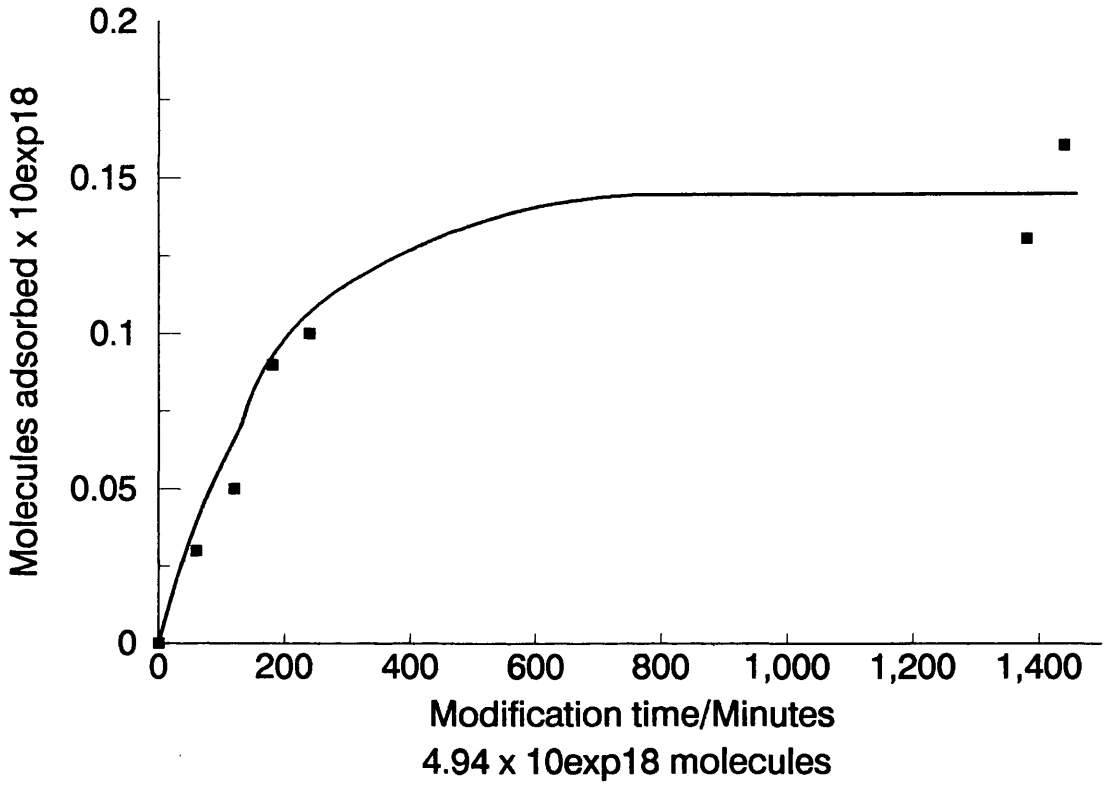

4.94 x 10exp18 molecules

Figure 4.41:-

Adsorption of S Diamine on to Pt/Cab-O-Sil

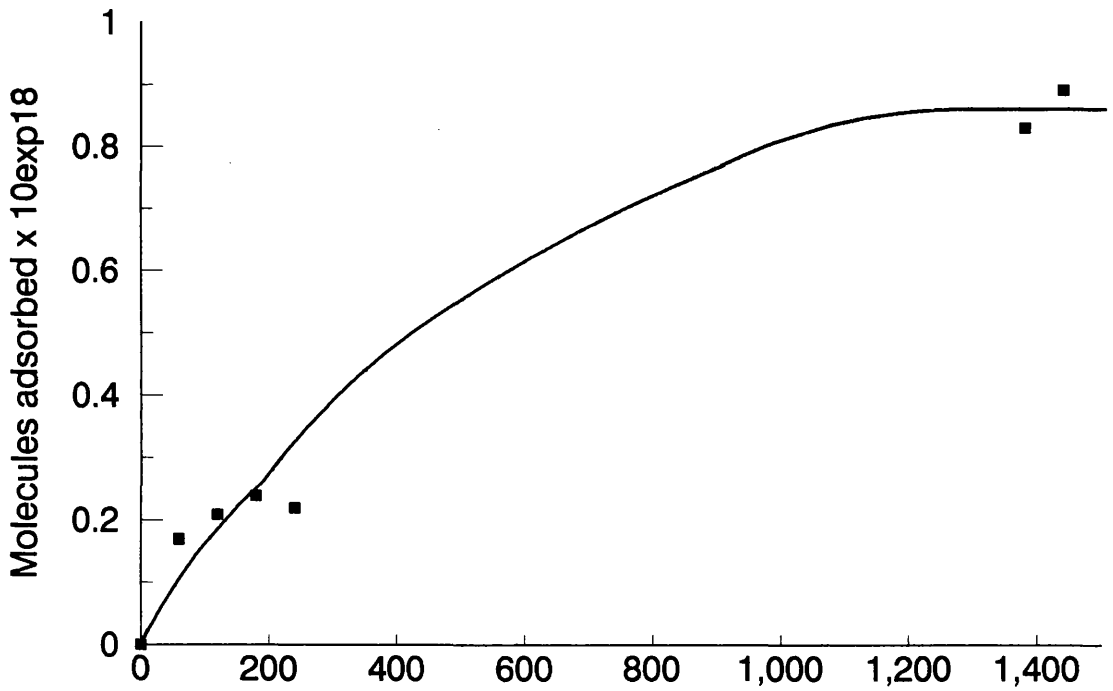

4.98 x 10exp18 molecules

Table 4.74:- Desorption of R diamine from diamine modified Pt/Cab-O-Sil		
Initial no. of modifier molecules added x 10^{18}	No. of molecules modifier remaining adsorbed after wash x 10^{18}	Nominal resultant ratio
7.97$^{\Phi}$	0.41$^{\phi}$	0.04$^{\phi}$
9.16$^{\Phi}$	2.12 (+ 0.43 Aminol + 0.07 Diol)	0.21 (+0.04 Aminol + < 0.01 Diol)
10.65$^{\Phi 1}$	0.19 (+ 0.11 Aminol)	0.02 (+ 0.01 Aminol)
17.61$^{\Phi}$	-0.83$^{\phi}$	N/A$^{\phi}$
19.12$^{\Phi 6}$	0.55 (+ 0.02 Aminol)	0.05 (+ < 0.01 Aminol)
26.01$^{\Phi}$	7.01 (+ 0.10 Aminol)	0.69 (+ 0.01 Aminol)
26.17$^{\Phi}$	2.13 (+ 0.16 Aminol)	0.21 (+ 0.02 Aminol)

Φ Unsintered
ϕ Includes aminol
1 At 273K
6 68 Hours

Table 4.75:- Adsorption of S Diamine on to Pt/Cab-O-Sil		
Initial no. of modifier molecules added x 10^{18}	No. of molecules modifier adsorbed x 10^{18}	Nominal ratio
19.61$^{\Phi}$	5.19 (+ 6.35 Aminol + 0.82 Diol)	0.51 (+ 0.63 Aminol + 0.08 Diol)

Φ Unsintered

Table 4.76:- Desorption of S diamine from diamine modified Pt/Cab-O-Sil		
Initial no. of modifier molecules added x 10^{18}	No. of molecules modifier remaining adsorbed after wash x 10^{18}	Nominal resultant ratio
19.61$^{\Phi}$	4.95 (+ 0.10 Diol and 0.41 Aminol)	0.49 (+ 0.01 Diol and 0.04 Aminol)

Φ Unsintered

Dimethoxy

As with the other two Pt-supported catalysts, Pt/Cab-O-Sil was used to study the adsorption of (±) dimethoxy. The dimethoxy was not adsorbed by either the sintered or unsintered form as shown by Table 4.77.

Table 4.77:- Adsorption of (±) dimethoxy on to Pt/Cab-O-Sil		
Initial no. of modifier molecules added x 10^{18}	No. of molecules modifier adsorbed x 10^{18}	Nominal ratio
4.35$^{\omega}$	0.00	N/A
4.65$^{\Phi}$	0.00	N/A

Φ Unsintered
ω Sintered
N/A Not applicable

Co-adsorption studies using two modifiers

Similar studies to those of Pt/γ-alumina were undertaken with Pt/Cab-O-Sil in the sintered and unsintered forms. Table 4.78 gives of the adsorption data for co-adsorption of diol and diamine, when the two modifiers are added simultaneously. The results for desorption following a washing of the modified catalyst are shown in Table 4.79. It can be noted that diol is created and in some circumstances aminol formation is observed. Tables 4.80 to 4.81 and Figures 4.42 to 4.45 show the extent of adsorption as a function of time.

Table 4.78:- Co-adsorption of diol and diamine on to Pt/Cab-O-Sil			
Modifier	Initial no. of modifier molecules added x 10^{18}	No. of molecules modifier adsorbed x 10^{18}	Nominal ratio
R Diol$^{\omega}$	4.94	0.13^{7}	0.03
R Diamine	4.98	1.15	0.26
R Diol$^{\omega}$	5.05	0.11^{7}	0.03
R Diamine	5.09	2.01	0.46
R Diol$^{\Phi}$	6.35	0.35^{7}	0.03
R Diamine	5.97	3.30 (+ 1.76 Aminol)	0.33 (+ 0.17 Aminol)
R Diol$^{\Phi}$	6.41	0.24^{7}	0.02
R Diamine	6.04	1.75	0.17
R Diol$^{\Phi}$	6.71	0.39^{7}	0.04
R Diamine	7.15	3.70	0.37
S Diol$^{\Phi}$	5.33	0.26^{7}	0.03
S Diamine	8.50	2.09 (+ 1.35 Aminol)	0.21 (+ 0.13 Aminol)
S Diol$^{\Phi}$	7.31	0.38^{7}	0.04
S Diamine	12.78	1.07	0.11
S Diol$^{\Phi 1}$	12.78	0.16^{7}	0.02
S Diamine	12.62	6.10 (+ 1.49 Aminol)	0.61 (+ 0.15 Aminol)

Φ Unsintered
ω Sintered
1 At 273K
7 Diol produced

Table 4.80:- Adsorption of R Diol and R Diamine on to Pt/Cab-O-Sil$^{\omega}$				
5.05×10^{18} diol molecules added initially				
5.09×10^{18} diamine molecules added initially				
Modification time/Minutes	No. of molecules diol created x 10^{18}	Nominal ratio	No. of molecules diamine adsorbed x 10^{18}	Nominal ratio
0	0	0	0	0
60	0.14	0.03	0.17	0.04
120	0.18	0.04	0.14	0.03
180	0.25	0.06	0.35	0.08
240	0.57	0.13	0.22	0.05
1380	1.05	0.24	0.83	0.19
1440	1.11	0.25	0.91	0.20

ω Sintered

Table 4.81:- Adsorption of R Diol and R Diamine on to Pt/Cab-O-Sil$^{\Phi}$						
6.35×10^{18} modifier molecules added initially						
5.97×10^{18} modifier molecules added initially						
Modification time/ Minutes	No. of molecules Diol created x 10^{18}	Nominal ratio	No. of molecules Diamine adsorbed x 10^{18}	Nominal ratio	No. of molecules Aminol created x 10^{18}	Nominal ratio
0	0	0	0	0	0	0
60	0.02	< 0.01	0.76	0.08	0	0
120	0.06	< 0.01	0.58	0.06	0	0
180	0.19	0.02	0.71	0.07	0.06	< 0.01
240	0.02	< 0.01	1.09	0.11	0.58	0.06
1380	1.56	0.15	1.58	0.16	1.84	0.18
1440	1.76	0.17	1.54	0.15	1.76	0.17

Φ Unsintered

Figure 4.42:-

Adsorption of R Diol and R Diamine on to Pt/Cab-O-Sil

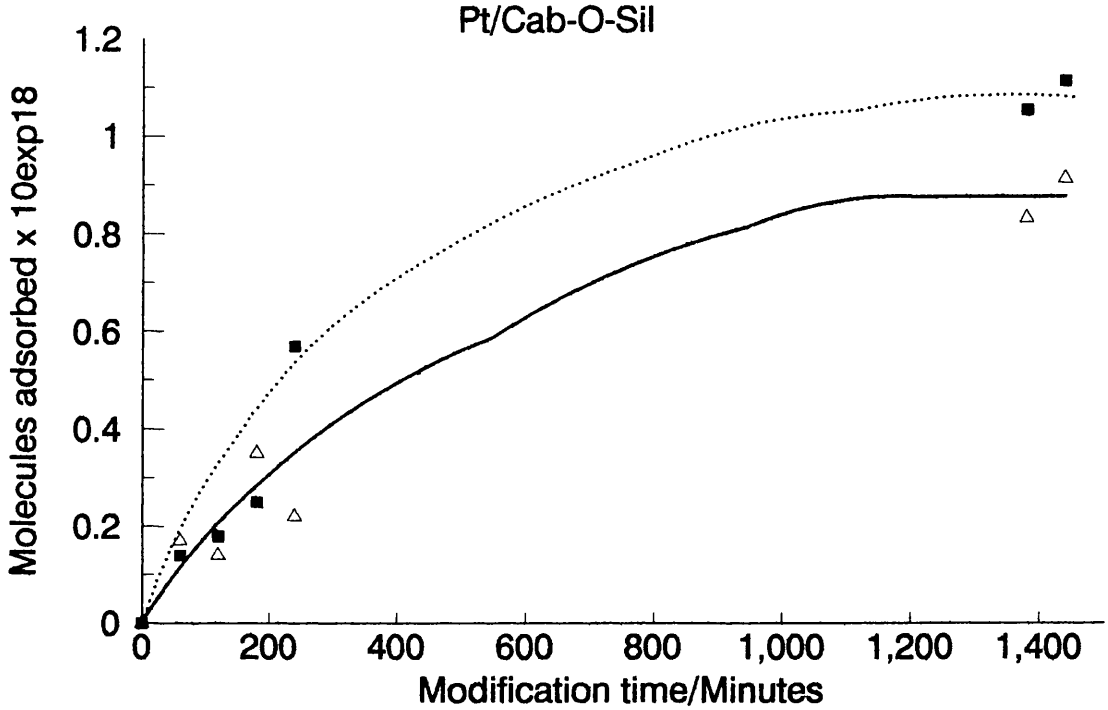

5.05 x 10exp 18 molecules diol ■ 5.09 x 10exp 18 molecules diam △

NB. diol created not adsorbed

Figure 4.43:-

Adsorption of R Diol and R Diamine on to Pt/Cab-O-Sil

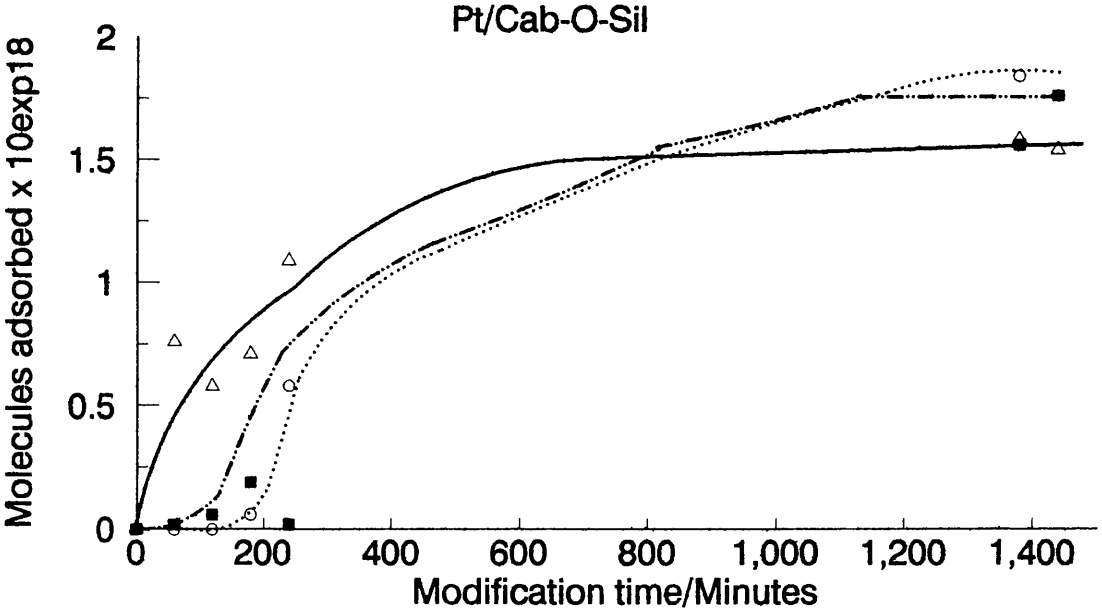

6.35 x 10exp 18 molecules diol ■ 5.97 x 10exp 18 molecules diam △

Aminol formation ○

NB. diol created not adsorbed

NB. aminol formation

Table 4.82:- Adsorption of S diol and S diamine on to Pt/Cab-O-Sil$^{\Phi}$						
5.33×10^{18} diol molecules added initially						
8.50×10^{18} diamine molecules added initially						
Modification time/Minutes	No. of molecules Diol created x 10^{18}	Nominal ratio	No. of molecules Diamine adsorbed x 10^{18}	Nominal ratio	No. of molecules Aminol created x 10^{18}	Nominal ratio
0	0	0	0	0	0	0
60	0.02	< 0.01	0.89	0.09	0	0
120	0.10	0.01	0.98	0.10	0	0
180	0.31	0.03	0.97	0.10	0.35	0.03
240	0.21	0.02	1.17	0.12	0.42	0.04
1380	0.43	0.04	1.85	0.18	1.38	0.14
1440	0.26	0.03	2.09	0.21	1.35	0.13

Φ Unsintered

Table 4.83:- Adsorption of S Diol and S Diamine on to Pt/Cab-O-Sil$^{\Phi}$ at 273K						
12.78 x 10^{18} Diol molecules added initially						
12.62 x 10^{18} Diamine molecules added initially						
Modification time/Minutes	No. of molecules Diol created x 10^{18}	Nominal ratio	No. of molecules Diamine adsorbed x 10^{18}	Nominal ratio	No. of molecules Aminol created x 10^{18}	Nominal ratio
0	0	0	0	0	0	0
60	0.23	0.05	0.19	0.04	0	0
120	0.36	0.08	0.24	0.06	0	0
180	0.47	0.11	1.02	0.23	0.44	0.10
240	0.52	0.12	1.92	0.44	0.78	0.18
1380	0.01	< 0.01	6.00	1.38	1.71	0.39
1440	0.16	0.04	6.10	1.40	1.49	0.34

Φ Unsintered

Figure 4.44:-

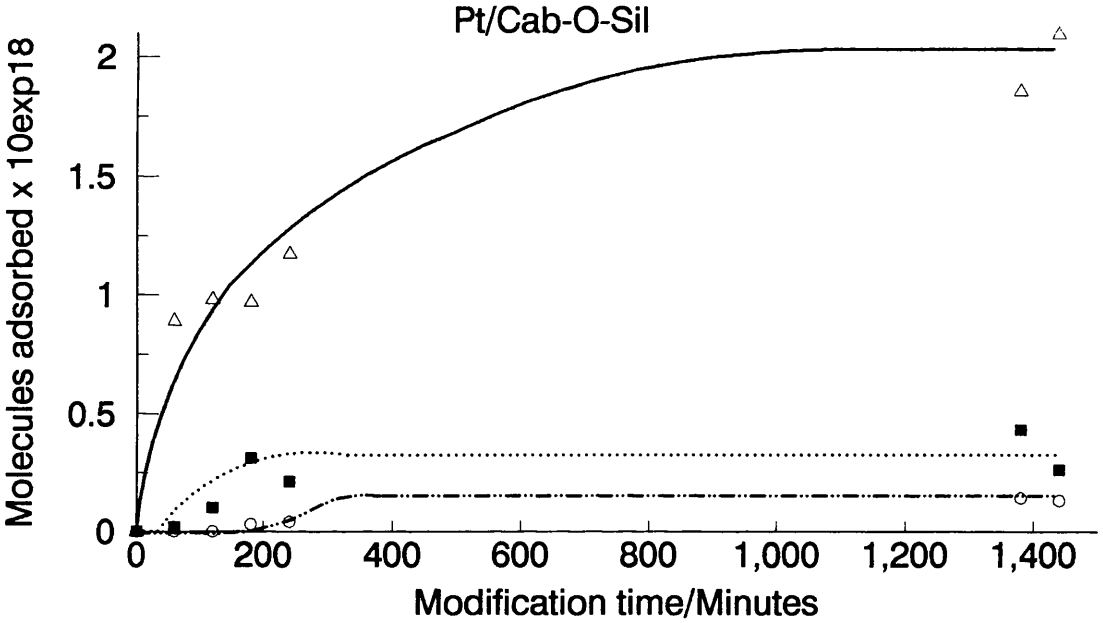

5.33 x 10exp 18 molecules diol ■ 8.50 x 10exp 18 molecules diam △

Aminol formation ○

NB. diol created not adsorbed

NB. aminol formation

Figure 4.45:-

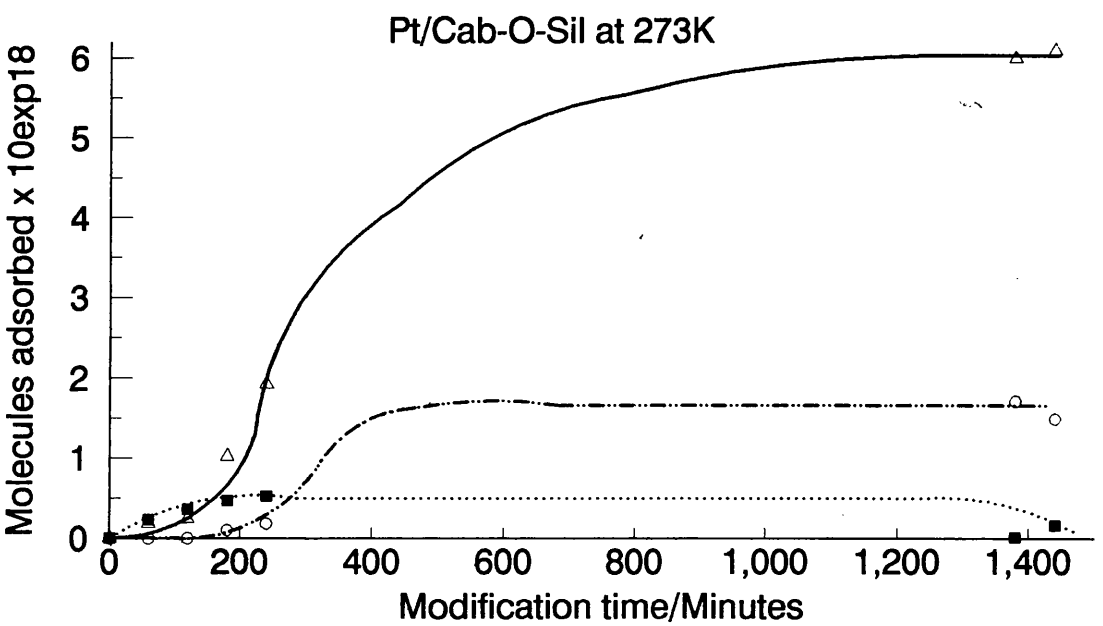

12.78 x 10exp18 molecules diol ■ 12.62 x 10exp18 molecules diam △

Aminol formation ○

NB. diol created not adsorbed

NB. aminol formation

Table 4.79:- Desorption of diol and diamine from diol/diamine modified Pt/Cab-O-Sil		
Modifier	No. of molecules modifier adsorbed x 10^{18}	Nominal resultant ratio
R Diol$^{\Phi}$	0.39[7]	0.04[7]
R Diamine	3.70	0.02
S Diol$^{\Phi}$	0.26[7]	0.09[7]
S Diamine	2.09 (+ 1.35 Aminol)	0.14 (+0.11 Aminol)
S Diol$^{\Phi 1}$	0.16[7]	0.16[7]
S Diamine	6.10 (+ 1.49 Aminol)	0.43 (+ 0.11 Aminol)

Φ Unsintered
1 At 273K
7 Diol produced

The tetrasubstituted hydroxy binaphthalene, tetra-ol was also studied for its adsorption on to Pt/Cab-O-Sil. The results are shown in Table 4.84.

Table 4.84:- Adsorption of tetra-ol on to Pt/Cab-O-Sil		
Initial no. of modifier molecules added x 10^{18}	No. of molecules modifier adsorbed x 10^{18}	Nominal ratio
5.71$^{\Phi}$	0.00	N/A

Φ Unsintered

Adsorption studies of the alternative modifiers

TFAE was studied. The results shown in Table 4.85.

Table 4.85:- Adsorption of TFAE on to Pt/Cab-O-Sil		
Initial no. of modifier molecules added x 10^{18}	No. of molecules modifier adsorbed x 10^{18}	Nominal ratio
4.39$^{\omega}$	0.02	< 0.01
4.40$^{\Phi}$	0.00	N/A

Φ Unsintered
ω Sintered
N/A Not applicable

The $(CH_2)_5$- and $(CH_2)_6$-bridged, pyridine based macrocycles were also studied. The

adsorption are results shown in Tables 4.86, 4.88 and 4.90 and the desorption results are shown in Tables 4.87 and 4.89. Table 4.90 and Figure 4.46 shows the extent of adsorption as a function of time.

Table 4.86:- Adsorption of $(CH_2)_5$-bridged, pyridine-based macrocycles on to Pt/Cab-O-Sil		
Initial no. of modifier molecules added x 10^{18}	No. of molecules modifier adsorbed x 10^{18}	Nominal ratio
2.52$^{\Phi}$	0.40	0.04
3.04$^{\Phi}$	0.48	0.05
25.28$^{\Phi}$	0.66	0.07

Φ Unsintered

Table 4.87:- Desorption of $(CH_2)_5$-bridged, pyridine-based macrocycle from $(CH_2)_5$-bridged, pyridine-based macrocycle modified Pt/Cab-O-Sil		
Initial no. of modifier molecules added x 10^{18}	No. of molecules modifier remaining adsorbed after wash x 10^{18}	Nominal resultant ratio
25.28$^{\Phi}$	0.09	< 0.01

Φ Unsintered

Table 4.88:- Adsorption of $(CH_2)_6$-bridged, pyridine-based macrocycles on to Pt/Cab-O-Sil		
Initial no. of modifier molecules added x 10^{18}	No. of molecules modifier adsorbed x 10^{18}	Nominal ratio
1.21$^{\Phi}$	0.39	0.04
2.40$^{\Phi}$	0.21	0.02
2.68$^{\Phi}$	0.13	0.01

Φ Unsintered

Table 4.89:- Desorption of $(CH_2)_6$-bridged, pyridine-based macrocycle from $(CH_2)_6$-bridged, pyridine-based macrocycle modified Pt/Cab-O-Sil		
Initial no. of modifier molecules added x 10^{18}	No. of molecules modifier remaining adsorbed after wash x 10^{18}	Nominal resultant ratio
1.21$^{\Phi}$	0.38	0.04
2.40$^{\Phi}$	0.15	0.01
2.68$^{\Phi}$	-0.05	N/A

Φ Unsintered
N/A Not applicable

Table 4.90:- Adsorption of $(CH_2)_6$-bridged, pyridine-based macrocycle on to Pt/Cab-O-Sil$^{\Phi}$		
2.68 x 10^{18} modifier molecules added initially		
Modification time/Minutes	No. of molecules modifier adsorbed x 10^{18}	Nominal ratio
0	0	0
60	0.02	< 0.01
120	0.05	< 0.01
180	0.06	< 0.01
1380	0.03	< 0.01
1440	0.13	0.01

Φ Unsintered

4.2.2 Supports

Adsorption and subsequent desorption of the modifiers was carried out on the catalyst support materials, namely; γ-alumina, Grace silica C10 (silica C10) and Cab-O-Sil in an analogous manner to that used for the catalysts themselves, using the apparatus outlined in sections 3.4.3.4 and 3.4.3.5. The supports were subjected to the same conditions as the corresponding catalyst, that is for example, γ-alumina was subjected to flowing dihydrogen for 2 hours at 573K followed by the purging of dinitrogen and cooling of the support in dinitrogen. Adsorption/desorption of the modifiers on to/from the supports was monitored as for the catalysts and analysis by HPLC. The modifiers studied for support adsorption properties were the diol, diamine, tetra-ol, TFAE and $(CH_2)_5$- and $(CH_2)_6$-bridged, pyridine based macrocycles.

4.2.2.1 γ-Alumina

The adsorption and desorption results of the diol, diamine, tetra-ol, TFAE and $(CH_2)_5$- and $(CH_2)_6$-bridged, pyridine based macrocycles for the γ-alumina support are shown in Table 4.91. All figures quoted for modifier addition and adsorption are per gram of support. Tables 4.92 and 4.93 and Figures 4.47 and 4.48 show the extent of adsorption as a function of time for diol, whilst Table 4.94 and Figure 4.49 show the desorption of diol from diol modified γ-alumina over time at ambient temperature. Tables 4.95 and 4.96 and Figures 4.50 and 4.51 show the extent of adsorption as a function of time for diamine adsorption on to γ-alumina. Table 4.97 and Figure 4.52 show the adsorption of tetra-ol on to the γ-alumina support and Tables 4.98 and 4.99 and Figures 4.53 and 4.54 show the extent of adsorption as a function of time for the $(CH_2)_5$- and $(CH_2)_6$-bridged, pyridine-based macrocycles on to the γ-alumina support.

Table 4.91:- Adsorption of modifier on to the γ-alumina support followed by desorption

Modifier	Initial no. of modifier molecules added x 10^{18}	No. of molecules modifier adsorbed x 10^{18}	No. of molecules modifier remaining adsorbed after wash x 10^{18}
R Diol	14.11	13.68	N/A
R Diol	14.75	13.51	13.51
R Diol	15.04	14.67	14.50
R Diol	15.20	14.48	N/A
R Diol	23.09	22.89	22.57
(±) Diamine	14.45	1.11	N/A
(±) Diamine	14.49	3.87	N/A
(-) Tetra-ol	5.68	5.28	N/A
R TFAE	14.47	0.00	N/A
$(CH_2)_5$-bridged, pyridine-based macrocycle	2.65	2.24	N/A
$(CH_2)_5$-bridged, pyridine-based macrocycle	2.67	0.44	0.32
$(CH_2)_5$-bridged, pyridine-based macrocycle	2.79	1.18	0.73
$(CH_2)_6$-bridged, pyridine-based macrocycle	2.78	0.40	0.09

N/A No data available

Table 4.92:- Adsorption of R Diol on γ-Alumina support	
14.11 x 10^{18} modifier molecules added initially	
Modification time/Minutes	No. of molecules modifier adsorbed x 10^{18}
0	0
60	7.93
120	9.11
180	11.52
240	12.34
1380	13.63
1440	13.68

Table 4.93:- Adsorption of R Diol on γ-Alumina	
15.18 x 10^{18} modifier molecules added initially	
Modification time/Minutes	No. of molecules modifier adsorbed x 10^{18}
0	0
60	6.20
120	8.61
180	10.62
390	13.33
1380	14.34
1440	14.48

Figure 4.46:-

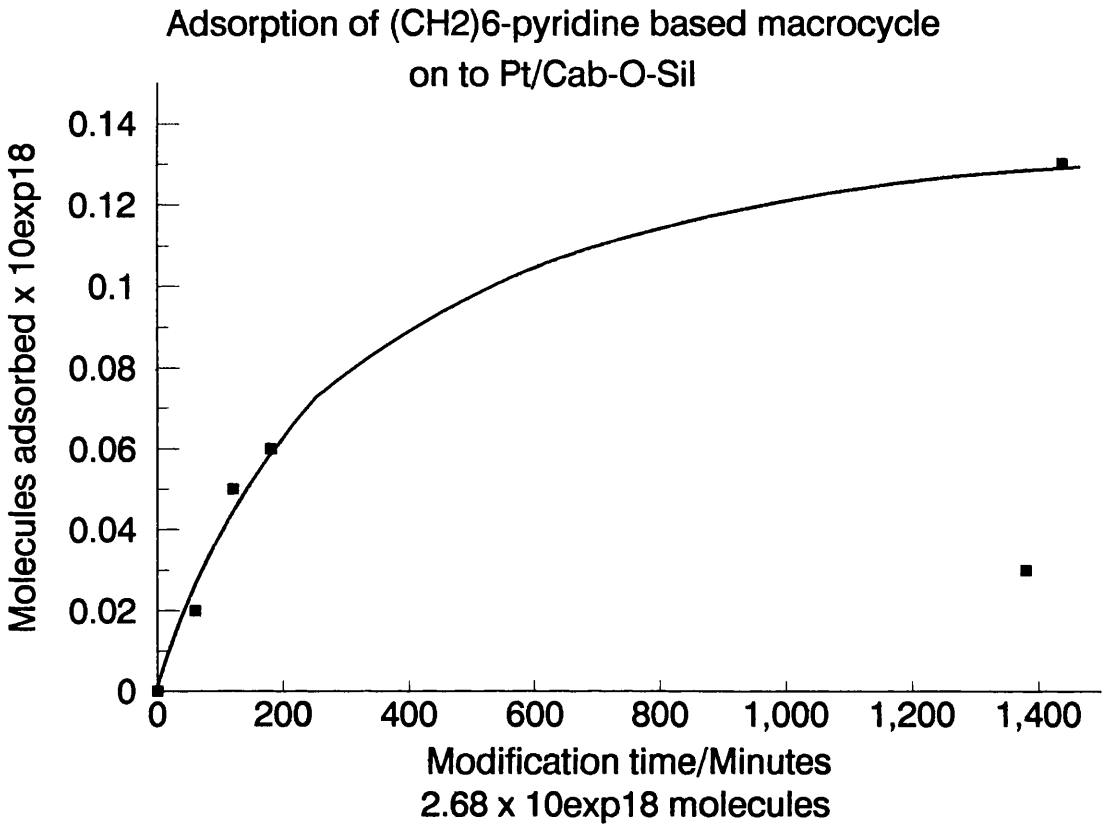

Figure 4.47:-

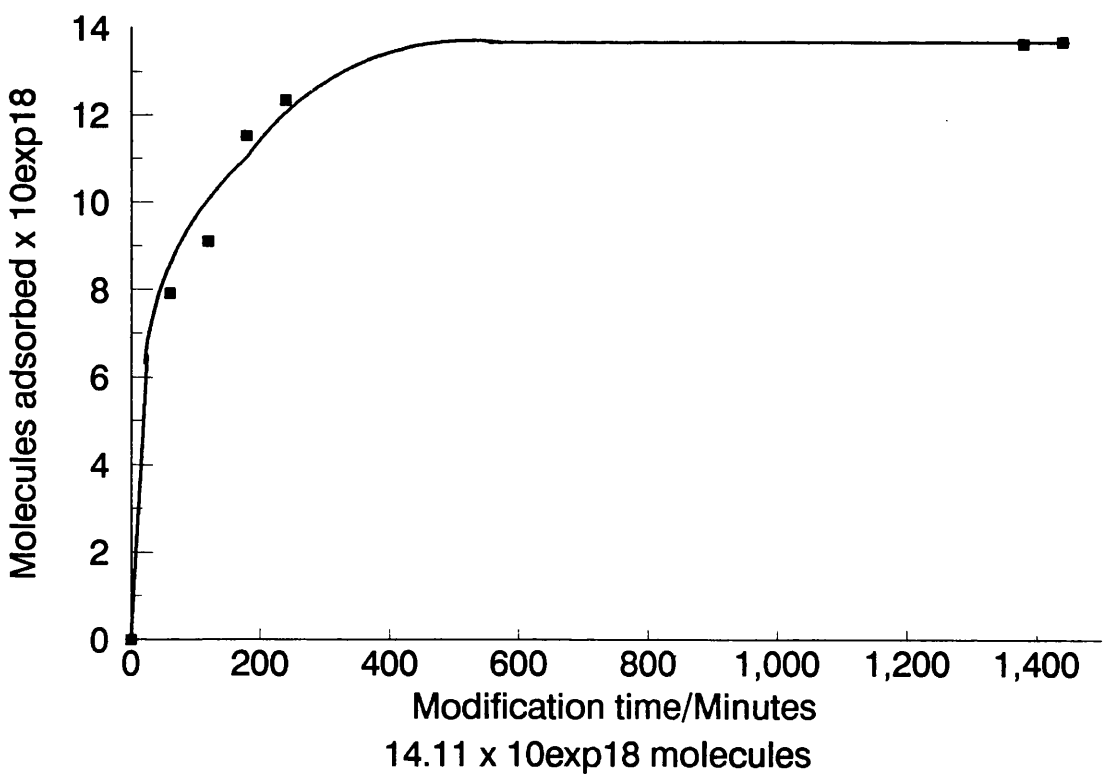

Table 4.94:- Desorption of R Diol from diol modified γ-Alumina	
15.04×10^{18} modifier molecules added initially	
Modification time at ambient temperature/Minutes	No. of molecules modifier desorbed x 10^{18}
Before wash	14.67
60	14.50
120	14.41
180	14.50
240	14.05
300	12.82

Table 4.95:- Adsorption of (±) Diamine on γ-Alumina	
14.45×10^{18} modifier molecules added initially	
Modification time/Minutes	No. of molecules modifier adsorbed x 10^{18}
0	0
60	2.88
120	2.93
180	3.00
240	3.39
1380	1.90
1440	1.11

Figure 4.48:-

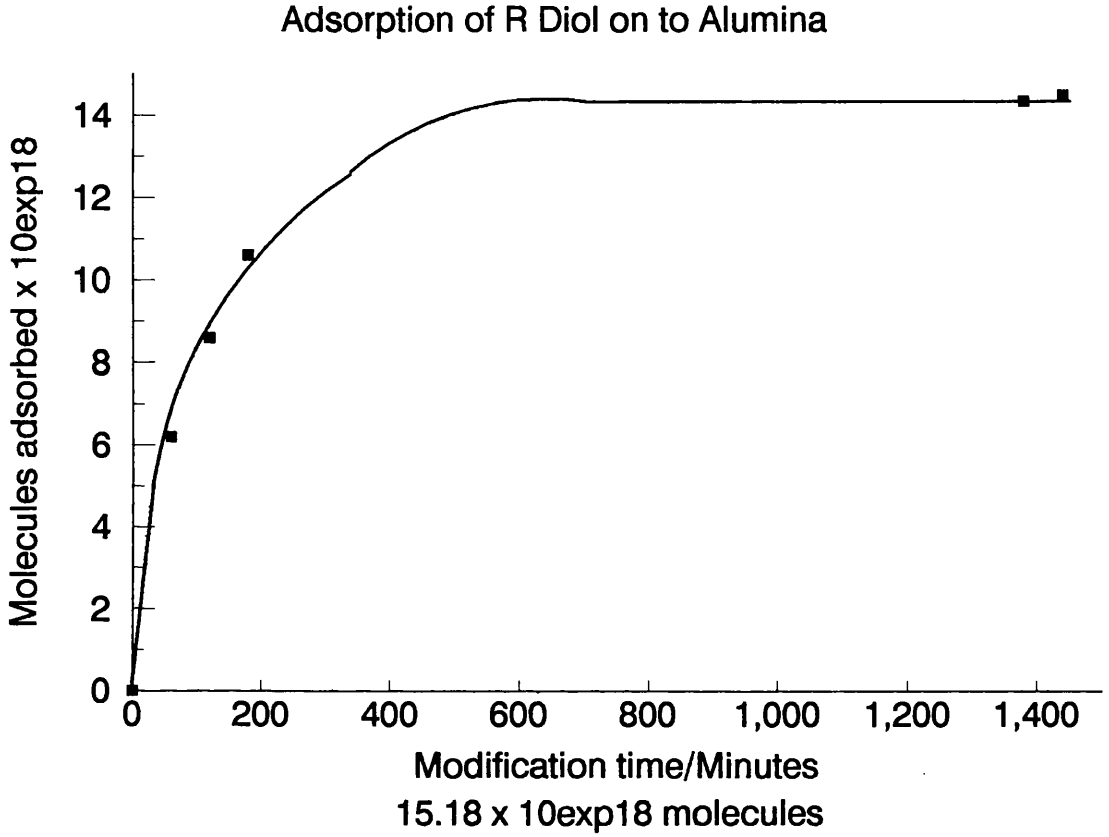

Figure 4.49:-

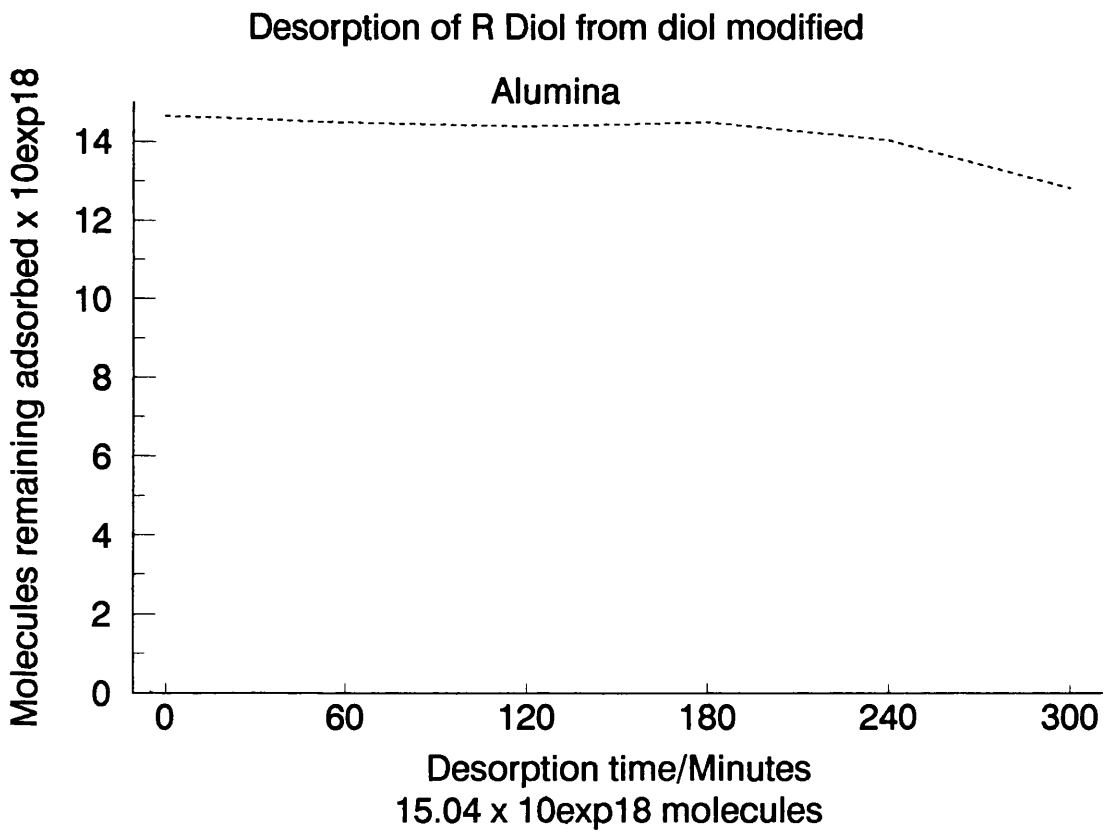

Table 4.96:- Adsorption of (±) Diamine on γ-Alumina	
14.49×10^{18} modifier molecules added initially	
Modification time/Minutes	No. of molecules modifier adsorbed x 10^{18}
0	0
60	2.17
120	3.69
180	3.97
240	4.47
1380	4.00
1440	3.87

Table 4.97:- Adsorption of Tetra-ol on to γ-Alumina	
5.68×10^{18} modifier molecules added initially	
Modification time/Minutes	No. of molecules modifier adsorbed x 10^{18}
0	0
10	1.48
20	2.18
30	2.85
40	3.42
50	3.84
60	4.08
90	4.47
120	4.71
180	4.94
240	5.08
1380	5.28
1440	5.29

Figure 4.50:-

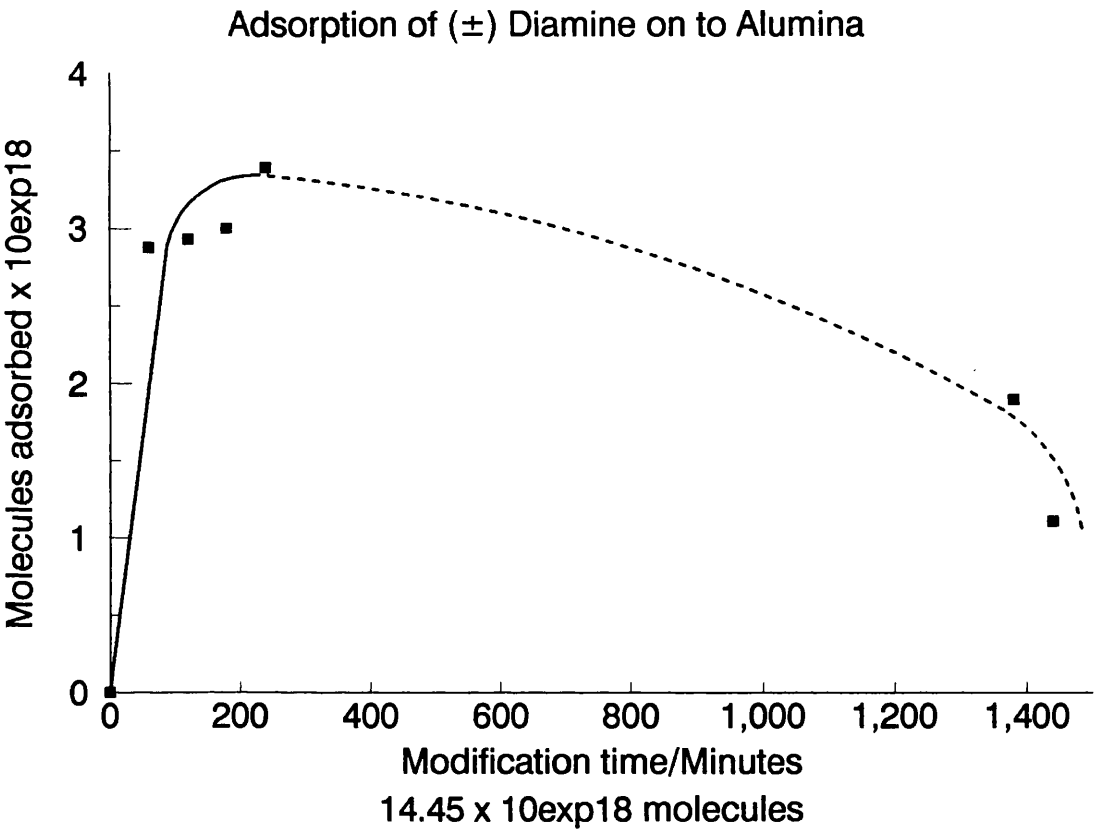

Figure 4.51:-

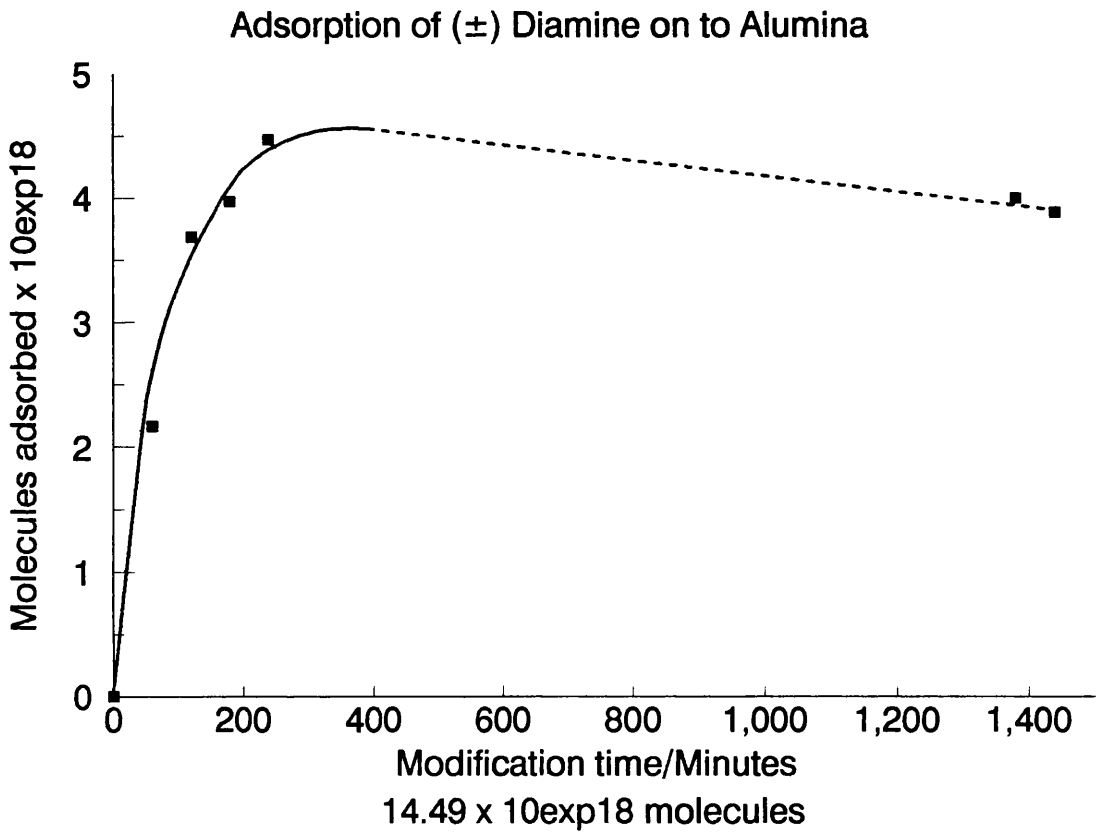

Table 4.98:- Adsorption of $(CH_2)_5$-bridged, pyridine-based macrocycle on to γ-Alumina	
2.67×10^{18} modifier molecules added initially	
Modification time/Minutes	No. of molecules modifier adsorbed x 10^{18}
0	0
60	0.08
120	0.17
180	0.23
240	0.25
1380	0.42
1440	0.44

Table 4.99:- Adsorption of $(CH_2)_5$-bridged, pyridine-based macrocycle on to γ-alumina	
2.79×10^{18} modifier molecules added initially	
Modification time/Minutes	No. of molecules modifier adsorbed x 10^{18}
0	0
60	0.12
120	0.39
180	0.51
240	0.73
1380	1.13
1440	1.18

4.2.2.2 Grace silica C10

Adsorption studies of the diol and diamine on the silica C10 support resulted in no adsorption of modifier.

4.2.2.3 Cab-O-Sil

The study for adsorption of diol, diamine and the $(CH_2)_5$- and $(CH_2)_6$-bridged, pyridine-based macrocycles on to the Cab-O-Sil support resulted on no adsorption being observed.

4.2.3 Polarimetry studies

The possibility of racemisation of the diol and diamine modifiers as a result of their

Figure 4.52:-

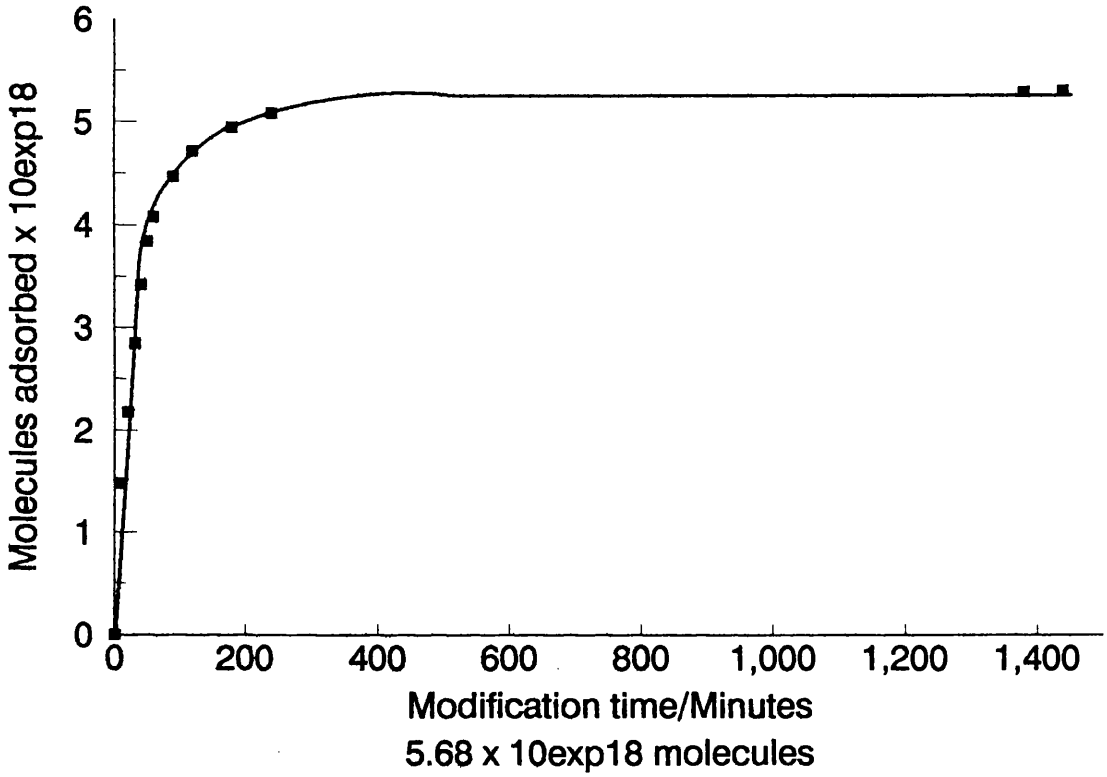

Figure 4.53:-

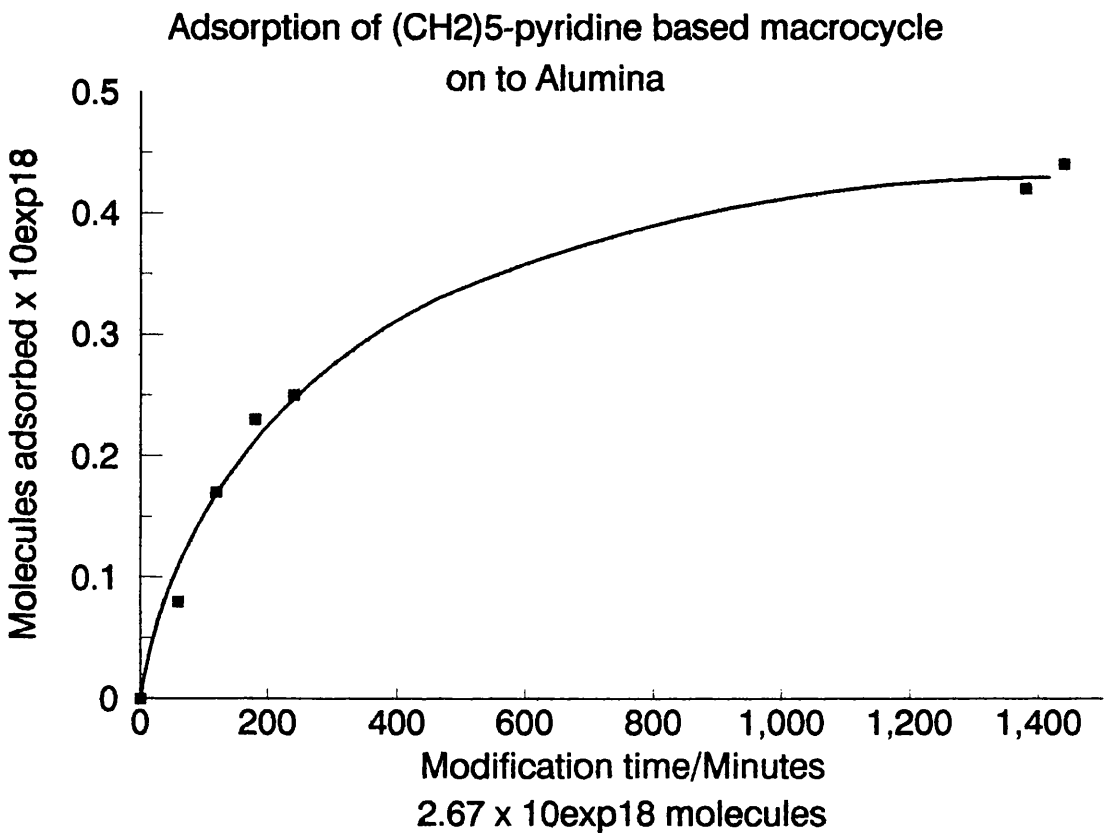

Figure 4.54:-

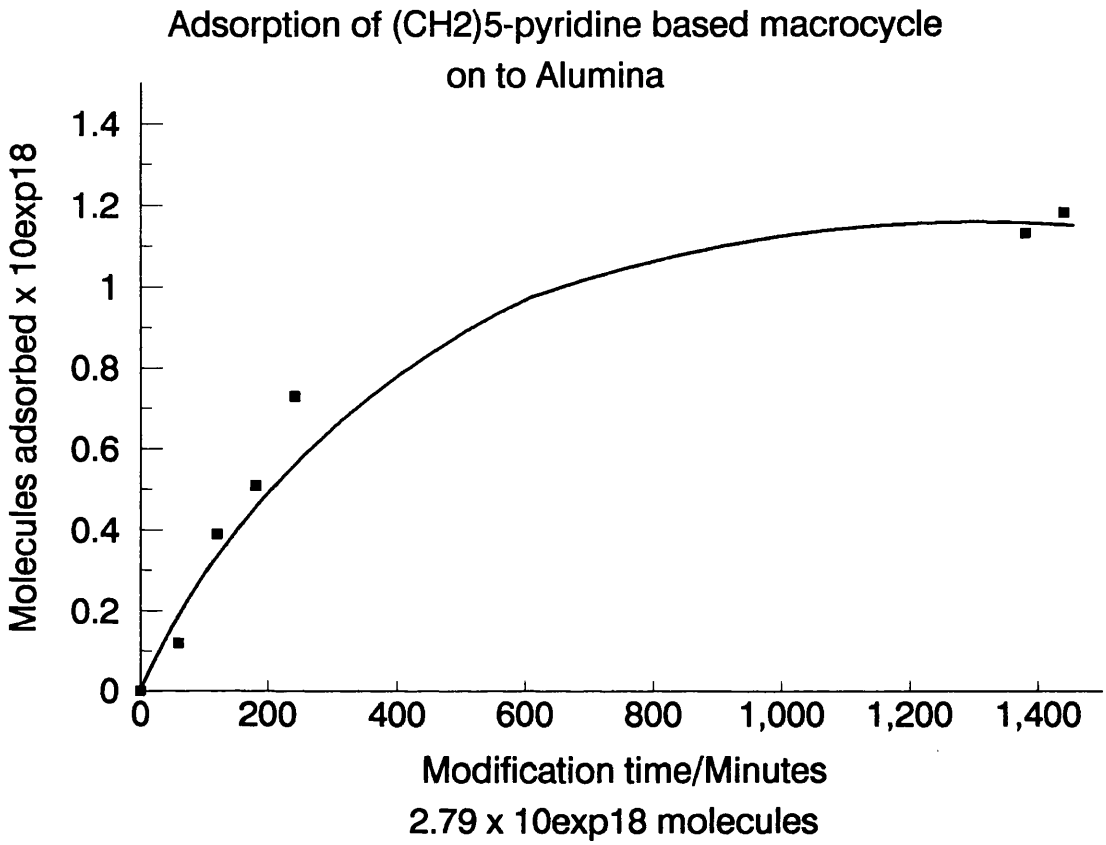
Adsorption of (CH2)5-pyridine based macrocycle
on to Alumina
Molecules adsorbed x 10exp18
1.4
1.2
1
0.8
0.6
0.4
0.2
0
0
200
400
600
800
1,000
1,200
1,400
Modification time/Minutes
2.79 x 10exp18 molecules

contacting the catalyst was studied for the Pt/γ-alumina and Pt/silica C10 catalysts as outlined in section 3.4.3.6. A control experiment with the γ-alumina support was carried out with the diol. Table 4.100 summarises the results of the polarimetry study with the catalysts and the γ-alumina support.

Table 4.100:- Polarimetry studies

Catalyst	Modifier	Racemisation
Pt/γ-alumina	R diol	YES
Pt/γ-alumina	R diamine	NO
Pt/silica C10	R diol	NO
Pt/silica C10	R diamine	NO
γ-alumina	R diol	YES

4.3 HYDROGENATION STUDIES

The hydrogenation of methyl tiglate, tiglic acid and 3-coumaranone were studied using the apparatus and conditions described in section 3.5.3. Initially a control experiment was performed with methyl tiglate and the γ-alumina support. Further control experiments were carried out using methyl tiglate, tiglic acid and 3-coumaranone with unmodified Pt/γ-alumina and Pt/Cab-O-Sil catalysts. Pt/silica C10 catalyst was not studied for hydrogenation properties for reasons explained elsewhere.

For the γ-alumina support, after 20 hours methyl tiglate was still present at its initial concentration. However, the control experiments for the unmodified catalysts showed that each of the reactants was hydrogenated and the products present from the unmodified reduced catalysts were in racemic form. For γ-alumina it could therefore be assumed that no reaction had occurred. For the unmodified supported Pt catalysts it could therefore be assumed that the catalyst hydrogenated the methyl tiglate, tiglic acid and 3-coumaranone but, since a racemic mixture was observed, that not unexpectedly the unmodified catalysts did not exhibit chiral qualities.

The various hydrogenations resulting over modified Pt/γ-alumina and Pt/Cab-O-Sil are shown by Tables 4.102 to 4.115. The appropriate adsorption and desorption data for the modifiers studied for their adsorption/desorption properties can be found in section 4.2, respectively. A range of modifiers which will be referred to as the alternative modifiers were chosen for their aromaticity and chiral pendent arm, that is the chiral centre was at least at the C atom α to the aromatic ring. Table 4.101 summaries in detail the acronyms used for the alternative modifiers which were not studied for their adsorption characteristics.

Table 4.101:- Summary of acronyms for alternative modifiers

Name of modifier	Acronym
R-(+)-N,N-Dimethyl-1-phenylethylamine	DMPEA
L-Histidine	His
R-(+)-α-Methoxy-α-trifluoromethylphenylacetic acid	MTFMPAA
L-Phenylalaninol	PhAla
L-α-Phenylglycinol	PhGly
(+)-Pseudoephedrine	Pseudo
L-Tryptophan	Trp

Tables 4.3.2 to 4.3.15 have a number of superscripts which can be summarised as follows:

N/A indicates that the data concerned was not obtained due to no hydrogenation being observed;

N/A* that hydrogenation was not monitored at this time;

† where the washing step of the modified catalyst was omitted;

1 that the modification and hydrogenation were studied at 273K;

ώ that the additional product was formed but no integration occurred;

a and b indicated the S and R enantiomer in excess, respectively;

Ω indicates the modifier which is used as the pre-conditioner; and

λ that aminol formation is observed.

The number of modifier molecules added to a freshly prepared catalyst sample is expressed per gram of catalyst.

4.3.1 Methyl tiglate hydrogenation

The hydrogenation of the C=C bond of prochiral methyl tiglate led to the formation of chiral methyl-2-methyl butyrate and in some cases an additional product which was found to be methyl angelate.

Tables 4.102 and 4.103 show the hydrogenation results for methyl tiglate over modified Pt/γ-alumina.

The hydrogenation of methyl tiglate modified Pt/Cab-O-Sil is shown in Tables 4.104 and 4.105 where the Pt/Cab-O-Sil is not sintered, while Table 4.106 shows the results for the sintered Pt/Cab-O-Sil catalyst.

4.3.2 Tiglic acid hydrogenation

The hydrogenation of the C=C bond of prochiral tiglic acid led to the formation of chiral 2-methyl butyric acid and, in some cases, an additional product.

The hydrogenation of tiglic acid is shown in Table 4.107 over modified Pt/γ-alumina and Table 4.108 for unsintered modified Pt/Cab-O-Sil.

4.3.3 3-Coumaranone hydrogenation

The hydrogenation of the C=O bond of prochiral 3-coumaranone led to the formation of chiral 3-benzofuranol and an additional product.

Modified Pt/γ-alumina, 3-coumaranone hydrogenation results are shown in Tables 4.109 to 4.112.

Table 4.113 shows the results for the hydrogenation of 3-coumaranone over a R diamine modified Pt/γ-alumina catalyst which had previously been used for the hydrogenation of a sample of 3-coumaranone.

The hydrogenation of 3-coumaranone over unsintered Pt/Cab-O-Sil is shown in Tables 4.114 and 4.115.

Table 4.102:- Hydrogenation of methyl tiglate by binaphthyl modified Pt/γ-alumina catalyst							
Modifier	Initial no. of modifier molecules added x 10^{18}	% Conversion of methyl tiglate		% Methyl angelate		% Enantiomeric excess (e.e.)	
		4 hours	20 hours	4 hours	20 hours	4 hours	20 hours
None	/	49.0	100.0	0.0	0.0	0.0	0.0
R Diol	15.33	N/A*	90.0	N/A*	0.0	N/A*	0.0
R Diamine	14.03	N/A*	80.0	N/A*	0.0	N/A*	0.0
R Diamine	14.08	N/A*	100.0	N/A*	0.0	N/A*	0.0
R Diamine	14.28	N/A*	30.0	N/A*	0.0	N/A*	0.0
S Diamine	14.10	45.0	87.0	0.0	0.0	0.0	0.0

Table 4.103:- Hydrogenation of methyl tiglate by modified Pt/γ-alumina catalyst						
Modifier	% Conversion of methyl tiglate		% Methyl angelate		% Enantiomeric excess (e.e.)	
	4 hours	20 hours	4 hours	20 hours	4 hours	20 hours
None	49.0	100.0	0.0	0.0	0.0	0.0
PhAla	50.0	99.5	0.0	0.0	0.0	0.0
His	37.0	99.0	30.0	0.0	0.0	0.0
DMPEA	24.0	84.0	ώ	ώ	0.0	0.0
PhGly	49.5	100.0	0.0	0.0	0.0	0.0
Trp	45.5	100.0	ώ	ώ	0.0	0.0
Pseudo	47.0	100.0	ώ	0.0	0.0	0.0
MTFMPAA	40.0	100	30.0	0.0	0.0	0.0

Table 4.104:- Hydrogenation of methyl tiglate by binaphthyl modified Pt/Cab-O-Sil catalyst unsintered							
Modifier	Initial no. of modifier molecules added x 10^{18}	% Conversion of methyl tiglate		% Methyl angelate		% Enantiomeric excess (e.e.)	
		4 hours	20 hours	4 hours	20 hours	4 hours	20 hours
None	/	89.0	100.0	0.0	0.0	0.0	0.0
R Diamine	5.93	47.0	100.0	0.0	0.0	0.0	0.0
S Diamine	6.03	27.0	100.0	0.0	0.0	0.0	0.0

Table 4.105:- Hydrogenation of methyl tiglate by modified Pt/Cab-O-Sil catalyst unsintered						
Modifier	% Conversionof methyl tiglate		% Methyl angelate		% Enantiomeric excess (e.e.)	
	4 hours	20 hours	4 hours	20 hours	4 hours	20 hours
None	89.0	100.0	0.0	0.0	0.0	0.0
PhAla	47.0	100.0	ώ	ώ	0.0	0.0
His	41.0	100.0	ώ	0.0	0.0	0.0
DMPEA	45.0	95.5	ώ	ώ	0.0	0.0
PhGly	27.0	97.0	ώ	ώ	0.0	0.0
Trp	85.0	100.0	ώ	0.0	0.0	0.0
Pseudo	57.0	98.5	23.0	0.0	0.0	0.0
MTFMPAA	37.0	96.0	30.0	0.0	0.0	0.0

Table 4.106- Hydrogenation of methyl tiglate by binaphthyl modified Pt/Cab-O-Sil catalyst sintered							
Modifier	Initial no. of modifier molecules added x 10^{18}	% Conversion of methyl tiglate		% Methyl angelate		% Enantiomeric excess (e.e.)	
		4 hours	20 hours	4 hours	20 hours	4 hours	20 hours
None	/	27.0	95.0	0.0	0.0	0.0	0.0
R Diamine	5.34	45.5	100.0	0.0	0.0	0.0	0.0
S Diamine	5.36	25.0	84.0	0.0	0.0	0.0	0.0

Table 4.107:- Hydrogenation of tiglic acid by modified Pt/γ-alumina catalysts

Modifier	Initial no. of modifier molecules added x 10^{18}	% Conversion of tiglic acid		% Angelic acid		% Enantiomeric excess (e.e.)	
		4 hours	20 hours	4 hours	20 hours	4 hours	20 hours
None	/	94	100.0	0.0	0.0	0.0	0.0
R Diol	21.62	65.6	98.4	0.0	0.0	0.0	0.0
R Diol	30.36	100.0	100.0	0.0	0.0	0.0	0.0
R Diamine	14.77	91.9	100.0	0.0	0.0	0.0	0.0
R Diamine†	14.75	91.4	99.6	0.0	0.0	0.0	0.0
R Diamine	47.04	100.0	100.0	0.0	0.0	0.0	0.0
R Diamine†	60.22	0.0	0.0	N/A	N/A	N/A	N/A
R Diol and R Diamine	7.77	0.0	88.7	N/A	0.0	N/A	0.0
	7.99						

Table 4.108:- Hydrogenation of tiglic acid by modified Pt/Cab-O-Sil catalysts							
Modifier	Initial no. of modifier molecules added x 10^{18}	% Conversion of tiglic acid		% Angelic acid		% Enantiomeric excess (e.e.)	
		4 hours	20 hours	4 hours	20 hours	4 hours	20 hours
None	/	64.6	100.0	1.0	ώ	0.0	0.0
R Diol	30.47	0.0	100.0	N/A	0.0	N/A	0.0
R Diamine	18.93	100.0	100.0	0.0	0.0	0.0	0.0

Table 4.109:- Hydrogenation of 3-coumaranone by binaphthyl modified Pt/γ-alumina catalyst

Modifier	Initial no. of modifier molecules added x 10^{18}	% Conversion of 3-coumaranone		% Additional product		% Enantiomeric excess (e.e.)	
		4 hours	20 hours	4 hours	20 hours	4 hours	20 hours
None	/	27.2	41.5	6.8	10.0	0.0	0.0
None[1]	/	8.6	64.8	1.6	9.3	0.0	0.0
R Diol	14.42	17.0	92.0	5.0	37.0	0.0	0.0
R Diol[†]	14.62	17.0	60.0	7.0	30.0	0.0	0.0
S Diol	14.31	8.5	43.0	4.0	23.0	0.0	0.0
R Diamine	13.98	0.0	23.0	N/A	11.5	N/A	11.0[a]
R Diamine[†]	14.22	12.5	71.0	4.0	17.0	5.0[a]	8.0[a]
R Diamine[1]	14.33	0.0	3.5	N/A	1.2	N/A	0.01[a]
R Diamine	15.82	35.5	54.5	11.0	16.0	1.0[a]	2.0[a]
R Diamine	31.93	23.0	59.0	10.0	24.0	4.0[a]	4.0[a]
S Diamine	14.23	10.0	54.5	5.0	21.5	3.0[b]	11.0[b]
S Diamine	15.82	23.0	53.0	7.0	22.0	5.0[b]	6.5[b]
S Diamine	19.93	3.2	43.3	1.3	17.9	9.0[b]	13.6[b]
S Diamine	24.88	5.0	27.0	2.7	9.5	0.01[b]	7.7[b]

Table 4.110a:- Hydrogenation of 3-coumaranone by binaphthyl modified Pt/γ-alumina catalyst

Modifier	Initial no. of modifier molecules added x 10^{18}	% Conversion of 3-coumaranone		% Additional product		% Enantiomeric excess (e.e.)	
		4 hours	20 hours	4 hours	20 hours	4 hours	20 hours
None	/	27.2	41.5	6.8	10.0	0.0	0.0
S Diol	14.31	8.5	43.0	4.0	23.0	0.0	0.0
S Diamine	14.23	23.0	53.0	7.0	22.0	5.0[b]	6.5[b]
R Diol	7.27	6.9	39.7	3.2	15.9	6.9[a]	11.8[a]
R Diamine	7.75						
R Diol[Ω]	7.25	0.0	16.9	N/A	8.0	N/A	10.7[b]
S Diamine	7.30						
R Diol	7.27	0.0	13.6	N/A	6.5	N/A	7.4[b]
S Diamine[Ω]	7.33						
R Diol	7.35	3.4	18.4	1.7	9.6	3.8[b]	10.7[b]
S Diamine	7.48						
R Diol[†]	7.40	7.6	17.9	2.8	7.9	7.5[b]	10.3[b]
S Diamine[†]	7.53						
S Diol	7.25	3.1	19.5	1.2	9.0	1.6[a]	8.9[a]
R Diamine	7.47						

Table 4.110b:- Hydrogenation of 3-coumaranone by binaphthyl modified Pt/γ-alumina catalyst

Modifier	Initial no. of modifier molecules added x 10^{18}	% Conversion of 3-coumaranone		% Additional product		% Enantiomeric excess (e.e.)	
		4 hours	20 hours	4 hours	20 hours	4 hours	20 hours
S Diol[Ω]	7.27	3.0	28.3	1.0	10.9	1.0[b]	12.2[b]
S Diamine	7.24						
S Diol	7.28	2.6	14.1	0.9	5.3	7.8[b]	10.2[b]
S Diamine	7.25						
S Diol	7.38	0.0	15.0	N/A	3.2	N/A	10.1[b]
S Diamine	12.9						
S Diol	7.87	4.7	24.3	1.7	10.0	8.3[b]	13.4[b]
S Diamine	7.25						
S Diol	8.53	6.8	52.7	2.8	21.6	9.7[b]	18.6[b]
S Diamine	17.00						
S Diol	13.41	7.1	67.3	3.3	22.0	8.7[b]	16.8[b]
S Diamine	13.33						
S Diol	19.60 (19.63)	N/A* (11.7)	44.5 (N/A*)	N/A* (3.6)	12.9 (N/A*)	N/A* (16.0[b])	19.2[b] (N/A*)
S Diamine	10.35 (10.39)						

Table 4.111:- Hydrogenation of 3-coumaranone by modified Pt/γ-alumina catalysts						
Modifier	% Conversion of 3-coumaranone		% Additional product		% Enantiomeric excess (e.e.)	
	4 hours	20 hours	4 hours	20 hours	4 hours	20 hours
None	27.2	41.5	6.8	10.0	0.0	0.0
PhGly†	9.3	74.6	4.2	21.8	0.0	1.2[a]
PhGly	12.0	62.5	4.0	25.0	0.0	0.0
PhAla†	10.8	75.6	4.7	28.7	2.5[b]	2.7[b]
MTFMPAA†	5.4	75.5	2.3	20.7	0.0	0.0
DMPEA†	12.0	69.9	4.4	17.3	0.5[b]	2.0[b]
Pseudo†	8.3	69.4	2.4	17.9	0.0	0.0
Trp†	25.9	90.1	9.9	26.9	0.2[b]	0.6[b]
His†	8.6	79.7	3.0	23.0	0.0	0.0

Table 4.112:- Hydrogenation of 3-coumaranone by pyridine based macrocycles modified Pt/γ-alumina catalyst							
Modifier	Initial no. of modifier molecules added x 10^{18}	% Conversion of 3-coumaranone		% Additional product		% Enantiomeric excess (e.e.)	
		4 hours	20 hours	4 hours	20 hours	4 hours	20 hours
None	/	27.2	41.5	6.8	10.0	0.0	0.0
$(CH_2)_5$-bridged, pyridine-based macrocycle	2.69	5.9	27.4	2.1	11.1	0.0	0.0
$(CH_2)_6$-bridged, pyridine-based macrocycle	2.80	0.0	20.3	N/A	9.6	N/A	0.0

Table 4.113:- Double hydrogenation of 3-coumaranone by R Diamine modified Pt/γ-alumina						
Initial no. of modifier molecules added x 10^{18}	% Conversion of 3-coumaranone		% Additional product		% Enantiomeric excess (e.e.)	
	1st hydrogenation	2nd hydrogenation	1st hydrogenation	2nd hydrogenation	1st hydrogenation	2nd hydrogenation
48.15	7.9	13.3	4.1	6.6	3.6[a]	3.6[a]

Table 4.114:- Hydrogenation of 3-coumaranone by binaphthyl modified Pt/Cab-O-Sil catalyst unsintered							
Modifier	Initial no. of modifier molecules added x 10^{18}	% Conversion of 3-coumaranone		% Additional product		% Enantiomeric excess (e.e.)	
		4 hours	20 hours	4 hours	20 hours	4 hours	20 hours
None	/	18.5	76.0	7.0	26.0	0.0	0.0
None[1]	/	3.1	36.8	0.9	7.6	0.0	0.0
S Diol	15.67	26.2	87.2	6.1	15.1	0.0	0.0
R Diamine[λ]	10.18	6.7	41.3	3.7	22.7	1.3[a]	4.5[a]
R Diamine[†]	10.65	2.8	8.8	1.6	4.1	0.0	1.3[a]
R Diamine[1†]	11.06	0.3	4.0	0.3	2.8	0.0	3.3[a]
R Diamine[λ]	26.01	16.2	48.2	5.9	15.7	15.8[a]	18.0[a]
S Diol[†]	7.31	N/A*	24.2	N/A*	10.8	N/A*	13.7[b]
S Diamine[†]	12.78						

Table 4.115:- Hydrogenation of 3-coumaranone by pyridine based macrocycles modified Pt/Cab-O-Sil catalyst unsintered							
Modifier	Initial no. of modifier molecules added x 10^{18}	% Conversion of 3-coumaranone		% Additional product		% Enantiomeric excess (e.e.)	
		4 hours	20 hours	4 hours	20 hours	4 hours	20 hours
None	/	18.5	76.0	7.0	26.0	0.0	0.0
$(CH_2)_5$-bridged, pyridine-based macrocycle	3.04	13.2	52.1	4.5	17.9	0.0	0.0
$(CH_2)_5^{\dagger}$-bridged, pyridine-based macrocycle	3.04	N/A*	22.3	N/A*	11.2	N/A*	0.0
$(CH_2)_6$-bridged, pyridine-based macrocycle	1.21	19.0	63.3	7.4	18.1	0.0	0.0
$(CH_2)_6$-bridged, pyridine-based macrocycle	2.40	30.1	75.2	10.4	25.8	0.0	0.0

CHAPTER 5
DISCUSSION

5 INTRODUCTION

The catalysts used in this study were characterised by UV-VIS spectroscopy, TPR, CO(g) and O_2(g) chemisorption and TEM. These characterised catalyst were then used to study their adsorption properties with respect to chiral modifiers and the chirally modified catalysts characterised with respect to asymmetric hydrogenation reactions.

5.1 CATALYST CHARACTERISATION

5.1.1 Ultra-violet-Visible spectroscopy

The ultra-violet and visible (UV-VIS) spectroscopy data compares well with the available literature on octahedral (IV) species.[119,120] The spectra of the precursors of both Pt/silica C10 (October 1992 and April 1994) and Pt/Cab-O-Sil catalyst are very similar to that of aqueous H_2PtCl_6.[118] The spectra of Pt/silica C10 (October 1992) and Pt/silica C10 (April 1994) exhibit similar transitions but the precise wavelengths of some of these transitions have changed. Both the d-d transitions have remained similar, while the ligand-to-metal charge transfer (LMCT) bands exhibited an increase in one and a decrease in the other going from October 1992 to April 1994. These changes in wavelength can be attributed to changes of the surface platinum species of the catalyst. The change in the LMCT bands are due to stronger interaction of $[PtCl_6]^{2-}$ with the OH^- groups on silica than is usually observed. Normally the absence of amphoteric OH^- groups on silica accounts for the similar absorbance of adsorbed $[PtCl_6]^{2-}$ with free $[PtCl_6]^{2-}$.

The spectrum of the Pt/γ-alumina sample is slightly different, as shown by the shift in the LMCT transition to 200nm, which is consistent with Chen *et al*[122] and Lietz *et al*[123] who claim that the $[PtCl_6]^{2-}$ anion absorbs on to positive sites of the γ-alumina and that an adsorbed $[PtCl_6]^{2-}$ is slightly different from the free anion. The wavelength for LMCT band decreased on the adsorption of the $[PtCl_6]^{2-}$ anion on to the positively charged Al site by ligand exchange of OH^- for $[PtCl_6]^{2-}$ (200nm, adsorbed $[PtCl_6]^{2-}$and 263nm, free $[PtCl_6]^{2-}$,[118]). Chen *et al*,[122] showed that the LMCT band increased on adsorption of the anion (that is; 200nm, free $[PtCl_6]^{2-}$ and 275nm, adsorbed $[PtCl_6]^{2-}$). While Lietz *et al*[123] also showed an increase in the wavelength of LMCT band from 262nm for the free $[PtCl_6]^{2-}$ to 275nm for the adsorbed $[PtCl_6]^{2-}$. Jackson *et al*,[118] however, showed that the wavelength of adsorbed $[PtCl_6]^{2-}$ (218nm) was less than that for the free $[PtCl_6]^{2-}$ (263nm). Jackson *et al*[118] showed that the spectrum for Pt/γ-alumina is in fact, similar to that for PtO_2/γ-alumina, in which the 209nm absorption is assigned to LMCT from O to Pt. The presence of an intermediate hydroxy- or oxy-chloro species such as $[PtCl_5OH]^{2-}$, formed by exchange reactions of the type

$$[PtCl_6]^{2-} + H_2O \rightleftharpoons [PtCl_5(OH)]^{2-} + H^+ + Cl^-$$

in aqueous solution could therefore account for the band observed at 200nm in the Pt/γ-alumina spectra. The unchanged d-d bands suggest that the octahedral complex with the six Cl^- ligands is preserved.

5.1.2 Temperature Programmed Reduction

Only the TPR profiles of Pt/γ-alumina, Pt/silica C10 and unsintered Pt/Cab-O-Sil

catalyst were obtained. Sensitivity problems of the TPR recorder did not permit the profile to be obtained for the sintered Pt/Cab-O-Sil catalyst. The profile of the Pt/γ-alumina catalyst, as shown by Figure 4.1, exhibited one peak. This peak at 491K corresponded to the reduction of a four-electron process.[124] The reduction of Pt/γ-alumina catalyst shows a similar temperature maximum and number of peaks to the TPR of Pt/γ-alumina catalyst reported by Jackson *et al.*[118] McNicol[124] concluded that the reduction temperature of the alumina-supported platinum was above the reduction temperature of unsupported tetravalent chlorides or oxides, therefore there must be an interaction between the platinum species and the γ-alumina surface and that the interaction took place during the calcination step. Blanchard[125] has shown for Pt/γ-alumina catalysts, prepared by impregnation from H_2PtCl_6 and then calcined and catalysts prepared by Yao *et al,*[126] have similar TPR profiles to the catalyst prepared by McNicol.[124] It is thought that the excellent dispersions of platinum on γ-alumina are achieved because of an interaction between the γ-alumina and the platinum species that occurs during the calcination step,[127] but the nature of this interaction is not well established.

The profile for the Pt/silica C10 catalyst (Figure 4.2) is that of the catalyst prior to ageing. One reduction peak is observed at 409K. However, the peak was asymmetric with a tail on the high temperature side of the maximum. Jackson *et al*[118] observed the same behaviour with an impregnated Pt/silica catalyst and showed that by increasing the ramping temperature from $10Kmin^{-1}$ to $35Kmin^{-1}$ that two peaks were observed. Therefore had the ramp temperature been increased in the case of the Pt/silica C10 this same behaviour may have been observed. As seen with the Pt/γ-alumina catalyst, the reduction process corresponds to the gain of four-electrons, that is, Pt(IV) → Pt(0). Jenkins *et al*[115] showed that a Pt/silica catalyst exposed to TPR conditions exhibited a profile consisting to three peaks. The first peak Jenkins *et al*[115] attributed to unsupported bulk $PtCl_4$ and H_2PtCl_6, still present after the drying step which was responsible for poor dispersions of metal in the impregnated catalyst. The other peaks observed by Jenkins *et al*[115] were the reduction of platinum supported on the silica. The absence of this first peak suggests very little or no unsupported bulk is present.

The Pt/Cab-O-Sil catalyst in the unsintered form gave rise to two different TPR profiles. The first TPR profile shows a single peak with a maximum at 468K (Figure 4.3), whilst the second set of profiles shows a single peak with a maximum at 613K (Figure 4.4). The TPR profile with the peak maximum at 468K was asymmetric with tailing to the high side of the peak maximum, as observed by Jackson *et al,*[118] while the TPR profile with the peak maximum at 613K is observed to be symmetric. This difference in maximum

reduction temperature was due to support metal interaction.

5.1.3 Chemisorption studies

As shown by the results presented in Table 4.3, the metal dispersions for the Grace supported platinum catalyst and sintered Cab-O-Sil supported platinum catalyst are lower than for the unsintered Cab-O-Sil supported platinum and γ-alumina supported platinum catalysts.

Platinum adsorbed both O_2(g) and CO(g) strongly, although carbon monoxide, in general, is shown to be adsorbed to a greater strength than dioxygen because the formation of a Pt-CO bond is thermodynamically more favourable than the a Pt-O bond. For the calculation of dispersion of surface metal, the mode of adsorption of the carbon monoxide on to Pt was assumed to be linear for both the Pt/silica catalysts and the Pt/γ-alumina catalyst, that is, the ratio Pt:CO is 1:1. Although infra-red studies done by other groups (Jackson *et al*,[128] Dorling and Moss[129] and Primet *et al*[130]) on supported platinum catalyst show that only approximately 80% of CO was linearly bound and the remaining CO bound in a bridging mode.

The adsorption of dioxygen occurs by a dissociative mechanism which assumes that for every oxygen molecule adsorbed, two metal atoms form a metal-oxygen bond. The linear adsorption of an oxygen atom on to the Pt metal surface therefore has a ratio of 1Pt:0.5O. For catalysts with small Pt particles, Wilson and Hall[131] proposed that the chemisorption of dioxygen on to a Pt catalyst surface was 1Pt:0.5O. Results obtained by Jackson *et al*,[128] for Pt catalysts with small particle sizes also consistent with a 1Pt:0.5O ratio. For the purpose of this study the Pt:O ratio is taken as 1:0.5 for dispersion calculations, independent of the particle size.

5.1.4 Transmission electron microscopy

The TEM results in Table 4.4, show the range of particle sizes for the catalysts. With the exception of the sintered Pt/Cab-O-Sil, the catalyst are generally of small particle size and it is likely that some of the smallest particles escaped detection. This hypothesis was supported by work reported by Huang *et al*[132] on a series of Pt/γ-alumina, Re/γ-alumina and Pt-Re/γ-alumina catalysts. Catalysts which have been shown to have high metal dispersion, invariably have small metal particles, for example, EUROPT-1 has a dispersion of 65% calculated form a Pt:H ratio of 1:1[133] and particles sizes ranging from 0.9nm to 3.5nm.[134] The sintering of a sample of Pt/Cab-O-Sil catalyst increases the particle sizes of the metal.

The TEM of the aged Pt/Grace silica C10 catalyst shows the presence of discrete metal particles although CO chemisorption[135] shows that no metal is exposed following

activation of the catalyst. These results suggest that the metal although visible to the electrons of the microscope are not on the surface of the silica. The structure of the Grace silica C10, as shown in Figure 5.1 suggests that the Pt metal could be incorporated into the silica ring and so the metal is unable to be fully reduced to the metallic state.

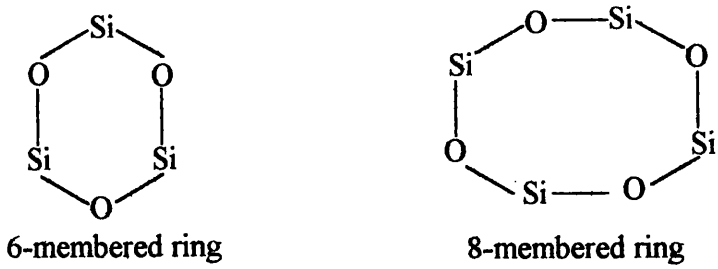

6-membered ring 8-membered ring

Figure 5.1:- Structure of Grace silica

5.2 ADSORPTION STUDIES OF CHIRAL MODIFIERS

As shown in the results section 4.2, adsorption studies of the binaphthalene derivatives have shown the following:

(1) All three catalysts (Pt/γ-alumina, Pt/silica C10 and Pt/Cab-O-Sil) were found to adsorb the diamine;

(2) Pt/γ-alumina and Pt/silica C10 catalysts were found to adsorb the diol;

(3) Pt/γ-alumina catalyst adsorbed the tetra-ol

(4) Pt/silica C10 catalyst was not investigated for its ability to adsorb tetra-ol

(5) Dimethoxy was not adsorbed by either the Pt/γ-alumina, Pt/silica C10 or Pt/Cab-O-Sil catalysts.

(6) As a result of ageing problems of the catalyst which were encountered with the Pt/silica C10 catalyst, were discussed earlier (section 5.1.4), the extent of adsorption of the diol and diamine modifiers diminished until no modifier adsorption was observed

(7) Diamine in some instances underwent a chemical reaction upon adsorption on to the Pt/Cab-O-Sil catalyst

Control experiments involving the supports show that the γ-alumina support adsorb the diol, diamine, tetra-ol and the $(CH_2)_5$- and $(CH_2)_6$-bridged, pyridine-based macrocycle and probably the $(CH_2)_6$-bridged, pyridine based macrocycle. The silica C10 support is shown not to adsorb either the diol or diamine and the Cab-O-Sil support does not adsorb the diol, diamine and $(CH_2)_5$- and $(CH_2)_6$-bridged, pyridine-based macrocycles.

Comparing the adsorption results obtained using the different reactors and reduction methods, initial adsorption studies of R diol on to the Pt/silica C10 catalyst were reproducible for reactor R1 and R2, indicating that the design of the reactor makes no difference to the adsorption properties of the catalyst prepared by static reduction. Using reactor R2, the method of catalyst reduction was changed from static to flow. Comparing the adsorption of R diol on to the Pt/silica C10 catalyst prepared by static reduction with flow reduction suggests a lack of reproducibility in the results for the two different reduction methods. However, this was found subsequently to be a result of the catalyst ageing. This same observation was made for the adsorption of (±) diamine on to Pt/silica C10, where the same ageing problem was encountered. However, comparison of results for the adsorption of R diol on to Pt/γ-alumina using the different reduction methods showed that the mode of reduction made no difference. The extent of adsorption is reproducible

when a similar initial number of modifier molecules are added to the freshly prepared catalyst. Comparisons are not available for the other catalyst/modifier systems. The adsorption of (±) diol is reproducible on to the Pt/γ-alumina catalyst irrespective of reactor type or reduction mode.

5.2.1 Adsorption of modifiers

Comparing of modifier adsorption on to the catalysts and their respective supports, the extent of diol adsorption on to the γ-alumina support is almost identical to the adsorption of the diol on to the Pt/γ-alumina catalyst, this suggested that the diol is mainly adsorbed on to the support of the catalyst rather than on to the Pt metal. The adsorption of diol on to the Pt/γ-alumina catalyst was shown to be reproducible. The Pt/silica C10 catalyst also adsorbed the diol modifier although it was not adsorbed on to the silica C10 support, indicating that the Pt metal has the capability of adsorbing the diol.

However, the Pt/Cab-O-Sil catalyst in either the sintered or unsintered form is found not to adsorb the diol. The Cab-O-Sil support is also found not to adsorb the diol.

As a result of the Pt metal of the Pt/Cab-O-Sil catalyst being unable to adsorb the diol, this suggests that the adsorption of diol by the Pt/silica C10 catalyst is mainly on the silica C10 support, but it has been previously shown that the silica C10 support is unable to adsorb the diol. A possible explanation for the adsorption of diol on to the Pt/silica C10 catalyst would be that the diol has been moved from the Pt metal on to the support and the metal has to be present in order for the diol to be adsorbed on to the silica C10 support. This phenomenon where the modifier moves from the metal of the catalyst to the support is described as spillover and is shown schematically in Figure 5.2 for the diol. Spillover, in general, involves the transport of an active species adsorbed on the metal surface on to another surface that cannot adsorb the species under the same conditions,[136] that is, the adsorbed species gains access to a different phase that is in contact with the original adsorbing phase.

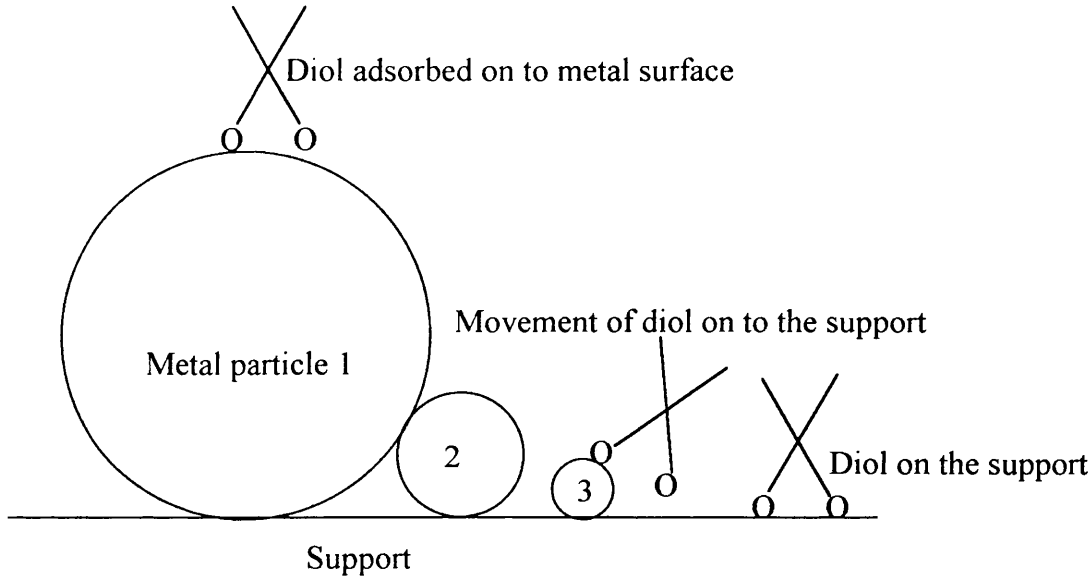

Figure 5.2:- Schematic diagram of modifier spillover

In the case of the diamine, the extent of adsorption of diamine on to the γ-alumina support was small in comparison to the amount adsorbed on the Pt/γ-alumina catalyst, when the same initial number of modifier molecules are added to the support as well as the catalyst. This suggests that the diamine adsorbed on to the catalyst is by both the support and the Pt metal. The extent of diamine adsorption on to the Pt/γ-alumina catalyst is shown to be irreproducible for the addition to a freshly prepared catalyst samples similar initial number of molecules.

The extent of adsorption of the modifiers on to the catalyst is also expressed as the nominal ratio of modifier molecules adsorbed per surface metal atom. The Pt/cinchona-alkaloid system has shown that each cinchona molecule can cover about 15 atoms[46] and in the case of the EUROPT-1 (6.3% w/w Pt/silica) some of the modifier was shown to be adsorbed on to the silica support.[15] Molecular modelling studies for the adsorption of diol on to the Pt metal surface as shown in Figure 5.3 shows that the diol molecule covers more than one metal atom. The model suggests that approximately 10 atoms are covered by the diol and, therefore it would be quite reasonable to assume that the maximum nominal ratio which could be accepted and relates to monolayer coverage of the modifier on the catalyst surface is 0.2. However, the nominal ratio for some of the modified catalyst is greater than 0.2 suggesting the modifier undergoes spillover from the metal on to the silica, as the silica has been shown not to be able to adsorb the modifiers, in the case of the silica supported Pt catalysts, while for the γ-alumina supported Pt catalyst the modifier

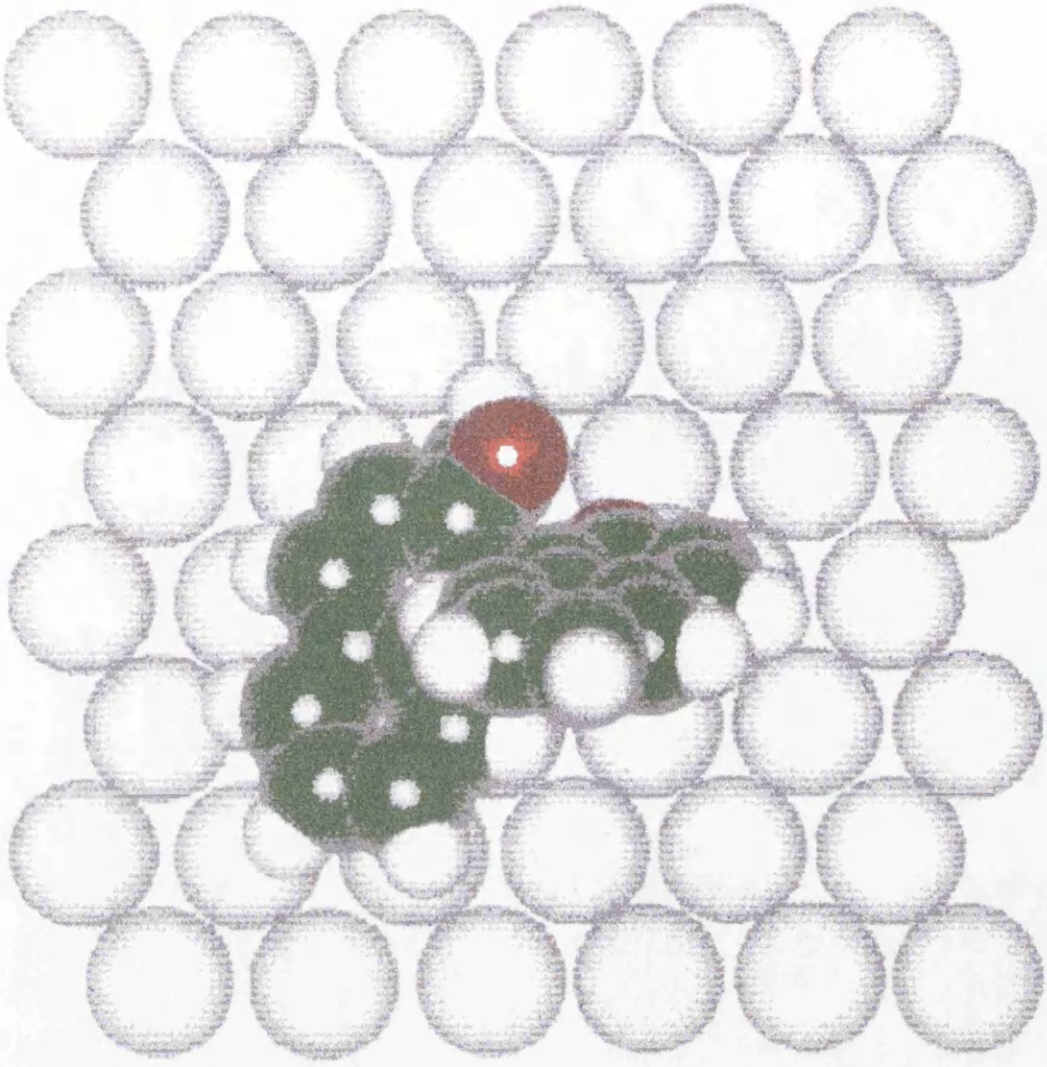

Figure 5.3:- Molecular modelling of the adsorption of diol on to the Pt metal surface

adsorbed in excess of the ratio of 0.2 must be via an acid/base interaction of the support and the modifier.

The suggestion that the diamine is adsorbed by Pt metal is further supported by the results of the adsorption of diamine on to both the Pt/silica C10 catalyst, before ageing, and the Pt/Cab-O-Sil catalyst; especially when both the silica C10 and Cab-O-Sil supports were found to be unable to adsorb the diamine.

With the Pt/Cab-O-Sil catalyst, the diamine is capable of being adsorbed but that the diamine is also capable of undergoing a chemical reaction with the formation of aminol and diol. When the diamine is adsorbed, without undergoing a chemical reaction, on to the Pt/Cab-O-Sil catalyst, it is shown that the extent of adsorption of diamine on to the Pt/Cab-O-Sil is irreproducible when similar initial number of modifier molecules are added to the freshly reduced catalyst samples. When the diamine undergoes a chemical reaction, the diamine is inter-converted to aminol and diol. Similar results were observed with a 1% w/w Pd/Cab-O-Sil catalyst,[137] although other products, for example as shown in Figure 5.4; (1) the replacement of one of the H atoms in each of the amine groups by a THF molecule as well as loss of aromaticity in half of one of the naphthalene rings, closest to one of the substituted amine groups; and (2) the loss of aromatic character in one of the naphthalene rings as well as the loss of aromaticity in half of the other naphthalene ring, closest to the amine group; were also observed. These results then suggests that the diamine inter-conversion is not a characteristic of the Pt metal but of the Cab-O-Sil support. However, with a 10% w/w Ni/Cab-O-Sil catalyst[137] this diamine inter-conversion was not observed, suggesting that the inter-conversion was not a characteristic of the Pt metal or of the silica support. The conclusion was that the increased metal loading of the Ni/Cab-O-Sil catalyst compared with the Pd/Cab-O-Sil catalyst, that is, 10% w/w Ni and 1% w/w Pd explained the apparent diamine inter-conversion observed for the Pd/Cab-O-Sil catalyst whilst not for the Ni/Cab-O-Sil catalyst because of the higher metal content, more of the support will be covered in metal. The diamine inter-conversion is then a characteristic of the Pt metal and not the Cab-O-Sil support, since the Cab-O-Sil support is unable to inter-convert the diamine as shown by the addition of diamine to a sample of the Cab-O-Sil support where no inter-conversion is observed as well as no adsorption. The optical purity of the diol and aminol formed from the diamine inter-conversion is not determined. The question arises as to where the hydroxyl groups in the aminol and the diol come from and to where the amine groups from the diamine go. The hydroxyl groups cannot come from the Cab-O-Sil support because this type of silica is non-porous. The hydroxyl groups may then have come from the solvent, THF, had the THF not been kept dry in a nitrogen

atmosphere. However, the use of a sample of diamine prepared with 'dry' THF led, in some cases, to diamine being adsorbed without any inter-conversion was observed, while in other cases inter-conversion being observed to occur. Similarly, the preparation of diamine in 'wet' THF led to similar results to those obtained with samples prepared in 'dry' THF, leading to the conclusion the THF is not involved in the inter-conversion, although work done by Young[137] with the Pd/Cab-O-Sil showed that the other products observed with this particular catalyst involved an association of the THF with the diamine.

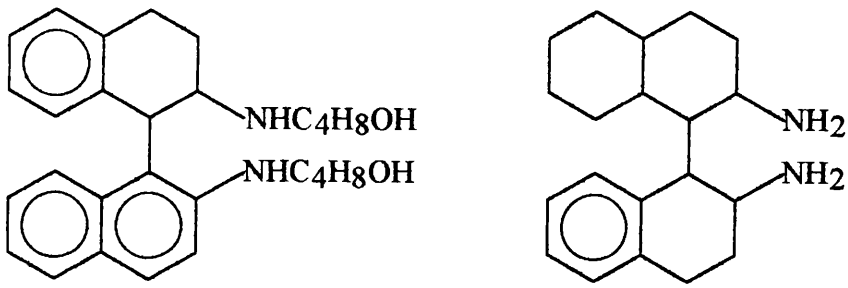

Figure 5.4:- A couple examples of the other products observed from the inter-conversion of diamine

The use of tetra-ol as a modifier led to the following conclusion. Comparing the extent of adsorption of tetra-ol on to the Pt/γ-alumina catalyst and on the γ-alumina support, for similar initial number of molecules modifier added, shows that the extent of adsorption is very similar. This observation would then lead to the conclusion that the tetra-ol has been mainly adsorbed by the support of the catalyst and not the Pt metal. This conclusion can be further supported by the fact that neither the Pt/Cab-O-Sil catalyst or the Cab-O-Sil support is unable to adsorb the tetra-ol. Comparison of the adsorption of the diol and tetra-ol modifiers for solutions of similar concentration, shows that the extent of adsorption are very similar. This suggests that the extra hydroxyl groups are not involved in the adsorption.

The γ-alumina support was found not to adsorb the TFAE, while the Pt/γ-alumina catalyst does adsorb TFAE. Whilst this suggests that the TFAE is adsorbed on to the Pt metal, although, as will be discussed later, the TFAE was only weakly adsorbed on to the Pt/γ-alumina catalyst and not on to the support, the Pt/Cab-O-Sil catalyst did not adsorb the TFAE suggesting that the Pt metal was not able to adsorb the TFAE.

Both the Pt/γ-alumina catalyst and the γ-alumina support adsorb the $(CH_2)_5$-bridged, pyridine-based macrocycle, although the extent of adsorption for similar initial number of modifier molecules is greater on the catalyst than on the support, indicating that

the $(CH_2)_5$-bridged, pyridine-based macrocycle was adsorbed by the Pt metal. The Pt/Cab-O-Sil catalyst also adsorbed the $(CH_2)_5$-bridged, pyridine-based macrocycle, while the Cab-O-Sil support did not, providing further evidence that the $(CH_2)_5$-bridged, pyridine-based macrocycle is adsorbed by the Pt metal.

$(CH_2)_6$-bridged, pyridine-based macrocycle is also used as a modifier. Both the Pt/γ-alumina and Pt/Cab-O-Sil catalysts are shown to adsorb the $(CH_2)_6$-bridged, pyridine-based macrocycle. Although the assumption can be made that the γ-alumina support could have adsorbed the $(CH_2)_6$-bridged, pyridine based macrocycle. However, the adsorption is still by the Pt metal as the only difference is the size of the bridge chain length.

The Pt/Cab-O-Sil catalyst was examined as either a reduced catalyst or as a catalyst reduced after exposure to a sintering process. Comparing the effect of introducing the sintering process for catalyst preparation with a catalyst sample which is not exposed to a sintering process prior to reduction with respect to the resultant adsorption of the diamine and TFAE modifiers shows that the unsintered and sintered forms of the Pt/Cab-O-Sil catalyst adsorb the diamine and TFAE; while the inter-conversion of diamine is observed for only the unsintered Pt/Cab-O-Sil catalyst.

When the diamine adsorption on to the Pt/Cab-O-Sil is shown to undergo inter-conversion, the extent of diamine adsorption is found to be irreproducible for a specific initial number of modifier molecules added to a freshly prepared catalyst sample, irrespective of whether the catalyst is sintered or not. As a consequence no conclusion can be drawn as to whether the sintering of the catalyst leads to a greater or lesser adsorption of the diamine.

Inter-conversion of the diamine is only observed with the unsintered Pt/Cab-O-Sil catalyst and the extent of inter-conversion is independent of the initial number of modifier molecules added to the freshly prepared catalyst sample, although adsorption of unreacted diamine is also observed. The formation of aminol was observed in all cases where inter-conversion occurred, while in some circumstances diol is also produced.

Although the unsintered form of Pt/Cab-O-Sil is found to adsorb a minute amount of TFAE, the sintered form does not adsorb any TFAE at all. However, the minute amount of TFAE adsorbed by the unsintered form is within the 5% detection error limit of HPLC, suggesting that the TFAE may not have been adsorbed by the unsintered form.

5.2.2 Co-adsorption studies

Co-adsorption studies of diol and diamine have been undertaken and the results of these studies compared with the single modifier adsorption studies. The co-adsorption on to the Pt/γ-alumina catalyst followed one of the three methods outlined in the

experimental chapter, that is (i) addition of mixed modifier solution, (ii) pre-conditioning of the catalyst followed by addition of a second modifier and (iii) pre-conditioning of the catalyst prior to the addition of the second modifier following the removal of the first modifier. The Pt/γ-alumina is able to adsorb both the diol and the diamine in the presence of the other one, that is, diol can be adsorbed on to a Pt/γ-alumina catalyst previously modified with diamine and vice versa.

Comparing the extent of co-adsorption with the appropriate adsorption of one of the modifiers has shown, in general, similar trends. The extent of adsorption of diol and diamine, where both modifiers have been added to the catalyst together as a mixture, have shown that for an initial number of diol molecules added, independent of the number of diamine molecules, that the extent to which the diol is adsorbed was similar to that of the diol adsorption, with a similar number of molecules added initially to the catalyst. However, for the diamine, the extent of adsorption is less than for the diamine adsorption, taking into account the irreproducible adsorption of diamine on to the Pt/γ-alumina catalyst. Assuming that the total initial number of modifier molecules in the mixture (diol and diamine) is similar to the total initial numbers of molecules of either diol or diamine, the total adsorption of modifier decreases, when compared to the diol adsorption as a result of the presence of diamine. However, independent of the irreproducible adsorption of diamine on to Pt/γ-alumina catalyst, the extent of co-adsorption is greater than that for diamine adsorption as a result of the presence of diol.

The co-adsorption studies, where the catalyst is pre-conditioned prior to the addition of the second modifier without the removal of the first modifier, has shown a similar extent of diol adsorption, when compared to the diol adsorption where similar initial numbers of diol molecules are added to the catalyst, when the diol is the pre-conditioner. However, the extent of diol adsorption decreases slightly when the catalyst has been pre-conditioned with diamine. Although no firm comparison can be drawn for the diamine adsorption with respect to either the pre-conditioner or as the second modifier with the appropriate diamine adsorption. Comparing the total number of modifier molecules for the mixture with diol leads to a decrease in the extent of adsorption independent of the order of modifier addition. The adsorption of the mixture compared to single diamine adsorption, increases as found for the single mixed addition of modifier due to the presence of the diol and is independent of the order of the modifier addition.

The removal of the pre-conditioning modifier prior to the addition of the second modifier is shown in the case of the diol to have no effect on the extent of adsorption when comparing it to the single diol adsorption. When the diamine is the pre-conditioner,

the comparison with adsorption of single diamine leads to a decrease in adsorption but this could be attributed to the irreproducible adsorption of diamine on to Pt/γ-alumina. However, no firm comparisons can be made for the second modifier with the adsorption of the appropriate single modifier addition as shown by two previous co-adsorption procedures, where the total number of modifier molecules in the mixture added are compared with adsorption of single diol and the extent of adsorption decreases as in previous studies due to the presence of diamine. While the comparing the mixture with adsorption of single diamine results in an increase in the adsorption due to the presence of the diol.

Therefore, in general, the mode of addition of a mixture of diol and diamine has very little effect on the extent of adsorption.

In the case of the Pt/Cab-O-Sil catalyst, the co-adsorption studies undertaken are of the type where both modifiers are added to the catalyst together as a result the adsorption on to the Pt/γ-alumina catalyst. These studies are also undertaken even although the diol has been shown not to adsorb on to the Pt/Cab-O-Sil catalyst (unsintered or sintered). Aminol formation is observed when diol and diamine are added to the unsintered Pt/Cab-O-Sil catalyst. However, the diol is formed on the addition of diol and diamine to the sintered Pt/Cab-O-Sil catalyst. Comparing the extent of adsorption diamine from the mixture with the extent of adsorption of single diamine leads, however, to no firm conclusions when the number of modifier molecules of diamine in mixture independent of the number of diol, because of the irreproducible adsorption of single diamine on to the Pt/Cab-O-Sil catalyst and the inter-conversion of diamine.

5.2.3 Similarities/differences in the adsorption of resolved modifier

As a result of the adsorption of the racemate, the adsorption properties of the R and S enantiomers of diol and diamine are studied. The (±), R and S enantiomers of diol are adsorbed to similar extent on to Pt/γ-alumina. However, for the (±), R and S enantiomers of diamine, are not adsorbed to a similar extent suggesting that the enantiomers are adsorbed differently. When the addition of similar numbers of diamine molecules of a specific enantiomer are added to the catalyst samples, the extent of adsorption is irreproducible suggesting the difference seen for (±), R and S is not a result of enantiomer adsorption property differences but could be due the number of metal atoms on the surface being different each time the catalyst is prepared, that is, although the catalyst was reduced using the same conditions every time a reduction took place the surface properties of the catalyst were slightly different each time.

The adsorption of (±) and R enantiomer of diol on to Pt/silica C10 was generally

unreliable to conclude whether there is differences in adsorption of (±) from R due to the ageing of the Pt/silica C10 catalyst.

The Pt/Cab-O-Sil catalyst is unable to adsorb R or S diol in either the unsintered or sintered form. The Rand S diamine adsorption on to the Pt/Cab-O-Sil catalyst is irreproducible independent of the catalyst activation process (unsintered or sintered form) and as a result of the inter-conversion of diamine to aminol in the adsorption of single diamine by the unsintered Pt/Cab-O-Sil catalyst.

5.2.4 Effect of temperature on adsorption

Catalyst modification is studied at both 273K and room temperature with the following conclusions, that for example, reducing the temperature for the modification of Pt/γ-alumina with diol ((±), R and S) from room temperature to 273K results in similar extends of adsorption when similar numbers of diol molecules are added. The adsorption at 273K for diamine is similar to that at room temperature taking into consideration the irreproducibility of diamine adsorption. The extent of adsorption of co-modifiers of diol and diamine is not affected by the decrease in adsorption temperature.

The sintered form of Pt/Cab-O-Sil was not used on the temperature effect studies, only the unsintered. The potential of diol is not studied at 273K, although a study at 195K leads to a slight adsorption which is within the HPLC detection error limit. The reducing of the adsorption temperature from room temperature to 273K shows diamine adsorption and on some occasions the inter-conversion of diamine to aminol, although the irreproducible adsorption of diamine makes the comparison between the temperatures difficult. The extent of aminol inter-conversion is not reproducible at room temperature or at 273K and so the effect of temperature is negligible on aminol formation. The comparison of the modification temperature for the co-adsorption of diol and diamine on to the unsintered Pt/Cab-O-Sil is difficult because of the mixture of diamine adsorption, aminol inter-conversion and diol formation occurring.

5.2.5 Size of macrocycle methylene bridge

Comparing of the lengths of the methylene (CH_2 groups) bridge in the $(CH_2)_5$- and $(CH_2)_6$-bridged, pyridine based macrocycles shows that increasing the methylene groups from 5 to 6 creates a decrease in the amount adsorbed for both the Pt/γ-alumina and Pt/Cab-O-Sil catalysts.

5.2.6 Strength of modifier adsorption

The strength to which the modifiers are adsorbed on to the catalysts was determined by the washing of the modified catalyst with a fresh sample of THF for 1 hour. From the wash results, the following conclusions can be drawn. The diol is found after the standard

wash procedure to be strongly adsorbed on to the Pt/γ-alumina catalyst although the actual strong adsorption is mainly on to the support itself. Extending the time of the wash procedure as far as the adsorbed diol was concerned made no significant difference to the extent of adsorbed diol. The same observation is made when the temperature of the wash procedure is increased, that is the diol is strongly adsorbed.

The diamine is also found to be strongly adsorbed on to the metal of the Pt/γ-alumina catalyst because the γ-alumina support has been shown to adsorb the diamine weakly.

The extent of tetra-ol adsorption on to the Pt/γalumina catalyst and the γ-alumina support has been shown to be similar to that of the diol. The assumption could be made that the tetra-ol, like the diol, is strongly adsorbed.

The Pt/γ-alumina catalyst is found to weakly adsorb the TFAE as shown by the washing procedure, almost all of the adsorbed TFAE is washed off.

The $(CH_2)_5$-bridged, pyridine-based macrocycle has been shown to adsorb strongly on to both the Pt/γ-alumina catalyst and the γ-alumina support suggesting a high degree of adsorption of the macrocycle on to the support of the catalyst as well as the metal. The adsorption of the macrocycle on to the Pt/Cab-O-Sil catalyst and not the Cab-O-Sil support suggests that the platinum metal is capable of macrocyclic adsorption.

The $(CH_2)_6$-bridged, pyridine-based macrocycle, although shown to adsorb to a lesser extent than the $(CH_2)_5$-bridged, pyridine-based macrocycle, is strongly adsorbed on to the catalyst when compared to the support suggesting less of the $(CH_2)_6$-bridged, pyridine-based macrocycle is adsorbed on to the support than the $(CH_2)_5$-bridged, pyridine-based macrocycle.

The Pt/silica C10 catalyst, prior to ageing, is able to adsorb diol strongly as is shown by both the standard wash procedure and washing the modified catalysts at a range of temperatures. This conclusion is further support by the fact that the support, silica C10, is unable to adsorb the diol. As a result of catalyst ageing, the strength of adsorption of diamine on to the Pt/silica C10 catalyst is of intermediate strength. The strength of adsorption of diamine on to the Pt/Cab-O-Sil catalyst is reasonably strong although adsorption of diamine which occurs in the presence of aminol inter-conversion, is stronger than when no reaction occurs.

The TFAE was very weakly adsorbed.

The adsorption of $(CH_2)_5$- $(CH_2)_6$-bridged, pyridine-based macrocycles has been shown to be strong on to the metal of the catalyst because of the inability of the Cab-O-Sil support to adsorb either of them.

5.2.7 Mode of modifier adsorption

Pt/γ-alumina catalysts

Considering the mode of modifier adsorption on to the three supported platinum catalysts, Isoda *et al*[30] and Izumi[34] have showed that the use of chiral modifiers based on benzene were able to induce optical activity in the hydrogenation of an oxazoline derivative of phenyl, shown in Figure 5.5, over tyrosine modified RaneyNi.[30,34] Yoshida and Harada[138] were also able to show the modification of Pd/C with ephedrine gave rise to optical activity when the C=N of the molecule shown by Figure 5.6 was reduced. Wang *et al*[139] showed that quinoline and naphthalene derivatives of chiral amino alcohols were able to induce a more substantial optical yield in the hydrogenation of ethyl pyruvate over Pt/alumina catalyst than the benzene and pyridine derivatives analogous because the extended aromatic π-system emitted by the former derivatives (Figure 5.7).

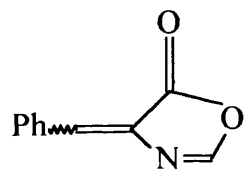

Figure 5.5:- Oxazoline derivative of phenyl hydrogenated over tyrosine modified RaneyNi

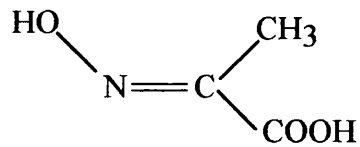

Figure 5.6:- C=N compound asymmetrically hydrogenated over ephedrine modified Pd/C

The substituted binaphthalene modifiers were chosen, to extend relative to the substituent groups the aromaticity from one benzene ring to two rings, so increasing the strength with which the modifiers can be anchored to the supported metal catalyst by increasing the continuous π-system. The adsorption of diol, diamine and tetra-ol on to the Pt/γ-alumina catalyst but not the dimethoxy suggests that the mode of modifier adsorption must occur via the substituent groups (near vertical mode), as shown for the diol in Figure 5.8 rather than by the naphthalene rings (horizontal mode), as shown for the diol in Figure

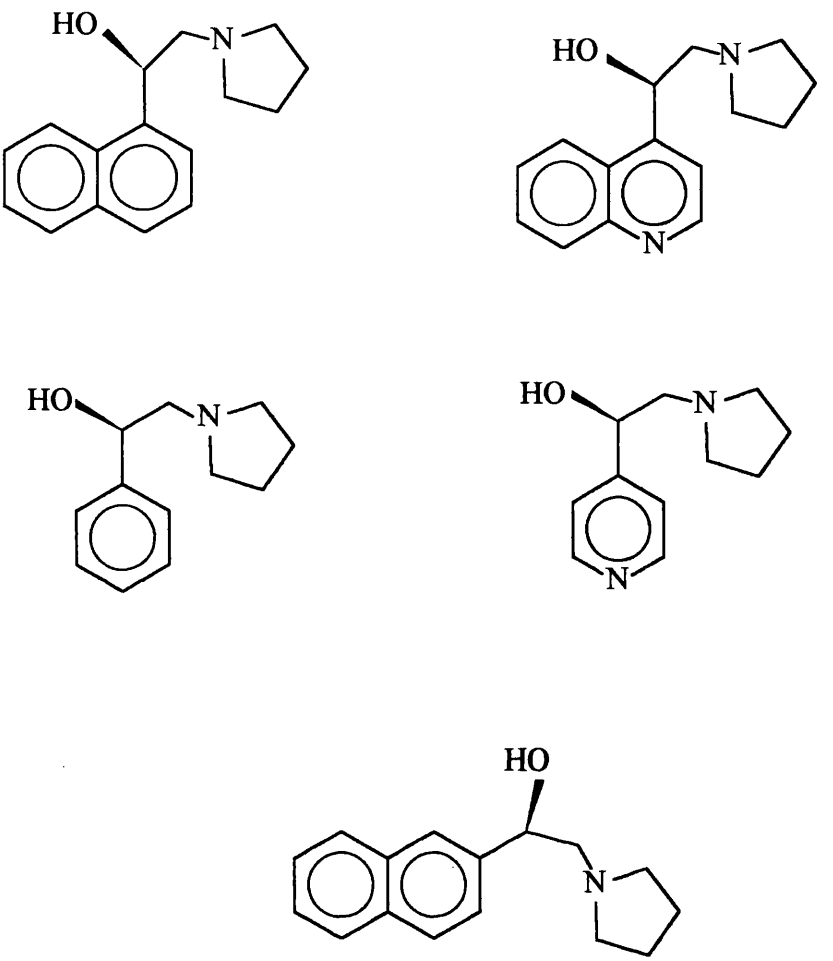

Figure 5.7:-Chiral amino alcohol modifiers

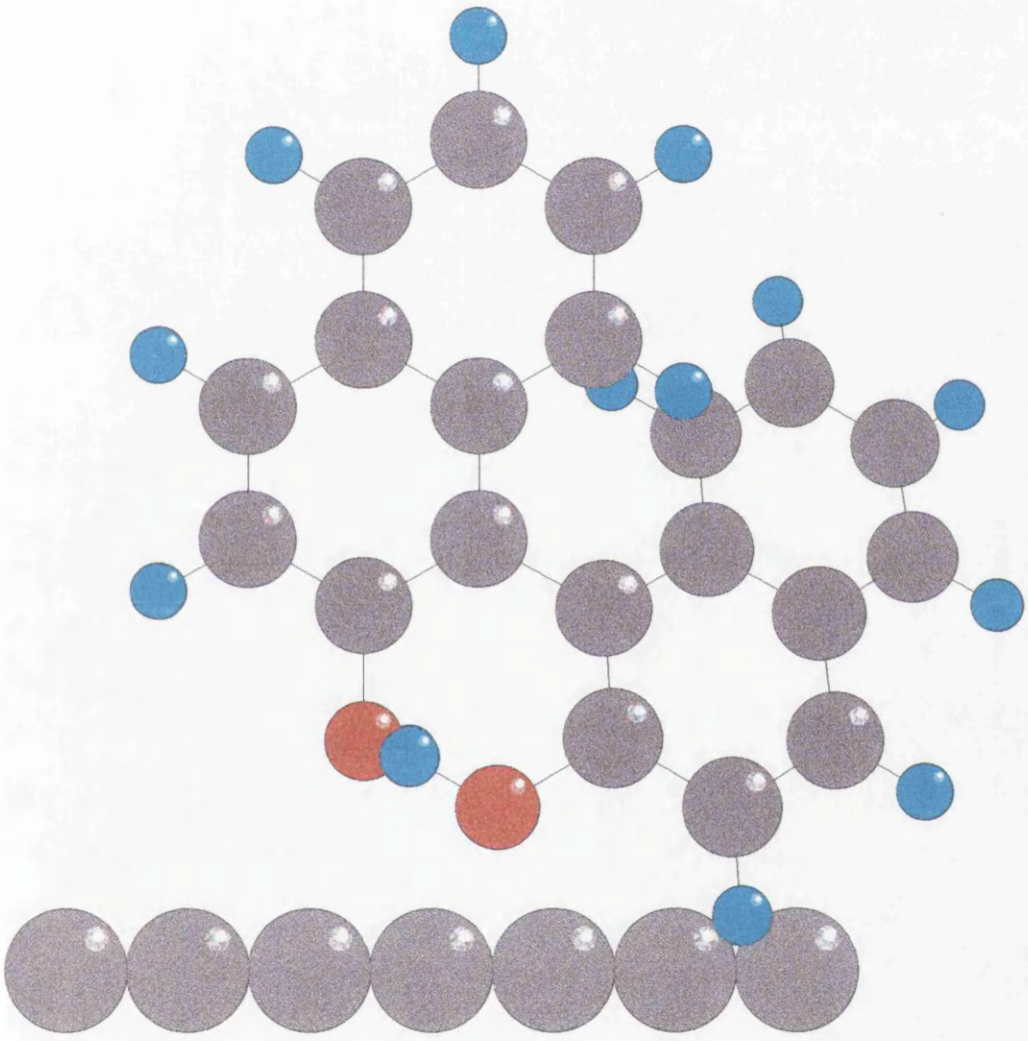

Figure 5.8:- Near vertical mode of diol adsorption on to the Pt surface

5.9. The adsorption is believed to be through the -OH and -NH_2 groups because if adsorption was in the horizontal mode the dimethoxy would have adsorbed. Adsorption in the near vertical mode by the -OH and -NH_2 groups of the diol and the diamine is possible because H atoms are able to dissociate from the O and N atoms, whilst the -CH_3 cannot dissociate from the O atom of the -OCH_3 groups.

The diamine adsorption has been shown to be mainly on to the metal, although the γ-alumina support has also been shown to adsorb the diamine to a small extent. The mode of adsorption must occur through the N atom of at least one of the -NH_2 groups. The adsorption of the N atom on to the metal is unlikely to be via the lone pair associated with N atom because this would have given rise to weak adsorption of the diamine whereas, from the wash procedure that the diamine is shown to be strongly adsorbed. The N atom will be strongly adsorbed if a H atom dissociates from the -NH_2 group, leaving a free electron pair which can then be adsorbed on to the platinum metal. Work done by Watson[140] on hydrogen/deuterium (H/D) studies on adsorbed diamine suggests that the diamine is adsorbed by the substituent groups, since H/D exchange was observed in the naphthalene rings was slower than that observed for the -NH_2 groups. Also, the adsorption through the N atom, means that the resonance structure of the naphthalene ring remains intact which, as will be discussed later, is important in the asymmetric hydrogenation of 3-coumaranone. The question also arises as to whether the diamine is anchored on to the metal surface by either one or both N atoms and whether it is important that the diamine is adsorbed by either one or both N atoms, in the asymmetric hydrogenation of 3-coumaranone. The adsorption of the number of N atoms could be determined by replacing the two H atoms of one of the -NH_2 groups with two -CH_3 groups (that is, -$N(CH_3)_2$), to see what effect this would have on the asymmetric 3-benzofuranol formation.

The diamine modified catalysts will also exhibit a surface which is partially oxidised because of the soft acid -soft base interaction of the Pt metal of the catalyst and the N atoms of the diamine. Generalisation made by Pearson[141] on acid-base interactions, showed that hard acids prefer hard bases and soft acids prefer soft bases. From this generalisation, Pt is described as a soft acid because of its size and molecules containing N atoms are described as soft bases. The metal surface could also have been oxidised by the solvent, THF, increasing the acidity of the metal and so increasing the acid-base interaction.

In the case of the diol as the modifier, which has been shown to be strongly adsorbed on to the γ-alumina support of the Pt/γ-alumina catalyst, the adsorption is through the -OH groups of the diol on to the surface acid sites of the γ-alumina. Diol

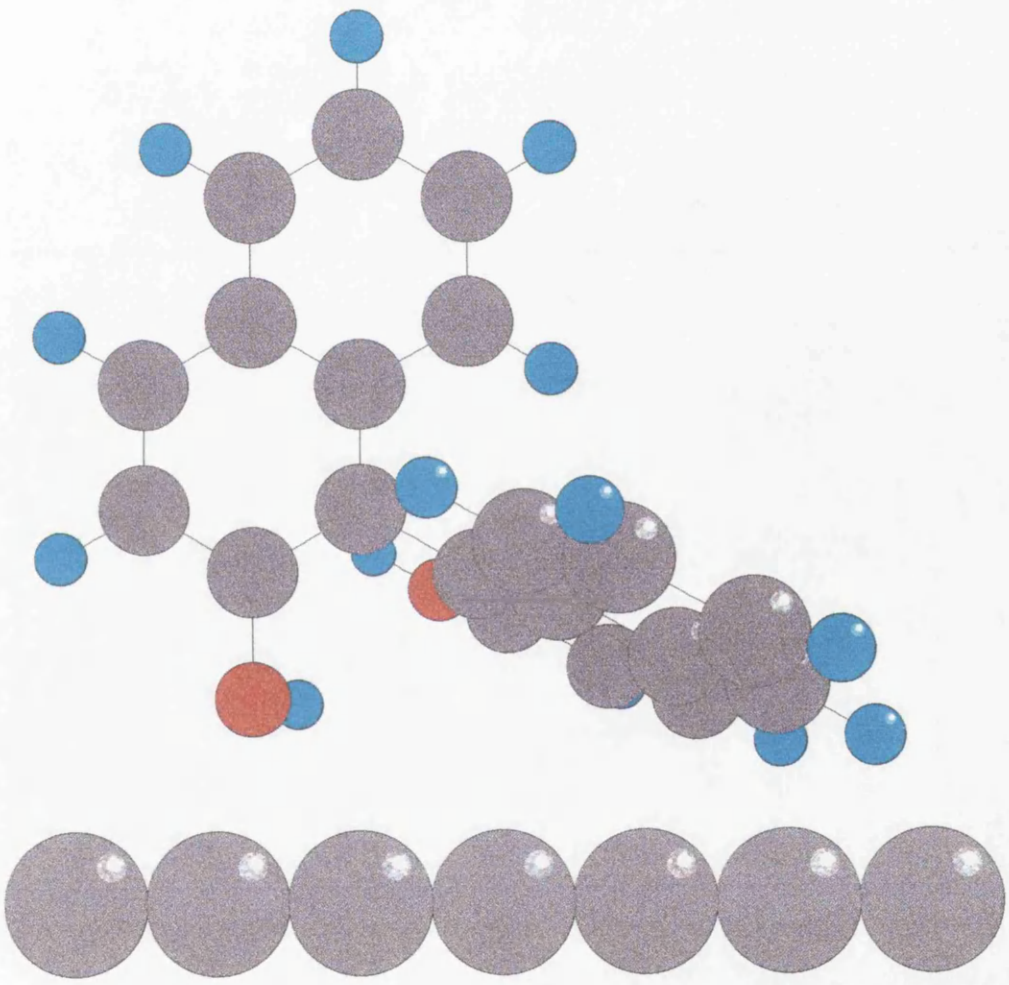

Figure 5.9:- Horizontal mode of diol adsorption on to the Pt surface

adsorption on to the platinum metal would be similar to that of the diamine, that is, the adsorption would occur through an electron pair on the oxygen atom of the -OH group as the result of the dissociation of H atom from the -OH group. Weak adsorption would have been observed if adsorption only occurred through the lone pairs on the oxygen atom. The atomic radius of a Pt atom (0.139nm) is such that the possibility exists, that if the diol has the correct geometry, that adsorption on the platinum metal could take place by both the O atoms (radius, 0.074nm).

The apparent inability of the diamine and the diol to adsorb on to the Pt/γ-alumina catalyst via one of the naphthalene rings is due to steric effects within the modifiers arising from the chirality in the axial position of the σ bond which holds the two naphthalene rings together. Both Heinz *et al*[142] and Wang *et al*[139] have suggested that the naphthalene based chiral amino alcohols are adsorbed on to a Pt/alumina catalyst by the naphthalene rings, but in the case of the chiral amino alcohols the chiral centre is at the C atom α to the naphthalene ring and so the chiral centre is held up and away from the catalyst surface as in the cinchona alkaloid modifiers.[139] The adsorption of the binaphthalene derivatives by the substituent groups mimics the idea of the chirality being held out from the catalyst surface, remembering that the chirality is at the axis of the bond between the two naphthalene ring. If the adsorption of the diamine, for instance, was through the ring system then the chirality would have been bound to the surface and not above it which, from the cinchona alkaloid modifiers is a prerequisite to optical activity.[140] It is also important to note that naphthalene itself has been shown[135] not to adsorb on to the Pt/γ-alumina catalyst, suggesting that the platinum particle sizes are not large enough to support the adsorption of naphthalene.

Adsorption of the tetra-ol modifier on to the Pt/γ-alumina catalyst has been shown to be similar to that for the diol. Therefore, like the diol, the tetra-ol is adsorbed mainly by the surface acidic sites of the γ-alumina support through the hydroxyl groups in the 2 position only because, if the hydroxyl groups in the 7 position had been involved in the adsorption as well as the hydroxyls in the 2 position, the extent of adsorption, when compared to the diol for both the Pt/γ-alumina catalyst and the γ-alumina support, would have decreased. As a result of the size of the tetra-ol and the conformation of the molecule, the hydroxyls at the 7 position are held further apart than those at the 2 position and if the adsorption of tetra-ol had occurred only by the hydroxyls at the 7 position, the amount of tetra-ol, when compared to the diol, would have been reduced.

The TFAE modifier is chosen for its increased π-system aromaticity and with the chiral centre being held away from the aromatic group. However, we have shown that

since the TFAE is weakly adsorbed, the adsorption is unlikely to have occurred through the π-system of the anthracene ring as then the adsorption would have been strong. Since the TFAE is not adsorbed on to the γ-alumina support, adsorption via the hydroxyl group can be ruled out in this case. An alternative adsorption mode of the TFAE is through the $-CF_3$ group since the F has electron withdrawing inductive effects, pulling electrons from the -OH group making the $-CF_3$ group electron rich. However, the -OH group has also the ability to withdraw electrons from the $-CF_3$ group making the -OH group electron rich. The F has a greater electron withdrawing inductive effect than the -OH, suggesting the weak adsorption is through the $-CF_3$ group. As a result of this competitive electron withdrawing inductive effect, the TFAE is only weakly adsorbed.

The $(CH_2)_5$- and $(CH_2)_6$-bridged, pyridine based macrocycles have been shown to absorb on to both the γ-alumina support and the platinum metal of the Pt/γ-alumina catalyst. There are a number of possibilities for the macrocycles to have adsorbed on to the catalyst. The adsorption could occur via the carbonyl groups, the π-system of the pyridine ring or the binding of the metal in the macrocyclic cavity by bonding to the metal through the O atoms of the ester groups and the N atoms of the amine groups. Kellogg[118] has used these macrocycles ligands for the formation of catalysts with a Mg^{2+} ion in the cavity bound to the O atoms of the ester groups and the N atoms of the amine groups. Therefore the adsorption of the macrocycles on to the Pt/γ-alumina catalyst may be similar to that of the Mg^{2+} ion binding where the platinum is concerned or by the pyridine ring and that the adsorption on to the γ-alumina support via the carbonyl groups. The increase in the size of the methylene bridge, that is the $-CH_2$ groups, leads to reduced adsorption due to the increased bulkiness of the macrocycle and reduced size of the cavity.

Pt/silica C10 catalysts

The adsorption of diol and diamine on to the Pt/silica C10 catalyst but not the dimethoxy suggests that the mode of adsorption of the modifier is in the near vertical position, that is via the substituent groups and not through a horizontal mode, that is via the naphthalene rings. The same argument can be made as for the Pt/silica C10 catalyst as the Pt/γ-alumina catalyst.

The adsorption of the diol modifier on to the Pt/silica C10 catalyst, prior to catalyst ageing, is via to the metal because the silica C10 support is unable to adsorb the diol. The extent of diol adsorption is such that the spillover of modifier from the metal to support must occur. The mode of the diol adsorption, following from the observed similarities between the diol and diamine adsorptions the argument presented for the diamine, is considered to be via the dissociated hydroxyl groups.

Pt/Cab-O-Sil catalysts

Adsorption of diamine which is not subjected to the inter-conversion to aminol and diol is adsorbed on to the platinum metal of the Pt/Cab-O-Sil catalyst in the vertical mode, that is via the $-NH_2$ substituent groups. The argument of adsorption through the $-NH_2$ substituent groups is further supported by the observation that, although sintered Pt/Cab-O-Sil is able to adsorb naphthalene,[135] it is not able to adsorb the diol.

The mode of TFAE adsorption is probably via the $-CF_3$ groups as deduced for the Pt/γ-alumina catalyst, because the adsorption is so slight. Furthermore, if the adsorption had occurred via the anthracene ring the amount adsorbed would have increased with the degree of sintering of the Pt/Cab-O-Sil.

The Pt/Cab-O-Sil catalyst unlike the Pt/γ-alumina catalyst, adsorption of the macrocycles is only on to the metal. As with the Pt/γ-alumina catalyst, the adsorption of the macrocycles on the Pt/Cab-O-Sil catalyst becomes more sterically hindered as the bridge size of the macrocycle is increased. The adsorption of the macrocycles by the platinum metal must have been via within the cavity by the N atoms of by the pyridine ring.

5.3 HYDROGENATION STUDIES

The hydrogenation of methyl tiglate and tiglic acid over binaphthalene based modified Pt/γ-alumina and Pt/Cab-O-Sil catalysts gave rise to racemic methyl-2-methyl butyrate and methyl butyric acid, respectively. The hydrogenation of methyl tiglate and tiglic acid over Pt/γ-alumina and Pt/Cab-O-Sil catalysts modified with PhGly, PhAla, DMPEA, Trp, MTFMPAA, Pseudo and His gave rise to the racemic products. The hydrogenation of methyl tiglate over His, DMPEA, Trp, Pseudo and MTFMPAA modified Pt/γ-alumina catalysts, resulted in the formation of an additional product, methyl angelate. An additional product, angelic acid,was also observed when tiglic acid was hydrogenated over unmodified Pt/Cab-O-Sil catalyst .However, the hydrogenation of 3-coumaranone over R diamine modified Pt/γ-alumina and Pt/Cab-O-Sil catalysts gave rise to the enantioselective formation of S-3-benzofuranol in (Figure 5.10a), whilst S diamine modified while Pt/γ-alumina and Pt/Cab-O-Sil catalysts gave rise to the R enantiomer of 3-benzofuranol in excess (Figure 5.10b). Although diol modified Pt/γ-alumina and Pt/Cab-O-Sil catalysts gave racemate 3-benzofuranol. Modification of the Pt/γ-alumina catalyst with PhGly, PhAla, DMPEA and Trp, enantioselectivity was observed in the hydrogenation of 3-coumaranone, however the inclusion of the wash step for the modification process of PhGly led to a loss of enantioselectivity suggesting that there is an interaction between the weakly bound PhGly and the 3-coumaranone, which is lost following the wash. While modification of Pt/γ-alumina catalyst with MTFMPAA, Pseudo and His, enantioselectivity was not observed in the hydrogenation of 3-coumaranone.In the hydrogenation over $(CH_2)_5$- and $(CH_2)_6$-bridged, pyridine-based macrocyclic modified Pt/γ-alumina and Pt/Cab-O-Sil catalysts, no enantioselectivity was observed. In addition to the formation of 3-benzofuranol, a second product was shown to be formed, this product which will be referred to the "additional" product, was formed independent of whether the catalyst was modified or unmodified.

5.3.1 Hydrogenation of 3-coumaranone

Pt/γ-alumina catalysts

Hydrogenation of 3-coumaranone over diol modified Pt/γ-alumina catalyst at ambient temperature results in a reduction in the extent of conversion in comparison with that observed for the unmodified catalyst after 4 hours. However, after 20 hours, the extent over the diol modified catalyst has increased in comparison with that observed for unmodified catalyst which suggests that the modifier is acting as a promoter. That is the diol interaction with the catalyst surface creates a surface which is favourable to the adsorption and subsequent hydrogenation of 3-coumaranone. Omission of the wash step

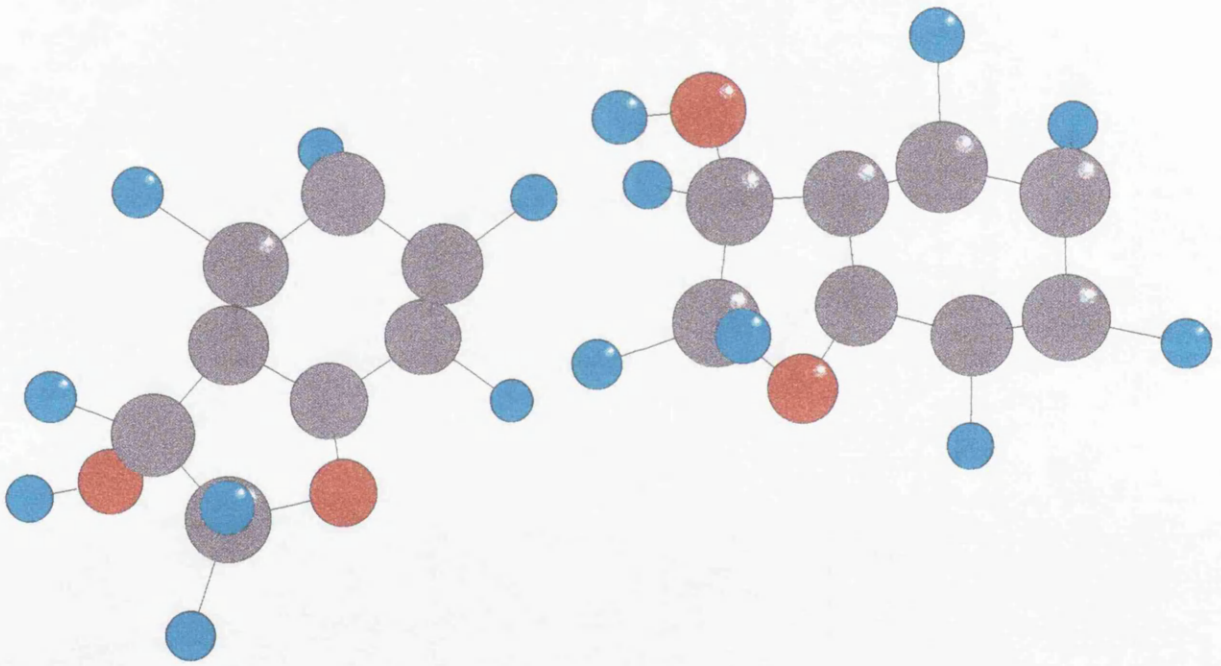

a b

Figure 5.10:- S and R enantiomers of 3-benzofuranol

of the standard modification procedure resulted in no significant effect on the extent of conversion of 3-coumaranone. The % conversion of 3-coumaranone seems to be reduced as the diol is was changed from the R enantiomer to the S enantiomer, which was unexpected in view of the observation that the γ-alumina support of the Pt/γ-alumina and catalyst is capable of racemising the pure enantiomer of diol. Even without the racemisation of the diol, the conversion would be expected to be similar considering that both the R and S enantiomers of diol adsorb on to the Pt/γ-alumina catalyst to the same extent and the amounts adsorbed are reproducible.

Hydrogenation of 3-coumaranone over diamine modified Pt/γ-alumina catalyst at ambient temperature results in a reduction in the extent of conversion in comparison with for the unmodified Pt/γ-alumina catalyst after 4 hours. Although, after 20 hours no clear trend is observed when the hydrogenation over the modified catalyst is compared with that for the unmodified catalyst. Reducing the temperature to 273K results in a reduction in the extent of conversion using modified catalyst in comparison with that observed with the unmodified catalyst. A reduction in the extent of conversion after similar reaction times is observed when the reaction temperature at ambient is compared to that of 273K for the hydrogenation of 3-coumaranone over R diamine modified Pt/γ-alumina catalyst. As the amount of diamine modifier added to the freshly prepared catalyst samples is increased, no clear trend is observed in the extent of 3-coumaranone hydrogenation to 3-benzofuranol and the additional product. This unclear trend in the extent of conversion over similar reaction times of 3-coumaranone with increased modifier addition results from the non-reproducible adsorption of diamine on to the Pt/γ-alumina catalyst. As with the diol modified Pt/γ-alumina catalysts, omission of the wash step from the standard catalyst modification procedure and the results in an increase in the extent of conversion. Although enantioselectivity is observed from this modified catalyst system there is no clear trend in the enantiomeric excess, which neither increases nor decreases as the amount of modifier added to the catalyst is increased. Polarimetry studies shows that no racemisation of the diamine occurs during either the modification or hydrogenation processes.

The adsorption studies show that the Pt/γ-alumina catalyst is capable of adsorbing both diol and diamine, independent of the order of addition of the modifiers and the amount of diol adsorbed, in general, is similar to that where only diol is added; while, in general, the amount of diamine adsorbed is reduced in comparison to where only diamine was added. The hydrogenation of 3-coumaranone by diol and diamine modified Pt/γ-alumina catalysts results in enantioselectivity and is independent of the procedure used to adsorb both of the modifiers. The extent of conversion of 3-coumaranone over diol/diamine

modified Pt/γ-alumina catalyst, when compared to the unmodified Pt/γ-alumina catalyst is reduced after similar reaction times. Comparison of the extent of conversion after similar reaction times of 3-coumaranone over diol/diamine modified Pt/γ-alumina catalyst, with diol modified Pt/γ-alumina catalysts, where the total number of diol and diamine molecules added to the catalyst is similar that of the diol, is reduced. The extent of conversion after similar reaction times is also reduced when the diol/diamine modified Pt/γ-alumina catalyst is compared to that of a diamine modified catalyst, where the total number of diol and diamine molecules is similar to that of the diamine. The enantioselectivity observed for diol/diamine modified Pt/γ-alumina catalysts is greater than that observed for the diamine modified Pt/γ-alumina catalysts. The increased enantioselectivity is independent of the modification procedure and the extent of diamine adsorption. The omission of the wash step makes no difference to the extent of conversion after similar reaction times.

The Pt/γ-alumina catalyst is modified with a number of modifiers: PhGly, PhAla, DMPEA, Trp, MTFMPAA, Pseudo and His; which all exhibit an aromatic moiety through which the adsorption might be expected to occur with the chiral centre held up and away from the catalyst surface. The modification of the Pt/γ-alumina catalyst with PhGly, PhAla, DMPEA, Trp, MTFMPAA, Pseudo and His results in a decrease in the extent of conversion after 4 hours when compared to the hydrogenation of 3-coumaranone over the unmodified catalyst. However, the extent of conversion after 20 hours over the PhGly, PhAla, DMPEA, Trp, MTFMPAA, Pseudo and His modified Pt/γ-alumina catalysts when compared to that for the hydrogenation of 3-coumaranone over the unmodified catalyst results in an increase. The increase in the extent of conversion by the modified catalysts compared to the unmodified catalyst after 20 hours suggests that the modifiers are acting as catalyst promoters, allowing the length of time the for the catalyst to add the hydrogen to the -C=O group, to be reduced. PhGly modified Pt/γ-alumina catalyst gives rise to the S enantiomer in excess and PhAla, DMPEA and Trp modified Pt/γ-alumina catalysts give rise to the R enantiomer in excess.

The modification of the Pt/γ-alumina catalyst with either the $(CH_2)_5$- or $CH_2)_6$-bridged, pyridine-based macrocycle results in the racemic of 3-benzofuranol being formed on hydrogenation. Comparing the hydrogenation of 3-coumaranone over the macrocyclic modified Pt/γ-alumina catalysts with the unmodified catalyst after similar reaction times results in a reduced conversion.

Pt/Cab-O-Sil catalysts

Although the unsintered Pt/Cab-O-Sil catalyst was found not to adsorb the diol, a sample of unsintered Pt/Cab-O-Sil catalyst is treated with a solution of diol according to

the standard adsorption procedure. Subsequent hydrogenation of 3-coumaranone with this catalyst results in an increase in the extent of conversion after similar reaction times when compared to a catalyst sample which was not treated with diol. This observed increase in the extent of conversion suggests that although the diol was not adsorbed on to the catalyst, that following the wash step, there must be diol molecules remaining. These remaining diol molecules are then acting as catalyst promoters.

The extent of conversion after similar reaction times for the hydrogenation of 3-coumaranone is reduced as a result of modification of the unsintered Pt/Cab-O-Sil catalysts and the extent is independent of the temperature at which the hydrogenation is studied. However, the reduction of temperature from ambient to 273K results in a decrease in the conversion after similar reaction times for the unmodified unsintered Pt/Cab-O-Sil catalyst. With diamine modified unsintered Pt/Cab-O-Sil catalysts the extent of conversion after similar reaction times is reduced when aminol formation is observed. The omission of the wash step from the modification procedure leads to a reduction in the extent of 3-coumaranone hydrogenated after similar reaction times. Enantioselectivity is observed from the diamine modified unsintered Pt/Cab-O-Sil catalysts in the presence of aminol, although the optical yield is decreased. The aminol seems to be acting as a hydrogenation suppressant and blocks some of the some enantioselective sites.

The addition of diol and diamine to the unsintered Pt/Cab-O-Sil catalyst results in enantioselectivity and a reduction in the extent of hydrogenation product after similar reaction times when compared to that of the unmodified catalyst. There does not appear to be any trends between the co-adsorbed modified catalyst with the diol or diamine modified catalysts.

The use of the $(CH_2)_5$- and $CH_2)_6$-bridged, pyridine-based macrocycles as chiral modifiers for the unsintered Pt/Cab-O-Sil catalysts has resulted in racemic 3-benzofuranol. The modification of the unsintered Pt/Cab-O-Sil catalyst results in a decrease in the extent of conversion of 3-coumaranone after similar reaction times compared to that of the unmodified catalyst. The omission of the wash step from the modification procedure results in reduced amount of hydrogenation after similar reaction times compared to that of the unmodified catalyst. The extent of 3-coumaranone hydrogenation increases as the amount of macrocycle added to the catalyst increases.

5.3.2 Hydrogenation of methyl tiglate and tiglic acid

Pt/γ-alumina catalysts

Modification of the Pt/γ-alumina catalysts with diol or diamine results in a decrease in the extent of conversion of methyl tiglate after similar reaction times compared to that

of the unmodified catalyst. The extent of conversion of tiglic acid over the modified catalysts is similar to that for the unmodified catalyst when compared after similar reaction times. Omission of the wash step from the modification process, observed in tiglic acid hydrogenation makes no significant difference to the amount of conversion. Increasing the amount of modifier added to the freshly prepared catalyst sample, made no difference to the amount of tiglic acid converted.

The inability of diol modified Pt/γ-alumina catalysts to induce enantioselectivity into the hydrogenation of methyl tiglate and tiglic acid could be a result of the racemisation of the diol by the γ-alumina support of the Pt/γ-alumina catalyst.

Modification of the Pt/γ-alumina catalyst with DMPEA, MTFMPAA, His, Trp, Pseudo, PhGly and PhAla modifiers for the hydrogenation of methyl tiglate results in the formation of the racemate. However, an additional product is observed with the His, DMPEA, Trp, Pseudo and MTFMPAA modified Pt/γ-alumina catalysts. The conversion using the modified catalyst is approximately the same as with the unmodified catalyst.

Pt/Cab-O-Sil catalysts

The modification of unsintered Pt/Cab-O-Sil catalysts with diamine for the hydrogenation of methyl tiglate results in the formation of the racemate. A similar result is observed for the hydrogenation of tiglic acid over diamine and/or diol modified unsintered Pt/Cab-O-Sil catalyst. The extent of hydrogenation of methyl tiglate over diamine modified unsintered Pt/Cab-O-Sil catalysts is less after 4 hours but is similar to the unmodified catalyst by 20 hours. Diol and/or diamine modified unsintered Pt/Cab-O-Sil catalysts show similar conversions in the hydrogenation of tiglic acid to those obtained with the unmodified catalyst. The formation of an additional product in the hydrogenation of methyl tiglate over the unmodified and diol and diamine modified catalyst is not observed. However, the hydrogenation of tiglic over unmodified unsintered Pt/Cab-O-Sil catalyst results in the formation of an additional product. Use of unsintered Pt/Cab-O-Sil catalyst in the presence of the alternative modifiers for the hydrogenation of methyl tiglate results in the formation of the racemate, and in some instances, the formation of an additional product. Comparing the extent of hydrogenation of the unsintered Pt/Cab-O-Sil catalyst modified with the alternative modifiers with the unmodified catalyst shows that there is a reduction of conversion at 4 hours but by the 20 hours the extents of hydrogenation are similar.

The sintering of a sample of Pt/Cab-O-Sil catalyst followed by the modification with diamine for the hydrogenation of methyl tiglate, results in the formation of the racemate. In general, when the extent of hydrogenation obtained with the modified sintered

Pt/Cab-O-Sil catalyst is compared with that over the unmodified catalyst, the amounts are very similar.

5.3.3 Hydrogenation mechanism for 3-coumaranone

The hydrogenation of prochiral molecules by supported metal catalysts results in racemic mixtures due to hydrogen being able to add to both sides of the double bond. The two sides or faces of the double bond in a molecule (C=O, C=C) with a prochiral centre have been designated the names *Re* and *Si*. The faces can be defined using an altered version of the Cahn-Ingold-Prelog rules to define the R and S configurations of chiral molecules. The assignment of the faces of C=C and C=O is on the basis of three ligands attached to the prochiral centre with the molecule visualised as lying flat on the plane of the paper as shown by Figure 5.11. In proceeding round the prochiral centre, the usual order of decreasing priority of the ligands, if the direction of travel highest to lowest priority is in a clockwise direction, the face turned upward towards us is specified as the *Re* face (rectus); if counterclockwise, it is specified as the *Si* face (sinister). However, asymmetric hydrogenation results in the addition of hydrogen to only one of the faces, that is the *Re* or *Si* face. To be able to restrict the hydrogen form being added to both faces, the reactant has to be held in a conformation which exposes only one face. The use of chirally modified catalysts, restricts the adsorption of the starting material to only one face because of the chirality of the modifier and so the catalyst sterically inhibits/directs the adsorption of the prochiral material.

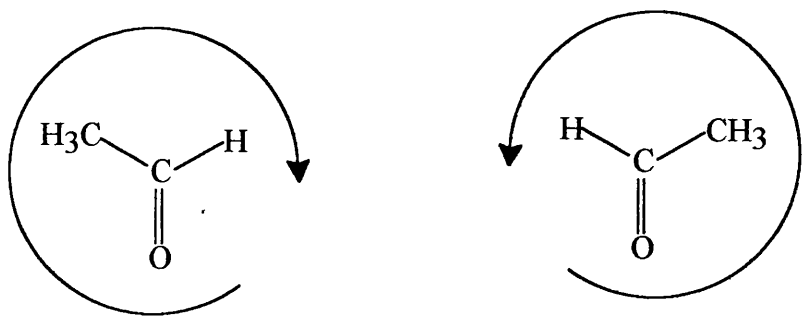

Re face *Si* face

Figure 5.11:- *Si* and *Re* faces of ethanal

The mechanism of asymmetric hydrogenation over chirally modified catalyst will be dependent on the generation of the surface chirality. The adsorption studies have shown that the substituted binaphthalene derivatives are adsorbed by the substituent groups, that is, -OH and -NH_2 groups of diol and diamine respectively, with the generation of a chiral adlayer on the catalyst surface. The formation of chiral centres on the catalyst surface with

the generation of a template, as had been initially proposed by Wells[46] with respect to the Pt/cinchona alkaloid hydrogenation of methyl pyruvate must be discarded because (1) the binaphthalenes are not adsorbed via a naphthalene ring, which would have resulted in ensembles of unmodified atoms and (2) the proposal of a 1:1 modifier:reactant by Blaser[143] and subsequently by Wells[66] for the Pt/cinchona alkaloid system.

5.3.3.1 Hydrogenation of 3-coumaranone over supported Pt catalysts modified with substituted binaphthalenes

The proposed mechanism for the asymmetric hydrogenation of the prochiral staring material, 3-coumaranone, is an interaction between the 3-coumaranone and the binaphthalene-based modifiers. The 3-coumaranone has to interact with the substituted binaphthalene molecule and this is possible through the π-system of the 3-coumaranone and one of the naphthalene rings. The π-π interaction between the 3-coumaranone and one of the benzene rings of the naphthalene unit could be fairly strong since, in general, even although the π electrons are more loosely held than the σ electrons of the carbon-carbon bonds and so the π electrons are thus particularly available to a reagent seeking electrons. Reeder *et al*[144] have shown that π-π interaction between 1,1'-substituted binaphthalenes can be used as chiral recognition agents for cinchona alkaloids. This interaction was proposed to be through one of the naphthalene groups and the quinoline ring of the cinchona alkaloid together with hydrogen bonding between the binaphthalene and the cinchona alkaloid to hold the conformation rigid. The loosely held π electrons in either 3-coumaranone of the furthest aromatic ring of a naphthalene unit from the substituent group are able to interact with similarly loosely held π electrons of the other material. The interaction of the two sets of π electrons allows the 3-coumaranone and the substituted binaphthalene to be held together, although this interaction could be reversible because of the presence of the π electron clouds existing above and below the plane of the ring. The π-π interaction of the 3-coumaranone with the substituted binaphthalene modifiers is not enough to allow the asymmetric hydrogenation of 3-coumaranone to take place, therefore another mode of interaction of the 3-coumaranone with the modifiers to create a rigid complex is required.

The adsorption of the diol modifier on to the metal of the supported Pt catalysts has been shown to occur through an O atom of the dissociated -OH group, although in the case of the Pt/γ-alumina catalyst, the adsorption is mainly on to the γ-alumina support. The main interaction between the 3-coumaranone and the diol is via the π-π interaction between the benzene substituent of 3-coumaranone and the ring of the naphthalene moiety furthest from the -OH group, although a weak interaction may occur between the carbonyl group

of the 3-coumaranone and the diol but this would not be strong enough to hold the 3-coumaranone in such a way that only one face is exposed for the addition of hydrogen. The racemisation of the diol by the γ-alumina support of the Pt/γ-alumina catalyst suggests that either no interaction exists between the 3-coumaranone and the diol or that the presence of the racemate of the diol suggests that the R diol produces one enantiomer of the 3-benzofuranol in excess and at the same time and at the same rate the S diol produces the other enantiomer in excess.

However, when the diamine is used as the modifier, enantioselectivity is observed. The adsorption of the diamine through the N atom of the $-NH_2$ group by the dissociation of at least one H atom, leaves a H atom still bound to the N atom. The presence of this H atom allows the formation of a strong hydrogen bond between the amine group of the diamine and the O atom of the carbonyl group of the 3-coumaranone. The existence of this hydrogen bonding is thought to be sufficient along with the π-π interaction, referred to as π stacking, for the 3-coumaranone to be held in such a way that only one face is exposed for the addition of hydrogen. R diamine modified supported Pt catalysts create the S enantiomer of 3-benzofuranol and S diamine, the R enantiomer of 3-benzofuranol.

The formation of the aminol over the Pt/Cab-O-Sil catalyst modified with diamine affects the overall conversion of 3-coumaranone to 3-benzofuranol and reduces the enantiomeric excess of 3-benzofuranol. Clearly the aminol is acting as a poison for both the enantiomeric sites and the racemic sites.

The proposed mechanism involving the π-π interaction of 3-coumaranone with the diamine modifier, where the 3-coumaranone is not bonded to the metal itself, is shown schematically in Figures 5.12 and 5.13, for R and S diamine respectively. From the model, the R diamine is able to form the S 3-benzofuranol when the 3-coumaranone exposes its *Si* face and the hydrogen is attached by *syn* addition to the front of the exposed face. *Syn* addition is described as the addition of hydrogen to the same face of the double bond as is shown in Figure 5.14a, whilst Figure 5.14b shows the alternative stereochemical addition of hydrogen (*anti* addition - addition of hydrogen to opposite faces of the double bond). This argument can be extended to the S diamine which forms the R 3-benzofuranol. Assuming that the hydrogen attaches itself to the C=O by *syn* addition from the front of the molecule, and if the *Si* face is exposed with the R diamine, then the *Re* face must be exposed upon interaction with the S diamine, therefore the expected configuration would be R, which is what is obtained.

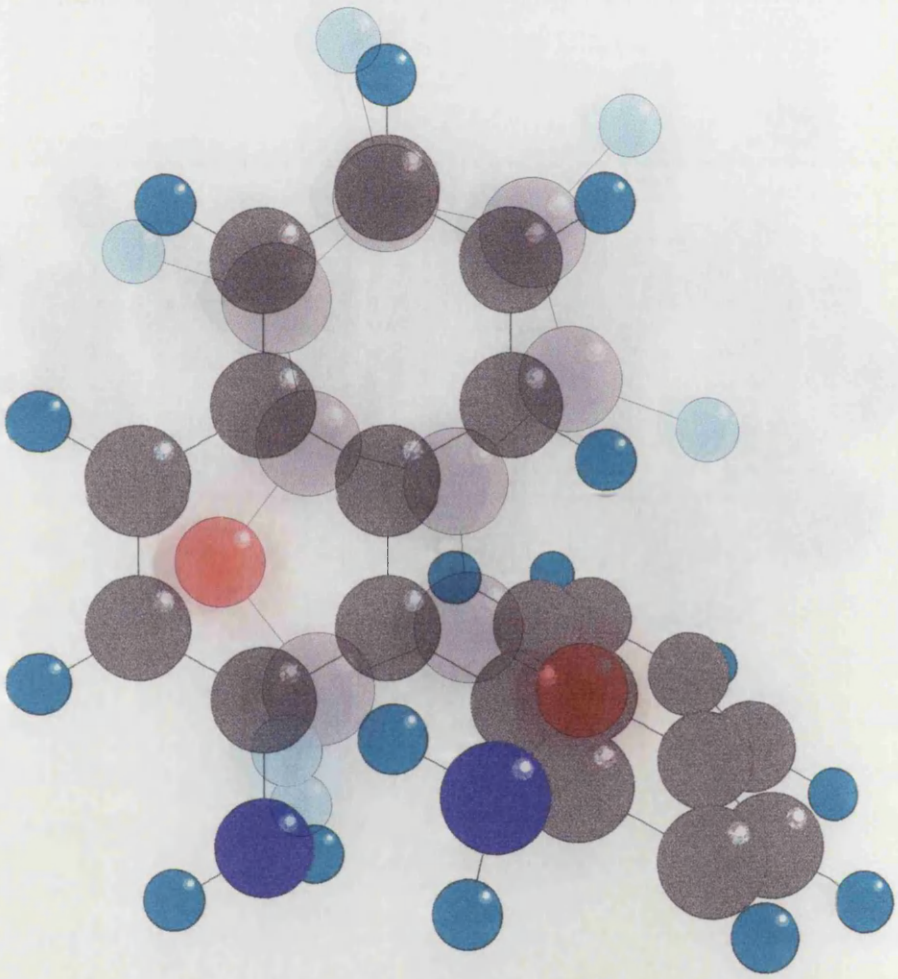

Figure 5.12:- Interaction of 3-coumaranone with R diamine

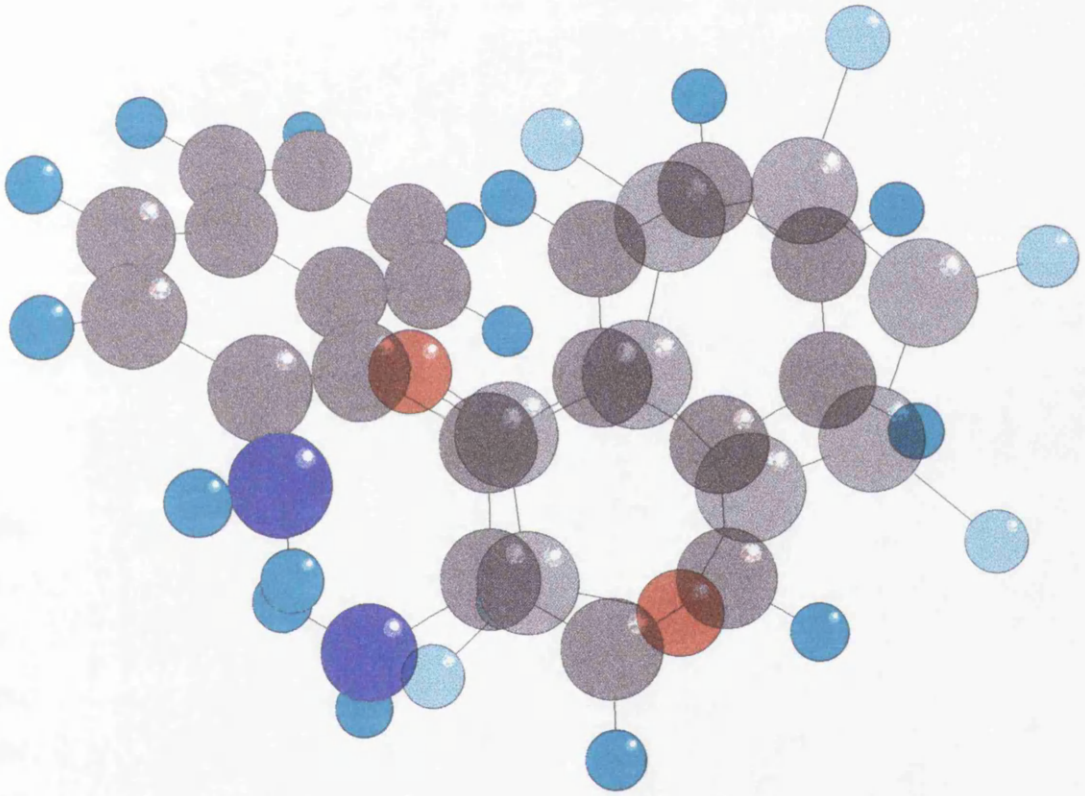

Figure 5.13:- Interaction of 3-coumaranone with S diamine

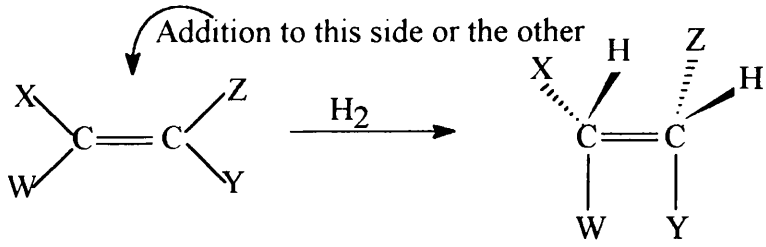

(a) Syn addition

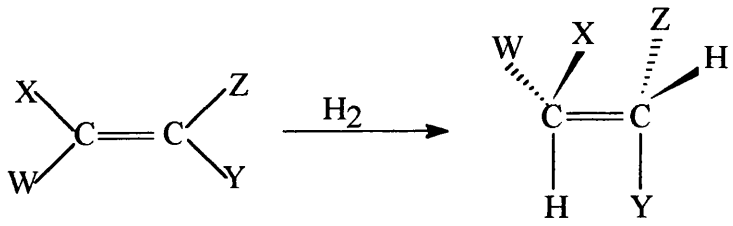

(b) Anti addition

Figure 5.14:- *Syn* and *anti* addition of hydrogen to a double bond

The *syn* addition of hydrogen to the carbonyl from the front is the most likely addition because of the small size of the H atoms. The exact source of the hydrogen atoms is not yet clear. It may be possible for the hydrogens to come from the diamine via the amine grouping to which the carbonyl oxygen is hydrogen bonded or, alternatively, the hydrogen atoms may come directly from the H_2(g). The addition of hydrogen to the carbonyl oxygen reduces the hydrogen bonding between the -N-H and O=C- continuing and so eventually the hydrogen bonding is broken and, following the addition of hydrogen to the carbonyl carbon, the 3-benzofuranol if formed and the π-π interaction lost and the 3-benzofuranol is then no longer bonded to the diamine.

5.3.3.2 Hydrogenation of 3-coumaranone over supported Pt catalysts co-modified with substituted binaphthalenes

The hydrogenation of 3-coumaranone over supported Pt catalyst modified with both diol and diamine is asymmetric. However, we know that the diol alone does not induce enantioselectivity and diamine does. It is not surprising, therefore, that the configuration of the benzofuranol is directed by the configuration of the diamine used to modify the catalyst. The presence of the diol, however, increases the enantioselectivity. This increase must be due to the diol blocking some of the racemic sites on the catalyst surface, thereby

reducing the racemic hydrogenation as well as reducing the overall conversion of 3-coumaranone to 3-benzofuranol. Essentially, the diol is acting as a poison to the racemic hydrogenation sites but not the asymmetric hydrogenation, which results from the surface complex formed by π-π stacking and hydrogen bonding of the diamine and 3-coumaranone.

5.3.3.3 Hydrogenation of 3-coumaranone over supported Pt catalyst modified with the macrocycles

The racemic hydrogenation found with the $(CH_2)_5$- and $(CH_2)_6$-bridged, pyridine-based macrocycles modified supported Pt catalyst is due to a lack of interaction between the modifier and 3-coumaranone.

5.3.3.4 Hydrogenation of 3-coumaranone over supported Pt catalysts modified with the alternative modifiers

The proposed model for the asymmetric hydrogenation of 3-coumaranone over the diamine modified supported Pt catalysts suggests the requirement of the presence of a N atom in the modifier. Therefore, the MTFMPAA modifier would not be expected to give rise to enantioselectivity in the 3-coumaranone hydrogenation. The presence of a H atom bonded to the N atom to enable the hydrogen bonding between the modifier and 3-coumaranone is a also requirement for the model. Of the other modifiers studied and which contain a N atom only PhGly, PhAla, His and Trp will possess the ability, following adsorption on to the metal surface assuming these molecules like the diamine adsorb via the N group and leave a N-H bond. Although, of these modifiers only the PhAla, PhGly and Trp exhibit enantioselectivity. However, what is surprising, is that DMPEA which does not contain an N-H bond is able to promote enantioselectivity. The extent of enantioselectivity found with the PhGly, DMPEA and Trp modifiers is very low and that the extent of enantioselectivity is within the detection limits of the GC suggesting no enantioselectivity occurred. The PhAla is very similar to modifiers used in the asymmetric hydrogenation of methyl pyruvate over Pt/γ-alumina catalysts modified with chiral amino alcohol derivatives,[5] where it was found that the chiral centre is between the N grouping and the aromatic moiety.

5.3.3.5 Additional product formation

During the hydrogenation of 3-coumaranone, an additional product is formed independent of whether the catalyst is modified or unmodified. The exact identity of this additional product could not be established during the present work. From GC-MS studies, the molecular mass is known to be 138, that is, the additional product has a molecular mass of 2 units more than the benzofuranol (136), suggesting that the additional product has an extra two hydrogen atoms. NMR analysis is difficult to interpret as a result of the

small quantity of additional product. Of the possible both, (±)-1-phenyl-1,2-ethanediol and 2-phenoxyethanol, shown in Figure 5.15, can be ruled out as shown by chiral GC analysis.

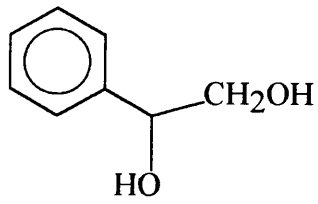

(±)-1-Phenyl-1,2-ethanediol

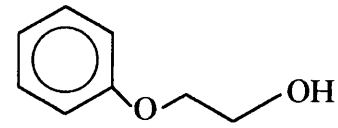

Phenoxyethanol

Figure 5.15:- Possible contenders for additional product formed from the hydrogenation of 3-coumaranone

5.3.4 Hydrogenation mechanism for methyl tiglate and tiglic acid

5.3.4.1 Hydrogenation of methyl tiglate and tiglic acid over supported Pt catalysts modified with substituted binaphthalenes

Extending the proposed mechanism of π-π interaction of staring material and chiral modifier to the hydrogenation of methyl tiglate and tiglic acid is reasonable due to the presence of the π bond on the C=C bond. However, the hydrogenation of methyl tiglate and tiglic acid over chirally modified supported Pt catalyst is not asymmetric. The methyl tiglate and tiglic acid molecules are therefore unable to interact with the modifiers to such an extent that the molecules have only one face exposed for hydrogen addition. From both TEM and chemisorption, the supported Pt catalysts are seen to be highly dispersed with small metal particles (~2nm). Unlike the 3-coumaranone which is not adsorbed on to the metal surface of the chirally modified supported Pt catalysts, the tiglic acid and methyl tiglate are adsorbed on to the metal surface of the modified catalyst. As a result of the small particle size, the ability of the modifier and prochiral material to be held sufficiently close enough to allow π-π interaction to occur is minimal. Furthermore, as shown by the 3-coumaranone, the π-π interaction is not sufficient to hold the prochiral molecule in a rigid conformation, allowing the preferential addition of hydrogen to one side of the double bond and that the presence of hydrogen bonding between the amine group of the diamine, as shown by O atom of the 3-coumaranone carbonyl group, is required. The tiglic acid has the ability to hydrogen bond to the amine group of the diamine through the dissociation of the H atom from the acid group and the adsorption of the acid to the metal via C=O group of -COOH. However, the small metal particle sizes does not seem to allow this proposed interaction to take place. Methyl tiglate, on the other hand, does not possess the

ability to dissociate a H atom from the acid grouping. Therefore, independent of the metal particle size, the methyl tiglate is unable to form a hydrogen bond with the amine group of the diamine modifier and so is not held in such a conformation that hydrogen is only able to be added from one side. Methyl tiglate, like tiglic acid, is adsorbed on to the metal.

Alternatively, the methyl tiglate and tiglic acid may have no interaction of any type with the diamine and the hydrogenation takes place only at the racemic sites.

5.3.4.2 Hydrogenation of methyl tiglate over supported Pt catalysts modified with the alternative modifiers

As is seen by the modification of the supported Pt catalysts with the substituted binaphthalene modifiers, the use of catalysts modified with the alternative modifiers results in racemic hydrogenation of the methyl tiglate. The formation of the racemate is probably due to a lack of interaction between the modifier and methyl tiglate. The formation of an additional product is found with His, DMPEA, Trp, Pseudo and MTFMPAA modifiers.

5.3.4.3 Additional product formation

Analysis by chiral GC shows the presence of an additional product during the hydrogenation with some of the modified catalysts. The peak arises between the two enantiomers of methyl-2-methyl butyrate from methyl tiglate hydrogenation and between the two enantiomers of methyl butyric acid from tiglic acid hydrogenation. These additional products were also observed from the hydrogenation of methyl tiglate and tiglic acid over modified supported Ni and Pd catalysts and GC-MS analysis on the these additional products by Young[145] showed that they have the same molecular mass as methyl tiglate and tiglic acid, respectively, and were identified as the *cis* isomer of the starting materials, that is, methyl angelate and angelic acid (Figure 5.16).

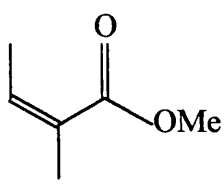

Methyl angelate

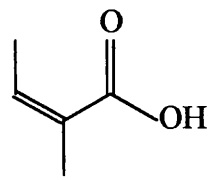

Angelic acid

Figure 5.16:- Methyl angelate and angelic acid, the additional products from methyl tiglate and tiglic acid hydrogenation

The formation of methyl angelate and angelic acid is by a *cis-trans* isomerisation. Cis-trans isomerisation has been shown to occur in the hydrogenation of 1-butene over a Pd/γ-alumina[7] catalyst to the *cis* and *trans* isomer of 2-butene and involved the reversible

formation of an butyl radical as the half-hydrogenated state as shown by Figure 5.17.

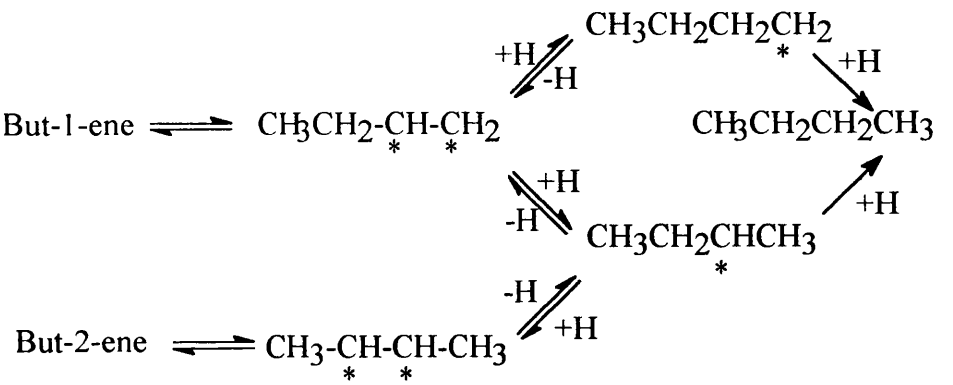

Figure 5.17:- *Cis-trans* isomerisation of 1-butene

The formation of methyl angelate and angelic acid, and its subsequent hydrogenation results in the usual hydrogenation products, therefore it is perhaps not surprising that the racemates are formed as shown in Figures 5.18 and 5.19, respectively.

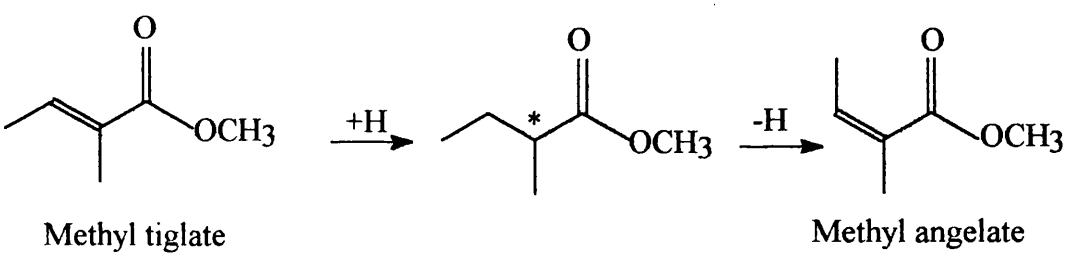

Figure 5.18:- *Cis-trans* isomerisation of methyl angelate and methyl tiglate

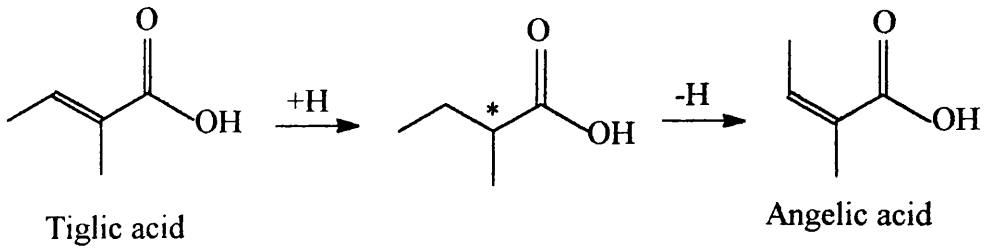

Tiglic acid

Angelic acid

Figure 5.19:- *Cis-trans* isomerisation of angelic acid and tiglic acid

REFERENCES

1. D. T. Benfrey (ed), In " Classics in Theory of Chemical Combinations", Dover New York, (1963), p151
2. L Pasteur, 2 lectures delivered before the Societe Chimique de Paris, Jan. 20th and Feb. 3rd, (1860)
3. Y. Izumi and A. Tai, In "Stereo-Differentiating Reactions", Kodansha Limited, Tokyo, (1977), p.2.
4. H.M. Leicester, In "The Historical Background of Chemistry", Dover Publications Inc., New York, (1971)
5. G.A. Somorjai, In "Introduction to Surface Chemistry and Catalysis", John Wiley and Sons Inc., USA, (1994), p444
6. J.W. Döbereiner, Scweigers, J. Chem. Phys., **38**, 321, (1823)
7. G.C. Bond, In "Heterogeneous Catalysis: Principles and Applications", (2nd ed), Claredon Press, Oxford, (1987)
8. J.J. Berzelius, Edinburgh New Philosophical Journal, **XXI**, 223, (1836)
9. R. Noyori, Chemtech, **22**, 366, (1992)
10. J. Mann, in "Secondary Metabolism", (2nd ed), Oxford University Press, Oxford, (1987), p9
11. R.K. Mackie, D.M. Smith and R.A. Aitken, In "Guidebook to Organic Synthesis", (2nd ed) Longman, (1987), p311
12. R.K. Mackie, D.M. Smith and R.A. Aitken, In "Guidebook to Organic Synthesis", (2nd ed) Longman, (1987), p313
13. Y. Izumi, T. Harada, J. Tanabe and K. Okadu, Bull. Chem. Soc. Jpn., **36**, 155, (1963)
14. J.T. Wehrli and A Baiker, J. Mol. Catal., **49**, 195, (1989)
15. I.M. Sutherland, A. Ibbotson, R.B. Moyes and P.B. Wells, J. Catal., **125**, 77, (1990)
16. W. Carruthers, In "Some Modern Organic Chemistry", (3rd ed) Cambidge Universtity Press, Cambridge, (1986), p464
17. F.A. Cotton and G. Wilkinson, In "Advanced Inorganic Chemistry", (5th ed) John Wiley and Sons, USA, (1988), p1244
18. J.A. Osborn, F.H. Jardine, J.F.Young and G. Wilkinson, J. Am. Chem. Soc. A, 1711, (1966)
19. H.B. Kagan and T.P. Dang, J. Am. Chem. Soc., **94**, 6429, (1972)
20. W.S. Knowles, B.D. Vineyard, M.J. Sabacky, G.L. Bachman and D.J. Weinkauff, J. Am. Chem. Soc., **99**, 5946, (1977)
21. G. Gelbard, H.B. Kagan and R. Stern, Tetrahedron, **32**, 233, (1976)

22. X-ray
23. R. Noyori and H. Takaya, Acc. Chem. Res., **23**, 345, (1990)
24. A. Miyashita, H. Takaya, T. Souchi and R. Noyori, Tetrahedron, 40, 1245, (1984)
25. H. Muramatsu, H. Kawano, Y. Ishii, M. Saburi and Y. Uchida, J. Chem. Soc., Chem. Commun., 769, (1989)
26. H. Takaya, T. Ohta, N. Sayo, H. Kumobayashi, S. Akutagawa, S. Innoue, I. Kasahara and R. Noyori, J. Am. Chem. Soc., **109**, 1596, (1987)
27. R. Noyori, T. Ohkuma, M. Kitamura, H. Takaya, N. Sayo, H. Kumobayashi and S. Akutagawa, J. Am. Chem. Soc., **109**, 5856, (1987)
28. E.J. Corey and J. O. Link, J. Am. Chem. Soc., **114**, 1906,
29. S. Akabori, S. Sakurari, Y. Izumi and Y. Fujii, Nature, **178**, 323, (1956)
30. T. Isoda, A. Ichikawa and T. Shimamoto, Rikagaku Kenkyusho Hokuku, **34**, 134 and 143, (1958)
31. Y. Izumi, Bull. Chem. Soc. Jpn., **32**, 932, (1959)
32. Y. Izumi, Bull. Chem. Soc. Jpn., **32**, 936, (1959)
33. Y. Izumi, Bull. Chem. Soc. Jpn., **32**, 942, (1959)
34. Y. Izumi, Adv. Catal., **32**, 215, (1983)
35. A.A. Kamatsu, Y. Izumi and S. Akabori, Bull. Chem. Soc. Jpn., **34**, 1067, (1961)
36. A.A. Kamatsu, Y. Izumi and S. Akabori, Bull. Chem. Soc. Jpn., **34**, 1302, (1961)
37. A.A. Kamatsu, Y. Izumi and S. Akabori, Bull. Chem. Soc. Jpn., **34**, 1706, (1961)
38. Y. Nakamura, Bull. Chem. Soc. Jpn., **16**, 367, (1941)
39 D. Lipkin and T.D. Stewart, J. Am. Chem. Soc., **61**, 3295, 3297, (1939)
40. Y. Orito, S. Imai, S. Niwa and G-H. Nguyen, J. Synth. Org. Chem. Jpn., **37**, 173, (1979)
41. Y. Orito, S. Imai and S. Niwa, J. Chem. Soc. Jpn., 1118, (1979)
42. Y. Orito, S. Imai and S. Niwa, J. Chem. Soc. Jpn., 670, (1980)
43. Y. Orito, S. Imai and S. Niwa, J. Chem. Soc. Jpn., 137, (1982)
44. H-U. Blaser and M. Muller, Stud. Surf. Sci. Catal., **59**, 73, (1991)
45. H-U. Blaser, Tetrahedron: Asymmetry, **2**, 843, (1991)
46. G. Webb and P.B. Wells, Catal. Today, **12**, 319, (1992)
47. H-U. Blaser, H.P. Jalett and J. Wehrli, J. Mol. Catal., **68**, 215, (1991)
48. H-U. Blaser, H.P. Jalett, D.M. Monti, J. F. Reber and J.T. Wehrli, Stud. Surf. Sci. Catal., **41**, 153, (1988)
49. J.R.G. Perez, J. Malthete and J. Jacques, C.R. Acad. Sc. Paris Serie II, 169, (1985)
50. H-U. Blaser and H.P. Jalett, Stud. Surf. Sci. Catal., 139, (1993)

51. W.A.H. Vermeer, A. Fulford, P. Johnston and P.B. Wells, J. Chem. Soc., Chem. Commun., 1053, (1993)

52. Jpn. Kokai Tokkyo Koho JP, **62**, 158, 268, (1987)

53. Y. Nitta, Y. Ueda and T. Imanaka, Chem. Lett (Jpn)., 1095, (1994)

54. H-U. Blaser, S.K. Boyer and U. Pittelkow, Tetrahedron: Asymmetry, **2**, 721, (1991)

55. J.T. Wehrli, A. Baiker, D.M. Monti and H-U. Blaser, J. Mol. Catal., **49**, 195, (1989)

56. J.T. Wehrli, A. Baiker, D.M. Monti, H-U. Blaser and H.P. Jalett, J. Mol.Catal., **57**, 245, (1989)

57. J.T. Wehrli, A. Baiker, D.M. Monti and H-U. Blaser, J. Mol. Catal., **61**, 207, (1990)

58. P.A. Meheux, A. Ibbotson and P.B. Wells, J. Catal., **128**, 387, (1991)

59. K.E. Simons, A. Ibbotson, P. Johnston, H. Plum and P.B. Wells, J. Catal., **150**, 321, (1994)

60. J.L. Margitfarli, B. Minder, E. Talas, L. Boltz and A. Baiker, Stud. Surf. Sci. Catal., **75**, 2471, (1993)

61. G. Bond, K.E. Simons, A Ibbotson, P.B. Wells and D.A. Whan, Catal. Today, **12**, 421, (1992)

62. M. Garland and H-U. Blaser, J. Am. Chem. Soc., **112**, 7048, (1990)

63. K.E. Simons, A. Ibbotson and P.B. Wells, In "Catalysis and Surface Characterisation" (T. Dines, C.H. Rochester and J. Thomson, Eds) Spec. Publ. No.114, Royal Soc. Chem., (1992), p174

64. H-U. Blaser, H.P. Jalett, D. Monti, A Baiker and J.T. Wehrli, Stud. Surf. Sci. Catal., **67**,147, (1991)

65. A. Saus, Zimmermann, K. Gurtler, O., Chemiker-Zeitung, **115**, 252, (1991)

66. K.E. Simons, P.A. Meheux, A. Ibbotson and P.B. Wells, Proc. 10th Intern. Congr. Catal. Vol. C, 2317, (1993)

67. B. Minder, T. Mallat, P. Skrabal and A. Baiker, Catal. Lett., **29**, 115, (1994)

68. H-U. Blaser, M. Garland and H.P. Jalett, **144**, 569, (1993)

69. E.N. Jacobsen, I. Marko, W.S. Mungall, G. Schröder and K.B. Sharpless, J. Am. Chem. Soc., **110**, 1968, (1988)

70. E.N. Jacobsen, I. Marko, W.S. Mungall, G. Schröder and K.B. Sharpless, J. Am. Chem. Soc., **111**, 737, (1989)

71. A. Ibbotson and P.B. Wells, Chem. Brit., 1004, (1992)

72. R.L. Augustine, S.K. Tanielyan and L.K. Doyle, Tetrahedron: Asymmetry, **4**, 1803, (1993)

73. O. Schwalm, B. Minder, J. Weber and A. Baiker, Catal. Lett., **23**, 271, (1994)

74. O. Schwalm, J. Weber, J. Margitfalvi and A. Baiker, I. J. Chem. Quant. Chem., **52**, 191, (1994)

75. O. Schwalm, J. Weber, J. Margitfalvi and A. Baiker, J. Mol. Struct., **297**, 285, (1993)

76. A. Tai, T. Kikukawa, T. Sugimura, Y. Inoue, S. Abe, T. Osawa and T. Harada, Bull. Chem. Soc. Jpn., **67**, 2473, (1994)

77. A. Tai and T. Harada, In "Tailored Metal Catalysts" (Y. Iwasawa, Ed.) D. Reiel, Dordrecht (1986), p265-324

78. A. Tai, T Harada, Y. Hiraki and S. Murakami, Bull. Chem. Soc. Jpn., **56**, 1414, (1983)

79. M.A. Keane and G. Webb, J. Mol. Catal., **73**, 91, (1992)

80. H. Brunner, M. Muschiol, T. Wishert and J. Wehrli, Tetrahedron: Asymmetry, **1**, 159, (1990)

81. M. Bartok, In "Stereochemistry of Heterogeneous Metal Catalyst", Chapter XI, J. Wiley, New York, (1985), p511-524

82. M.A. Keane, Can. J. Chem., **72**, 372, (1994)

83. Y. Nitta, F. Sekine, T. Imanaka and S. Teranshi, Bull. Chem. Soc. Jpn., **54**, 980, (1981)

84. Y. Nitta, F. Sekine, T. Imanaka and S. Teranshi, J. Catal., **74**, 382, (1982)

85. Y. Nitta, O. Yamanishi, F. Sekine, T. Imanaka and S. Teranshi, J. Catal., **79**, 475, (1983)

86. Y. Nitta and T. Imanaka, Bull. Chem. Soc. Jpn., **61**, 295, (1988)

87. L. Fu, H.H. Kung and W.M.H. Sachtler, J. Mol. Catal., **42**, 29, (1987)

88. M.A. Keane and G. Webb, J. Catal., **136**, 1, (1992)

89. M.A. Keane, Catal. Lett., **19**, 197, (1993)

90. M.A. Keane and G. Webb, J. Chem. Soc. Chem Commun., 1619, (1991)

91. A. Tai, K. Tsukioka, Y. Imachi, Y. Inoue, H. Ozaki, T. Harada and Y. Izumi, Proc. 8th Int. Congr. Cat. 531, (1984)

92. A. Tai, K. Tsukioka, H. Ozaki, T. Harada and Y. Izumi, Chem. Lett., 2083, (1984)

93. M.J. Fish and D.F. Ollis, Cat. Rev-Sci. Eng., 18, 259, (1978)

94. G. Webb, In "Proc. European Symposium on Chiral Reactions in Heterogeneous Catalysis", (G. Jannes, Ed.), Plenum, (1995), in press

95. W.M.H. Sachtler, In "Catalysis in Organic Reactions", (L. Augustine, Ed.) Chem. Ind., **22**, 189, (1985)

96. P. Weisz, Adv. Catal., **13**, 137, (1962)

97. P. Weisz and R.D. Goodwin, J. Catal., **6**, 227, (1966)

98. F.A. Cotton, G. Wilkinson and P.L. Gaus, In "Basic Inorganic Chemistry",(2nd ed), John Wiley and Son, Singapore, (1987)

99. Handout from Fuji-Davidson Chemical Ltd "Synthetic Bead Type Silica for Catalyst Supports - CARIACT"

100. F.A. Cotton and G. Wilkinson, In "Advanced Inorganic Chemistry", (5th ed), John Wiley and Sons, (1988)

101. E.P. Parry, J. Catal., **2**, 371, (1963)

102. S.E Voltz, A.E. Hirschler and A. Smith, J. Phys. Chem., **64**, 1594, (1960)

103. C.A. Spitler and S.S. Pallack, J. Catal., **69**, 241, (1981)

104. G. Marcelin and R.F. Vogel, J. Catal., **81**, 252, (1983)

105. P. Burton, J.P. Brunnelle, M. Pijolat and M. Soustelle, App. Catal., **34**, 225, (1987)

106. K. Tanabe, M. Misono, Y. Ono and H. Hattori, In "New Solid Acids and Bases - their Catalytic Properties", Elsevier, Japan, (1989)

107. J.T. Richardson, In "Principles of Catalyst Development", Plenum Press, New York, (1989)

108. A.W. Adamson, In "Physical Chemistry of Surfaces", (5th ed), John Wiley and Sons, USA, (1990)

109. P. Wynblatt and N.A. Gjosteib, Prog. Solid State Chem., **9**, 21, (1974)

110. C.N.R. Rao, In "UV-Vis Spectroscopy: Chemical Applications", (3rd ed), Butterworth, London, (1975)

111. A.R. West, In "Solid State Chemistry and Its Applications", John Wiley and Sons, Norwich, (1984)

112. J.W. Jenkins, Gordon Research Conference on Catalysis, Colby-Sawyer College, New London, New Hampshire, (1975)

113. S.D. Robertson, B.D. McNicol, J.H. DeBaas, S.C. Kloet and J.W. Jenkins, J. Catal., **37**, 424, (1975)

114. N.W. Hurst, S.J. Gentry, A. Jones and B.D. McNicol, Catal. Rev., **24**, 233, (1982)

115. J.W. Jenkins, B.D. McNicol and S.D. Robertson, Chem. Technol., **7**, 316, (1977)

116. J.L. Lemaitre, P.G. Menon and F. Delannay, In "Characterisation of Heterogeneous Catalysis", (F. Delannay Ed), Marcell Dekker Inc., New York, (1984), Chpt. 7

117. C. Dalgleish, J. Chem. Soc., 137, (1952)

118. S.D. Jackson, J. Willis, G.D. McLellan, G. Webb, M.B.T. Keegan, R.B. Moyes, S. Simpson, P.B. Wells and R. Whyman, J. Catal., **139**, 191, (1993)

119. A.B.P. Lever, In "Inorganic Electronic Spectroscopy", Elsevier, Amsterdam, (1984)

120. D.L. Swihart and W.R. Mason, Inorg. Chem., **9**, 1749, (1970)
121. R.M. Kellogg, Agnew. Chem. Int. Ed. Engl., **23**, 782, (1984)
122. L. Chen, Y. Ni, J. Zang, L. Lin, X. Luo and S. Cheng, J. Catal., **145**, 132, (1994)
123. G. Lietz, H. Lieske, H. Spindler, W. Hanke and J. Völter, J. Catal., **81**, 17, (1983)
124. B.D. McNicol, J. Catal., **46**, 438, (1977)
125. G. Blanchard, H. Charcosset, M.T. Chenebaux and M.Primet, Proc. 2nd Intern. Symp. on Scientific Bases for Prep. of Heterog. Catalysts, Louvain, La Neuve, Belgium, (1978)
126. H.C. Yoa, M. Seig and H.K. Plummer Jr., J. Catal., **59**, 365, (1979)
127. M.F. Johnson and C.D. Keith, J. Phys. Chem., **67**, 200, (1963)
128. S.D. Jackson, B.M. Glanville, J. Willis, G.D. McLellan, G. Webb, R.B. Moyes, S. Simpson, P.B. Wells and R. Whyman, J. Catal., **139**, 207, (1993)
129. T.A. Dorling and R.L. Moss, J. Catal., **7**, 378, (1967)
130. M. Primet, M.El. Azhar, R. Frety and M. Guerin, Appl. Catal., **59**, 153, (1990)
131. G.R. Wilson and W.K. Hall, J. Catal., **17**, 190, (1970)
132. Z. Huang, J.R. Fryer, C. Park, D.Stirling and G. Webb, J. Catal., **148**, 478, (1994)
133. A. Frennet and P.B. Wells, Appl. Catal., **18**, 243, (1985)
134. J.W. Geus and P.B. Wells, Appl. Catal., **18**, 231, (1985)
135. E. Allan, unpublished results
136. J.L. Falconer and W.C. Conner, Appl. Catal., **56**, N28, (1989)
137. N. Young, PhD Thesis, University of Glasgow, (1995)
138. T. Yoshida and K. Harada, Bull. Chem. Soc. Jpn., **44**, 1062, (1971)
139. G. Wang, T. Heinz, A. Pfaltz, B. Minder, T. Mallat and A. Baiker, J. Chem. Soc., Chem. Commun., 2047, (1994)
140. S.R. Watson, private communication
141. A. Dowden, R. Hutchinson and F. Ross, In " Hard and Soft Acids and Bases", (R.G. Pearson Ed.), Stroudsburg, (1973)
142. T. Heinz, G. Wang, A. Pfaltz, B. Minder, M. Schürch, T. Mallat and A. Baiker, J. Chem. Soc., Chem. Commun., 1421, (1995)
143. H.U. Blaser and M. Müller, 1st EUROPA Cat. Conference on Catalysis, Montpelier, (1994)
144. J. Reeder, P.P. Castro, C.B. Knobler, E. Martinborough, L. Owens and F. Diederich, J. Org. Chem., **59**, 3151, (1994)
145. N. Young, private communication

APPENDICES

Appendix 1

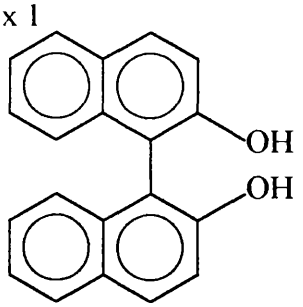

(±)-2,2'-Dihydroxy-1,1'-binaphthalene

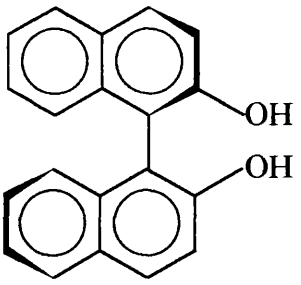

R-(+)-2,2'-Dihydroxy-1,1'-binaphthalene

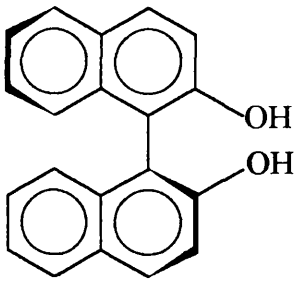

S-(-)-2,2'-Dihydroxy-1,1'-binaphthalene

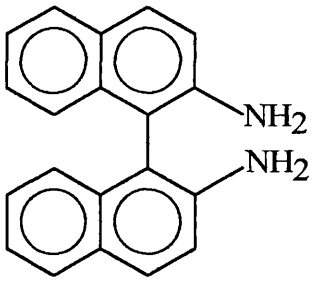

(±)-2,2'-Diamino-1,1'-binaphthalene

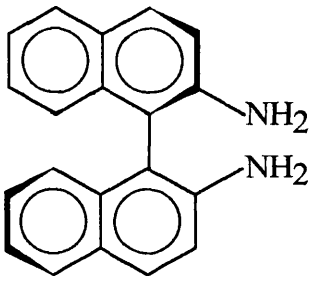

R-(+)-2,2'-Diamino-1,1'-binaphthalene

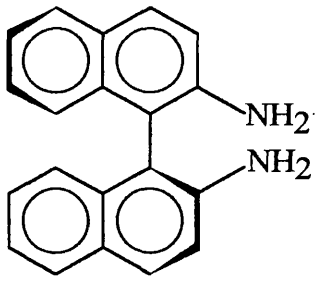

S-(-)-2,2'-Diamino-1,1'-binaphthalene

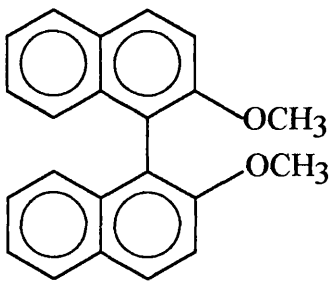

(±)-2,2'-Dimethoxy-1,1'-binaphthalene

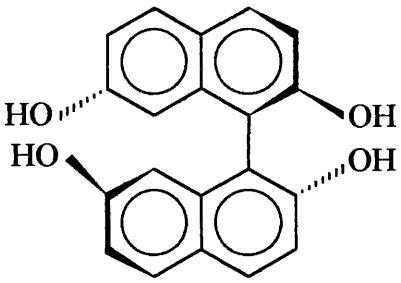

(-)-2,2',7,'7'-Tetrahydroxy-1,1'-binaphthalene

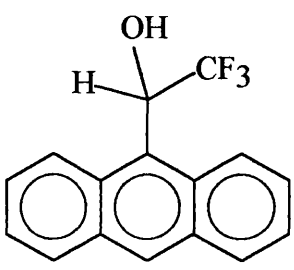

R-(-)-1-(9-Anthryl)-2,2,2-trifluoroethanol

Figure A.1:- Substituted binaphthalenes and R-(-)-(9-anthryl) -2,2,2-trifluoroethanol modifiers

Appendix 2

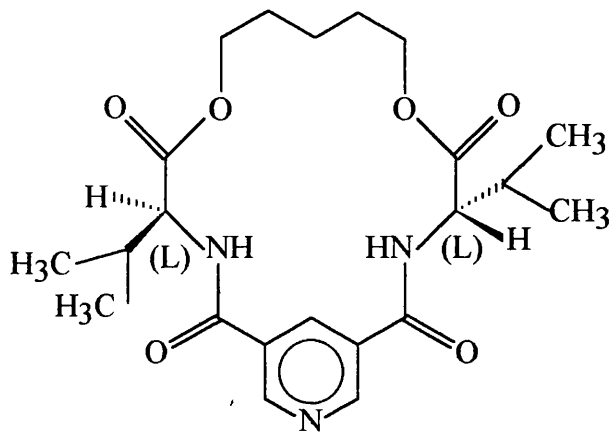

(S,S)-Di-(-2-propyl)-6,12-dioxa-2,5,13,16-tetraoxo-3,15,19-triazabicyclo[15.3.1] heneicosa-1 (21),17,19-triene '$(CH_2)_5$-bridged pyridine-based macrocycle'

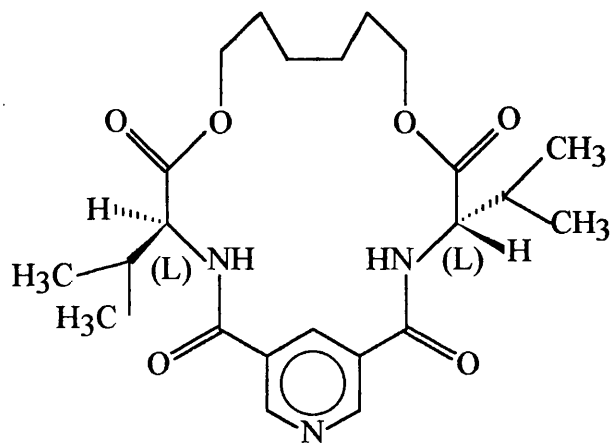

(S,S)-Di-(-2-propyl)-6,13-dioxa-2,5,14,17-tetraoxo-3,16,20-triazabicyclo [16.3.1] docosa -1(22),18,20-triene '$(CH_2)_6$-bridged pyridine-based macrocycle'

Figure A.2:- Macrocyclic modifiers

Appendix 3

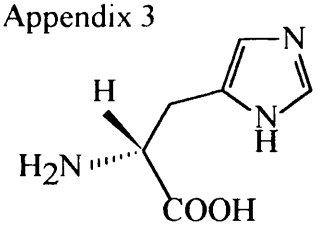

L-Histidine
'His'

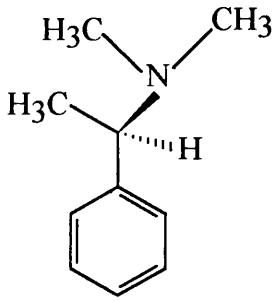

R-(+)-N,N-Dimethyl-1-phenylethylamine
'DMPEA'

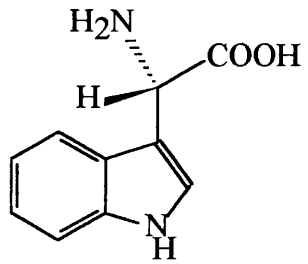

L-Tryptophan
'Trp'

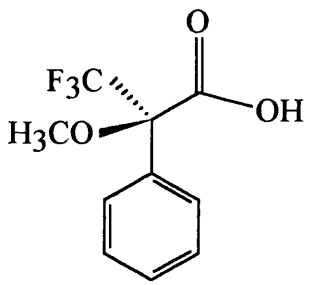

R-(+)-α-Methoxy-α-trifluoromethylphenylacetic acid
'MTFMPAA'

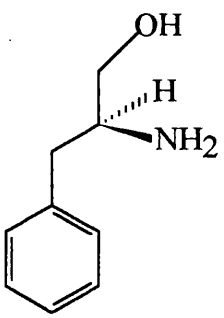

L-Phenylalaninol
'PhAla'

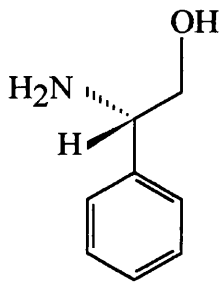

L-(+)-α-Phenylglycinol
'PhGly'

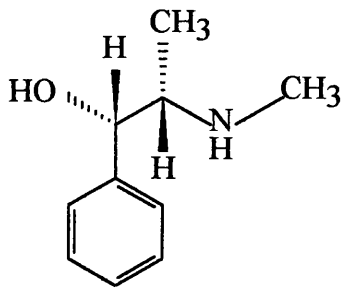

(+)-Pseudoephedrine
'Pseudo'

Figure A.3:- Alternative modifiers

Appendix 4

Preparation of R-(+)-2,2'-dihydroxy-1,1'-binaphthalene (diol)

(±)-2,2'-dihydroxy-1,1'-binaphthalene was resolved from diastereomeric salts by Hunter[1] according to Kawashima and Hirayama.[2] The diastereomeric salts were formed from reaction of the (±)-diol with 1,2-diaminocyclohexane. The (-)-1R, 2R-diaminocyclohexane, results in the formation of the resolved R-(+)-diol. After separation of the diastereomeric salts, acid was added and the resolved diol precipitated.

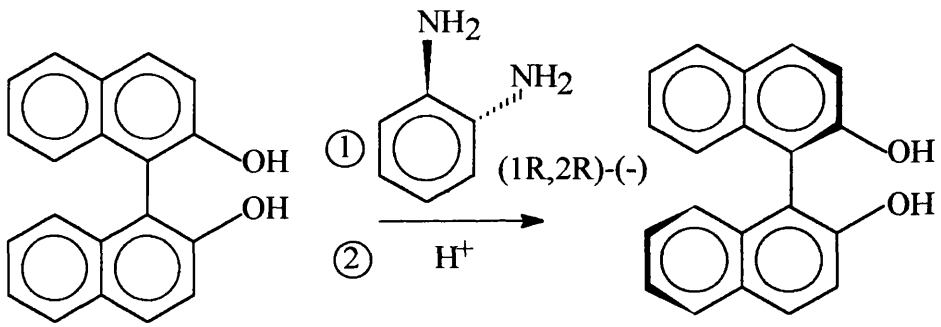

(±)-2,2'-Dihydroxy-1,1'-binaphthalene R-(+)-2,2'-Dihydroxy-1,1'-binaphthalene

Figure A.4:- Outline of R-(+)-diol preparation

1. D. Hunter, PhD Thesis, University of Glasgow, (1995)

2. M. Kawashima and A. Hirayama, Chem. Letts., 2299, (1990)

Appendix 5

Preparation of (±)-2,2'-diamino-1,1'-binaphthalene (diamine)

Hunter[1] prepared the (±)-diamine according to Brown *et al*[2] from β-naphthol and hydrazine monohydrate.

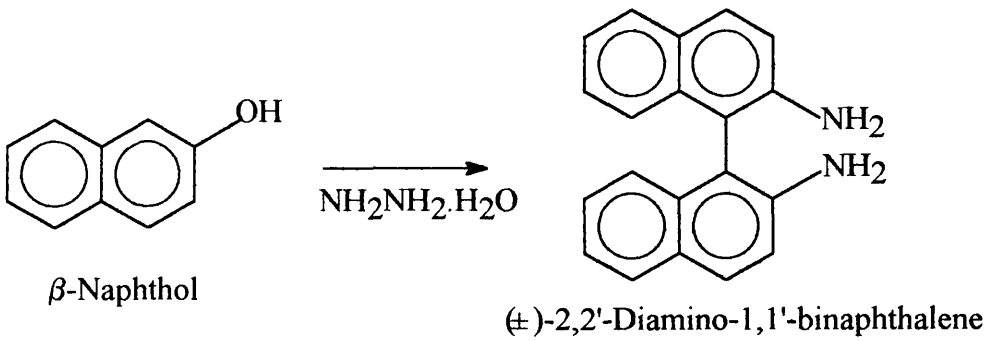

β-Naphthol

(±)-2,2'-Diamino-1,1'-binaphthalene

Figure A.5:- Outline of (±)-diamine preparation

1. D. Hunter, PhD Thesis, University of Glasgow, (1995)

2. K.J. Brown, M.S. Berry and J.R. Murdoch, Org. Chem., **50**, 4345, (1985)

Appendix 6

Preparation of (±)-2,2'-dimethoxy-1,1'-binaphthalene (dimethoxy)

Hunter[1] prepared the (±)-dimethoxy by using $NaBH_4$ to abstract H atoms from the -OH groups and replacing the CH_3 groups from CH_3I.

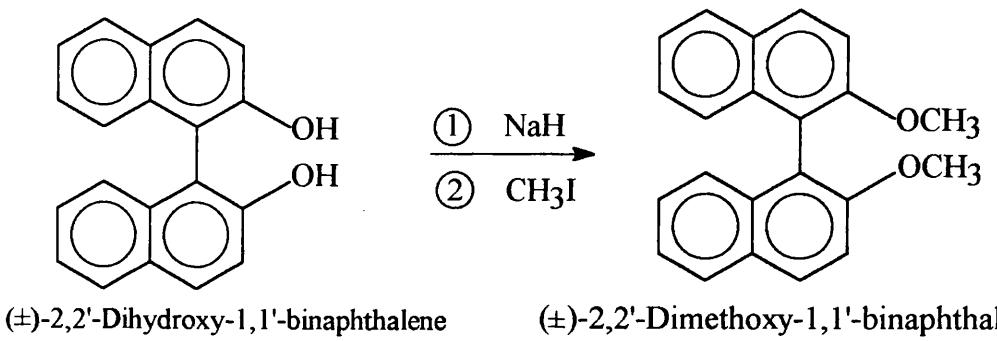

(±)-2,2'-Dihydroxy-1,1'-binaphthalene (±)-2,2'-Dimethoxy-1,1'-binaphthalene

Figure A.6:- Outline of (±)-dimethoxy preparation

1. D. Hunter, PhD Thesis, University of Glasgow, (1995)

Appendix 7

Preparation of (-)-2,2',7,7'-tetrahydroxy-1,1'-binaphthalene (tetra-ol)

Hunter[1] prepared the (-)-tetra-ol according to Horiuchi *et al.*[2] The (-)-tetra-ol was prepared by the coupling of two molecules of 2,7-dihydroxynaphthalene. The racemic mixture was resolved by forming diastereomeric salts with quinine.

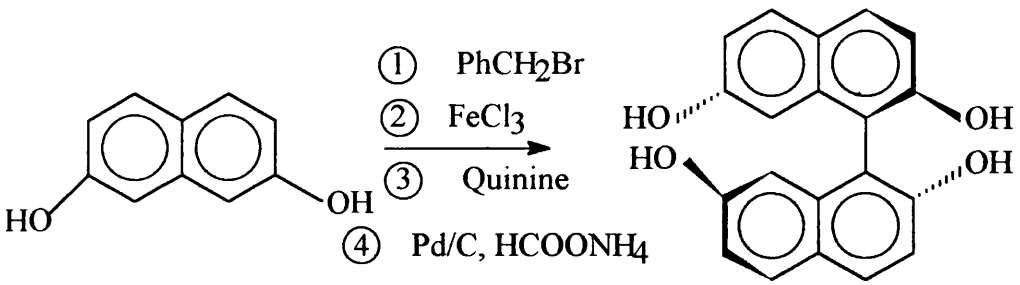

(-)-2,2',7,'7'-Tetrahydroxy-1,1'-binaphthalene

Figure A.7:- Outline of (-)-tetra-ol preparation

1. D. Hunter, PhD Thesis, University of Glasgow, (1995)
2. T. Horiuchi, T. Ohta, M. Stephan and H. Takaya, Tetrahedron: Asymmetry, **5**, 325, (1994)

Appendix 8

Preparation of (S,S)-Di-(2-propyl)-6,12-dioxa-2,5,13,16-tetraoxo-3,15,19-triazabicyclo [15.3.1] heneicosa -1 (21),17,19-triene [$(CH_2)_5$-bridged, pyridine based macrocycle]

This $(CH_2)_5$-bridged, pyridine based macrocycle was prepared as detailed in a paper by Kellogg *et al*[2] by Hunter.[1] 3,5-Pyridine dicarboxylic acid (Figure A.8a) was reacted with $SOCl_2$ to from the acid chloride of the pyridine dicarboxylic acid (Figure A.8b). An alkaline solution of L-valine methyl ester.HCl was then reacted with the acid chloride with the formation of a pyridine valine methyl ester (Figure A.8c). The ester groups of the pyridine valine methyl ester are then reduced to the acid grouping (Figure A.8d) by an alkaline solution [bis-(L-valinamide) of pyridine-3,5-dicarboxylic acid]. To the bis-(L-valinamide) of pyridine-3,5-dicarboxylic acid, Cs_2CO_3 and 1,5-dibromopentane was added. The 1,5-dibromopentane added to the two carboxylic groups form the $(CH_2)_5$-bridge.

1. D. Hunter, PhD Thesis, University of Glasgow, (1995)
2. A.G. Talma, P. Jouin, J.G. De Vries, C.B. Troostwijk, G.H.W. Bening, J.K. Waninge, J. Visscher and R.M. Kellogg, J. Am. Chem. Soc., **107**, 3981, (1985)

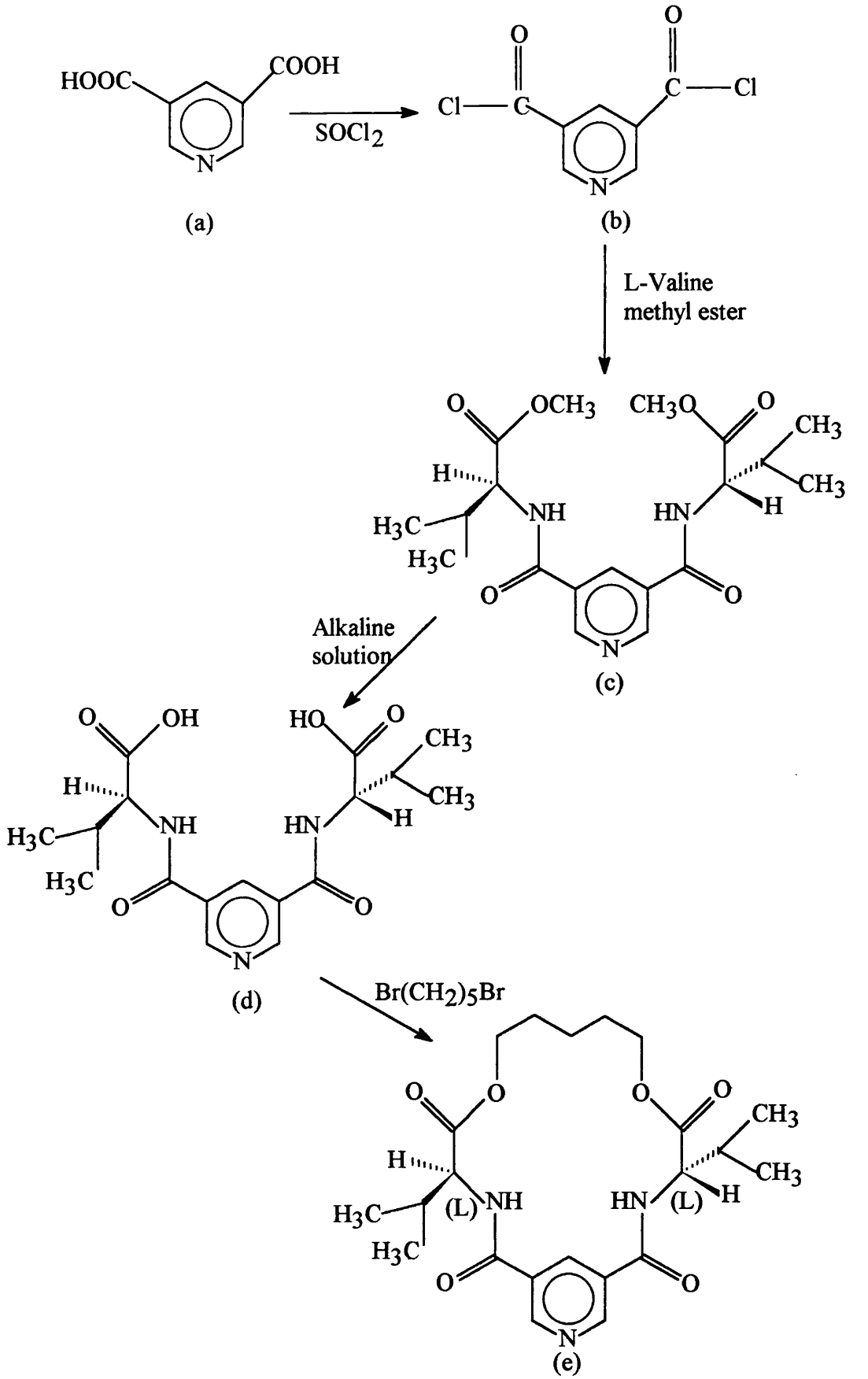

(S,S)-Di-(-2-propyl)-6,12-dioxa-2,5,13,16-tetraoxo-3,15,19-triazabicyclo[15.3.1] heneicosa-1 (21),17,19-triene

Figure A.8:- Preparation of $(CH_2)_5$-bridged, pyridine-based macrocycle

Appendix 9

Preparation of (S,S)-Di-(2-propyl)-6,13-dioxa-2,5,14,17-tetraoxo-3,16,20-triazabicyclo [16.3.1] docosa -1 (22),18,20-triene [$(CH_2)_6$-bridged, pyridine based macrocycle]

The $(CH_2)_6$-bridged, pyridine based macrocycle was prepared along the same procedure as for the $(CH_2)_5$-bridged, pyridine based macrocycle except that at the last step 1,6-dibromohexane instead of 1,5-dibromopentane was used.

Appendix 10

Preparation of (±)-3-benzofuranol

Racemic 3-benzofuranol was prepared by Hunter[1] by the reduction of 3-coumaranone using a standard reducing agent, $NaBH_4$. The 3-benzofuranol was purified on silica using 50% diethyl ether/hexane.

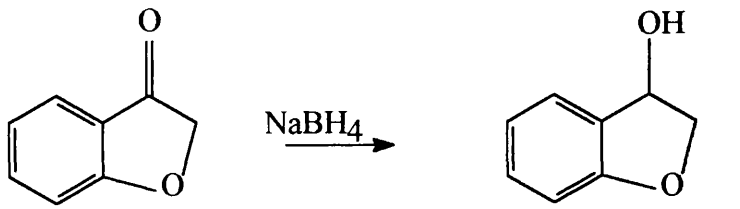

3-Coumaranone (±)-3-Benzofuranol

Figure A.9:- Outline of preparation of (±)-3-benzofuranol

1. D. Hunter, PhD Thesis, University of Glasgow, (1995)

Appendix 11

CASE FOR SUPPORT

THE GENERATION OF CHIRAL CENTRES AT HETEROGENEOUS SURFACES

The following is an abstract from the case for support:-

AIMS OF THE PROJECT

The main objective of this project is to establish a general framework for the generation of chiral centres on heterogeneous catalyst surfaces. It is the formation of sites having pre-determined, shaped environments, that will confer on the surface the capacity to catalyse the formation of products with both chemical specificity and optical purity. To achieve these objectives we intend to take principles from catalyst promotion and poisoning, polymer chemistry, synthetic organic chemistry and macrocyclic chemistry and fuse them into new concepts for the development of catalytically active chiral centres at heterogeneous surfaces.

SCIENTIFIC PROGRAMME

The scientific programme has been separated into distinct sections for ease of presentation and explanation, however this study will be fully integrated with both academic centres and ICI working to achieve common goals.

1 Test Reactions

As we have intimated earlier, previous studies have concentrated on single reaction systems, whereas it is our intention to examine a range of reactions on a range of metals, which are typical of those transformations required in current pharmaceutical synthesis. Catalytically active metals that will be most used in the study are platinum, palladium and nickel. The use of reactions which have different spatial and chemical requirements, in terms of their specificity, allows a more rigorous interrogation of the chiral centres prepared on these metals (or on their oxide forms). Therefore the following reactions have been chosen. (1) The hydrogenation of a substituted alkene, X-CH=C(CH_3)-CO_2CH_3, where X may be CH_3 or CF_3: the functional groups associated with the carbon-carbon double bond make hydrogenation of these compounds of significant interest. (2) The hydrogenation of ketones, both an amino-ketone, Ph-CO-CH_2-N(CH_3)$_2$, and an alpha-beta unsaturated ketone, Ph-CH=C(t-butyl)-CO-CH_3: hydrogenation of the latter puts considerable spatial constraints on the site geometry, gives information on chemical

selectivity (hydrogenation of ketone or alkene or both) as well as having two prochiral centres. (3) A Diels Alder coupling of CH_2=CH-CHO: this reaction is being used as a model system for coupling reactions. By use of these test reactions we will probe the chiral centres generated, on the metal (or oxidic) phase, by the methods outlined in the following sections.

2. Catalyst Modification

2.1 Generation of Chiral Centres by Use of Templates

Enantioselectivity can be achieved if a chiral modifier is adsorbed strongly to a metallic surface and leaves exposed shaped ensembles of metal atoms at which reactant molecules can adsorb in only one configuration (the template model developed by the Hull group (8,9,11)). Conformational selection in reactant adsorption leads directly enantioselectivity and the chiral sense of the product is correctly predicted by this model.

We propose to use as templates a family of binaphthyls (Figure A.10a) where X = -OH, -SH, PPh_2, PR_2, $-NR_2$, -SR, and CR_3. These materials are chiral because the two naphthyl units are tilted with respect to each other. By use of these molecules, which may be adsorbed either by one naphthyl unit parallel to the surface (horizontal mode), or by dissociation of H from the -OH or -SH groups (near vertical mode), the template concept can be examined in both surface and spatial regimes.

With adsorption in the horizontal mode, the shape of the template can be varied at will by specification of the X-group. Hence the geometry of the shaped ensembles of unoccupied metal atoms, available as sites for enantioselective reaction, will, accordingly, be variable and under our experimental control. This is a hitherto unavailable facility in terms of chiral centres on heterogeneous catalyst surfaces.

9,10-Dihydro-3:4,-5:6-dibenzophenanthrene (Figure A.10b), which can be regarded as a binaphthyl bridged between the 2- and 2'- positions is photosensitive. Illumination with circularly polarised light at ca. 300nm results in enantiomeric enrichment (12). The use of such compounds as templates will open up the tantalising possibility of engineering on the molecular level a photochemically switchable catalyst, so that the sense of the chirality of the product can be reversed at will.

We return to the use of systems having binaphthyls adsorbed in a near-vertical mode in paragraph 2.3.

2.2 Generation of Chiral Centres by Template Desorption

The second strategy is almost the reverse of that described in 2.1 and involves (i) templating the metal surface with a chiral substance (for example, cinchona alkaloid, or

a binaphthyl derivative), (ii) annihilation of the shaped ensembles of metal atoms so created by adsorption of a stable blocking agent, and (iii) the desorption of the template, thus leaving exposed a differently shaped ensembles of metal atoms bearing in two dimensions the chiral imprint of the modifier. The adsorption of such chiral templates has been shown to be easily reversible under certain conditions. Suitable blocking agents that would be used are sulphur compounds (e.g. H_2S, C_2H_5SH, thiophen). The value of this method resides in its flexibility; it provides for the exact determination of the size and shape of the imprint by variation of the binaphthyl derivative used and would be highly cost effective in industrial terms in that the chiral modifier could be used repeatedly.

2.3 Generation of Chiral Surfaces by the Irreversible Adsorption of Chiral Substances

Methods in 2.1 and 2.2 are designed to lead to the creation of shaped ensembles of exposed metal atoms, that is chiral centres. However, drawing on aspects of catalyst poisoning and promotion, we now propose a quite different approach to the generation of enantioselectivity, which has as its objective the establishment of a chiral quality at the surface which provides for conformational orientation or selection during the approach of the reactant to the catalyst site.

Metal catalysts performing organic molecules transformations contain hydrocarbonaceous residues on their surface. For 25 years the Glasgow Group has been the world leader in the identification and characterisation of the hydrocarbonaceous species on working supported metal catalysts (13). These residues are a permanent feature of the catalysts, they are necessary for the good health of the working catalyst, they increase catalyst selectivity, and play a crucial role in H-transfer and as such determine (and enhance) reaction rates.[157] By the generation of such species from optically active substances we expect to be able to condition metal surfaces to achieve this type of conformational selection. Adsorption of, for example, a chiral butene (CH_3-CHX-CH=CH_2, where X = NH_2, Cl, -Ph, etc) will produce on the metal surface an array of substituted butylidenes (Figure A.10c) that will create an adlayer that appears chiral to molecules approaching from the fluid phase. Use of a more complex chiral alkene will produce residue arrays that can be likened to an array of corkscrews: reactant molecules that eventually arrive at the reaction sites at the metal surface will be those the conformational characteristics of which best for the spatial geometry of the adsorption path. Such conformational selection in adsorption should allow the attainment of both chemical and chiral selectivity. Further control over the reaction sites will be exercised by variation of the size of substituent X.

Vertically orientated binaphthyls (referred to in section 2.1) fall into this category

and provide variations of this concept.

2.4 Chiral Centres Generated Using Macrocyclic Ligands

Metal complexes are known to catalyse asymmetric synthesis in the homogeneous phase but, as outlined in the introduction, such systems have severe limitations form a process engineering standpoint. Heterogenising these complexes has not proved very successful although the concept of making such complexes more robust and easier to handle has attractions. It is not our intention to go down such a well trodden path; rather, we intend to develop the use of metal-modifier complexes supported on the metal surface of a heterogeneous catalyst (a model which has recently been developed by the Glasgow group (10)). We see this is a natural development of the concepts detailed in 2.3.

`The synthesis of metal complexes of the type shown in Figure A.10d (M= Ni), in which the transition metal ion forms a chelate complex with a chiral macrocyclic ligand, are now well established at Glasgow (14). Chiral macrocyclic sulphides of the type shown in structures in Figure A.10e and in Figure A.10f are also readily prepared (15) and are more suitable for use with platinum and palladium, where S-ligand complexes are more stable than the corresponding N- or O-ligand complex. Use of these species as modifiers will not produce the template behaviour outlined in sections 2.1 and 2.2, because it is the complexed metal atom which acts as the chiral centre at which catalysis takes place. Adsorbing these metal complexes on the metal function of a heterogeneous catalyst (where the metal is the same as that in the macrocycle) will produce a hybrid system which maximises the benefits of both components. The underlying metal surface will supply dissociated hydrogen thereby enhancing rates, the macrocycle will ensure high chemical and chiral selectivity, while the physical properties will allow ease of separation and handling.

8. Y. Orito, S. Imai and S. Nai, Collected papers of the 43rd Catalyst Forum, (1978), p30
9. G. Webb and P.B. Wells, Catalysis Today, 12, (1992), 319
10. M.A. Keane and G. Webb, two papers accepted for publication in J. Catal.
11. I.M. Sutherland, A. Ibbotson, R.B. Moyes and P.B. Wells, J. Catalysis, 125, 77, (1990)
12. P.H. Schippers and H.P.J.M. Dekkers, Tetrahedron, 38, 2089, (1982)
13. G. Webb, Catalysis Today, 7, 139, (1990)
14. R.D. Peacock, J.Chem. Soc., Daton Trans., 931, (1989)
15. R.M. Kellogg, Agnew. Chem., 23, 782, (1984)

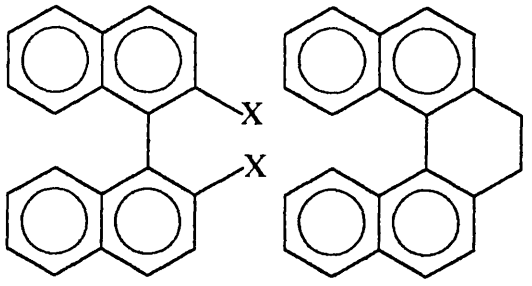

(a)

(b)

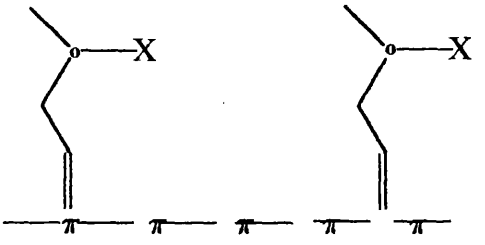

(c)

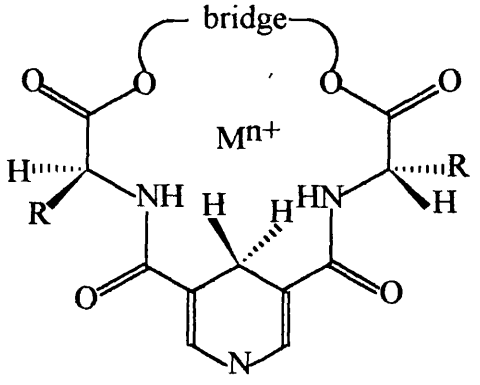

(d)

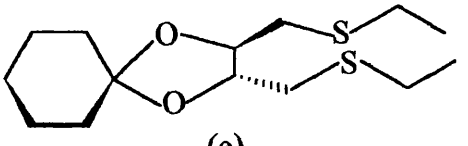

(e)

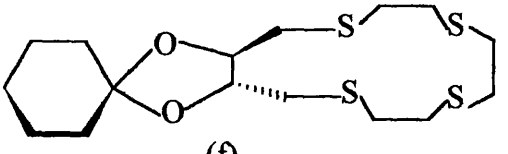

(f)

Figure A.10

Identification of the additional product formed from the hydrogenation of 3-coumaranone

Subsequent to the completion of the main thesis, the additional product formed upon hydrogenation of 3-coumaranone has been identified by Zeneca Pharmaceuticals from ^{13}C and mass spectroscopy. Figure A.11 gives the equation.

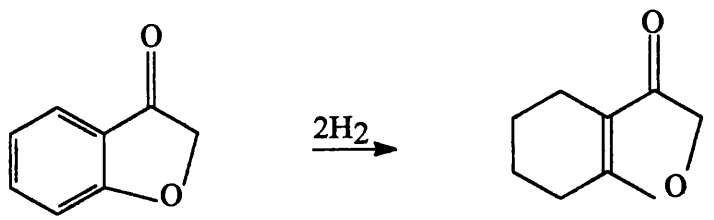

Figure A.11:- Additional product formation